PART 1. SYNTHESIS OF STABLE-ISOTOPE LABELED AMINO ACIDS

PART 2. SYNTHESIS OF MECHANISTIC PROBES OF RETINOID ACTION

DISSERTATION

Presented in Partial Fulfillment of the Requirements

for the Degree Doctor of Philosophy

in the Graduate School of The Ohio State University

By

Derek W. Barnett, B.S., Chemistry

*****

The Ohio State University

2002

Dissertation Committee:

Robert W. Curley, Jr., Ph.D., Adviser

Werner Tjarks, Ph.D.

Karl A. Werbovetz, Ph.D.

Approved By

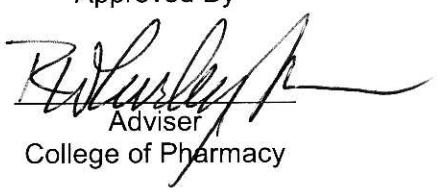

Adviser

College of Pharmacy

ABSTRACT

Stable-isotope labeled amino acids are valuable research tools. They are frequently used in mechanistic enzymology to study biosynthetic pathways and the stereochemical outcome of enzyme mediated processes. These materials are also relied upon in NMR spectroscopy where they facilitate protein structure determination with the use of isotope edited or filtered experiments. Previous work in our laboratory has led to the synthesis of ^{15}N-labeled glycine stereoselectively deuterated at the α-carbon. This molecule was used to stereospecifically assign the glycine α-proton resonances in FK506 binding protein in drug binding studies.

As an expansion of this previous work, we are currently developing synthetic routes to ^{15}N containing amino acids that have been stereoselectively deuterated at the β-carbon. Once incorporated into a protein of interest, these molecules can be used to obtain stereospecific assignments of the prochiral β-methylene protons. These assignments greatly increase the precision of the structure determination process and are critical to accurately establishing the orientation of amino acid side-chains within the protein. The utility of this strategy has been demonstrated by the synthesis of the (2*S*, 3*R*)-[3-^{2}H,^{15}N]-phenylalanine and (2*S*, 3*S*)-[3-^{2}H,^{15}N]-tyrosine derivatives. The key step in the syntheses is the alkylation of a chiral lithium enolate derived from ^{15}N-(-)-8-phenylmenthylhippurate with an enantiotopically deuterated benzylic electrophile.

A prominent feature of this strategy is its versatility. By selecting the appropriate protecting groups and electrophile, any of the four possible diastereomers can be synthesized. In addition, the method is amenable to the incorporation of various isotope labeling patterns owing to the commercial availability of different isotopomers of glycine. The details of the phenylalanine and tyrosine syntheses are presented as well as a summary of the efforts to optimize the strategy and extend the methodology to the production of several other labeled β-methylene unit containing amino acids.

N-(4-Hydroxyphenyl)retinamide (4-HPR) is a synthetic amide analog of retinoic acid that has been studied extensively as a cancer chemopreventive and chemotherapeutic agent. However, the mechanism through which 4-HPR exerts its antiproliferative effects remains unclear. It has been demonstrated that 4-HPR induces apoptosis in many tumor cell lines despite having virtually no affinity to the nuclear retinoid receptors. This is in direct contrast to retinoic acid, which possesses very high affinity for the retinoic acid receptors and induces differentiation in tumor cell lines. This data suggests that 4-HPR and retinoic acid may act at different cellular targets. In an effort to identify possible targets of 4-HPR binding, we have synthesized a series of electrophilic and photo affinity label analogs of 4-HPR. The details of the syntheses and preliminary chemical reactivity are presented.

Dedicated to mom and dad

ACKNOWLEDGMENTS

There are several people that I would like to acknowledge because of their help and support during my graduate school career. First of all, I would like to thank my adviser, Dr. Robert W. Curley Jr., for his help and guidance during my studies. I have certainly learned a great deal from you during our time together. I would also like to thank the rest of the faculty and students in the Division for all of their help along the way. I am also very grateful for the sharing of technical expertise by Mr. John Fowble and Dr. Charles Cottrell. Both of you certainly proved to be a valuable resource. I would also like to thank Ms. Joan Dandrea and Ms. Kathy Brooks for all of their assistance. If I ever had a question, one of you always had the answer.

I would especially like to recognize my most recent labmates: Joel, Kevin, and Serena. Each of you spent a lot of time with me in the trenches day in and day out and helped to make this experience something I will never forget. We had fun (sometimes too much) during the good times, and we still managed to laugh (most of the time) during the not so good times. I think that Joel and Kevin would have to agree that this part of my life has provided me with some of my best comedic material (just take a look at the ever expanding list of memories).

I would like to thank my wife Tara for all of her support during my studies. It really helped to know that you were there, especially when things got to be stressful. Thank you for being understanding about all of your events that I missed due to work

committments.

Joel, I am glad that our paths crossed and we got the chance to become such good friends and to serve time together in Shawshank. Just remember all we have is time but your day will come, so get busy living or get busy making 4-HBRCG. Finally, I would like to thank the members of Benzene (and our groupies) for all of the great concerts. For those of you that do not know, Benzene is arguably the greatest cover band of all time. The following quote was taken from one of the 10 or 12 lucky people in the universe who have actually seen Benzene perform at their semi-annual free concerts at The Wine Cellar.

> "Their energy on stage is amazing which is good because that almost begins to cover up the obvious lack of vocal or instrumental skills. With Joel 'Never A Mistake' Walker on bass, Robert 'Pink Floyd Rules' Curley on electric lead guitar, Derek 'Just Tell Me When To Come In' Barnett on acoustic rhythm guitar, and sometimes touring with Serena Mershon on harmonica and drums, I must admit they make the most of their very limited talent. It is definitely worth the cover charge." – groupie who wished to remain anonymous, The Wine Cellar, Fall 2002.

Please look for their first greatest hits album, entitled "Benzene Greatest Hits - Spheres of Sodium", on record store shelves in the summer of 2150 with a world tour soon to follow. Also, be sure to check out their full-length concert film, "Fleeing the Fleakers", produced by H.T. Productions.

VITA

May 11, 1973……Born – Little Rock, Arkansas

1996……...B.S., Chemistry
University of Arkansas at Little Rock

1995-1996……Undergraduate Research Assistant
University of Arkansas at Little Rock

1996-1997……Graduate Teaching Assistant
The Ohio State University

1997-2002……Graduate Research Assistant
The Ohio State University

PUBLICATIONS

Barnett, D. W.; Panigot, M. J.; Curley, R. W., Jr. Stereoselective route to ^{15}N-labelled-β-deuterated amino acids: synthesis of (2*S*, 3*R*)-[3-^{2}H,^{15}N]-phenylalanine. *Tetrahedron: Asymmetry* **2002**, *13*, 1893-1900.

Curley, R. W. Jr.; Mershon, S. M.; Barnett, D. W.; Clagett-Dame, M.; Chapman, J. S. Solid phase synthesis of arylretinamides. U.S. patent pending.

FIELDS OF STUDY

Major Field: Pharmacy

Specialization: Medicinal Chemistry

TABLE OF CONTENTS

LIST OF TABLES

LIST OF FIGURES

LIST OF SYNTHETIC SCHEMES

LIST OF NMR SPECTRA INCLUDED IN APPENDIX

LIST OF ABBREVIATIONS

Abbreviation	Term
4-AcPR	*N*-(4-acetamidophenyl)retinamide
4-AzPR	*N*-(4-azidophenyl)retinamide
4-AzOHPR	*N*-(4-azido-2-hydroxyphenyl)retinamide
4-HPR	*N*-(4-hydroxyphenyl)retinamide
4-NCSPR	*N*-(4-isothiocyanatophenyl)retinamide
4-TfaPR	*N*-(4-trifluoroacetamidophenyl)retinamide
9-BBN	9-borabicyclo[3.3.1]nonane
Å	angstrom
amp	ampere
amu	atomic mass unit
aq.	aqueous
atRA	all-*trans*-retinoic acid
calcd	calculated
CCIC	Campus Chemical Instrumentation Center
COSY	correlation spectroscopy
de	diastereomeric excess
DEAD	diethyl azodicarboxylate
ee	enantiomeric excess
eq	equivalent
ES	electrospray
EtOH	ethanol

FGI	functional group interconversion
FMOC	9-fluorenylmethylchloroformate
h	hour
HCA	hexachloroacetone
HMBC	heteronuclear multiple bond coherence
HMQC	heteronuclear multiple quantum coherence
HPLC	high performance liquid chromatography
HRE	hormone response element
HRMS	high resolution mass spectrometry
HSQC	heteronuclear singular quantum coherence
HTH	helix-turn-helix
g	gram
IR	infrared
K_d	dissociation constant
kDa	kilodalton
LDA	lithium diisopropylamide
MHz	mega hertz
mL	milliliter
mm	millimeter
mmol	millimole
mol	mole
mp	melting point
NBS	*N*-bromosuccinimide
nm	nanometer
NMR	nuclear magnetic resonance
NOE	nuclear Overhauser enhancement

PAL	phenylalanine ammonia lyase
PCC	pyridinium chlorochromate
ppm	parts per million
ppt	precipitate
psi	pounds per square inch
quant.	quantitative
RA	retinoic acid
RAL	retinal
RAR	retinoic acid receptor
RARE	retinoic acid response element
rb	round bottom
R_f	retention factor
ROL	retinol
rt	room temperature
RXR	retinoid X receptor
RXRE	retinoid X response element
S_N1	substitution nucleophilic unimolecular
S_N2	substitution nucleophilic bimolecular
TBAF	tetrabutylammonium fluoride
TBDMS	*tert*-butyldimethyl silyl
TFA	trifluoroacetic acid
TFAA	trifluoroacetic anhydride
THF	tetrahydrofuran
TIPS	triisopropylsilyl
TIPSCl	triisopropylsilyl chloride
TLC	thin layer chromatography

TMEDA	tetramethylenediamine
TMSI	trimethylsilyl iodide
TOCSY	total correlation spectroscopy
TPP	triphenylphosphine
t_r	retention time
UV	ultraviolet
UV-vis	ultraviolet-visible
Z	benzoyl

PART 1. SYNTHESIS OF STABLE-ISOTOPE LABELED AMINO ACIDS

CHAPTER 1

USE OF STABLE-ISOTOPE LABELED AMINO ACIDS

Isotopically labeled compounds are invaluable research tools that have countless applications in many fields of science.[1-3] Many of the advances in basic science today are a result of experiments which relied, either directly or indirectly, on isotopically labeled materials. The fields of astronomy, biology, chemistry, medicine, and physics are disciplines which make extensive use of isotopes. In addition to the basic sciences, isotopes play pivotal roles in the social sciences by helping us to develop our understanding of the past. For example, one of the techniques used to date archaeological relics is based on the analysis of the isotopic composition of matter. Regardless of their application, the importance of isotopes is undeniable. The first part of this document details our contribution to the synthesis of isotopically labeled compounds. We have developed a synthesis of stable-isotope labeled amino acids which has significant implications in several fields including nuclear magnetic resonance (NMR) spectroscopy. Compounds produced by this method can be used to facilitate protein structure determination using NMR methods. These materials can also be used to aid mechanistic enzymology and drug discovery studies. This first chapter provides an introduction to terms and concepts, followed by the necessary background information for an understanding of our synthetic method.

1.1 Introduction

A good starting point for this discussion is with a brief review of the structure of the atom and the definition of nomenclature and several terms that are commonly encountered when discussing isotopes. In the Bohr atomic model, an atom is visualized as having a positively charged nucleus that is charge balanced by a negative charge which surrounds the nucleus in defined orbitals. The source of the positive charge is a fundamental unit of matter known as a proton. Protons are constituents of all atomic nuclei, the number of which is defined as the atomic number of the element. A single proton carries one unit of positive charge, defined as 1.60×10^{-19} coulombs, and a mass of approximately one atomic mass unit (amu), defined as 1.66×10^{-24} grams. The neutron is another fundamental unit of matter that is present in the nucleus. It is electrically neutral and has a mass slightly greater than that of the proton. Together, these two particles account for essentially all of the mass associated with a particular element. To balance the positive charge in the nucleus, negatively charged electrons occupy orbitals around the nucleus. An electron carries an equal and opposite charge of a proton, but a mass 1/1837 that of a proton. Elements are defined by their atomic number, whereas “nuclides” have specified numbers of protons and neutrons. To represent a particular nuclide, the appropriate element symbol is used and the mass number (number of protons and neutrons) of the nuclide is written as a superscript to the left of the symbol. Thus, a nuclide of carbon having a mass number of 12 is written ^{12}C and is referred to as “carbon-12”.

Isotopes are groups of nuclides that have the same number of protons, but different numbers of neutrons and hence different mass numbers. All elements can exist in several isotopic forms. In general, isotopes can be characterized as being stable or

unstable. Unstable isotopes are termed “radioisotopes” or “radionuclides” and are classified by the type of “radioactive decay” processes they undergo. Radioactive decay processes are characterized by nuclear reactions involving specific emissions from the nucleus and result in the “transmutation” of one element into another element. For example, ^{14}C is an unstable isotope of carbon and undergoes radioactive β-decay to yield a ^{14}N nuclide plus a quantity of emitted energy. The different types of radioactive decay are classified according to the types of emissions that are observed. Stable isotopes do not undergo these decay processes and therefore, do not transmutate into other elements. Both stable and unstable isotopes are used extensively in many different areas of research, each type having a vast number of applications.

The compounds of interest for the purpose of this document are stable-isotope labeled amino acids. The use of these chemical entities in an experiment allows for these materials to be selectively observed within an experimental system. This ability to observe or “track” a label through an experiment makes these molecules extremely useful in obtaining data about the system under study. Stable-isotope labeled amino acids are frequently employed in mechanistic enzymology to study biosynthetic pathways and the stereochemical course of enzyme mediated reactions.[4-6] Since a comprehensive discussion of these applications is not the primary intent of this document, the reader is directed to the cited references as a starting point for additional reading.

1.2 Protein NMR Spectroscopy

One of the most significant uses for these labeled amino acids is facilitating protein structural studies using NMR spectroscopy.[7-10] Knowledge of the three-dimensional (3D) structure of proteins with atomic resolution is required for a complete understanding of their function and mechanisms of action. There are currently two major methods used to obtain such structures, X-ray crystallography and NMR spectroscopy. X-ray crystallography is based on the analysis of the diffraction patterns produced when a single protein crystal is irradiated with X-rays. The first protein structure solved using X-ray crystallography was reported in 1959 by Kendrew and co-workers.[11] Addressing the limitations of this method was the impetus behind the development of protein NMR spectroscopy. These limitations include the observation that many proteins fail to crystallize, and many that do not fail, often yield unsuitable crystals for diffraction studies.[12] In a NMR experiment, data is usually collected from a soluble protein which eliminates the need for protein crystallization. The use of a soluble protein has other important implications; there can be significant differences between the crystalline structure and the solution structure of a protein. In natural systems, proteins most often mediate their activity in the soluble state, therefore, NMR solution structures may be more biologically relevant.[13] Finally, many dynamic processes, such as protein folding, ligand-binding, and enzyme catalysis, are amenable to study using NMR spectroscopy because the protein is not confined to a static state.[13]

However, NMR methods possess their own requirements and limitations. Nuclear magnetic resonance is an inherently insensitive technique as compared to other spectroscopic methods such as infrared (IR) and ultraviolet-visible (UV-vis) spectroscopy. The energies associated with the fundamental processes which permit

NMR phenomena to be observable are very weak and therefore, sensitivity is a key consideration. This necessitates that for protein NMR studies, often times samples of millimolar concentrations are required. This demands that the sample be soluble at these high concentrations and that aggregate formation does not occur. In addition, signal line width and sensitivity become limiting as the size of the protein increases. These phenomena arise from the short transverse (spin-spin) relaxation times (T_2) of nuclei in larger molecules due to slower rotational correlation times (τ_c) and the resulting more efficient depolarization.[10] As a result of these limitations, early studies using these techniques failed to yield the 3D structure of any protein. However, much effort went into addressing these limitations, culminating with the first NMR solution structure of a protein being reported in 1985.[14-16] Since those initial reports, NMR technology has undergone a quantum leap forward in all aspects. The result is that today, hundreds of protein structures have been elucidated using NMR, including structural analysis of protein complexes with molecular weights of 900 kDa.[17] These advancements have established NMR spectroscopy as a ubiquitous tool in structural biology studies.

1.2.1 Basic NMR concepts and definitions

An exhaustive review of NMR principles is beyond the scope of this document, however, a working understanding of some of the terms and concepts encountered in NMR discussions is essential. The reader is directed to the Appendix for a listing of relevant NMR definitions. In its most basic form, a NMR experiment involves perturbing induced magnetization present within certain nuclei of a sample from an equilibrium state and observing the sample's response to the disturbance. Therefore, the concept of induced magnetization and how it responds to this disturbance is essential to an understanding of NMR theory. In most experiments, the induced magnetization is a

consequence of the sample being placed in a static magnetic field (B_o) of a fixed strength. The response of the induced magnetization is based on the relaxation or decay of magnetization after it has been disturbed from its equilibrium state.

As described in section 1.1, all nuclei have a positive charge originating from protons in the nucleus. In some nuclei this charge can be described as possessing the quantum mechanical property of "spin". This spinning of nuclei generates a magnetic dipole along the axis of spin. The angular momentum of the spinning charge can be described in terms of the spin number "I"; I can have values of 0, 1/2, 1, 3/2, etc… An I value of 0 is defined as having no spin. Nuclei having a nonzero I value are observable by NMR; nuclei with I values of 1/2 are the most common.

1.2.2 Protein structure elucidation strategies using multi-dimensional NMR

One of the major advances in protein NMR is the advent of stable-isotope labeling strategies.[10,18,19] The advent of $^{13}C/^{15}N/^{2}H$ labeling of proteins has facilitated the development of 3- and 4D heteronuclear experiments which in turn have permited larger protein structures to be analyzed.[20] These experiments accomplish this by addressing two fundamental problems encountered with NMR of proteins: resonance overlap and loss of sensitivity. As mentioned in section 1.2, as the size of a protein increases, the more difficult it becomes to solve its structure using NMR methods. The vast number of signals begin to overlap making it impossible to extract useful information. The development of 2D-NMR methods addressed this problem, and these experiments are useful for proteins consisting of approximately one-hundred residues.[12] At sizes greater than one-hundred residues, once again resonace overlap becomes a limiting factor. The concept of increasing dimensionality to obtain useful information may be best understood by the following analogy described by Clore and Gronenborn.[12] Consider all

of the information contained in a set of encyclopedias. In a 1D representation, all of that information would be condensed into a single line. Upon expansion of that line into a 2D representation (a page), the information would still not be discernable. However, when the page is further expanded into three-dimensions (a book representing one volume of the set), some of the information may become intelligible. Finally, upon expansion into 4D (the complete set of books), all of the information becomes clear.

It is in this manner that multidimensional NMR techniques have facilitated protein NMR. With techniques based on this principle, it is possible to solve protein structures with sizes up to 30 kDa using homonuclear techniques.[10] In addition, experiments relying on isotope editing and/or filtering strategies are now commonly used to make resonance assignments and to simplify NMR spectra.[21] In general terms, isotope editing experiments select for resonances of protons attached to either ^{13}C or ^{15}N while editing the resonances of protons attached to other nuclei; isotope filtering experiments select for resonance of protons attached to either ^{12}C or ^{14}N while filtering the signals from protons attached to ^{13}C and ^{15}N. Deuterium labeling of proteins directly addresses the limitation of loss of sensitivity when studying large molecules and will be discussed in detail later in this chapter. However, the use of ^{2}H labeling in conjunction with ^{13}C and ^{15}N labeling extends the effective size limit of proteins that can be studied up to 60-70 kDa.[10]

Shown in Figure 1.1 is the general strategy used for solving many 3D structures of macromolecules by NMR.[9] In brief, the first step is to obtain backbone sequential resonance assignments using a combination of through-bond and through-space correlations. These assignments provide the primary structure, sequences of amino acids, of the protein and this information can often times be used to identify elements of

secondary structure that are present. The second step is to obtain stereospecific assignments at chiral centers and torsion angle restraints using three-bond scalar couplings combined with NOE data. This step begins the process of collecting data that will be used to build a 3D representation of the global structure of the protein. The third step is to identify through-space connectivities between protons separated by less than five Å using NOE derived data. Data collected from these experiments will be used as constraints to refine the model of the structure. Finally, the fourth step involves calculating 3D structures on the basis of the experimental NMR restraints using one or more of a number of algorithms such as distance geometry and/or simulated annealing.[22-24] Often times several structures are initially produced that fit all of the constraints due to ambiguities arising from incomplete assignments. Once a set of low resolution structures are obtained, it is possible to use iterative methods to resolve most ambiguities and produce refined low-resolution structures. These initial structures are often refined by additional constraints obtained from further experimentation to resolve any remaining ambiguities in the structure. This process is repeated until a small number of structures are obtained with acceptable resolution.

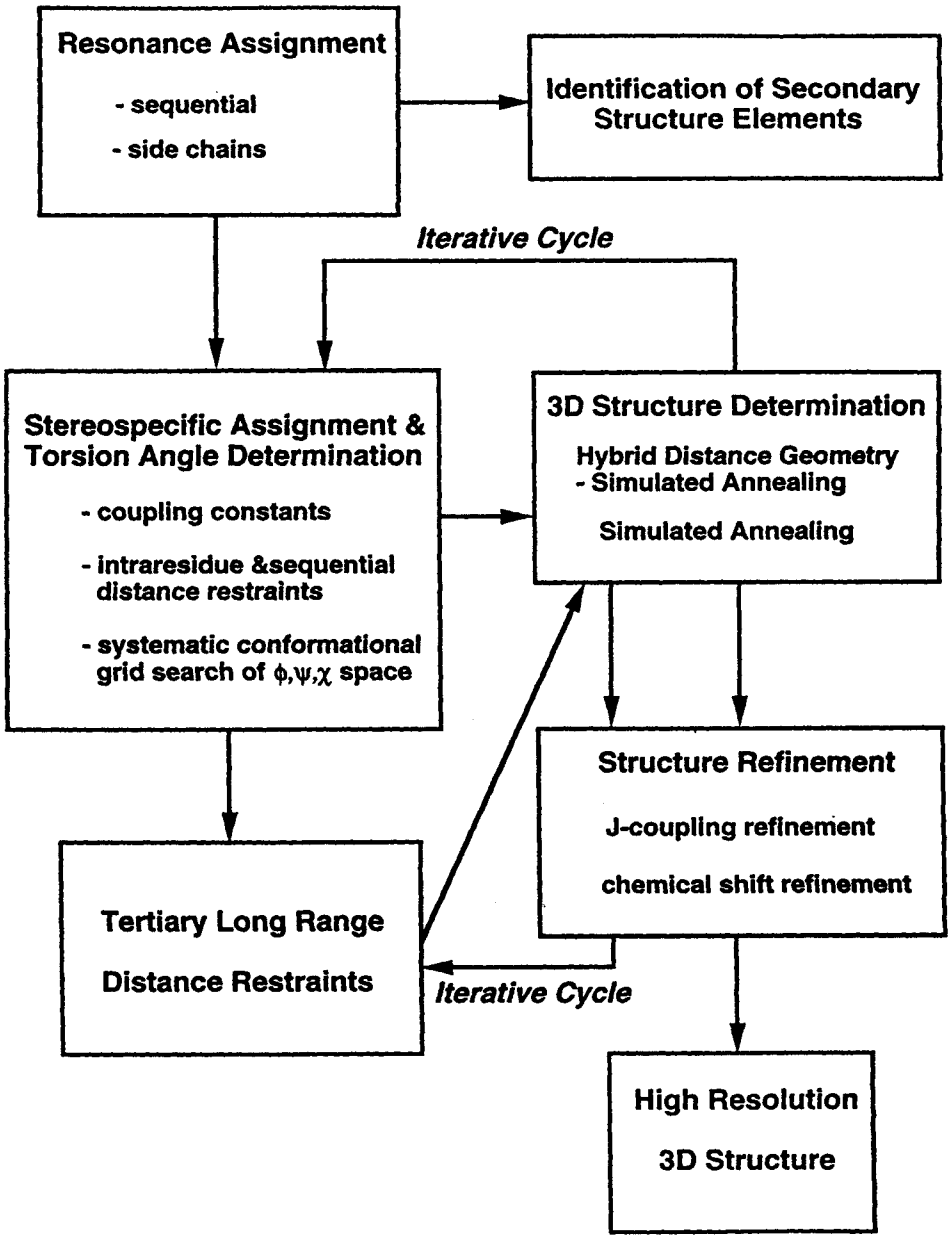

Figure 1.1 General NMR strategy used to solve 3D structures of macromolecules. (figure taken from reference 9)

1.2.3 Stereospecific assignments

1.2.3.1 Karplus equations

The determination of stereospecific assignments and torsion angle constraints is a key step in obtaining high resolution NMR structures. These assignments are often determined using a combination of homonuclear and heteronuclear three-bond coupling contants (^3J) and NOE data[9,25-27] The magnitude of the ^3J coupling constant is a function of the dihedral angle θ, originally derived for ^{1}H-C-C-^{1}H coupling from the theoretical calculations of Karplus[28,29] and in its most general form is represented as:

$$^3J = A\cos^2(\theta) + B\cos(\theta) + C$$

The coefficients A, B, and C are empirical parameters that depend on the type of coupled nuclei and their environment. Specific equations have been derived for most of the relevant homonuclear and heteronuclear coupling constants found in proteins.[30] However, caution must be taken when these equations are invoked in the absence of additional information because multiple bond angle values may exist for every ^3J value. In spite of this degeneracy, these couplings can at the very least be used to resolve ambiguities or as restraints for molecular dynamics calculations.

1.2.3.2 Prochiral β-methylene protons and χ_1 torsion angle

Shown in Figure 1.2 are the common torsion angles encountered in protein structural studies.[31]

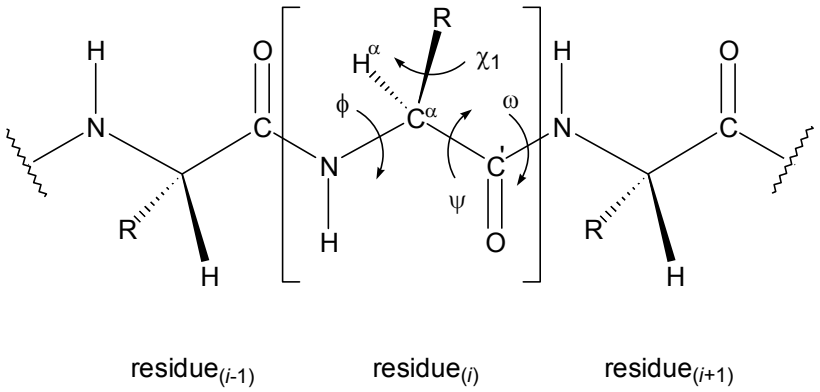

Figure 1.2 Polypeptide segment with the backbone torsion angles ϕ, ψ, ω and the first sidechain torsion angle χ_1.

Torsion angles ϕ, ψ, and ω correspond to the backbone of the peptide while χ_1 defines the projection of the side-chain from the backbone. If a protein is considered as a polymer of peptide units as shown above, these torsion angles define the 3D conformation of each peptide unit and taken collectively, they globally describe the protein. It has long been established that stereospecific side-chain resonance assignments greatly enhance the precision of NMR structures of proteins.[32] For amino acid residues containing a β-methylene unit, unambiguous assignment of the prochiral β-protons greatly facilitate determining χ_1 torsion angles because the appropriate couplings can be associated with the correct protons (Figure 1.3). The coupling constants that are often used to determine torsion angle values and the relevant Karplus equations that have been derived for these angles are listed in Figure 1.4.[13]

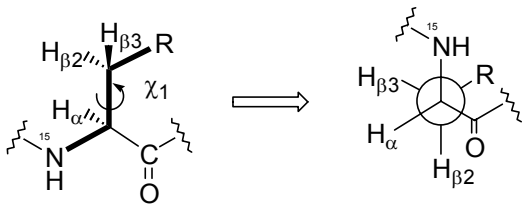

Figure 1.3 General representation of the χ_1 torsion angle in peptide for β-methylene unit containing amino acid residue.

Torsion angle	Relevant *J*-couplings
ϕ	$^3J_{NH\text{-}H\alpha}$, $^3J_{C\beta\text{-}NH}$. $^3J_{C\gamma\text{-}H\alpha}$, $^3J_{H\alpha\text{-}C'(i\text{-}1)}$
ψ	$^3J_{H\alpha\text{-}N(i+1)}$
ϕ and ψ	$^1J_{C\alpha\text{-}H}$
χ_1	$^3J_{H\alpha\text{-}H\beta}$, $^3J_{C'\text{-}H\beta}$, $^3J_{N\text{-}H\beta}$

Karplus Equations:

$$^3J_{NH\text{-}H\alpha}(\phi) = 6.4\cos^2(\phi - 60°) - 1.4\cos(\phi - 60°) + 1.9$$

$$^3J_{H\alpha\text{-}H\beta2}(\chi 1) = 9.5\cos^2(\chi_1 - 120°) - 1.6\cos(\chi_1 - 120°) + 1.8$$

$$^3J_{H\alpha\text{-}H\beta3}(\chi 1) = 9.5\cos^2(\chi_1) - 1.6\cos(\chi_1) + 1.8$$

$$^3J_{N\text{-}H\beta2}(\chi 1) = -4.5\cos^2(\chi_1 + 120°) + 1.2\cos(\chi_1 + 120°) + 0.1$$

$$^3J_{N\text{-}H\beta3}(\chi 1) = 4.5\cos^2(\chi_1 - 120°) + 1.2\cos(\chi_1 - 120°) + 0.1$$

Figure 1.4 Peptide torsion angles as defined by their ^3J couplings and relevant Karplus equations.[13]

Early efforts to obtain stereospecific assignments of the prochiral β-methylene protons relied on a method of approximation known as pseudo-atom replacement strategies.[13] In this strategy, prochiral β-methylene protons with indistinguishable chemical shifts (<0.001 ppm) were treated as a single "pseudo-atom" located at the geometric center between the two protons. Distances derived from NOE data involving the prochiral β-methylene protons were approximated as a single distance to the "pseudo-atom" with a 0.3 Å correction added to the upperbound of the measured distance to correct for the difference in position of the "pseudo-atom" relative to the true proton. This method has proven to be inadequate as it results in a reduction of the precision of the experimental conformational constraints.[32] More recently, multidimensional NMR techniques have been used to obtain these stereospecific assignments.[9] The usual strategy for obtaining these stereospecific assignments of the β-methylene unit is outlined in Figure 1.5.

Newman projections

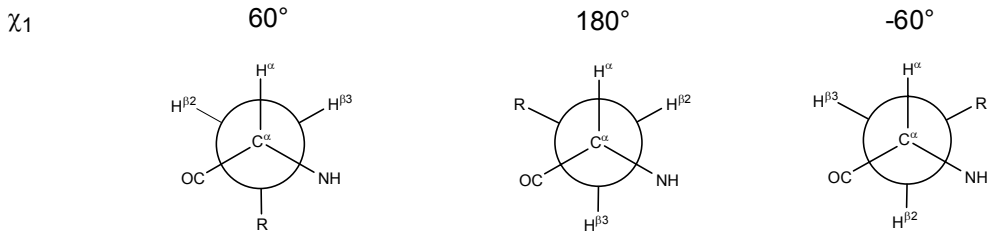

Scheme for establishing conformation

$^3J_{H\alpha\text{-}H\beta2}$ (Hz)	< 4	< 4	< 4
$^3J_{H\alpha\text{-}H\beta3}$ (Hz)	< 4	> 10	< 4
NOEs	$H_\alpha\text{-}H_{\beta2} \sim H_\alpha\text{-}H_{\beta3}$	$H_\alpha\text{-}H_{\beta2} > H_\alpha\text{-}H_{\beta3}$	$H_\alpha\text{-}H_{\beta2} < H_\alpha\text{-}H_{\beta3}$
NOEs	$N\text{-}H_{\beta2} < N\text{-}H_{\beta3}$	$N\text{-}H_{\beta2} \sim N\text{-}H_{\beta3}$	$N\text{-}H_{\beta2} > N\text{-}H_{\beta3}$

Figure 1.5 Scheme for obtaining stereospecific assignments of β-methylene protons on the basis of ^3J coupling constants.

It is often possible to obtain stereospecific assignments of these protons on the basis of qualitative interpretation of the homonuclear $^3J_{H\alpha\text{-}H\beta}$ coupling constants and the intraresidue NOE data involving the NH, $C^\alpha H$, and $C^\beta H$ protons.[26,27] A more rigorous approach, which also permits one to obtain ϕ,ψ, and χ restraints, involves the application of a conformational grid search of ϕ,ψ,χ_1 space on the basis of the homonuclear $^3J_{NH\text{-}H\alpha}$ and $^3J_{H\alpha\text{-}H\beta}$ coupling constants, which are related to ϕ and χ_1 respectively, and the intraresidue and sequential interresidue NOEs involving the NH, $C^\alpha H$, and $C^\beta H$ protons.[32,33] This information can be supplemented by the measurement of heteronuclear $^3J_{N\text{-}H\beta}$ and $^3J_{CO\text{-}H\beta}$ couplings, which are also related to χ_1.[34] However, due to spectral overlap, these types of experiments do not always provide this information.[35]

An alternative method to obtain stereospecific assignments is found in stable-isotope labeling strategies.

The incorporation of deuterium into proteins is often used to simplify ^{1}H NMR spectra and to improve the relaxation properties of the remaining protons.[36] Exchange of proton for deuteron simplifies ^{1}H NMR spectra by reducing the number of proton resonances. However, the most profound effect of deuteration of large molecules is on the relaxation properties of ^{13}C nuclei. As described in section 1.2, a fundamental problem of NMR of macromolecular systems is rapid T_2 relaxation times. Rapid T_2 relaxation, especially for covalently bound ^{13}C-^{1}H pairs, reduces the sensitivity of heteronuclear experiments used for resonance assignments as well as isotope-edited NOESY experiments used to extract distance constraints.[10] Replacement of ^{1}H with ^{2}H eliminates this relaxation pathway and many scalar and dipolar ^{1}H-^{1}H interactions that also result in a loss of sensitivity. Therefore, the transverse relaxation rates of the ^{13}C nuclei and remaining protons are prolonged, resulting in narrower ^{1}H line widths which leads to increased resolution and sensitivity in multidimensional experiments.[10] For example, the strategy of partial fractional deuteration has been used to help interpret *J*-values and NOE results in the stereospecific side-chain assignment and conformational analysis of thioredoxin.[37,38] These assignments were facilitated by stereospecific β-deuterated aspartate and asparagine being incorporated into the protein. As demonstrated by these examples, stereoselective deuteration of the prochiral β-methylene unit can aid obtaining coupling constant data related to the χ_1 torsional angle which is necessary for stereospecifically assigning side-chain resonances.

1.2.3.3 Stereospecific β-deuteration

Incorporation of these stereoselectively β-deuterated amino acids into a protein allows NMR spectra of these labeled proteins to be directly compared to spectra from unlabled "control" proteins. The disappearance of a specific cross-peak in a multidimensional NMR experiment helps to establish unambiguous assignments of these prochiral protons. The three-bond coupling constant between the remaining β-proton and α-proton ($^3J_{H\alpha\text{-}H\beta}$), which is critical for determining the χ_1 torsion angle, is now readily measurable. Double labeling of these amino acids, particularly by incorporating ^{15}N, allows for simplification of NMR spectra using spectral editing/filtering techniques.[39-41] In addition determination of $^3J_{N\text{-}H\beta}$ would now be readily obtainable which would also faciltate accurately determing χ_1. The incorporation of the deuteron at the prochiral β-methylene unit would have a significant effect on $^{13}C\beta$ T_2 relaxation rates such that assignments of the β-carbons would be aided.[20] Not only would these labeled amino acids be useful in protein structure determination studies, they would be valuable tools in the conformational analysis of peptides.

1.3 Conformational Analysis of β-Deuterated Peptide Ligands

NMR has other applications besides macromolecular structure determination. Its role in the drug discovery process is continuously expanding from structure determination of therapeutically relevant targets to a screening tool for chemical libraries and instrument for lead compound optimization. The reader is directed to recent reviews for further reading.[21,42-44] The use of NMR in this capacity is based on its ability to detect weak ligand-receptor interactions and the ability to provide structure information with atomic resolution to guide structure-based drug-design efforts. Isotope labeling of

ligands plays a role in the myriad of screening strategies.[44] A related application of NMR which relies on ligand labeling is the conformational analysis of peptide ligands with interesting bioactivities.[45,46] When a lead compound is conformationally flexible, knowledge of its conformation when bound to its receptor provides valuable information to guide analog synthesis. These studies have been facilitated with the use of stereoselectively β-deuterated amino acids.

The most common NMR approach to determining interatomic distances is using NOE data. A common failing of NOE-derived distance constraints for small peptides is the uncertainity imposed by the inability to stereospecifically assign resonances from prochiral protons.[45] When one proton in a pair of prochiral protons exhibits a specific NOE interaction, this lack of stereospecific assignment manifests itself as an imprecise internuclear distance.[45] These imprecisions lead to ambiguities in the structure. In a recent example, Etzkorn and Travins used stereospecific β-deuteration to aid their studies on the structure determination of a helix-turn-helix (HTH) peptide mimic.[46] Their cyclic tripeptide structure (Figure 1.6) is a constrained mimic of the turn in the HTH motif found in DNA-binding proteins. This structural motif is found in transcription factors which are essential for cellular differentiation during development.[47,48]

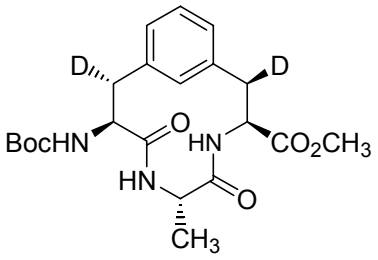

Figure 1.6 β-Deuterated cyclic HTH mimic.[46]

Analysis of NMR data collected from undeuterated HTH mimic revealed spectral overlap that prohibited stereospecific assignments and, therefore, the use of valuable NOE derived distance constraints necessary for conformational analysis. The use of stereoselective β-deuteration aided conformational analysis by permitting the use of fifteen additional NOE distance constraints that were unobtainable when analyzing data from the unlabeled HTH mimic. These fifteen added constraints represented 62% of the total distance constraints used for the final conformational analysis. Using this additional data, the authors were able to determine the solution structure of the HTH mimic and establish that the constrained cyclic tripeptide exists in the same conformation as predicted for an unconstrained mimic using computational methods.[46]

1.4 Summary

It is clear from the information presented above that stereoselectively β-deuterated amino acids have many uses. Their use has important implications in the fields of NMR, drug discovery, and mechanistic enzymology. Syntheses of specific β-deuterated amino acids have been reported in the literature.[4] Most of these can be characterized as relying on enzymatic strategies to induce chirality or resolve stereoisomers. Of those that are based solely on chemical methods, most can be characterized by their use of the reduction of dehydro amino acid derivatives. It is our goal to develop a chemical method that could be generalized to include all β-methylene unit containing amino acids. In addition, a key consideration was that the method not only be amenable to deuterium labeling, but also to the incorporation of ^{15}N and ^{13}C to take full advantage of the array of heteronuclear multidimensional NMR experiments that are available. The following two chapters of this document detail our synthetic method

and our efforts on the production of the first doubly labeled amino acids generated using this methodology.

CHAPTER 2

TOWARDS A GENERAL APPROACH TO STEREOSELECTIVELY β-DEUTERATED ^{15}N-LABELED AMINO ACIDS: SYNTHESIS OF (2*S*, 3*R*)-[3-^{2}H,^{15}N]-PHENYLALANINE

2.1 Statement of the Problem

Stable isotope labeled amino acids are valuable biochemical tools that are used in many different areas of research. They are frequently employed in mechanistic enzymology to study biosynthetic pathways and the stereochemical course of enzyme mediated processes.[4-6] These materials are also relied upon in NMR spectroscopy where they facilitate protein structure determination with the use of isotope edited or filtered experiments.[8-10] The incorporation of deuterium labeled amino acids into a protein greatly simplifies the ^{1}H NMR spectrum.[36,49] Stereospecific ^{1}H NMR assignments of prochiral protons can be obtained using chiral deuteration, and these assignments assist obtaining coupling constant information and distance constraints, and thus aid conformational analysis of the molecules under study. Previous work from our laboratory has led to the synthesis of (2*R*)-[2-^{2}H,^{15}N]-glycine that has been used for NMR studies of FK506 binding protein (FKBP).[50,51] Once incorporated into the protein, stereospecific NMR assignments of the glycine α-protons of FKBP bound to the immunosuppressant ascomycin were obtained using ^{15}N-edited TOCSY (**TO**tally **C**orrelated **S**pectroscop**Y**) experiments.

As an expansion of this previous work, we are currently interested in developing a general route to ^{15}N-labeled aromatic amino acids that are stereoselectively deuterated at the β-carbon. These materials will permit the stereospecific NMR assignments of the prochiral β-methylene protons, which will aid conformational studies of amino acid side-chains and conformational analysis of receptor-bound peptide ligands.[32,38,45,46,52]

2.2 Review of Alternative Synthetic Methodologies

Several synthetic routes to diastereotopically β-deuterated phenylalanine derivatives are known. These routes can be generally characterized as methods that utilize the reduction of dehydro amino acids[53-55] or halogenated derivatives,[56,57] or methods that rely on enzymatic steps to introduce chirality and/or resolve stereoisomers[58-60]. The work of Oba and co-workers utilizes the dioxopiperazine shown in Figure 2.1 to prepare α,β-dideuterio phenylalanine and tyrosine derivatives.

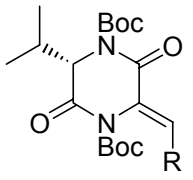

R
Ph
4-$MeOC_6H_4$
3,4-$(MeO)_2C_6H_3$

Figure 2.1 Dioxopiperazine derivatives used to prepare α,β-dideuterio amino acids.

The authors are interested in using these labeled materials as probes for the conformational analysis of peptide side-chains using NMR spectroscopy. Treatment of the dioxopiperazine derivatives with deuterium gas over palladium-carbon followed by hydrolysis gives the α,β-di-deuterio L-amino acid derivatives stereospecifically with high optical purity. The authors have observed that by varying the reaction conditions they

can induce the reduction to proceed by a *trans* addition to give the less accessible L-*erythro* isomer via the (*Z*)-dehydroamino acid derivative.[61]

The work of Easton and Hutton relied on the side-chain bromination of *N*-phthaloylamino acid derivatives using *N*-bromosuccinimide (NBS) to generate labeled phenylalanine derivatives (Figure 2.2).[56]

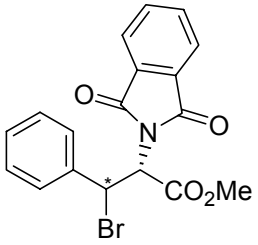

Figure 2.2 Brominated phenylalanine derivatives used to generate β-deuterated phenylalanines. *denotes chiral center

The authors were interested in studying the stereochemical course of the deamination reaction of (*R*)-phenylalanine by (*S*)-phenylalanine ammonia-lyase (PAL) and thus, required the deuterated D-amino acid derivatives. The compound shown in Figure 2.2 was obtained by the regiospecific mono-bromination of the protected phenylalanine derivative using NBS to give the bromides as a mixture of diastereomers. They report that under the appropriate conditions the deuteriolysis of the bromides using palladium-carbon proceeded with retention of configuration at the benzylic center to give the deuterated compounds. The 3-position epimers were then separated using chromatography after further derivatizations.

Kirby and Michael were interested in investigating the stereochemistry of the biosynthesis of various alkaloids and prepared β-labeled phenylalanine and tyrosine using α-acylamino cinnamic acid derivatives to facilitate their studies (Figure 2.3).[59,60]

Reduction of these materials using hydrogen over palladium-carbon gave the amino acid derivatives as racemic mixtures which required resolution.

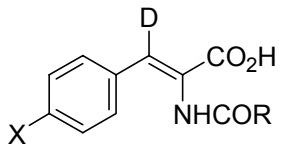

X = H, OH

Figure 2.3 Deuterated cinnamic acid derivatives used for the synthesis of phenylalanine and tyrosine derivatives.

Nagai and Kobayashi attempted to improve on the synthesis by incorporating enzymatic steps to induce asymmetry and provide resolution of stereoisomers[58] Their synthesis of a phenylalanine derivative was characterized by the enzymatic reduction of benzaldehyde-α-*d* to give (*S*)-benzyl-α-*d*-alcohol, conversion of this alcohol to the chiral tosylate, followed by the alkylation of a *N*-acetyl-glycine ethyl ester to give the racemic α-amino acid derivative. The enantiomers were then resolved using α-chymotrypsin to selectively hydrolyze the L-amino acid ester.

The method reported here is intended to be a chemical synthesis of ^{15}N-labeled stereoselectively β-deuterated aromatic amino acids. The synthetic method is based on the alkylation of a chiral glycine equivalent. The versatile nature of the strategy allows for the synthesis of multiple diastereomers and should allow for easy incorporation of multiple isotopic labeling patterns.

2.3 Experimental Design

2.3.1 Alkylation of glycine equivalents

Alkylation of glycine equivalents is well precedented and represents a common route to α-amino acid derivatives.[62-74] Excellent stereochemical control of the nascent carbon-carbon bond can be achieved with the use of the appropriate chiral protecting groups, establishing the desired stereochemistry at the α-carbon. If a stereoselectively deuterated electrophile were employed in the alkylation reaction, it would be possible to introduce asymmetry at the β-carbon during construction of the C2-C3 bond, assuming an S_N2 reaction mechanism (Figure 2.4). With this in mind, the alkylation of a glycine equivalent with an enantioselectively deuterated electrophile was adopted as the preferred synthetic strategy.

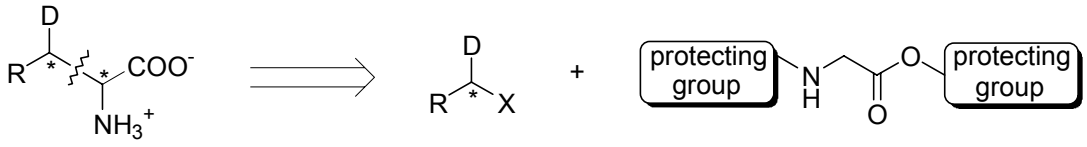

Figure 2.4 Retrosynthesis of chirally β-deuterated α-amino acids by alkylation of a glycine equivalent. *denotes chiral center

This methodology has several features that make it an attractive approach to these materials. The availability of labeled glycine in multiple isotopomeric forms allows for the incorporation of different isotope labels into the final product that may be beneficial to certain NMR experiments. In addition, the strategy is versatile, allowing synthetic access to all stereoisomers at the α- and β-carbons by varying the chirality of the protecting groups and electrophile. Finally, the method should be general enough to allow for the synthesis of other β-methylene unit containing amino acids.

2.3.2 Stereoselectivity considerations

2.3.2.1 Enolate conformation

As demonstrated by McIntosh and co-workers, *N*-benzoyl glycinate (hippurate) esters undergo C-alkylation stereoselectively when esterifed with the appropriate chiral alcohol.[75-77] With (-)-8-phenylmenthol serving as the chiral discriminator, formation of the C2-C3 bond proceeds with stereoselectivity exceeding 90% de to give the L-amino ester derivative.[77] The predictive model proposed for the induction of asymmetry is based on both the sterics of the auxiliary and stereoelectronic effects of the chelated enolate species (Figure 2.5).[76,77]

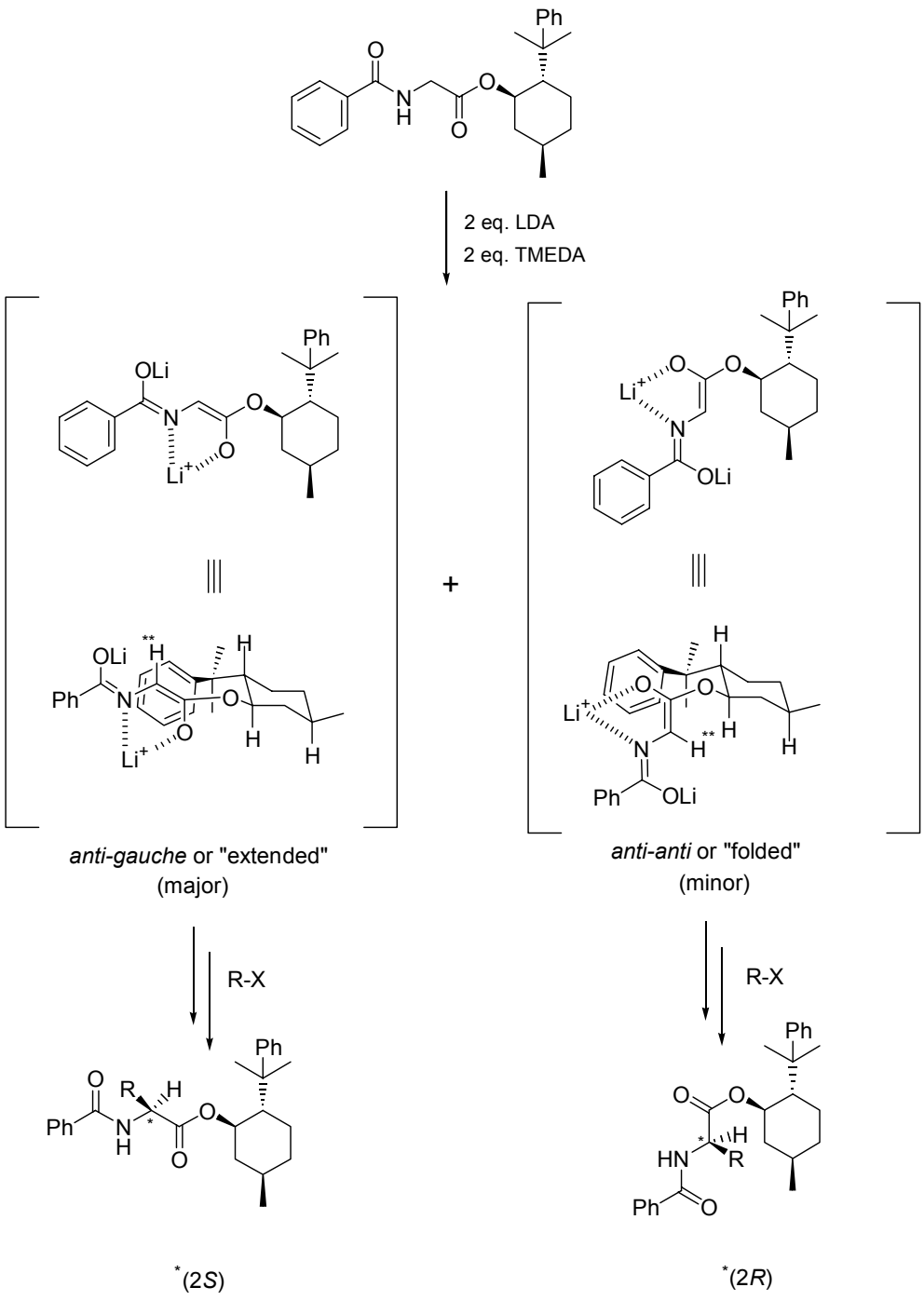

Figure 2.5 Model of stereoselectivity proposed for the alkylation of the lithium enolate derived from (-)-8-phenylmenthylhippurate.[73,76,77] **denotes position of α-methyl group in alanine derivatives.[73]

The anomeric effect predicts the preferred conformation of acetals and dialkoxycarbenium ions to be *anti-gauche* as opposed to *anti-anti* which sterics alone would predict.[78] In this preferred conformation, the repulsion between the lone pairs of electrons on the oxygen atoms is minimized. In the (-)-8-phenylmenthylhippurate system, the cyclohexane ring is constrained to the all-equatorial form which places the substituents in the preferred equatorial conformation, and a 5-member cyclic coordination between the lithium cation, the enolate oxygen atom, and the nitrogen atom is present to give the *trans* enolate derived from the benzamide portion of the molecule.[76] The *anti-gauche* conformation of the enolate derived from the ester predicts the stereochemical outcome of the major product, whereas the *anti-anti* conformation predicts the minor product.[76]

2.3.2.2 Sterics

Work by Berkowitz with related systems also suggests a similar model. However, steric hinderance is advanced as the controlling factor in the observed stereoselectivity.[73] In that work, the authors were alkylating dianions derived from protected alanine equivalents with high diastereoselectivity, and their model for chiral induction was based on “folded” and “extended” conformations of the enolates.[73] In the “extended” conformation, the α-methyl group that would be present in the alanine equivalent would be arranged to minimize any unfavorable steric interactions. However, in the “folded” conformation, the interaction between the α-methyl group and the axial carbinol proton would result in an unfavorable steric interaction (Figure 2.5).

2.3.2.3 π-Stacking

Another principle governing the alkylation model is that of π-π stacking interactions in the chiral enolate.[79] The phrase "π-stacking" refers to the spatial arrangement of multiple bonds, typically carbon-oxygen bonds or carbon-carbon bonds, parallel to and approximately 3.5 Å over an aromatic ring (Figure 2.6).[79]

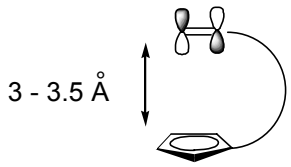

Figure 2.6 Alkene–arene π-stacking.

The exact nature of the π-stacking effect remains unclear and is still an ongoing area of research in organic and computational chemistry. Researchers are studying the contribution of charge transfer interactions as well as simple van der Waals forces to this phenomenon. Work by McIntosh has established that π-electrons do impact the stereochemical course of alkylation reactions using enolates derived from chiral hippurate esters.[75] In this work, higher diastereoselectivities were observed in the alkylation reaction when the π-electron nature of the system was increased, presumably due to greater π-π stacking interactions contributing to a more rigid intermediate.

2.3.3 Synthetic versatility

Using the same reaction conditions described by McIntosh[77], the C-alkylation of the diastereomeric lithium enolate derived from ^{15}N-labeled 8-phenylmenthylhippurate with a chirally deuterated benzylic electrophile should yield a doubly labeled phenylalanine derivative (Figure 2.7). The use of the enantiomeric 8-phenylmenthyl

alcohols allows for the generation of both α-position epimers while the chirality of the electrophile controls synthetic access to both β-position epimers. However, incorporating and maintaining chirality at the sensitive benzylic position throughout the synthesis poses a significant challenge. Therefore, the synthesis of the chirally deuterated electrophile and its properties in the ensuing alkylation chemistry are of paramount interest.

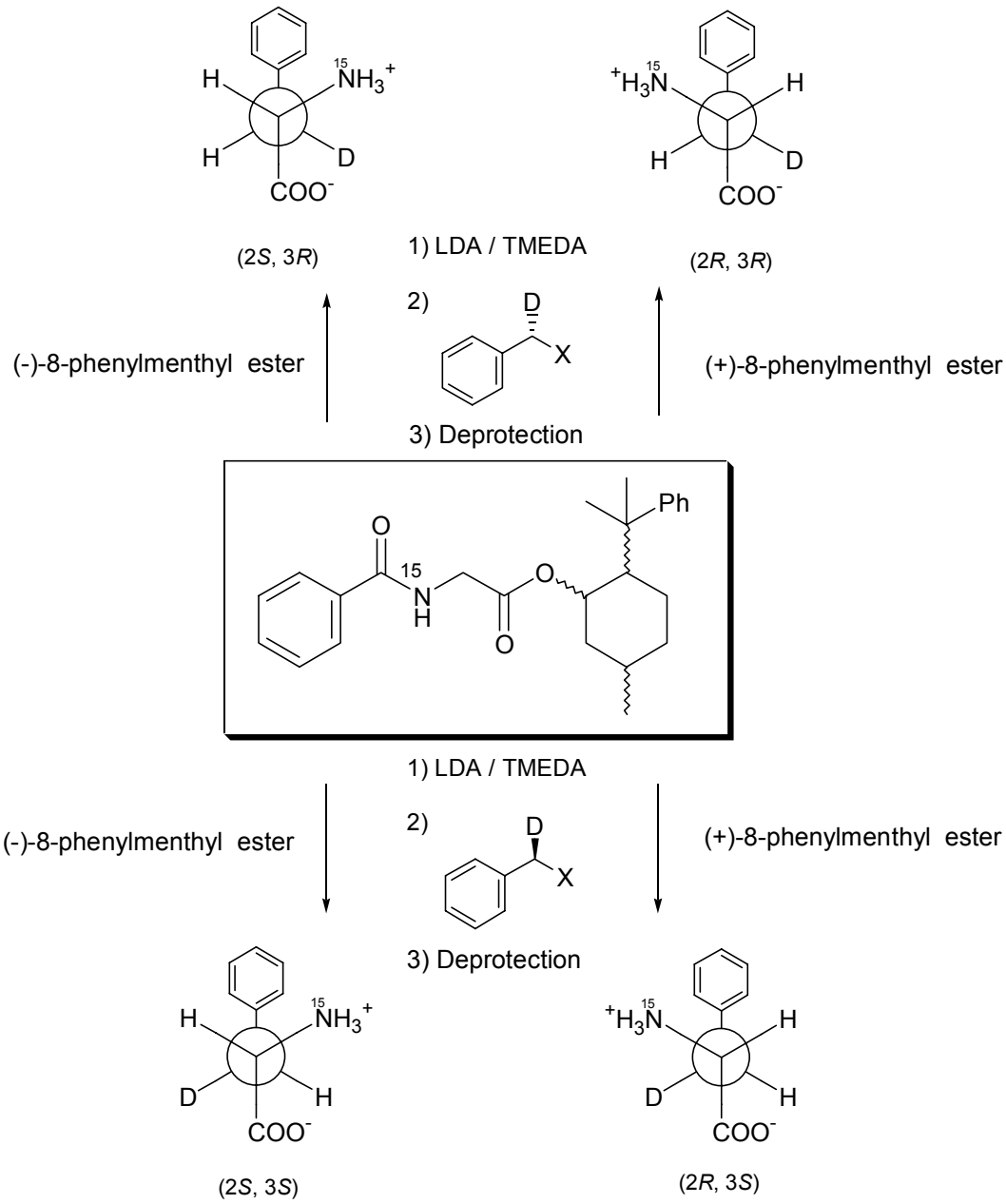

Figure 2.7 Synthesis of stereoselectively β-deuterated ^{15}N-labeled phenylalanines using 8-phenylmenthylhippurates as chiral glycine equivalents.

2.3.4 Deuterium incorporation

A key aspect to this strategy is the synthesis of deuterated compounds. The incorporation of deuterium into the synthetic scheme needed to be efficient and cost-effective. In addition, the method selected needed to be adaptable to large scale syntheses. It was decided that using the *umpolung* chemistry of the morpholineacetonitrile derivatives of aldehydes would be a method that satisfies these criteria (Figure 2.8).[80] Using this strategy, the source of deuterium would be deuterium oxide, which is relatively inexpensive and available in isotopically pure forms. In addition, the morpholineacetonitrile intermediates tend to be crystalline compounds which would facilitate purification.

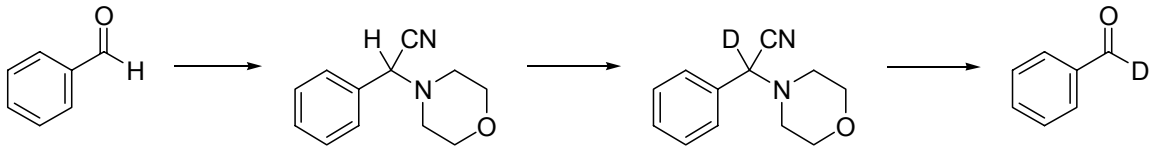

Figure 2.8 *Umpolung* method of proton-deuteron exchange.

2.3.5 Introduction of asymmetry

Midland and co-workers first demonstrated that (*R*)-Alpine Borane® is a highly effective asymmetric reducing agent for aldehydes.[81] In that paper, the authors described the reduction of benzaldehyde-α-*d* with the chiral borane reagent to give (*S*)-(+)-benzyl alcohol-α-*d* with very high enantioselectivity. The reagent is prepared from the hydroboration of (+)-α-pinene with 9-borabicyclo[3.3.1]nonane (9-BBN) (Figure 2.9).

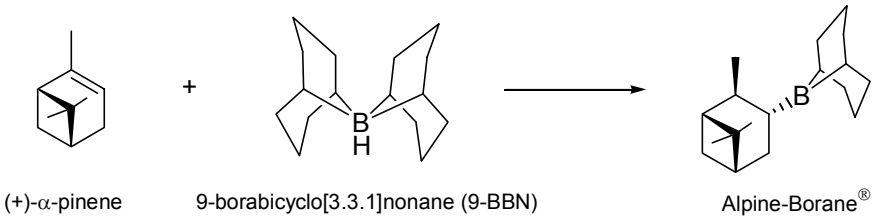

Figure 2.9 Hydroboration of (+)-α-pinene with 9-BBN to give (*R*)-Alpine Borane®

The basis for the chiral discrimination of the reagent resides in the high optical purity of (+)-α-pinene, which provides an asymmetric environment, and the steric bulk provided by the 9-BBN portion of the molecule. As a result, very high stereoselectivities can be observed in the reduction reaction.

In subsequent studies of the reagent, the model of stereochemical induction was rigorously established.[82] In that paper, the authors used a deuterated form of the reagent to further confirm that the organoborane reagent prepared using (+)-α-pinene led to (*S*)-(+)-benzyl-α-*d* alcohol in the reduction of benzaldehyde (Figure 2.10). Reagent based on (-)-α-pinene would give the enantiomeric alcohol.

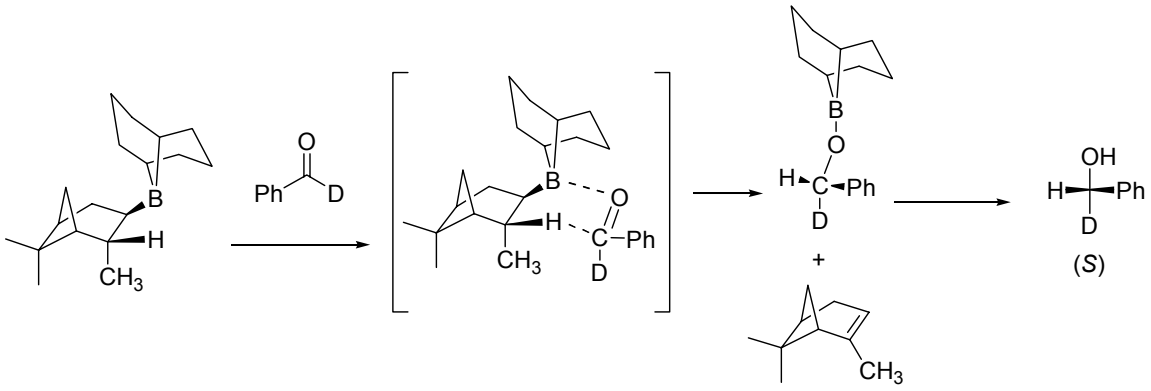

Figure 2.10 Model of asymmetric induction of (*R*)-Alpine Borane®.[82]

2.4 Methods Development

Initial efforts were focused on the synthesis of unlabeled compounds that were needed for model reactions. These included model alkylation substrates, HPLC reference compounds, and the chiral auxiliary. The goal was to develop an efficient synthesis of the amino acid derivatives with good α-position stereoselectivity, and then use an optimal deuterated electrophile to introduce diastereoselectivity at the β-position. Another important consideration was obtaining optimal yields for reactions involving isotope labeled materials.

2.4.1 Synthesis of ethyl hippurate

Ethyl hippurate was chosen as a simple achiral model for the alkylation substrate; the synthesis is depicted in Scheme 2.1. The first step was a benzoylation reaction first described by Schotten and Baumann[83,84] and adapted by Steiger.[85] The esterification of the carboxylic acid was accomplished using sulfuric acid catalyzed conditions in ethanol.

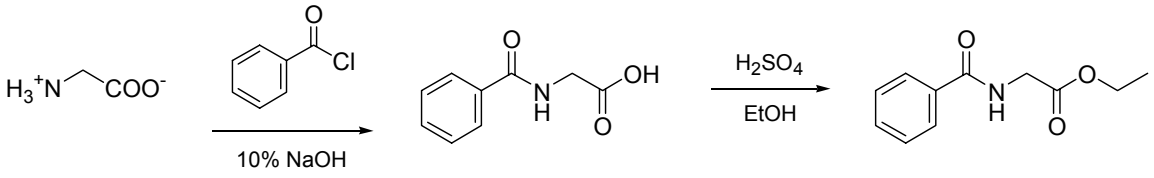

Scheme 2.1 Synthesis of ethyl hippurate.

2.4.2 Synthesis of (-)-8-phenylmenthol

The source of asymmetric induction at the α-carbon in the amino acid derivatives originates from using (-)-8-phenylmenthol as a chiral auxiliary.[86] The synthesis of the chiral alcohol is shown in Scheme 2.2.[87] The first step in the synthesis was a conjugate

addition of phenyl Grignard reagent to (*R*)-(+)-pulegone, the resulting mixture of ketones was then epimerized in base to give an equilibrated mixture of *trans*/*cis* diastereomers in the approximate ratio of 85:15. Next, the ketones were reduced to the corresponding alcohols using sodium metal and isopropanol in toluene followed by derivatization to the chloroacetate esters. The desired stereoisomer was then obtained by fractional crystallization from ethanol, which was hydrolyzed in basic conditions to give the desired product.

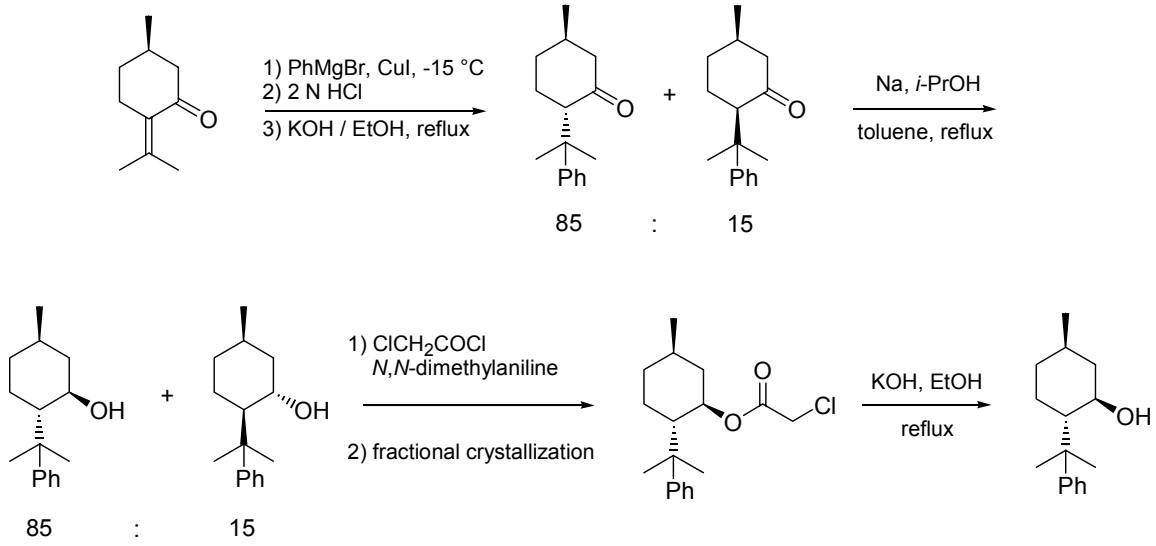

Scheme 2.2 Synthesis of (-)-8-phenylmenthol.[87]

2.4.3 Synthesis of (-)-8-phenylmenthylhippurate (1)

The synthesis of (-)-8-phenylmenthylhippurate **(1)** is shown in Scheme 2.3. The esterification reaction was carried out under Dean-Stark conditions to facilitate removal of water from the reaction.

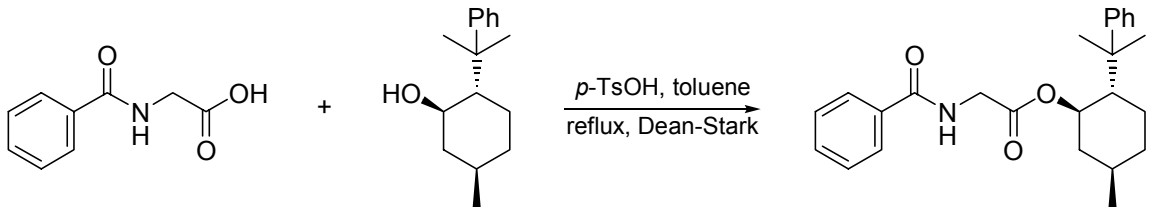

1

Scheme 2.3 Synthesis of (-)-8-phenylmenthylhippurate (**1**).

2.4.4 Synthesis of phenylalanine reference samples for stereochemical analyses

Standard samples were needed as HPLC and NMR references to accurately assess the stereochemical outcome of the alkylation reactions. Compounds were prepared by derivatizing commercially available L-phenylalanine and DL-phenylalanine as the benzamides and (-)-8-phenylmenthyl esters as previously described. These reference samples provided clear indicators of stereochemistry. Shown in Figure 2.11 is the ^{1}H NMR spectrum recorded at 400 MHz for (2*S*)-*N*-benzoyl-phenylalanine-(-)-8-phenylmenthyl ester.

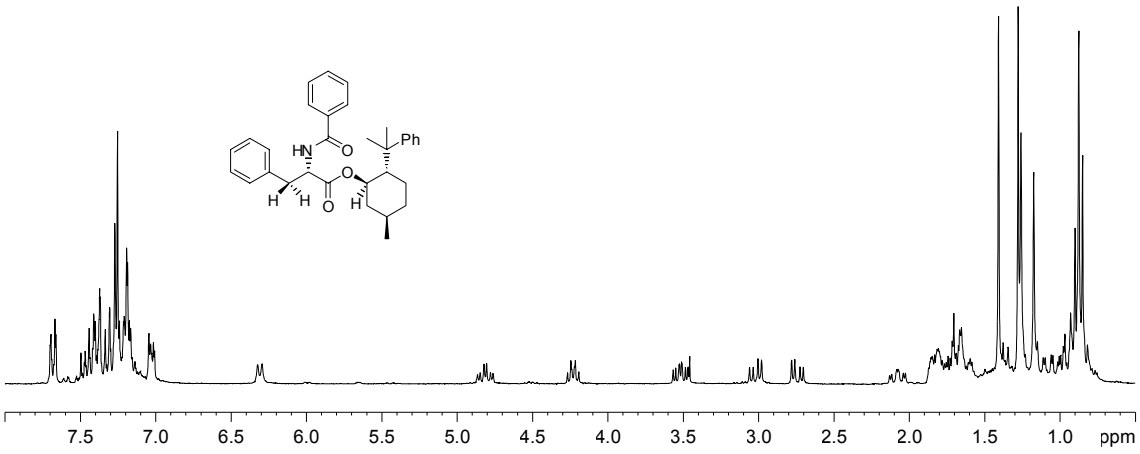

Figure 2.11 ^{1}H NMR spectrum (400 MHz) of (2*S*)-*N*-benzoyl-phenylalanine-(-)-8-phenylmenthyl ester.

This compound would represent the major product from the alkylation reaction. The doublet at approximately 6.3 ppm is from the amide proton, and the pair of doublets of doublets centered at approximately 2.9 ppm are from the benzylic protons. In addition, the resonances from the α-proton and carbinol proton are clearly visible at 4.2 ppm and 4.8 ppm respectively. The doublet of triplets at 3.5 ppm is from unreacted (-)-8-phenylmenthol that was present in the reaction mixture. Resonances from the chiral alcohol also contribute to the complex appearance of the aliphatic region of the spectrum.

Shown in Figure 2.12 is the ^{1}H NMR spectrum recorded at 400 MHz for the (2*R*)-epimer.

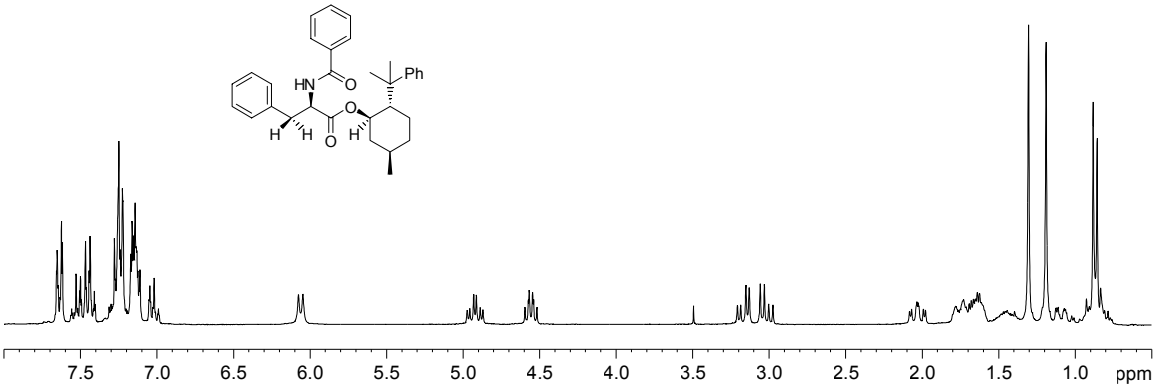

Figure 2.12 ^{1}H NMR spectrum (400 MHz) of (2*R*)-*N*-benzoyl-phenylalanine-(-)-8-phenylmenthyl ester.

This material was obtained from fractional crystallization of the racemic mixture of the DL-phenylalanine derivative. This compound would represent the minor product from the alkylation reaction. This material has similar proton resonances as the (2S)-epimer, however, the chemical shifts of the amide, alpha-, and benzylic protons are distinct and

thus provide diagnostic indicators of stereochemistry at both the α- and β-carbons. In addition to NMR spectroscopy, HPLC was also used to analyze stereochemistry. The (2*R*) diastereomer had a retention time of approximately 16 minutes in the separation conditions employed and the (2S) epimer had a retention time of 21 minutes.

2.4.5 Evaluating electrophile reactivity in the alkylation reaction

The goal of the model alkylation reactions was to find an optimal benzylic electrophile that would alkylate the protected glycine template in high chemical yield, and when stereoselectively deuterated, would undergo the alkylation reaction in a S_N2 type reaction resulting in a high stereoselectivity of the benzylic position in the alkylated product. Initially, several electrophiles were tested for the ability to undergo the alkylation reaction with the protected templates.

2.4.5.1 Benzyl sulfonate esters

Benzyl tosylate served as the starting point for the electrophile study. It was believed that the tosylate offered sufficient reactivity necessary for the alkylation chemistry and the advantage that for the chirally deuterated synthesis, the benzylic center would not be involved in the conversion to the electrophilic tosylate, thereby minimizing any possible racemization of the sensitive benzylic position. Benzyl tosylate was prepared from benzyl alcohol via sulfonate ester formation and the reactivity was evaluated in the alkylation reaction. It was found that benzyl tosylate did alkylate ethyl hippurate with an acceptable yield. However, it did not undergo the reaction when the bulky (-)-8-phenylmenthyl ester **1** derivative was used. It is reasonable to argue that the increased sterics of the chiral system combined with the bulky nature of the electrophile impedes the progress of the reaction. In addition, benzyl tosylate was found to be

somewhat unstable and difficult to purify. Considering these issues for the formation of what would have to ultimately be a stereoselectively detuerated material, it was decided to investigate other potential electrophiles rather than optimize this synthesis.

The other sulfonate ester that was investigated as a potential electrophile was benzyl mesylate, which was synthesized from benzyl alcohol using mesyl chloride and 4-dimethylaminopyridine (DMAP) catalyzed conditions. The mesylation reaction of benzyl alcohol was high yielding, and the product was easily purified using silica gel chromatography. As an electrophile, benzyl mesylate alkyated **1** in good chemical yield and with 92% de to give the L-isomer as determined by ^{1}H NMR spectroscopy and HPLC.

2.4.5.2 Benzyl halides

Benzyl bromide was the first halide studied as a potential electrophile. It was found to have the greatest reactivity in the alkylation reaction of any of the electrophiles investigated. In addition, the alkylation reaction proceeded with excellent stereoselectivity, 92% de at the 2-position. However, due to the high reactivity, care had to be taken during isolation to avoid decomposition.

Benzyl chloride possessed similar properties as that of the bromide. Although less reactive than benzyl bromide, the alkylation reaction proceeded with equally good stereoselectivity at the 2-position. In addition, benzyl chloride appeared to be moderately more stable than the bromide due to its attenuated reactivity.

Data from these preliminary studies indicated that both of the benzyl halides and benzyl mesylate were candidates for further study as enantioselectively deuterated electrophiles. The data from the alkylation reactions suggested that these electrophiles could alkylate the chiral lithium enolate generated from **1** to give a protected

phenylalanine derivative with good stereoselectivity and good chemical yield. It remained to be determined if a chirally deuterated electrophile could be used in the alkylation reaction to give a chirally β-deuterated product as well.

2.5 Synthesis of Deuterated Electrophiles

Chirally deuterated electrophiles are one of the keys to this synthetic strategy. A method is needed that yields products of high deuterium incorporation and optical purity. Two different synthetic routes have been investigated for deuterium incorporation, while the asymmetric reduction of a deuterated aldehyde with a chiral organoborane reagent is the method of choice for the introduction of chirality.

2.5.1 Synthesis of (*S*)-(+)-benzyl-α-*d*-alcohol (2)

Scheme 2.4 depicts the synthesis of (*S*)-(+)-benzyl-α-*d*-alcohol **(2)**, which served as the precursor for deuterated electrophile synthesis. This strategy, which was based on the generation of a deuterated aldehyde[80] and the subsequent asymmetric reduction with a chiral borane reagent[81], was the method of choice for several reasons. The chemistry proceeded exceptionally well on a large scale with excellent deuterium incorporation and represented a simple way to obtain these materials in a cost effective manner. In addition, the morpholineacetonitrile intermediates were crystalline materials which facilitated purification of large amounts of material by recrystallization.

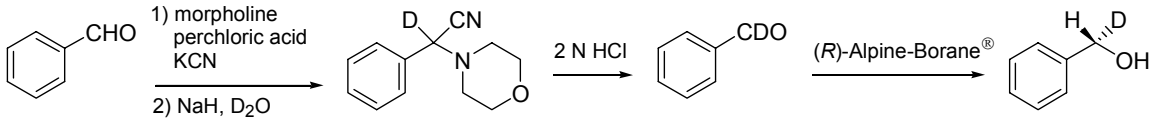

2

Scheme 2.4 Synthesis of (*S*)-(+)-benzyl alcohol-α-*d* (**2**)..

Treating benzaldehyde with morpholine perchlorate and potassium cyanide gave the morpholineacetonitrile derivative in excellent yield. This intermediate could easily be prepared on a one-hundred gram scale. Proton-deuteron exchange was accomplished by reaction with sodium hydride and deuterium oxide to yield the deuterated analog essentially quantitatively with excellent deuterium incorporation as determined by ^{1}H NMR spectroscopy. Acid hydrolysis gave deuterated benzaldehyde, which was then reduced asymmetrically with (*R*)-Alpine Borane®, to yield **2** as the major product with approximately 96% ee as determined by ^{1}H NMR analysis of the (-)-camphanate ester derivative (Figure 2.13).[88]

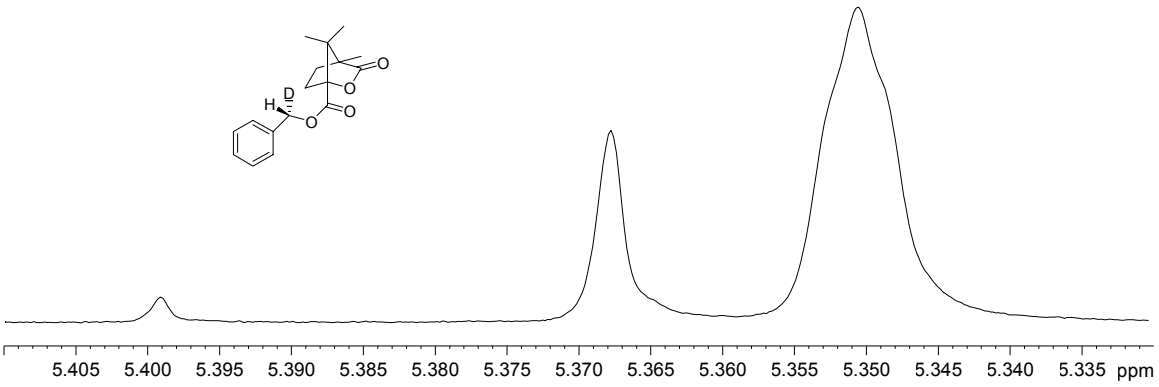

Figure 2.13 Benzylic region of ^{1}H NMR spectrum (800 MHz) of the (-)-camphanate ester[88] of **2**.

The broadened triplet at approximately 5.35 ppm is the benzylic proton resonance from the ester of **2** and the signal at approximately 5.4 ppm is from the ester of the (*R*)-(-)-benzyl alcohol-α-*d* (minor product). The resonance at approximately 5.37 ppm is from the benzylic protons from the ester that contains residual di-protio benzyl alcohol (approximately 10% after hydrolysis).

Another strategy that was initially investigated as a route to these deuterated materials is shown in Scheme 2.5. This method relied on the reduction of the ethyl ester moiety with lithium aluminum deuteride to give the di-deuterio benzylic alcohol, which was then oxidized with pyridinium chlorochromate to yield the deuterated benzaldehyde. This aldehyde was then treated in a similar fashion as described above to give **2**. This approach was generally lower yielding and led to products with lower deuterium incorporation due to the metal hydride reagent not being available in an isotopically pure form. In addition, this strategy would not be cost effective on a large scale when compared to the morpholineacetonitrile method.

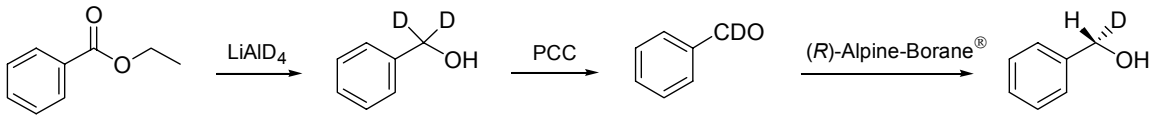

2

Scheme 2.5 Alternative deuterium incorporation strategy.

2.5.2 Functional group interconversion of labeled benzylic alcohol

It was believed that the bromide would be the preferred halide as an electrophile due to its apparent greater reactivity in the alkylation reaction. This increased reactivity would possibly result in a higher chemical yield of the amino acid derivative, and

perhaps, enhanced stereoselectivity at C3 in the benzylic position in the alkylated product. However, use of any of the halides for the alkylation reaction would require two formal inversions of configuration at the benzylic center, one for the functional group interconversion from **2** and one for the alkylation reaction. The use of the mesylate would have the apparent advantage of only requiring one formal inversion during the process. However, the impact of its attenuated reactivity in the alkylation reaction, as compared to the bromide, on the benzylic position stereochemistry in the product was unknown. Deuterated benzylic electrophiles were prepared from **2** by halogenation reactions known to proceed with inversion of configuration[89-91] and the mesylate was synthesized by methyl sulfonate ester formation as previously described. The labeled electrophiles were used to alkylate **1** and the products were analyzed by ^{1}H NMR spectroscopy to investigate stereochemistry at C2 and C3.

2.5.2.1 Halogenation reactions using CX_4/PPh_3

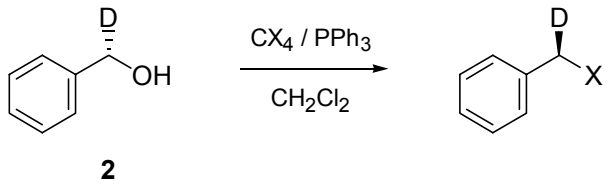

2

Figure 2.14 Functional group interconversion of **2** using carbon tetrahalide and triphenylphosphine.[89]

The chlorination of alcohols using carbon tetrachloride and triphenylphosphine was first described by Downie and co-workers (Figure 2.14).[89] The authors were searching for mild conditions for the preparation of halo-sugars and halo-terpenes using phosphorus containing reagents. In the course of their work, they found that the use of

triphenylphosphine and carbon tetrachloride rapidly effected the chlorination of alcohols in mild, essentially neutral conditions. The authors speculated on the nature of the mechanism of the reaction, but no implications of the stereochemical course of the transformation were described. In later work by Weiss and Snyder, many of the mechanistic details were investigated including the stereochemical aspects of the reaction.[92,93] It was found that in most cases the chlorination reaction proceeds with essentially complete inversion of configuration at the reaction center. To explain the observed stereoselectivity, the authors proposed the reaction proceeded through an intermediate such as the one shown in Figure 2.15. However, the authors admit that much more work needed to be done before a rigorous model could be established.

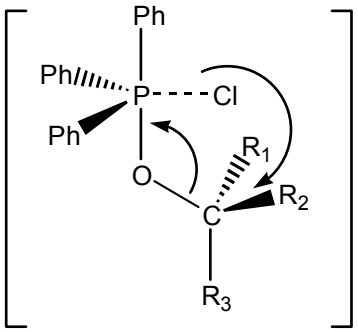

Figure 2.15 Proposed intermediate for CCl_4/PPh_3 chlorination leading to inversion of configuration.[93]

Since that early work, much work has been done to further study these reaction conditions. Today, these conditions are commonly employed in halogenation and dehydration reactions, as well as reactions for constructing phosphorous-nitrogen linkages.[94] It is generally agreed that for halogenation of alcohols these conditions give inversion of configuration in most cases and the reaction proceeds through a tight ion-pair mechanism as depicted in Figure 2.16.[94]

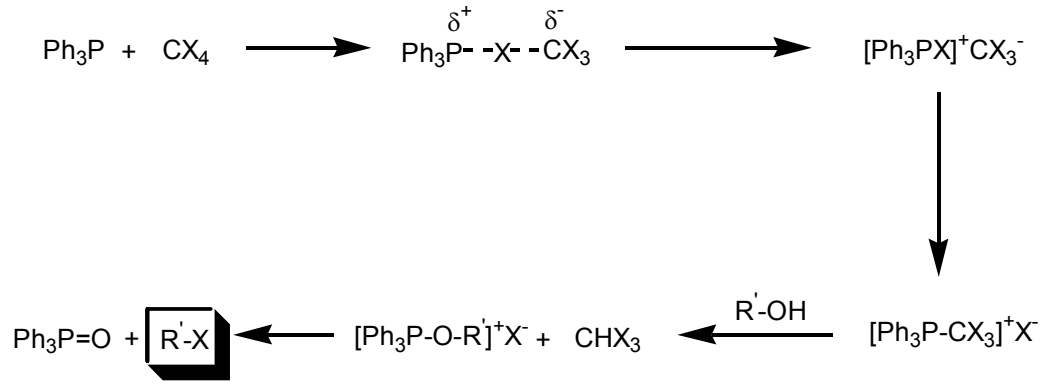

Figure 2.16 Proposed ion pair mechanism of CX_4/PPh_3 halogenation.[94]

2.5.2.2 Halogenation reactions using modified Mitsunobu conditions

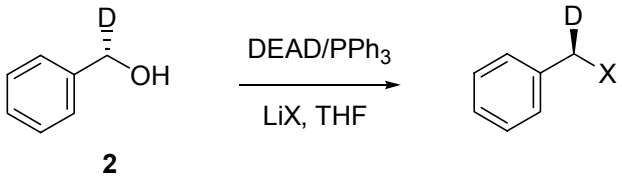

2

Figure 2.17 Functional group interconversion of **2** using the modified Mitsunobu conditions.[91]

The Mitsunobu reaction has been widely utilized in organic synthesis, usually as a means of inverting stereochemistry of secondary alcohol derivatives.[95,96] Manna and Falck have reported a modified version of the reaction to prepare alkyl halides and cyanides from the corresponding alcohols (Figure 2.17).[91] In that paper, the authors report that the halogenation of 3β-cholestanol to the analogous 3α-halides proceeds with complete stereochemical inversion. The general mechanism of the Mitsunobu reaction as it applies to this "modified" version is depicted in Figure 2.18.

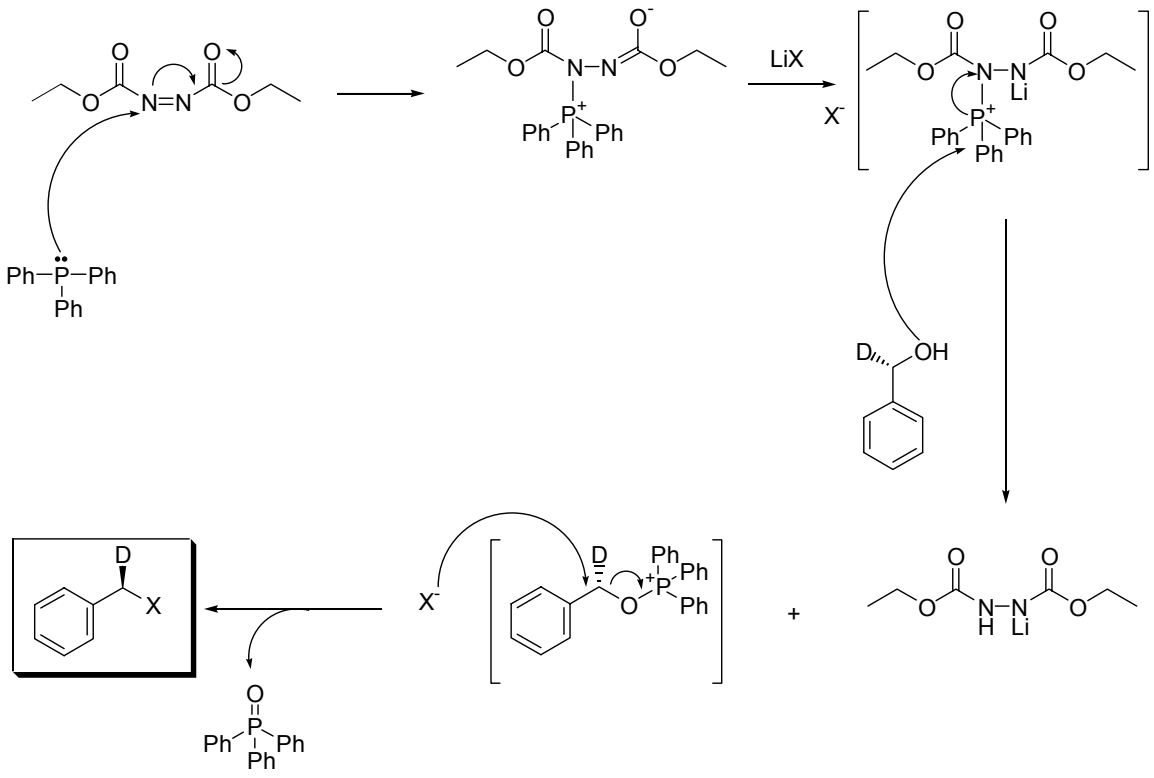

Figure 2.18 General mechanism of the modified Mitsunobu reaction.[91,96]

It is generally accepted that triphenylphosphine undgergoes an addition reaction with diethyl azidodicarboxylate (DEAD) to form a quaternary phosphonium salt. This salt then reacts with a lithium halide to form the species which reacts with the alcohol. The addition of the alcohol forms the alkoxyphosphonium salt that undergoes a displacement reaction with the halide counterion generating the alkyl halide and triphenylphosphine oxide as a byproduct.

2.5.2.3 Methane sulfonate ester formation conditions

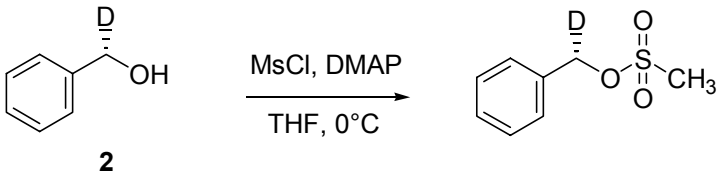

2

Figure 2.19 Functional group interconversion of **2** using DMAP catalyzed mesylation conditions.

The mesylation conditions that were employed utilized DMAP catalysis. Formation of the mesylate from the chiral alcohol should not involve the chiral carbon center (Figure 2.19).

2.6 Evaluation of Deuterated Electrophiles

The deuterated electrophiles **(3a-e)** were synthesized using the reaction conditions described above and then used to alkylate **1** to determine stereoselectivity at the β-carbon in the amino ester derivative. The results are summarized in Table 2.1 and Figure 2.20.

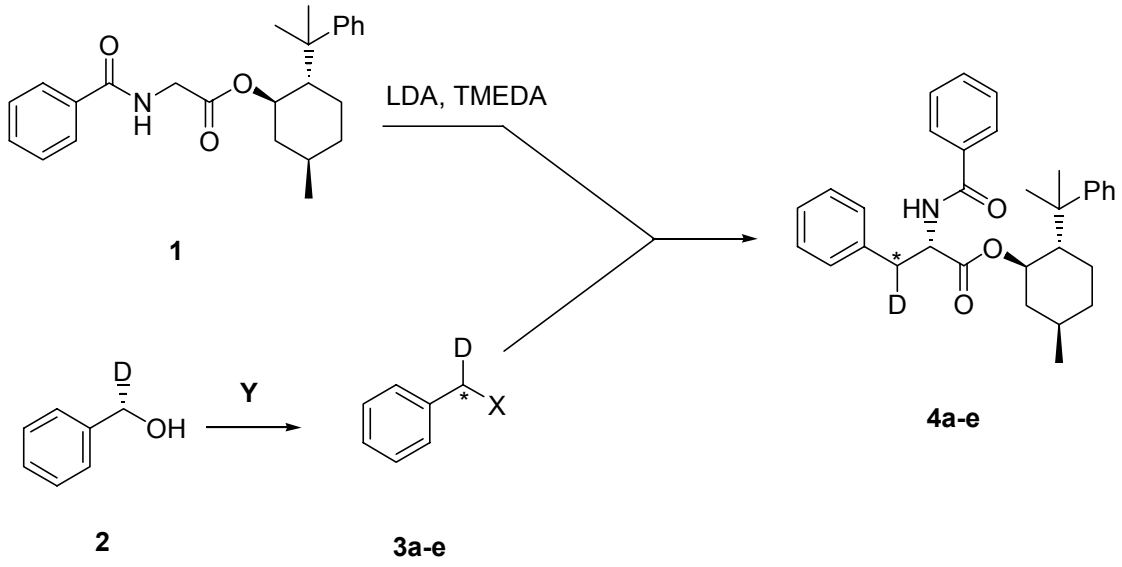

1 **2** **3a-e** **4a-e**

E^+	**Y**	X	CONFIGURATION OF **3a-e**	ALKYLATION RXN TEMP.	PRODUCT	(3*R*):(3*S*) IN **4a-e**
3a	Ph_3P/CBr_4	Br	(*R*)	- 78 °C	**4a**	1:1
3b	Mitsunobu	Br	(*R*)	- 78 °C	**4b**	1:1
3c	Ph_3P/CCl_4	Cl	(*R*)	21 °C	**4c**	2:3
3d	Mitsunobu	Cl	(*R*)	- 15 °C	**4d**	1:9
3e	DMAP/MsCl/NEt_3	OMs	(*S*)	- 42 °C	**4e**	9:1

Table 2.1 Evaluation of deuterated electrophiles

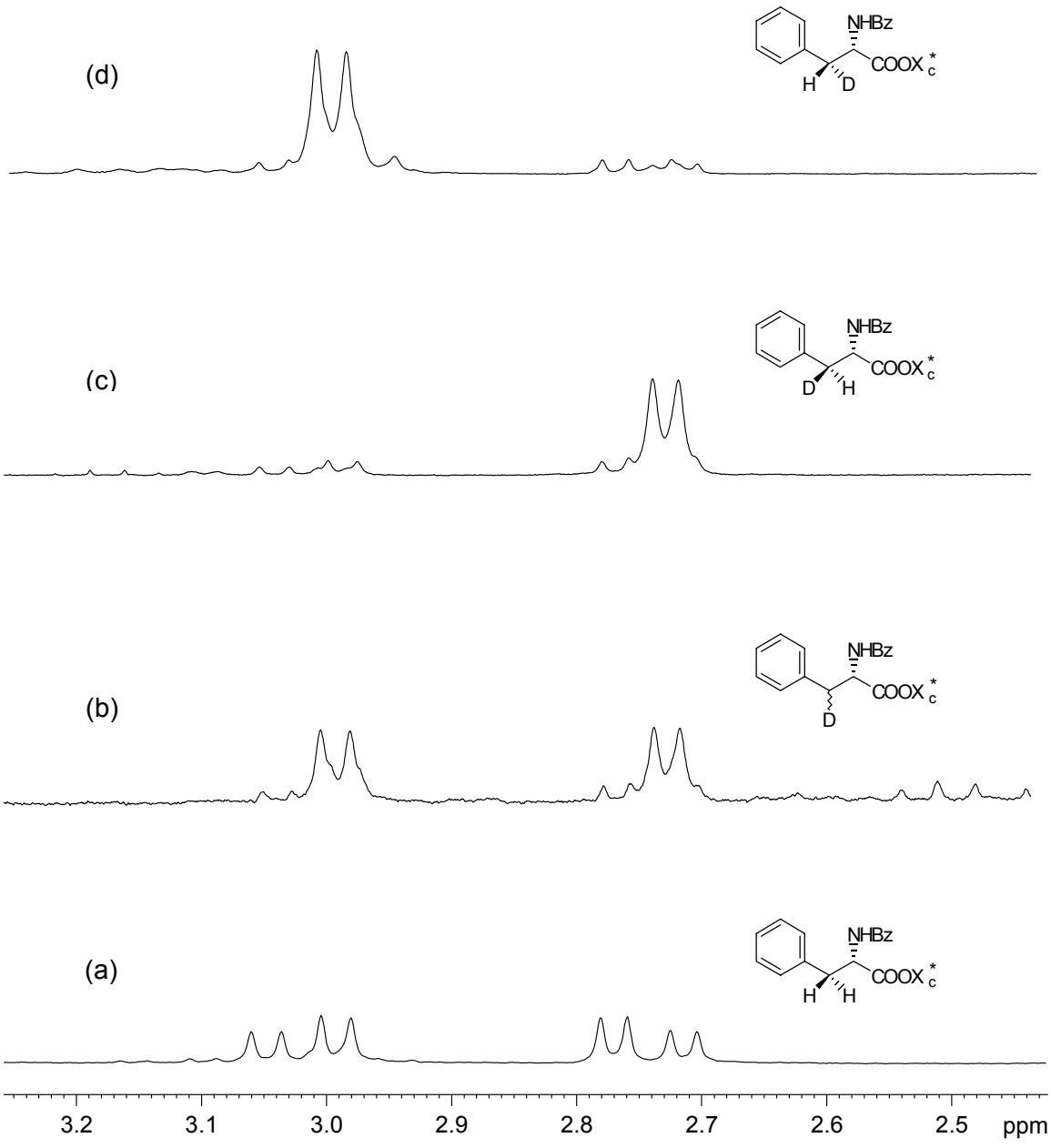

Figure 2.20 Benzylic region of ^{1}H NMR (400 MHz) spectra of alkylation products from electrophile evaluation studies, X_c* = (-)-8-phenylmenthol. (a) undeuterated compound from authentic L-phenylalanine reference sample. (b) representative spectrum of alkylation products **4a/b** from reactions employing deuterated benzyl bromides **3a/b**, showing complete racemization at benzylic center. (c) alkylation product **4d** from reaction employing deuterated benzyl chloride **3d**, showing an approximate 3*R*/3*S* of 1:9. (d) alkylation product **4e** from reaction employing deuterated benzyl mesylate **3e**, showing an approximate 3*R*/3*S* of 9:1.

2.6.1 (*R*)-Benzyl bromides-α-*d* (3a/b)

The first deuterated electrophile investigated in the alkylation reaction was (*R*)-benzyl bromide-α-*d* **3a** prepared using carbon tetrabromide and triphenylphosphine.[90] Unfortunately, the alkylation product **4a** showed a 1:1 ratio of stereoisomers at the benzylic position as assessed by ^{1}H NMR spectroscopy (Table 2.1 and Figure 2.20b). Similarly, the labeled bromide **3b** prepared using the modified Mitsunobu conditions, resulted in a similar lack of selectivity in the alkylated product **4b** (Table 2.1 and Figure 2.20b).

2.6.2 (*R*)-Benzyl chlorides-α-*d* (3c/d)

Alkylation product **4c,** which was obtained from using the labeled chloride prepared from using triphenylphosphine and carbon tetrachloride, showed a slight stereoselectivity of approximately 2:3 for 3*R*/3*S*. In this particular experimental run, no product was observed until the reaction mixture was allowed to warm to room temperature, therefore, the reaction was maintained at room temperature before quenching at ambient temperature. Investigating other chlorination conditions to perhaps enhance this modest selectivity, the modified Mitsunobu conditions were employed to generate chloride **3d**, which resulted in an approximate selectivity of 9:1 in favor of the (3*S*)-epimer of **4d** when used to alkylate **1** (Table 2.1 and Figure 2.20c). During this experimental run, product formation was observed at -15 °C and therefore the reaction was maintained and quenched at this temperature.

2.6.3 (*S*)-(+)-Benzyl mesylate-α-*d* (3e)

It was expected that the mesylate **3e** would yield the (3*R*)-epimer of the alkylated product as the major product since the mesylate was of opposite configuration from the chloride. Indeed, **4e**, showed a similar degree of selectivity (9:1), but in favor of the (3*R*)-epimer (Table 2.1 and Figure 2.20d).

2.6.4 Summary of deuterated electrophile studies

These results were very encouraging and demonstrated that a high degree of stereoselectivity could be introduced at the β-carbon while simultaneously constructing the C2-C3 bond to give the desired α-carbon stereoisomer. The racemization observed in the alkylation products **4a/b** synthesized from the bromides **3a/b** may be due to the inherent enhanced reactivity of the electrophile. It is possible that benzyl bromide was reactive enough to undergo bromide displacement reactions that ultimately resulted in racemization of the electrophile. The attenuated reactivity of the chlorides **3c/d** and mesylate **3e** may have been sufficient enough to minimize this racemization, which ultimately led to the observed stereoselectivity. Other researchers have also observed differences in the stereoselectivity of chlorination and bromination reactions when using the triphenylphosphine and carbon tetrahalide halogenation conditions to prepare halides of optically active alcohols.[97]

With regard to the observed difference in stereoselectivity between **4c** and **4d**, definitive comparisons of the stereoselectivity of the Mitsunobu and carbon tetrachloride/triphenylphosphine chlorination conditions can not be made based on this data alone due to the different reaction conditions. However, this data suggests that the temperature of the alkylation reaction plays an important role in determining stereoselectivity of the β-position. Based on these results, the mesylate **3e** was selected

as the electrophile for the synthesis of the doubly labeled material, however, these results clearly indicate that the labeled chloride could be used to generate the 3-position epimer.

2.6 Synthesis of (2*S*, 3*R*)-[3-^{2}H,^{15}N]-Phenylalanine (9)

Shown in Scheme 2.6 is the synthesis of ^{15}N-(-)-8-phenylmenthylhippurate **(7)** which served as one of the key starting materials for the synthesis of the labeled phenylalanine derivative. This material was obtained in high yield in two steps from commercially available ^{15}N-labeled glycine **(5)** which was greater than 98% isotopically pure.

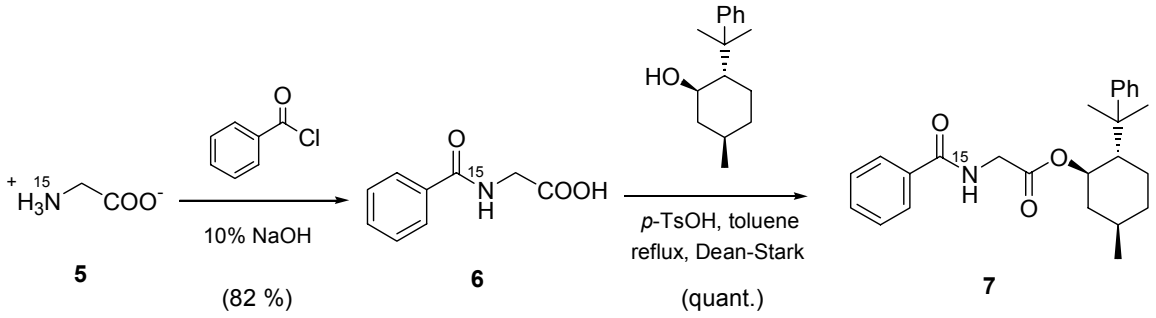

Scheme 2.6 Synthesis of ^{15}N-(-)-8-phenylmenthyhippurate **7**.

Shown in Scheme 2.7 are the remaining steps in the synthesis of the doubly labeled phenylalanine derivative **9**. Mesylate **3e** was obtained from **2** in 86% yield using DMAP catalyzed conditions. Treatment of **7** with 2 equivalents of LDA and TMEDA followed by the addition of **3e** yielded the doubly labeled alkylation product **8** in 74% chemical yield.

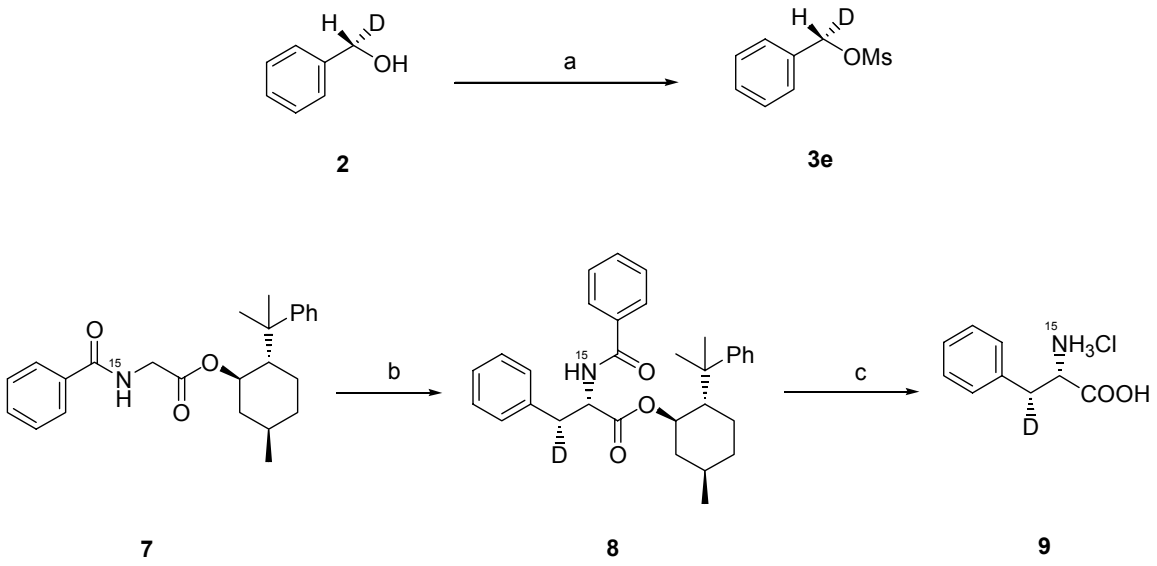

Scheme 2.7 Synthesis of **9**. (a) DMAP, MsCl, NEt_3, THF, 0°C, (86%); (b) i, 2 eq. LDA, 2 eq. TMEDA, THF, -78 °C; ii, 1.1 eq. **3e**, -42 °C, 12 h, (89%); (c) 6 N HCl, reflux in sealed bottle, 36 h, (86%).

Stereochemical analysis of **8** by ^{1}H NMR spectroscopy and HPLC suggested an approximate 90% de at C2 (Figures 2.21-2.23). In early model reactions with unlabeled compounds, the (2*R*)-epimer was obtained optically pure from the alkylation product mixture by crystallization from hexanes/ethyl acetate and was used as a standard for HPLC analyses. This fractional crystallization represents a way to obtain further enriched mixtures of the (2*S*)-epimer of **8**.

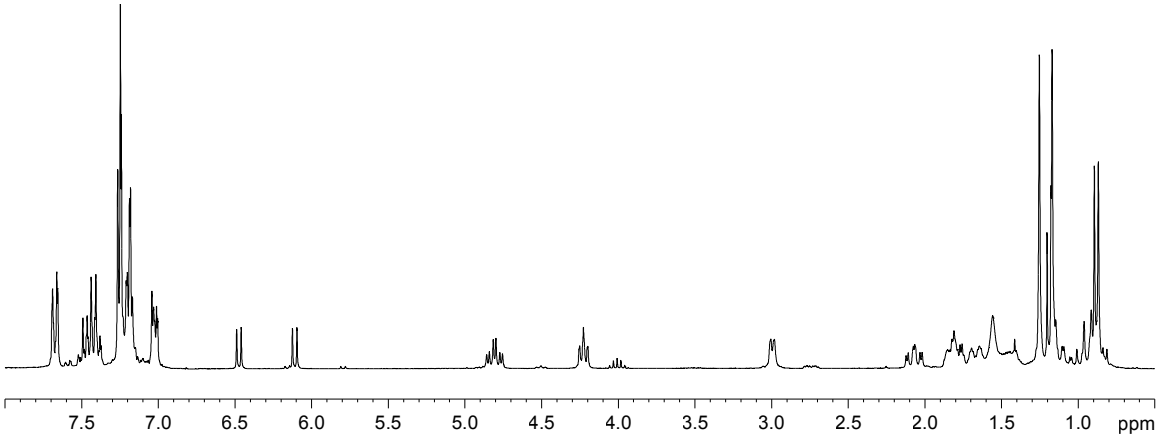

Figure 2.21 ^{1}H NMR spectrum (400 MHz) of **8**.

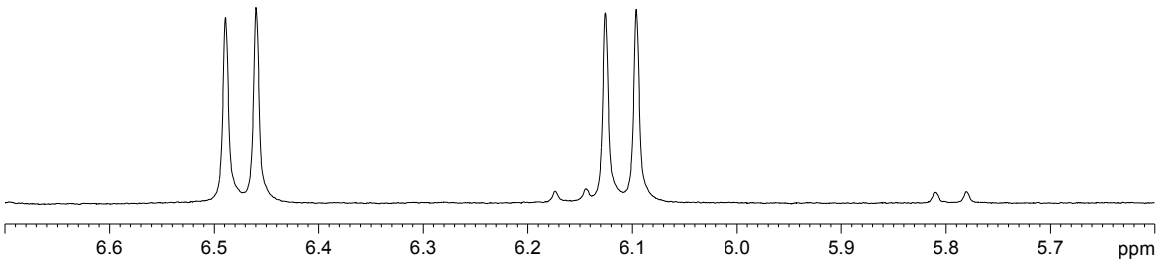

Figure 2.22 Amide region of ^{1}H NMR spectrum (400 MHz) of **8** showing the ratio of (2*S*) to (2*R*) epimers to be approximately 95:5. Also note the 1-bond ^{15}N-^{1}H coupling constant (91 Hz) and the 3-bond ^{15}N-^{1}H$_{\alpha}$ coupling constant (7.3 Hz) are apparent.

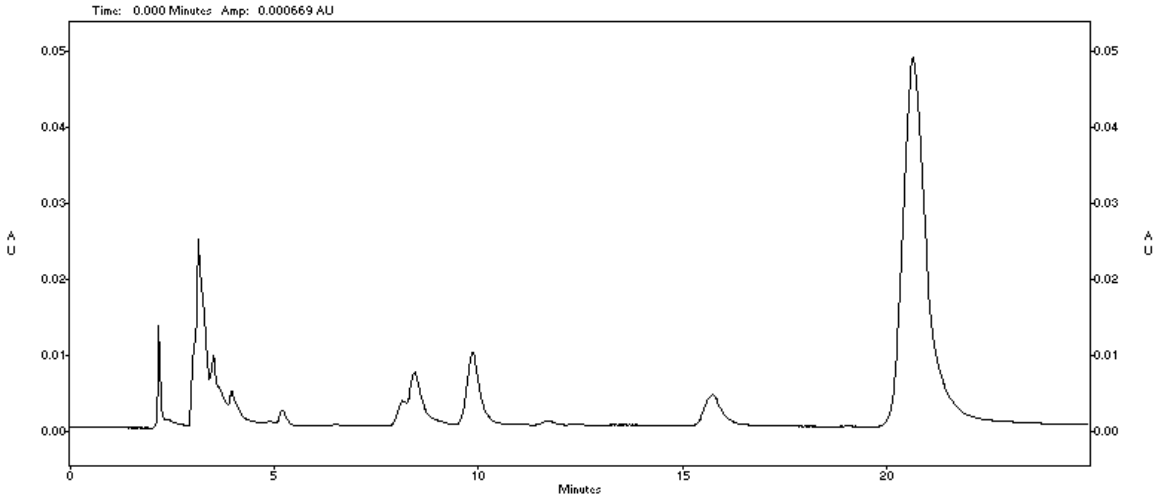

Figure 2.23 HPLC chromatogram of **8** from crude reaction mixture showing an approximate 90% de at C2. The minor (2*R*)-epimer has a retention time of approximately 16 minutes and the major (2*S*)-epimer elutes at approximately 21 minutes.

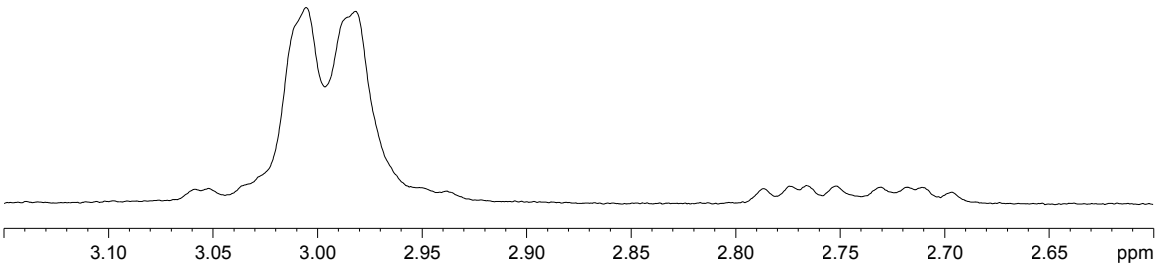

Figure 2.24 Benzylic region of ^{1}H NMR spectrum (400 MHz) of **8** showing an approximate 74% de at C3.

Stereochemcial analysis of the β-position in **8** by ^{1}H NMR spectroscopy revealed an approximate 74% de (Figure 2.24). Acidic conditions were employed in the hydroysis of **8** in an attempt to avoid any racemization of the α-carbon that might be induced by the hydrolysis reaction carried out in basic conditions. The acidic hydrolysis of the hindered

benzamide portion of **8** proved to be problematic, requiring long reaction times under reflux conditions in a closed vessel. The doubly labeled phenylalanine derivative **9** was purified by recrystallization from an isopropanol/water mixture. The partial ^{1}H NMR spectrum of **9** is shown in Figure 2.25. The doublet at approximately 4.0 ppm is the α-proton resonance and the β-proton is visible as a broadend triplet at approximately 3.2 ppm.

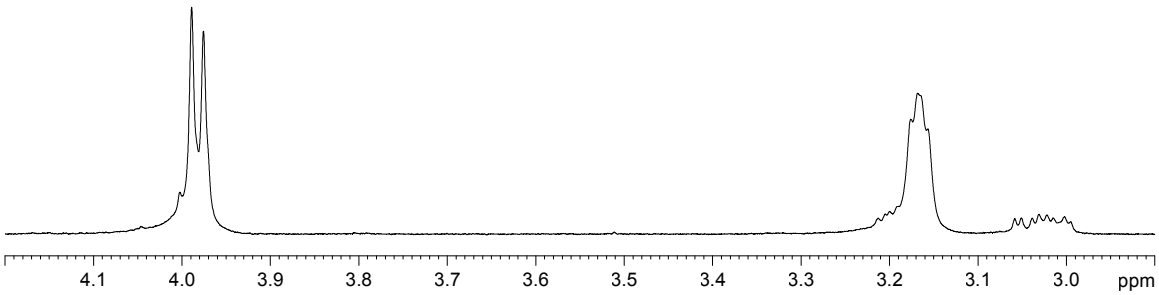

Figure 2.25 Alpha- and β-proton region of ^{1}H NMR (400 MHz) spectrum of **9**.

Stereochemical analysis of **9** revealed only partial degradation of the optical purity at the α-carbon relative to **8**. Analysis of the (-)-camphanamide methyl ester[98] of **9** (Figure 2.26) by HPLC showed 76% de at the α-carbon (Figures 2.27-2.29).

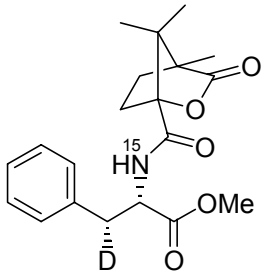

Figure 2.26 (-)-Camphanamide methyl ester derivative of **9** used for stereochemical analysis by HPLC.[98]

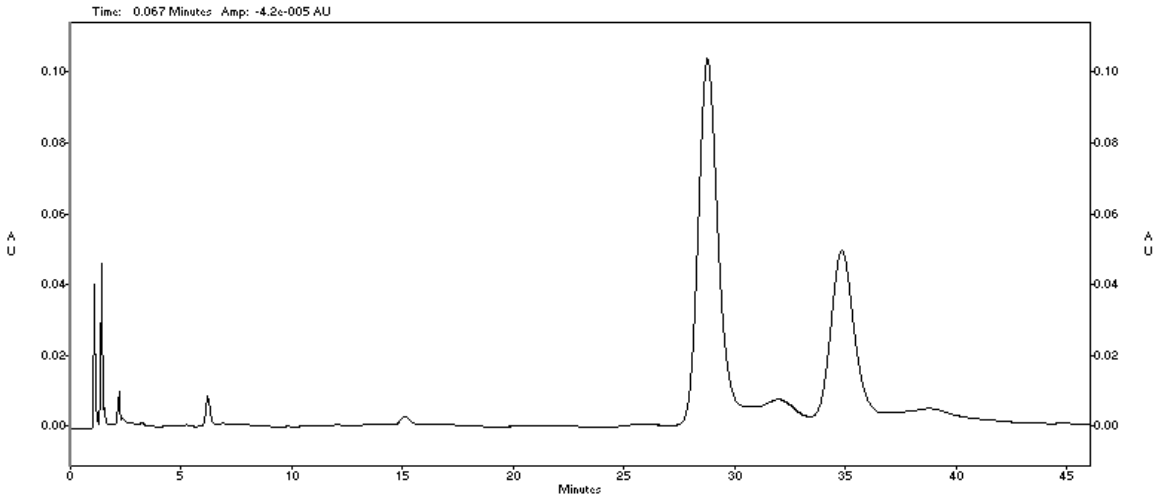

Figure 2.27 HPLC chromatogram of reference sample containing a mixture of D- and L-phenylalanine-(-)-camphanamide methyl esters.

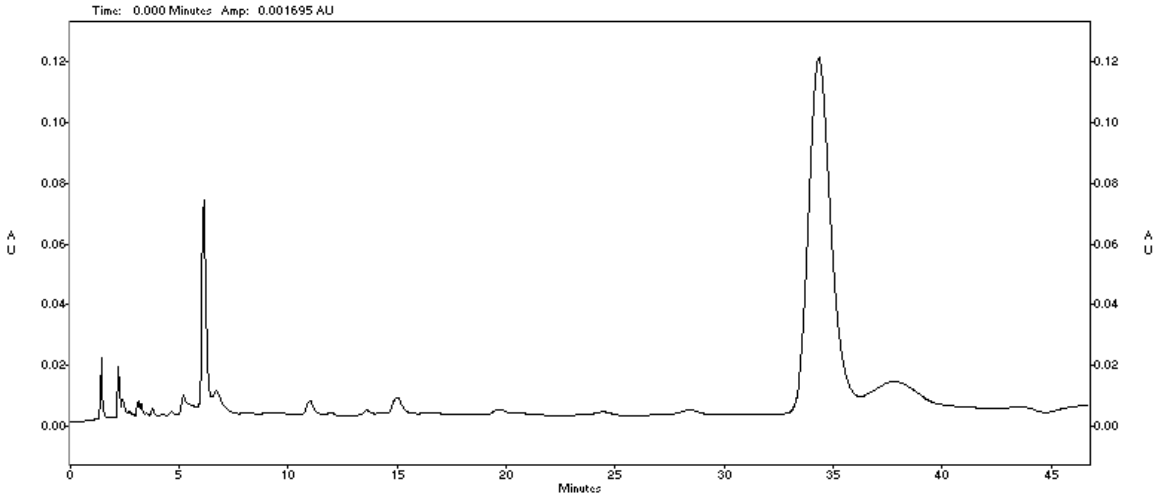

Figure 2.28 HPLC chromatogram of reference sample containing L-phenylalanine-(-)-camphanamide methyl ester.

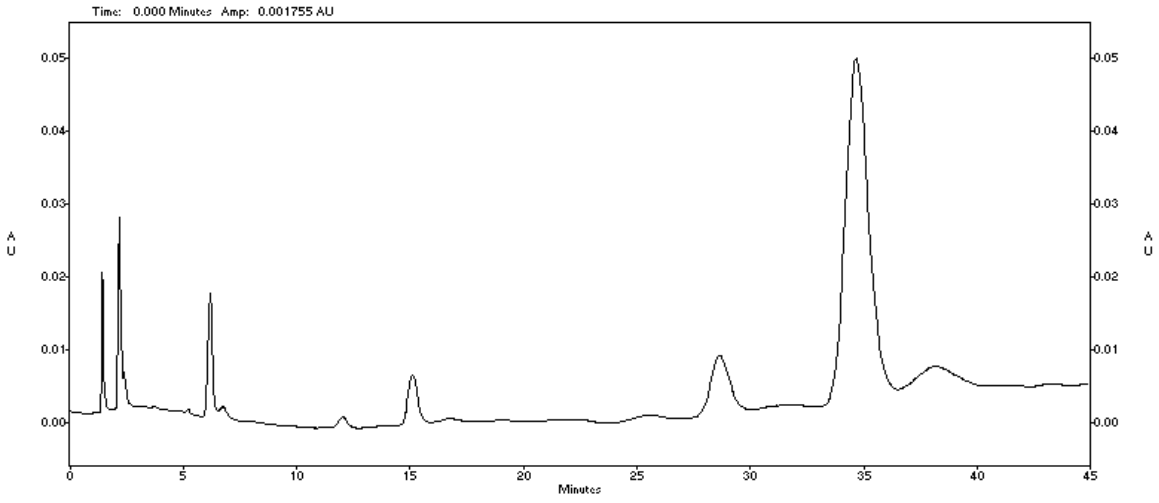

Figure 2.29 HPLC chromatogram of (-)-camphanamide derivative of **9**, showing an approximate 76% de at C2.

From NMR studies of **9** and its (-)-camphanamide derivative (free acid), an approximate value of 72% de at the 3-position was obtained (Figures 2.30 and 2.31) which is consistent with the measured value from **8**.

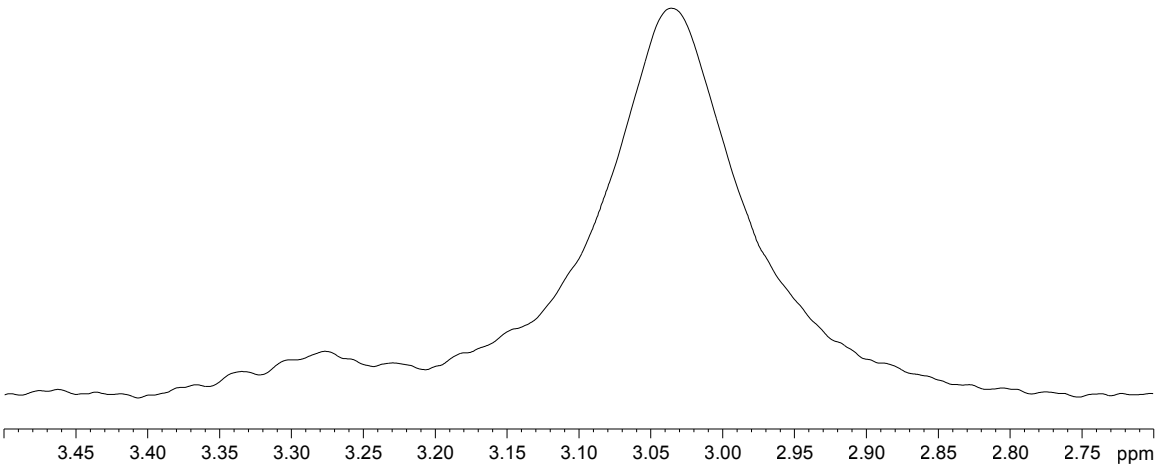

Figure 2.30 ^{2}H NMR Spectrum (600 MHz) of (-)-camphanamide derivative (free acid) of **9** showing an approximate 72% de at C3 as determined by Lorentzian line analysis.

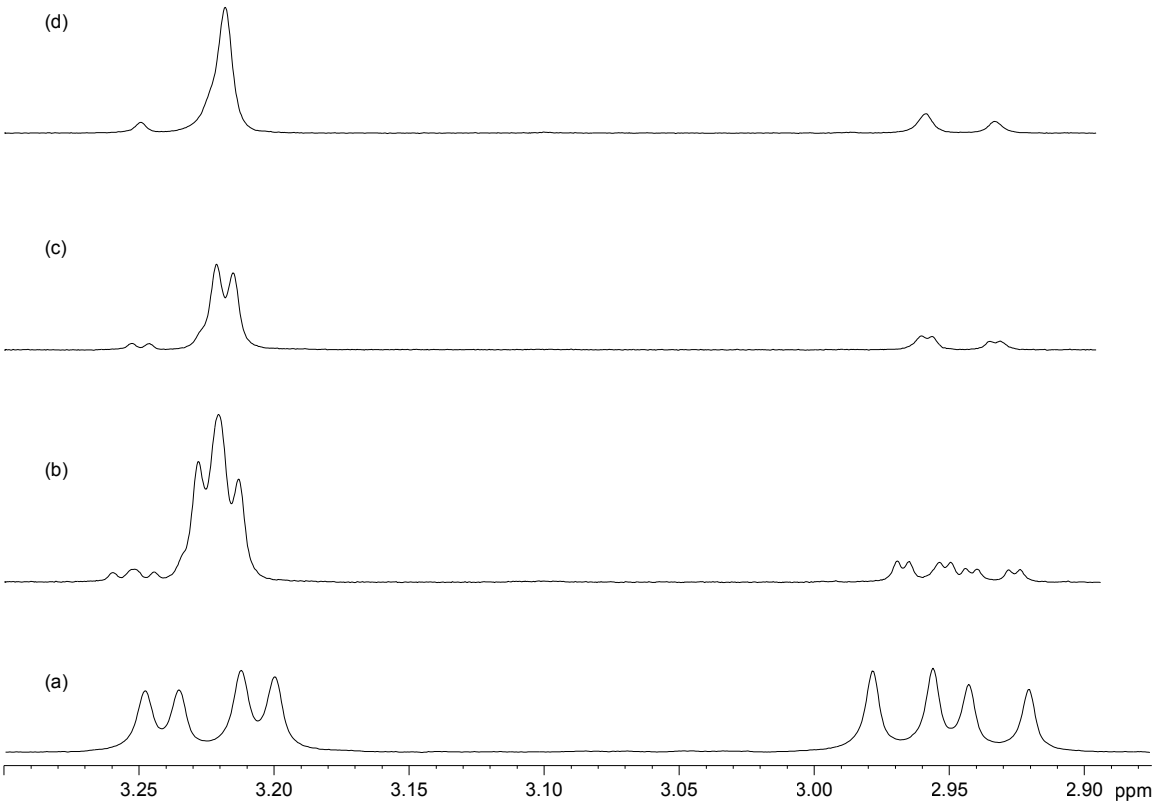

Figure 2.31 Benzylic region of ^{1}H NMR spectra of (-)-camphanamide derivatives (free acid) of L-phenylalanine reference sample and of **9**. (a) from L-phenylalanine (400 MHz) reference sample. (b) from **9** (600 MHz), no decoupling. (c) from **9** (600 MHz), α-proton decoupled. (d) from **9** (600 MHz), α-proton and ^{15}N decoupled.

2.8 Model NMR Application

As already described, our laboratory has previously synthesized (*R*)-[2-^{2}H,^{15}N]-glycine to facilitate NMR studies of FKBP.[51] In those studies, the chiral glycine was incorporated into FKBP and aided making stereospecific assignments of the prochiral α-proton resonances of the glycine residues when the protein was bound to the immunosuppressant ascomycin. Shown in Figure 2.32 is a comparison of some of the NMR spectra obtained from those experiments.

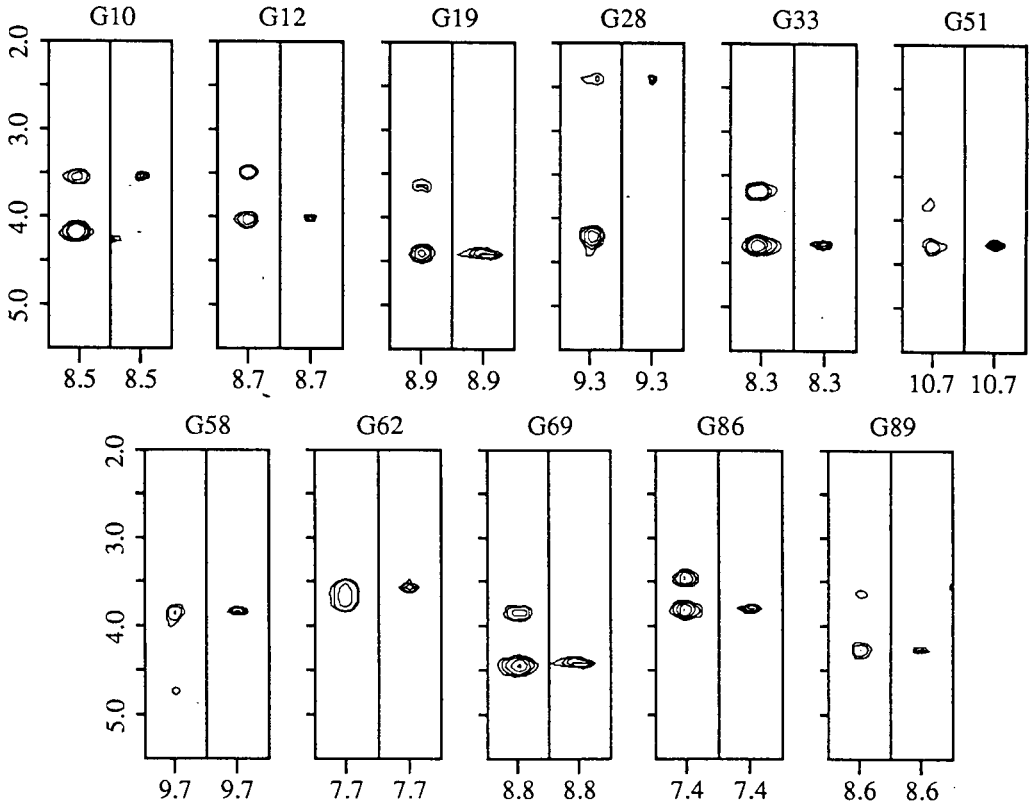

Figure 2.32 NMR spectra from FKBP studies using deuterated glycine. (figure taken from reference 51)

The data in the left hand panels are from spectra collected from control experiments. These experiments were conducted on FKBP incorporated with undeuterated ^{15}N-labeled glycine. These panels depict resonances originating from both prochiral α-protons. The data in the right panels are from the same experiment, only conducted on FKBP incorporated with the doubly labeled chiral glycine. A direct comparison of each of the data sets reveals the disappearance of one resonance in the right panel relative to the control experiment. Since the stereochemistry of the remaining resonance is known, this type of direct comparison allowed stereospecific assignments of the prochiral resonances to be made.

Similar studies could be conducted using the phenylalanine derivative **9** to obtain assignments of the prochiral β-methylene protons of incorporated phenylalanine residues. As a model for these studies, a 2D ^{15}N-^{1}H HMBC (**H**eteronuclear **M**ultiple **B**ond **C**orrelation) experiment was performed using **8**. The data provided by this experiment is similar to that obtained from the experiments associated with Figure 2.32. In this experiment, ^{15}N resonances are correlated with scalar coupled protons. This experiment, or variations of it, can be optimized to observe couplings from one to three bonds. In these model studies, the two and three bond couplings from the ^{15}N nucleus to the α and β-protons are observed. For the purpose of demonstrating the concept, compound **8**, a di-protected amino acid derivative, could be considered a model for a labeled peptide residue in a protein albeit with many more rotational degrees of freedom Figure 2.33 shows the results obtained from using the ^{15}N-labeled undeuterated analog of **8**.

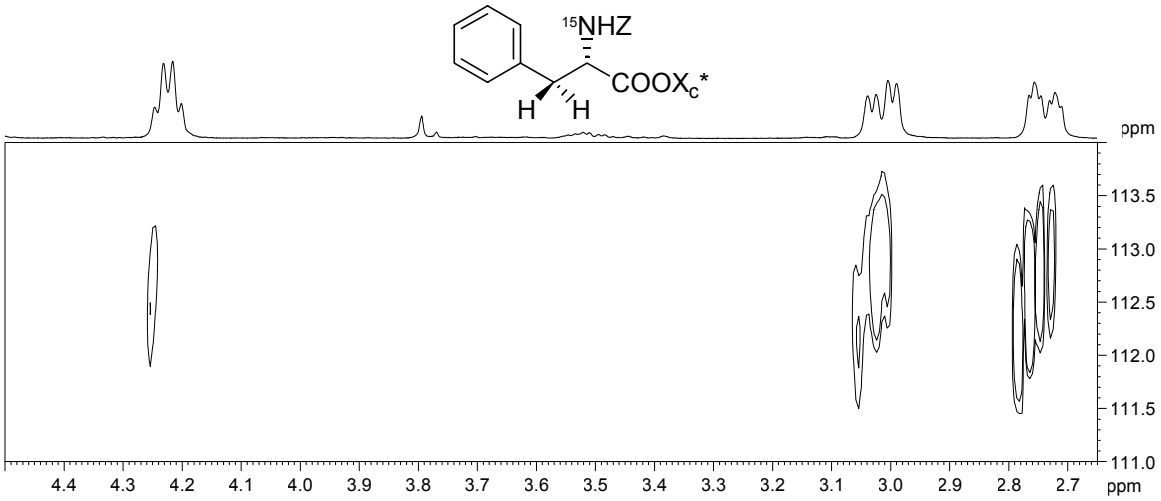

Figure 2.33 Section of gradient selected ^{15}N-^{1}H HMBC optimized for long range correlations.

This experiment represents the control experiment were ^{15}N-^{1}H cross-peaks are observed from both prochiral β-methylene protons at 2.75 and 3.05 ppm in the ^{1}H dimension. The cross-peak to the α-proton is also visible at approximately 4.25 ppm. Shown in Figure 2.34 are the results obtained from the same experiment but with using **8**. It is apparent from this data that the cross-peak originating from the *pro-R* proton is no longer visible. In this manner, compound **9** could be used to aid stereospecific assignments of the prochiral β-methylene protons of phenylalanine residues in proteins into which **9** was incorporated.

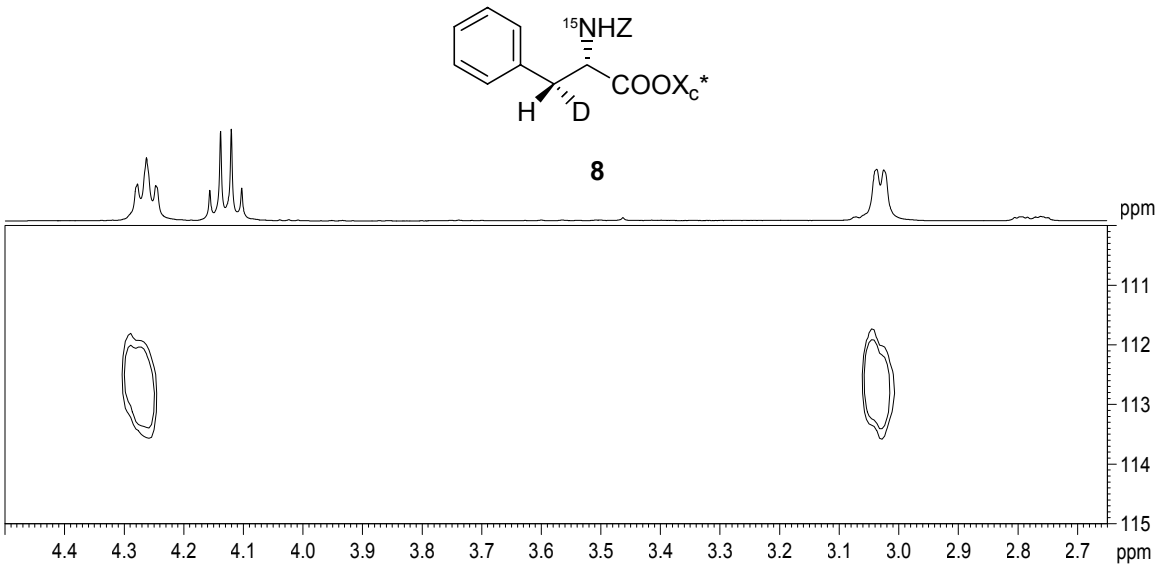

Figure 2.34 Section of gradient selected ^{15}N-^{1}H HMBC of **8** showing 2 and 3 bond correlations.

Perhaps a more useful experiment in an actual system would be the ^{15}N-resolved 3D HSQC-TOCSY (**H**eteronuclear **S**ingle **Q**uantum **C**oherence-**TO**tal **C**orrelation **S**pectroscop**Y**) experiment.[25] The information provided by this experiment is similar in nature to the ^{15}N-^{1}H HMBC experiment, however, it correlates all protons in a "coupled network" that are scalar coupled to an amide proton attached to nitrogen-15. For example, the α-proton of an amino acid residue in a ^{15}N-labeled protein is three-bond coupled to the ^{15}N nucleus. The α-proton is also three-bond coupled to the β-proton which in turn is coupled to a γ-proton if one is present. These relayed couplings define a "coupled network", and the coupling of the α-proton to the ^{15}N nucleus can be used to identify individual members of the network. Data derived from this experiment can be used to obtain ^{15}N-H_β coupling constants which can then be used in χ_1 determinations. However, in the simple model case presented above, all of the coupling information is obtainable from analysis of the 1D ^{1}H spectrum. This would not be the case in an actual

experiment involving a protein, and resolving the data into three dimensions using different ^{15}N frequencies would likely be required. From analysis of the 1D ^{1}H spectrum of the undeuterated analog of **8**, three coupling constants are apparent for each of the benzylic protons. These are most easily observed by considering the *pro-S* proton (Figure 2.35).

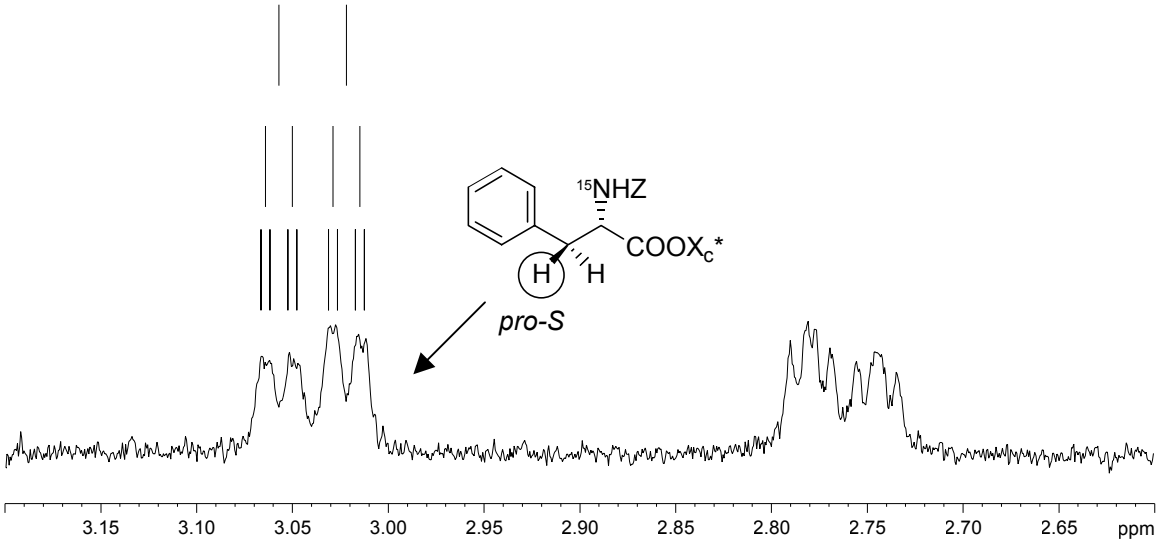

Figure 2.35 Benzylic region of ^{1}H NMR spectrum (800 MHz) of undeuterated analog of **8**.

The largest coupling is the two-bond geminal coupling between the benzylic protons. This coupling is approximately 14 Hz and is the same for both the *pro-R* and *pro-S* protons. The second largest coupling of the *pro-S* proton is the three-bond coupling between the α- and β-protons; this coupling is approximately 6 Hz. However, for the *pro-R* proton, this coupling is closer to 3 Hz. Finally, the smallest observed coupling is the three-bond coupling between the benzylic protons and the nitrogen-15

nucleus. For the *pro-S* proton, this coupling is approximately 2 Hz and for the *pro-R* proton, it is 1 Hz.

It is possible to speculate about the preferred conformation of the side-chain of the phenylalanine residue mimic **8** using this coupling constant information and the Karplus equations for the χ_1 torsion angle (Chapter 1, section 1.2.3.2). The average magnitude of χ_1 predicted by those equations is 61 degrees. The three possible staggered conformations for χ_1 are shown in Figure 2.36.

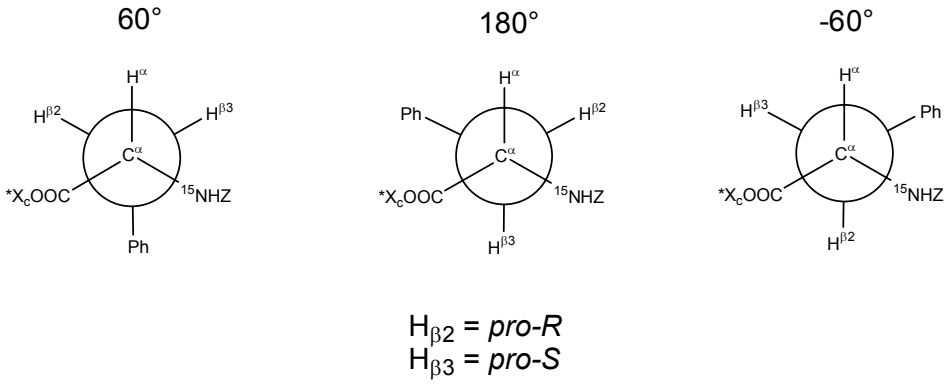

Figure 2.36 Newman projections of **8** showing possible χ_1 conformations. X_c* = (-)-8-phenylmenthyl

In the absence of additional information, a χ_1 torsion angle of 60° could correlate to either the -60° or the 60° conformation. In the 60° conformation, the coupling constants between the α and β protons would be expected to be very similar. This is not what is observed as the coupling of the α-proton to $H\beta_3$ is measured as 6 Hz and to $H\beta_2$ it is 3 Hz. In the -60° conformation, the coupling constant between the α-proton and $H\beta_2$ would be expected to be larger than the one between the α-proton and $H\beta_3$ based on the Karplus relationship between vicinal protons. Again, this is not what is observed. The

180° conformation satisfies the coupling constant prediction of $^3J_{H\alpha H\beta 3} > {}^3J_{H\alpha H\beta 2}$, however, it is not in agreement with the torsion angle value. It is likely that the torsion angle value is only approximated by the equations. For example, a χ_1 angle of 45°, which is fairly close to 60°, would also satisfy the coupling constant requirements. This slight twist could possibly arise from possible π-stacking interactions that would be available between the aromatic rings in this conformation. A complicating factor in this study is that the peptide mimic is not as conformationally restricted as would be the case in an actual polypeptide. This results in much more free rotation of the side-chain and consequently, the derived conformational information depicts an average conformation of the side chain. Although several possible solutions exist, the ability to make the stereospecific assignments aids the process and allows preliminary models to be developed. The actual result can only by determined with additional information. The difficulty with this simple model system illustrates the requirement for quality information to solve these types of problems, especially when working with an actual macromolecular system.

2.9 Summary

A simple yet versatile strategy for the chemical synthesis of ^{15}N-labeled diastereoselectively β-deuterated amino acids has been presented. The utility of the method has been demonstrated with the synthesis of a phenylalanine derivative **9**. The key step in the synthesis was the alkylation of ^{15}N-labeled hippurate **7** with deuterated mesylate **3e** to yield the doubly labeled protected phenylalanine derivative **8** in 89% chemical yield with approximately 90% de at the α-position and 74% de at the β-position. Deprotection of **8** under acidic conditions gave the desired (2*S*, 3*R*)-[3-^{2}H,^{15}N]-

phenylalanine **9** with only partial degradation of the optical purity at the α-carbon. Similar epimerization of the α-position of amino acids under these conditions has been previously observed.[99-102]

The final product **9,** if incorporated into a protein, could be used to obtain stereospecific assignments of the prochiral β-methylene protons of the labeled phenylalanine residues. Model NMR studies have been conducted using **8** as a peptide residue mimic. Two-dimensional NMR experiments, analogous to the 3D experiments that would be required in an actual study, have been conducted and demonstrate the utility of this compound. Preliminary side-chain conformational studies are possible by comparing data from **8** with an undeuterated analog. These preliminary studies allow initial models of side-chain orientation to be developed.

CHAPTER 3

SYNTHESIS OF OTHER ISOTOPICALLY LABELED MOLECULES

3.1 Statement of the Problem

A versatile strategy for the chemical synthesis of ^{15}N-labeled stereoselectively β-deuterated amino acids has been presented. These types of molecules are valuable biochemical tools that find uses in mechanistic enzymology and protein structural studies using NMR methods. The utility of the method has been demonstrated by the synthesis of (2*S*, 3*R*)-[3-^{2}H,^{15}N]-phenylalanine (Chapter 2). One of the goals of this strategy is that it be a general approach to other diastereoselectively deuterated β-methylene unit containing amino acids. Efforts to extend this strategy to other amino acids, as well as efforts to optimize the strategy, will now be reported. Additionally, work on the synthesis of other isotopically labeled amino acids and the development of novel conditions to effect the stereoselective chlorination of benzylic alcohols will be presented.

3.2 Extending the Strategy to Tyrosine

The synthesis of the corresponding labeled tyrosine derivative is a logical extension from the phenylalanine derivative. It is apparent that a similar strategy should be viable with the appropriate modifications to the electrophile. A key element to this approach would be the protecting group chemistry required for the *para*-oxygenated electrophile and how it impacts the subsequent alkylation chemistry. The details of the

synthetic approach taken to the doubly labeled tyrosine derivative will now be presented. This synthetic route evolved from several pathways that were initially investigated. Review of these early observations provides valuable insight into the development of the final synthesis.

3.3 Developing and Optimizing the Alkylation Strategy

Extending the strategy to tyrosine from phenylalanine, although logical and straightforward, provided an opportunity to investigate phenol protecting group strategies, alternative electrophilic species and glycine equivalents, and new chlorination conditions. These variables were investigated in an effort to achieve the most general and efficient synthesis possible. In this section, much of the developmental work will be presented as it provides insight into the evolution of the methodology. Early on, an advanced intermediate in the doubly labeled tyrosine synthesis was obtained and started the investigation of different phenol protecting groups when it was determined more efficient routes to the final product should be possible by changing the phenol protecting group.

3.3.1 4-Methoxy benzyl chloride

Initial efforts to synthesize the labeled tyrosine derivative were focused on the use of 4-methoxy protected benzylic electrophiles owing to the stability of the methyl ether.[103] As with the phenylalanine derivative, the enantioselectively deuterated alcohol was to serve as the key starting material for electrophile synthesis. Shown in Scheme 3.1 is the synthesis of (*S*)-(+)-4-methoxybenzyl-α-*d*-alcohol (**10**), which was prepared in a similar fashion as previously described for **2**. In general, the reaction sequence was

high yielding and proceeded with deuterium incorporation comparable to that observed in the simple benzylic case.

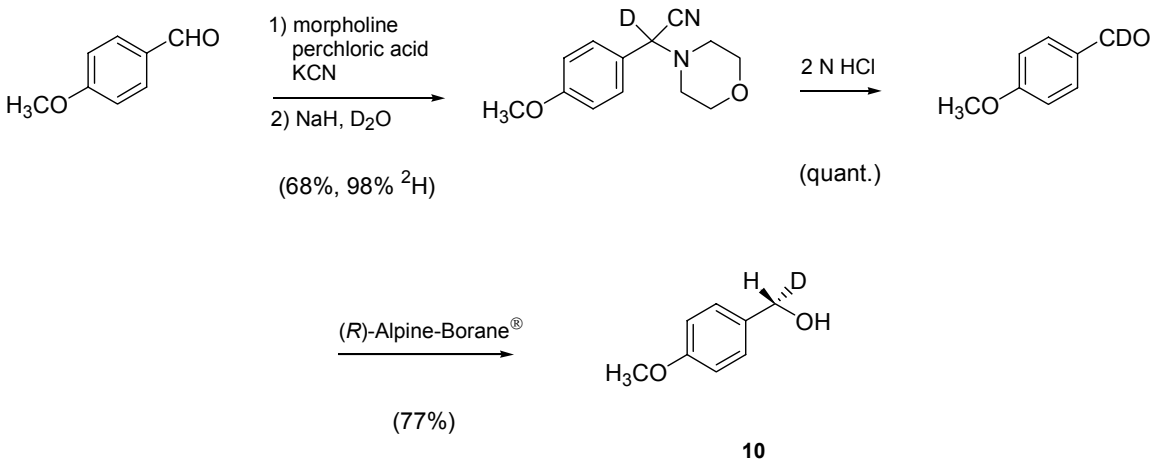

Scheme 3.1 Synthesis of **10**.

To demonstrate the versatile nature of the synthetic strategy, the chloride would be used as the electrophilic species in the alkylation reaction. The use of the chloride would provide the β-position epimer of the tyrosine derivative when compared to the labeled phenylalanine synthesis. Initially, (*R*)-(-)-4-methoxybenzyl-α-*d*-chloride (**11**) was prepared from **10** using the modified Mitsunobu conditions previously described (Scheme 3.2).[91]

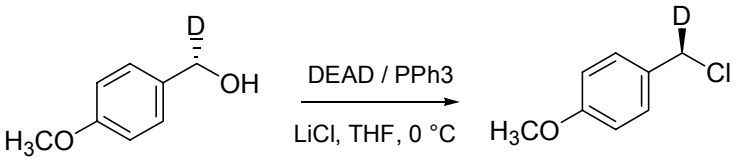

10 **11**

Scheme 3.2 Synthesis of **11** using the modified Mitsunobu conditions.[91]

However, it became apparent that purification of the unstable chloride would be hindered by the generation of byproducts from the Mitsunobu reaction. In this case, the chromatographic separation of the product from the crude reaction mixture was tedious and did not represent an ideal situation to obtain purified labeled product from a small scale reaction. This was an important consideration because optimal alkylation of the glycine equivalent required that the electrophilic species be relatively free of contaminating side products. The Mitsunobu reaction, although commonly used in organic chemistry, is infamous for the production of stoichiometric amounts of triphenylphosphine oxide and hydrazinecarboxylate as byproducts, which often prevent the isolation of the desired products. In addition, excess triphenylphosphine can also interfere with the isolation of the reaction product.

Despite these difficulties, small quantities of the labeled chloride **11** was obtained and used to alkylate **7** using the conditions previously described for the phenylalanine synthesis (Scheme 3.3).

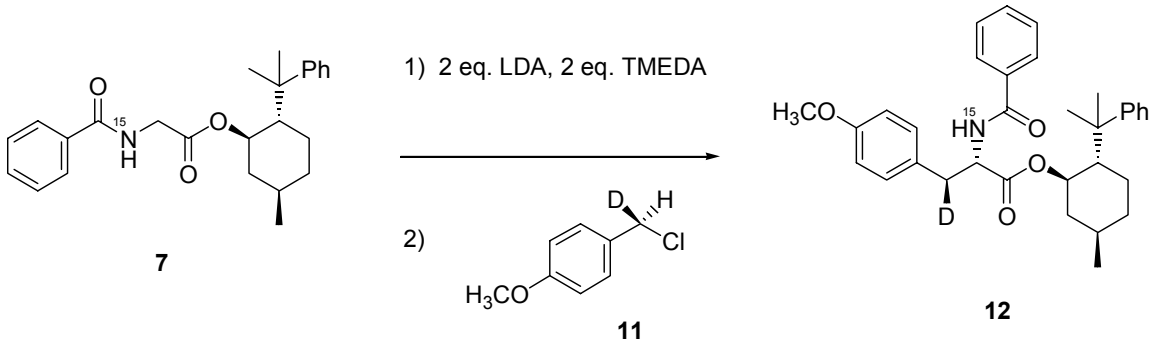

Scheme 3.3 Synthesis of a doubly labeled tyrosine derivative **12** using chloride **11**.

Unfortunately, the alkylation reaction did not proceed in good chemical yield, however, reasonable diastereoselectivies were observed at the α- and β-positions in the product **12** (Figure 3.1). The de at the β-carbon was determined to be approximately 64% from the integration of the benyzlic resonance in the ^{1}H NMR spectrum (Figure 3.2).

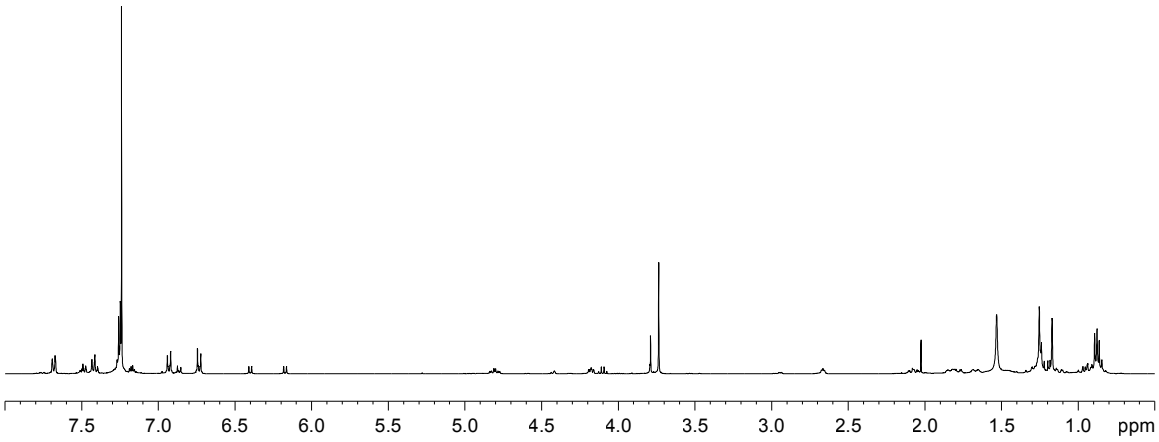

Figure 3.1 ^{1}H NMR spectrum (400 MHz) of **12** in $CDCl_3$.

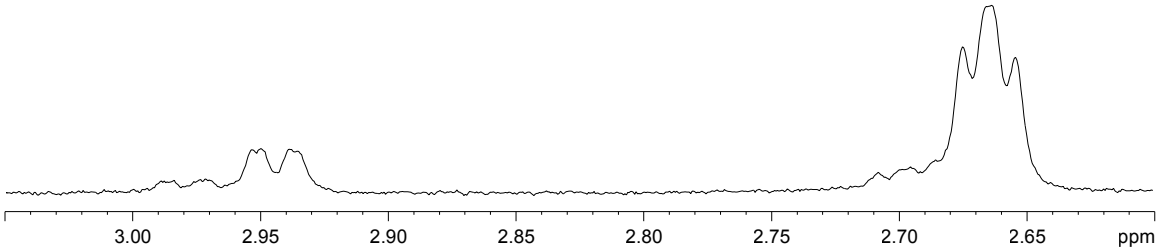

Figure 3.2 Benzylic region of ^{1}H NMR spectrum (400 MHz) of **12** showing an approximate 64% de at C3.

The next step in the synthesis would be the deprotection of the phenol methyl ether. The disadvantage of using the robust methyl ether as a phenol protecting group was that harsh conditions would be required for its removal. Achieving efficient deprotection without racemization of the α-carbon was a concern. Upon investigation, evidence in the literature suggested that some methods used for methyl ether cleavage result in racemization of the α-carbon of various amino acids derivatives.[100-102,104] Model compounds were used to investigate several deprotection conditions including HBr/NaI, TMSI, and thiol based deprotection strategies.[104-106] Unfortunately, none of these methods seemed to give acceptable yields in these model reactions. In an effort to optimize the strategy, several modifications were considered at this point in the project. It was believed that an alternative electrophile would provide easier synthetic access to the desired labeled tyrosine derivative. Additionally, an alternative chiral glycine equivalent had been reported in the literature[107] that appeared to be easily adaptable to the current synthesis and could potentially address some of the problematic aspects of the present strategy (Figure 3.3) including deprotection efficiencies and alkylation with alternative 4-oxygenated benzylic electrophiles.

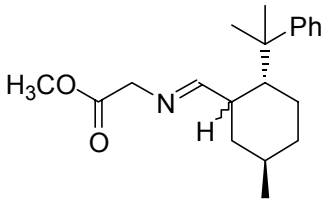

13

Figure 3.3 Alternative chiral glycine equivalent.[107]

3.3.2 Alternative glycine equivalent

The approach taken by Meyer and co-workers possesses similar qualities as the current strategy.[107] However, there are subtle differences that make a comparison very interesting. They report the use of various electrophiles, including 4-benzyloxybenzyl bromide, in the alkylation of **13** to produce amino acid derivatives in high chemical yield, as high as 96%, with stereoselectivity typically greater than 99%. The asymmetric induction originates from a chiral aldehyde derived from (-)-8-phenylmenthol, which is then used to prepare the glycine iminoester **13** that serves as the alkylation substrate. The chiral aldehyde exists as a mixture of two epimers which gives rise to major and minor conformations of the lithium enolate species (Figure 3.4)**.**

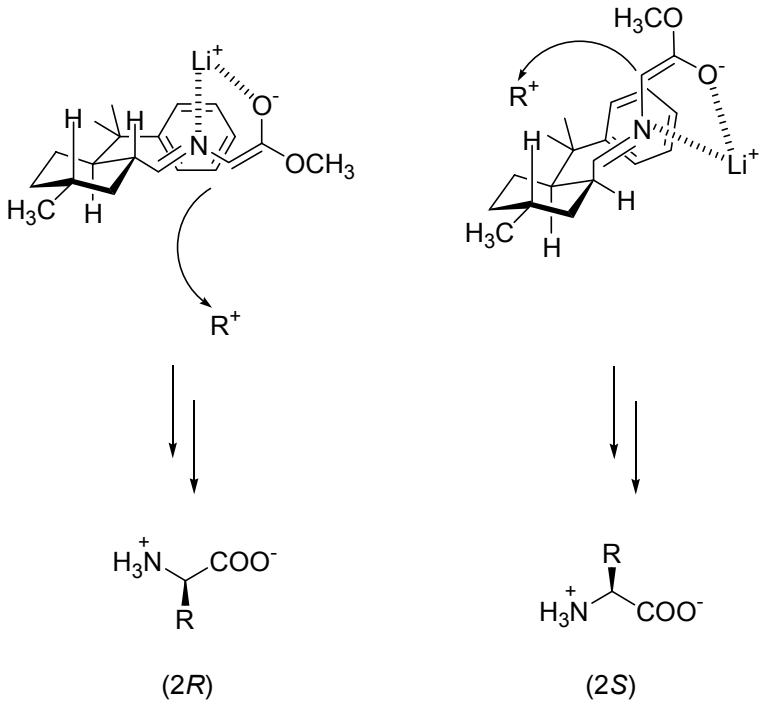

Figure 3.4 Chiral induction model for alkylation of lithium enolates derived from **13**.[107]

The same principles govern this proposed model as with the (-)-8-phenylmenthyl hippurate example. The sterics of the auxiliary, π-stacking interactions, and the preferred conformation of the chelated species all interact to direct the ensuing alkylation reaction. It is interesting to note that the major enolate, the all equatorial epimer, gives the less desired (*R*)-amino acid derivative as the major product. This is in contrast to the (-)-8-phenylmenthylhippurate example which produces the more common (*S*)-amino acid derivative as the major product. In their paper, the authors report the use of 4-benzyloxybenzyl bromide as an electrophile to produce a tyrosine derivative in 90% chemical yield with 98.5% ee at the α-carbon in the deprotected final product.[107] Perhaps more importantly, the deprotection conditions are mild and proceed with high chemical yield. With all of these considerations in mind, it was determined to attempt to adapt this strategy to the synthesis of a doubly labeled tyrosine derivative to improve the

chemical yield and deprotection steps of the current synthesis. The first requirement would be the synthesis of the chiral aldehydes. Shown in Scheme 3.4 is the synthesis of the chiral epimeric aldehydes starting from the previously synthesized (-)-8-phenylmenthol.

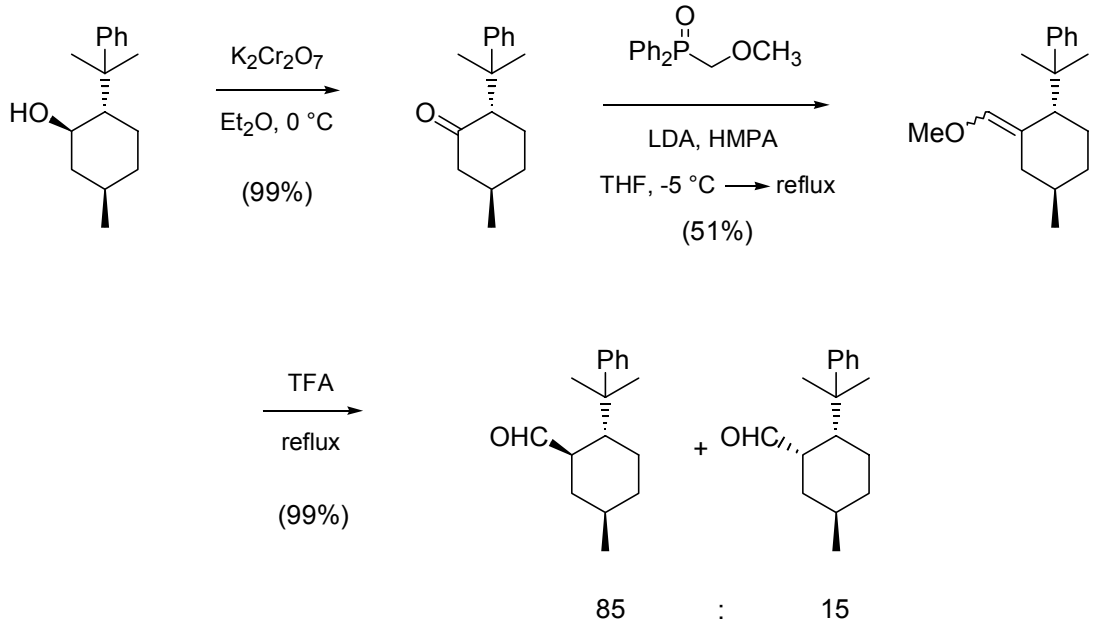

Scheme 3.4 Synthesis of the chiral aldehydes to be used in glycine imine formation.

Oxidation of (-)-8-phenylmenthol with potassium dichromate yielded the 8-phenylmenthone derivative in essentially quantitative yield. Treatment of the ketone with methoxymethyldiphenylhosphine oxide, synthesized from triphenylphosphine and methoxymethyl chloride, gave the vinyl ether as a 3:1 mixture of double bond isomers.[108] Hydrolysis of the vinyl ethers in trifluoroacetic acid yielded the epimeric mixture of aldehydes in high yield with a 70% de. The epimeric aldehydes were separated using silica gel chromatography. Next, the glycine portion of the molecule was prepared by

treating ^{15}N-labeled glycine in ethanol with HCl gas to give ethyl glycinate in quantitative yield (Scheme 3.5).

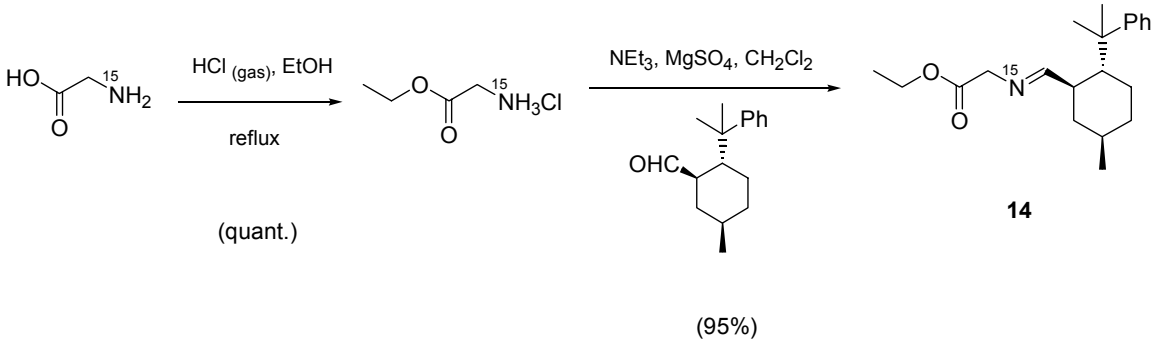

Scheme 3.5. Synthesis of ^{15}N-labeled glycine iminoester **14**.

Imine formation was accomplished at room temperature using triethylamine in dichloromethane. Model alkylation reactions were performed using unpurified imine as similarly reported by Meyer, however in our hands, adequate results were not obtained. Unfortunately, efforts to purify **14** using silica gel, reverse-phase, and alumina chromatography failed due to the apparent instability of **14** under these purification conditions. Based on these preliminary observations and the fact that the preferred α-position stereochemistry could be more readily obtained, it was decided to abandon the use of **14** and to continue investigating the alkylation of **7** with other electrophiles as the preferred synthetic route.

3.3.3 4-Benzyloxy benzylic electrophiles

In the course of their work, Meyer and co-workers reported the use of 4-benzyloxybenzyl bromide to successfully alkylate the chiral lithium enolate derived from a glycine iminoester.[107] In addition, the authors used hexamethylphosphoramide (HMPA) as an additive to increase the reactivity of the electrophiles. Based on this

work, it was decided to investigate 4-benzyloxybenzyl halides as potential electrophiles to alkylate (-)-8-phenylmenthylhippurate as well as the use of HMPA. Various alkylation reaction conditions were examined using 4-benzyloxybenzyl chloride and bromide with and without HMPA. Unfortunately, none of these seemed to offer any substantial improvements in the synthesis of a tyrosine derivative over the previously described protocol utilized for the phenylalanine synthesis.

3.3.4 4-*tert*-Butyldimethylsilyloxy benzylic electrophiles

The next option investigated was the use of silyl ether based protecting groups for the 4-oxygenated electrophiles. The first silyl ether studied was the *tert*-butyldimethylsilyl ether (TBDMS or TBS).[103] Undeuterated electrophiles were synthesized from the corresponding alcohol (Scheme 3.6).

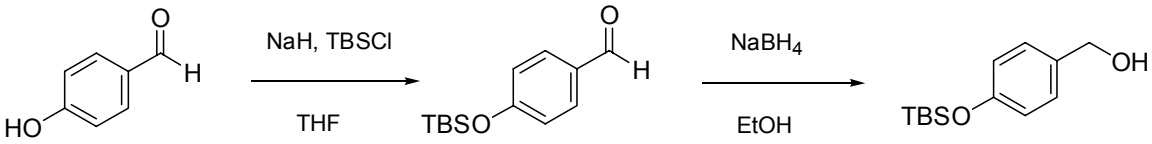

Scheme 3.6 Synthesis of 4-TBSO-benzyl alcohol.

Model alkylation reactions were performed using electrophiles generated from 4-TBSO-benzyl alcohol. Although the reactions were moderately successful, it became apparent that the TBS ether was not entirely stable under the alkylation reaction conditions as some de-silylated product was obtained. It was believed that the triisopropylsilyl ether would be a more robust protecting group under the reaction conditions.[103] Therefore, the 4-TIPSO-benzyl alcohol was prepared using similar conditions. In the course of model alkylation reactions using 4-TIPSO-benzyl chlorides,

it was found that the TIPS group did offer better stability and could be easily removed using TBAF.

3.4 Synthesis of (2*S*, 3*S*)-[3-^{2}H,^{15}N]-Tyrosine

Depicted in Scheme 3.7 is the synthesis of (*S*)-(+)-4-triisopropylsilyloxybenzyl-α-*d* alcohol (**15**), which served as the immediate precursor to the deuterated chloride that was to be used as the electrophile. The key elements of the synthetic route, deuterium incorporation and asymmetric induction, are identical to the method previously described.

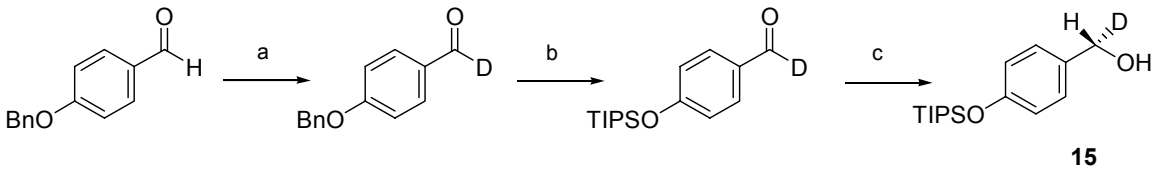

15

Scheme 3.7 Synthesis of **15**. (a) i, morpholine, perchloric acid, KCN, 90 °C, (quant.); ii, NaH, D_2O, THF, (86%; 99% ^{2}H); iii 2N HCl, (92%; 99% ^{2}H); (b) i, TMSI, CH_2Cl_2, (59%); ii, TIPSCl, NEt_3, THF; (c) (*R*)-Alpine Borane®, (79% from unprotected phenol; 99% ee).

Treatment of 4-benzyloxybenzaldehyde with morpholine perchlorate and KCN gave the morpholinoacetonitrile derivative in quantitative yield. Proton-deuteron exchange was accomplished with high efficiency using NaH and D_2O. Acid hydrolysis of the deuterated product gave the benzyl protected deuterated aldehyde in 92% yield. Removal of the benzyl protecting group was accomplished using trimethylsilyl iodide (TMSI) in dichloromethane in moderate yield. Treatment of the unprotected phenol with triisopropylsilyl chloride (TIPSCl) and triethylamine yielded the protected aldehyde-*d*. Finally, treatment with (*R*)-Alpine Borane® gave **15** with excellent enantioselectivity in 79% yield over the reprotection and reduction steps.

Shown in Scheme 3.8 is the synthesis of (*R*)-(-)-4-triisopropylsilyloxybenzyl-α-*d* chloride (**16**). The product chloride was obtained in 88% yield after chromatography using silica gel.

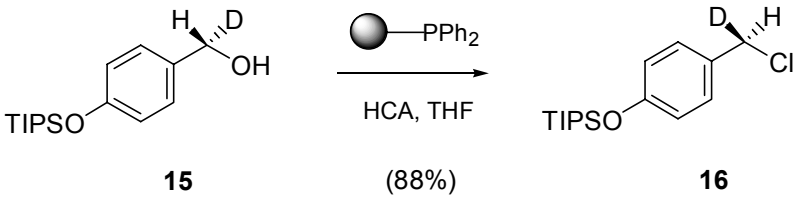

15 (88%) **16**

Scheme 3.8 Synthesis of **16** using HCA and polymer-supported TPP.

The halogenation conditions used hexachloroacetone (HCA) and polymer-supported triphenylphosphine (TPP) to generate the chloride stereoselectively from the alcohol. The chlorination of alcohols using HCA and soluble TPP was first reported by Magid and co-workers.[109] The authors detailed the regio- and stereoselective conversion of allylic alcohols into the corresponding chlorides under very mild conditions with excellent yields, minimal rearrangements, high selectivity, and with ease of purification. In later work,[110] Magid and co-workers propose several possible mechanisms by which the chlorination is mediated, however, conclusive data is not presented. Villeneuve and Chan report these conditions to be an acid-free procedure for the preparation of acyl chlorides.[111] They propose that the chlorination is mediated by the intermediate shown in Figure 3.5. This hypothesis is founded on their study of the reaction dependence on the stoichiometry of the reagents. They suggest that optimal results were obtained when using two mole equivalents of phosphine per mole equivalent of HCA.

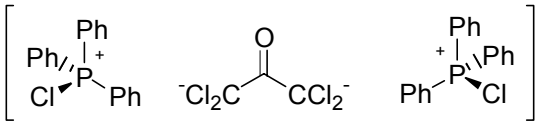

Figure 3.5 Proposed chlorinating species from HCA/TPP reaction.

In the current synthesis, a filterable source of TPP was used to facilitate product purification. In model reactions with soluble TPP, excess phosphine reagent, which was critical for ensuring maximal yield of the labeled products, greatly hindered product purification using chromatographic methods. In general, the chlorination reactions were performed on a small scale that was best suited for chromatographic purification as opposed to distillation. Unreacted triphenylphosphine had the same retention factor (R_f) as **16** in the many solvent systems evaluated, which resulted in the co-elution of the two compounds. The filterable source of phosphine eliminated this problem and greatly simplified the isolation of **16**.

Depicted in Scheme 3.9 are the details of the alkylation of **7** with labeled chloride **16** to give the labeled tyrosine derivative **17**. The alkylation reaction produced **17** in 62% chemical yield with approximately 86% de at the α-carbon and 82% de at the β-position as determined by ^{1}H NMR spectroscopy and HPLC (Figures 3.6 and 3.7).

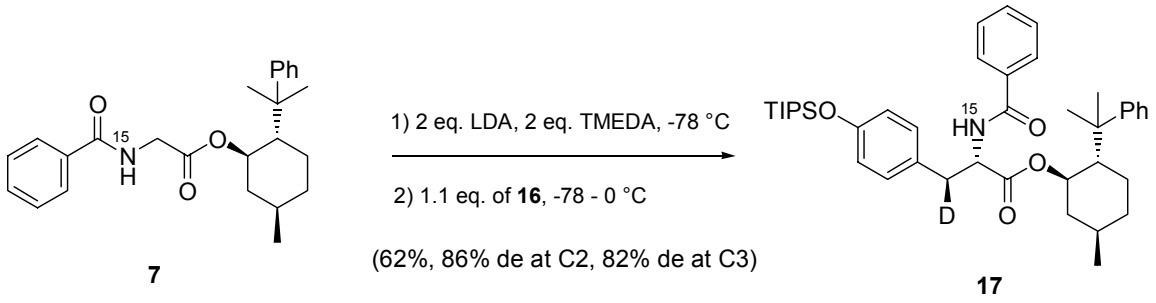

Scheme 3.9 Synthesis of the doubly labeled tyrosine derivative **17**.

Shown in Figure 3.6 is the amide region of the ^{1}H NMR spectrum of crude product **17**. This region of the spectrum is used to determine α-position stereoselectivity. The pair of doublets centered at 6.27 ppm is the resonance from the amide proton of the (2*S*) product; likewise, the doublet centered at approximately 5.90 ppm originates from the amide proton of the (2*R*) product. The large one-bond ^{15}N–H coupling (~90 Hz) is apparent, as is the smaller three-bond coupling to the α-proton (7.5 Hz). The pair of triplets centered at 6.03 ppm are from unreacted starting material and show the extra coupling of the additional α-proton.

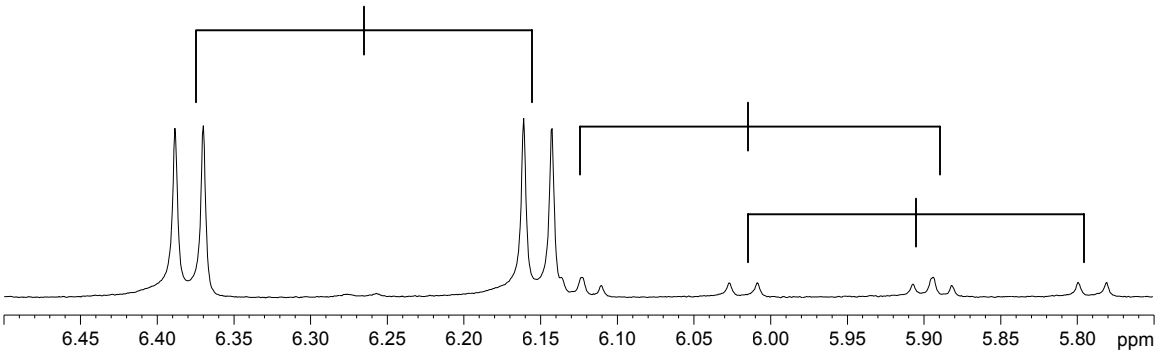

Figure 3.6 Amide proton region of ^{1}H NMR spectrum (400 MHz) of **17** showing an approximate 86% de at the α-carbon.

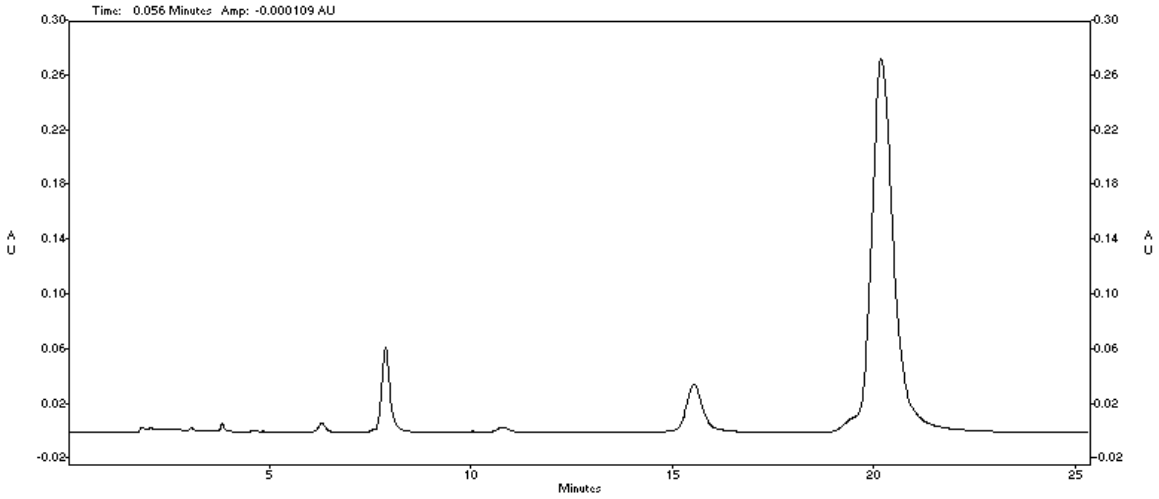

Figure 3.7 HPLC chromatogram of crude product reaction mixture of **17**.

In Figure 3.7, the HPLC chromatogram shows that, as with the case of the phenylalanine derivative, the (2*S*)-diastereomer after the (2*R*)-diastereomer in the separation conditions that were used. The (2*S*) diastereomer of **17** has a t_r of approximately 21 minutes and the (2*R*) diastereomer elutes at approximately 16 minutes; starting material is visible at a t_r of 8 minutes. Integration of these peaks is consistent with analysis from the NMR derived data (Figure 3.6), and suggests an approximate de of 86% at the α-position. Diastereoselectivity at the β-position was estimated to be approximately 82% de from integration of the benzylic resonance of the ^{1}H NMR spectrum of **17** (Figure 3.8).

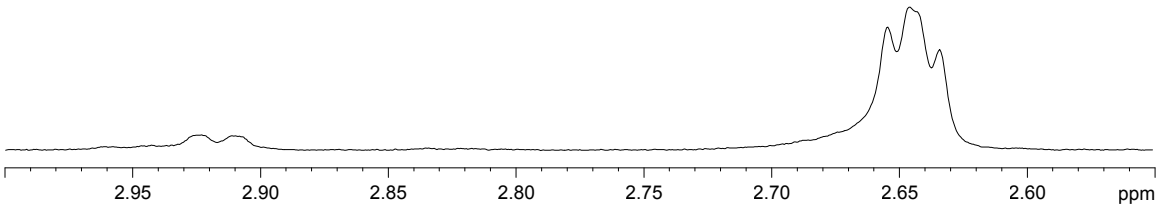

Figure 3.8 Benzylic proton region of ^{1}H NMR spectrum (400 MHz) of **17** showing an approximate 82% de at C3.

The next step in the synthesis was the deprotection of the phenol. It was believed that *N*-tetrabutylammonium fluoride (TBAF) could easily affect this transformation.[103] These deprotection conditions were first investigated using the unlabeled (-)-menthyl ester (Figure 3.9) as a model of the actual substrate. These studies were performed to confirm these conditions would not impact the stereochemistry of the α-carbon. This model compound was obtained from the alkylation of (-)-menthylhippurate with 4-TIPSO-benzyl chloride. Analysis of the deprotection products by ^{1}H NMR spectroscopy and HPLC revealed that the cleavage of the silyl ether protecting group had no detrimental effect on the stereochemistry of the α-carbon (data not shown).

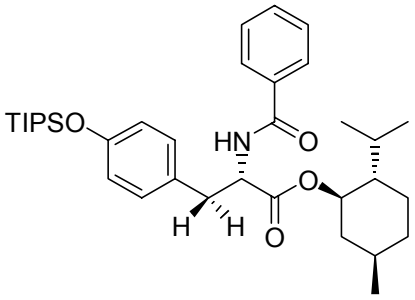

Figure 3.9 Unlabeled (-)-menthyl ester model compound used to study TBAF desilylation conditions.

Shown in Scheme 3.10 are the details of silyl ether deprotection of **17**. The reaction gave the deprotected phenol **18** in excellent yield. As evident from analysis of the ^{1}H NMR spectra and HPLC chromatograms, the stereochemistry at the α-carbon was unaffected (Figures 3.10 and 3.11).

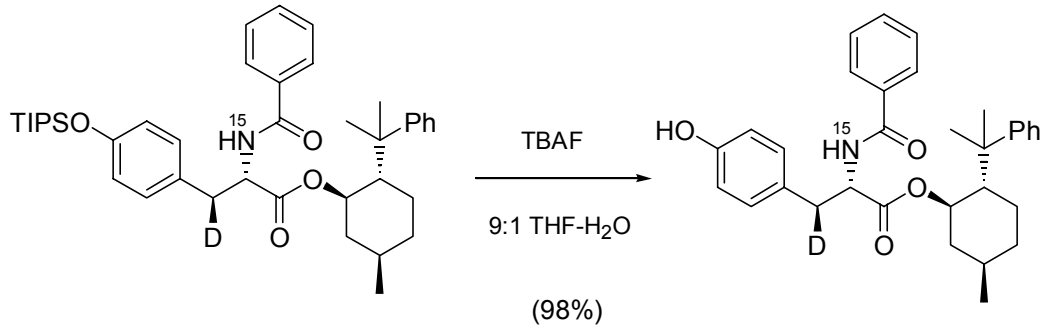

17 **18**

Scheme 3.10 TBAF deprotection of doubly labeled tyrosine derivative **17**.

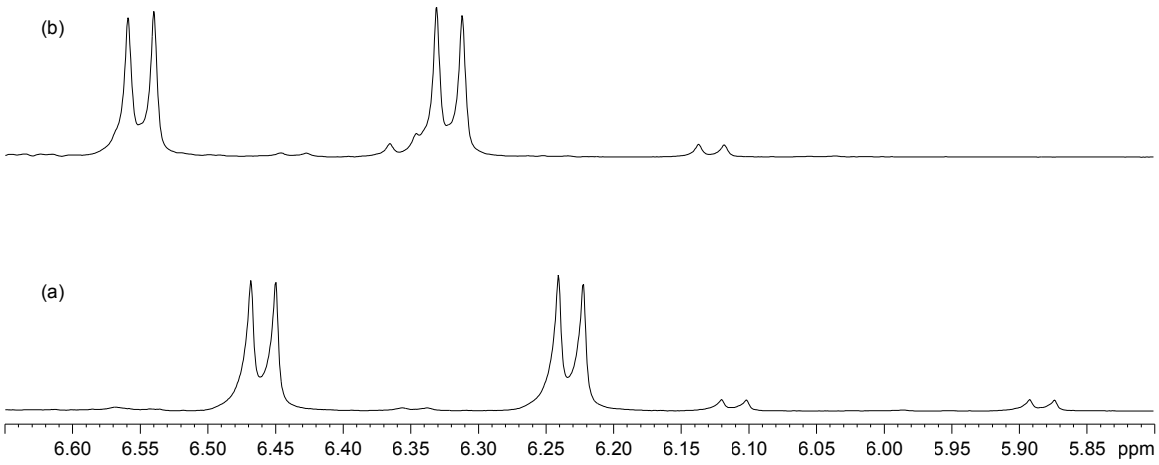

Figure 3.10 Amide proton region of ^{1}H NMR spectra (400 MHz) of labeled tyrosine derivatives showing the same de is maintained during silyl ether cleavage. (a) **17**, phenol silyl ether; (b) **18**, product from desilylation reaction.

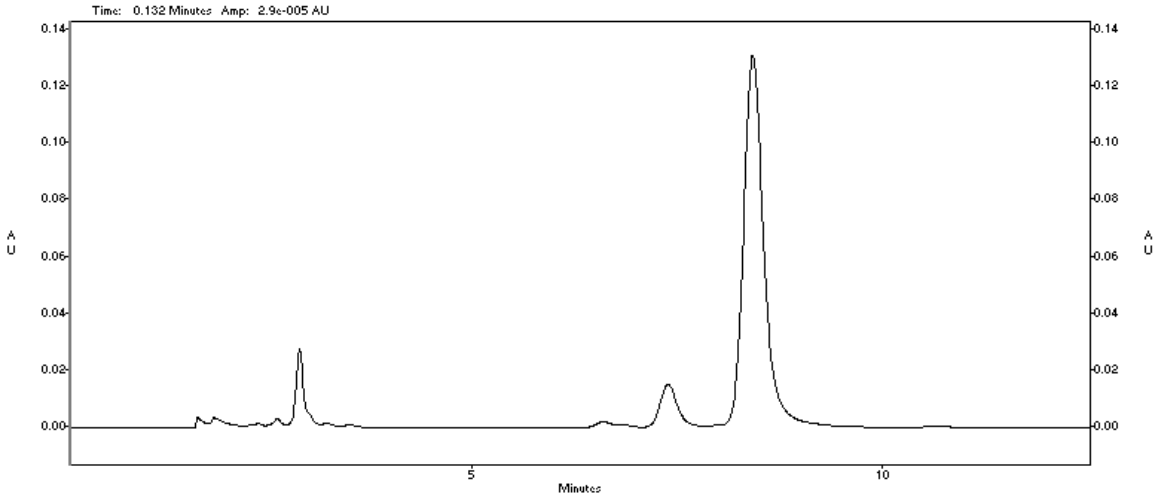

Figure 3.11 HPLC chromatogram of **18**. Optical purity at α-carbon is unaffected in silyl ether cleavage conditions (compare to Figure 3.7).

Shown in Scheme 3.11 is the final deprotection of **18** to yield (2*S*, 3*S*)-[3-^{2}H,^{15}N]-tyrosine hydrochloride (**19**). Treatment of **18** with hydrochloric acid at 70 °C yielded the final product as the hydrochloride salt in 59% yield. Unfortunately, significant epimerization was observed at the benzylic position. Figure 3.12 is a partial ^{1}H NMR spectrum of **19** as obtained from the crude reaction mixture showing the α- and β-proton region.

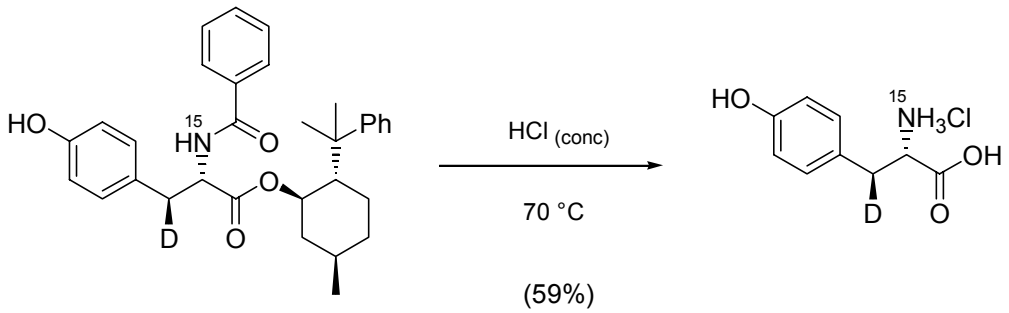

18 **19**

Scheme 3.11 Hydrolysis conditions to give doubly labeled tyrosine derivative **19**.

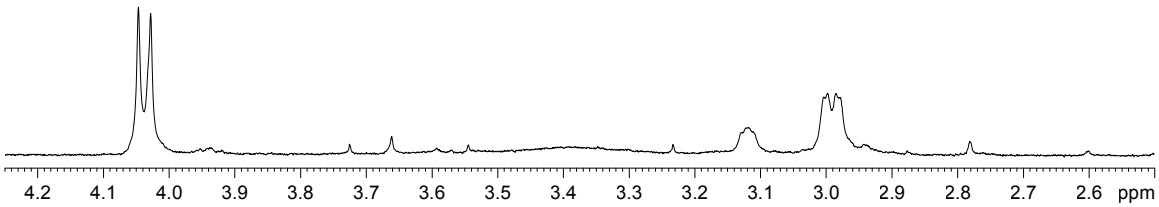

Figure 3.12 Partial ^{1}H NMR spectrum (400 MHz) of crude **19**.

Inspection of the ^{1}H NMR spectrum reveals an approximate 73% de at the α-carbon and 44% de at the β-position. The epimerization observed at the α-carbon is similar to that observed in the case of the phenylalanine derivative (approximately 7%) and is consistent with studies reported in the literature.[100-102] However, the apparent magnitude of β-position epimerization is surprising. Current efforts are focused on fully understanding this apparent loss of stereochemistry at the benzylic center. One possible mechanism for this epimerization would involve the formation of a quinone methide species (Figure 3.13).

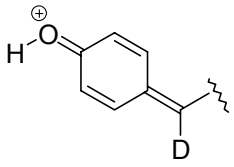

Figure 3.13 Putative quinone methide intermediate leading to β-position epimerization.

These types of intermediates are known to form in many chemical and biological processes. For a recent review, the reader is directed to another reference.[112] These species have also been implicated in the epimerization of chiral benzylic centers of phenol-containing natural products under acidic conditions and high temperatures.[113] The formation of this type of intermediate could be possible with the tyrosine derivative,

but not with the phenylalanine derivative; this is consistent with our observations. The effect of acid concentration and temperature on the reaction is currently being investigated. In the meantime, as a possible improvement in regards to a potential NMR application, the use of DCl in the hydrolysis is being evaluated. If the epimerization is mediated by the formation of the quinone methide species, then deuteration of the methide from DCl may yield a product with an "apparent" reduced epimerization at the β-position in the ^{1}H NMR spectrum because the β-di-deuterio product will be produced.

It is currently believed that the problem may lie with the harsh conditions required to cleave the benzamide protecting group of **18**. Preliminary ^{1}H NMR evidence suggests that the ester protecting group is cleaved initially and that the stereochemical integrity at C3 of the partially deprotected **18** is not compromised. However, long reaction times are required to fully deprotect **18**, and by this time significant benzylic epimerization is observed in product **19**. The benzamide protecting group of **18** is thought to play a critical role in ensuring high stereoselectivities of the alkylation reaction at the α-position (Chapter 2). Therefore, alternative deprotection conditions are being studied for the benzamide protecting group. For example, pyridinium polyhydrogen fluoride has been reported to cleave benzamide protecting groups in peptides in high yields at room temperature.[114] It is hoped that these reaction conditions may minimize the apparent epimerization. However, it is not known if alternative deprotection conditions will have any effect on the apparent epimerization.

3.5 HCA/Polymer-Supported TPP Chlorination Study

The synthetic details presented above represent the final route to the doubly labeled tyrosine derivative. The synthesis is similar to the phenylalanine derivative, however, the use of the required 4-oxygenated benzylic electrophiles had a significant

impact on the required chemistry. Not only was an additional protecting group issue introduced, but also a benzylic halide was used as the electrophile. A chloride was used as the electrophilic species for two reasons: 1) initial investigations of 4-oxygenated benzylic sulfonate esters revealed that these materials were too unstable to be useful as enantiotopically deuterated materials, and 2) the use of the chloride would demonstrate the versatility of the strategy by providing access to the β-position epimer relative to the phenylalanine derivative. Several chlorination conditions were evaluated, however, none proved optimal for the isolation of the 4-oxygenated benzylic chlorides. This led to the HCA/polymer-supported TPP conditions being investigated for this transformation. As previously described, these conditions facilitated the production and isolation of these materials. These reaction conditions were not previously described in the literature. Therefore, it was decided to study the stereochemical outcome of this reaction by investigating the chlorination of a small number of 4-substituted benzylic alcohols.

It is well established that nucleophilic substitution reactions are governed by many principles.[115] Two common nucleophilic substitution pathways are substitution-nucleophilic-unimolecular (S_N1) and substitution-nucleophilic-bimolecular (S_N2). These two mechanisms represent the opposite extremes of reactivity within nucleophilic substitution reactions. Reactions governed by a S_N1 mechanism are characterized by an extensively ionized transition state. The extent of ionization is dependent upon many factors including properties of the solvent and reactants. Conversely, reactions governed by a S_N2 mechanism are characterized by a transition state with significant covalent coordination; the extent of which is also dictated by properties of the solvent and reactants. It well known that S_N1 and S_N2 processes exist as a continuum, with reactions often showing evidence for the existence of both pathways.[115] Benzylic

electrophiles are known to react by both mechanisms. This is partly due to the inherent stability of the benzylic carbocation which can facilitate S_N1 processes.[115] As a result of this continuum of reactivity, reactions involving chiral benzylic centers can yield unexpected stereochemical results.[115-118] Our strategy is dependent on the use of chiral benzylic electrophiles, and maintaining chirality at the benzylic position. It is from this perspective that we were interested in studying the stereochemical course of these chlorination conditions.

3.5.1 Synthesis of stereoselectively deuterated benzylic alcohols

Most of the deuterated alcohols were prepared using the prototypical synthesis shown in Scheme 3.12. As previously described, this synthetic strategy proceeded with excellent chemical yield and deuterium incorporation in most cases.

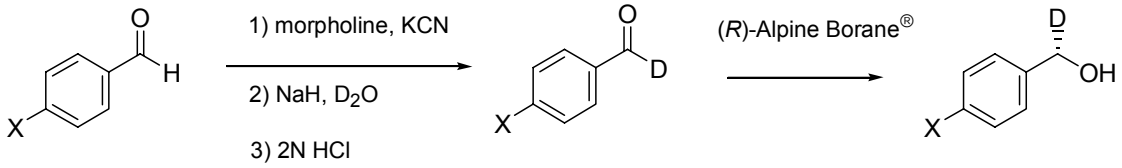

X = H, OTIPS, OCH_3, OBn, NO_2

Scheme 3.12 Prototypical synthesis of enantiotopically deuterated alcohols.

However, with the 4-nitro derivative, the above route yielded unsatisfactory results. The hydrolysis reaction to generate the deuterated aldehyde was low yielding and led to deuteron-proton exchange, presumably via the formation of the resonance stabilized benzylic carbanion species. The exchange problem was overcome by using deuterated mineral acids and D_2O in the hydrolysis reaction. However, the chemical yield of the

aldehyde was not sufficient, therefore, an alternative synthetic route was used to obtain 4-nitrobenzaldehyde-*d* (Scheme 3.13).

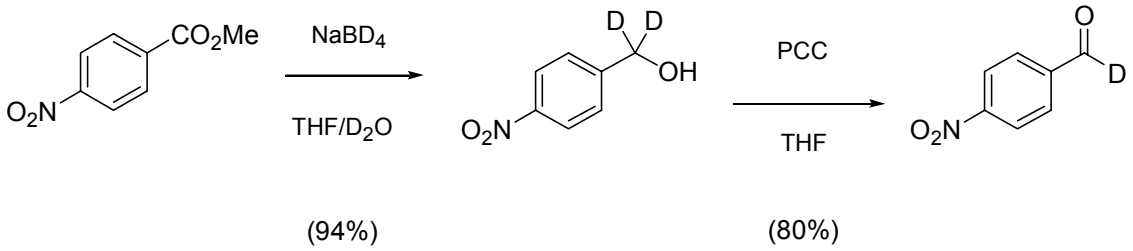

Scheme 3.13 Alternative synthesis of 4-nitrobenzaldehyde-*d.*

The methyl ester of 4-nitrobenzoic acid was prepared using methanol and HCl gas. The methyl ester was reduced using sodium borodeuteride in THF/D_2O to give the di-deuterio alcohol in high yield. This alcohol was then oxidized using pyridinium chlorochromate (PCC) in THF to give the deuterated aldehyde in good yield. This aldehyde was then treated with (*R*)-Alpine Borane® to give the corresponding chirally deuterated alcohol in 51% yield.

The enantioselectively deuterated chlorides were prepared from the alcohols using the HCA/polymer-supported TPP conditions. Optical rotations of both the alcohols and chlorides were recorded. The optical purities of the alcohols were determined using the (-)-camphanate ester as described in Chapter 2. The results are summarized in Table 3.1.

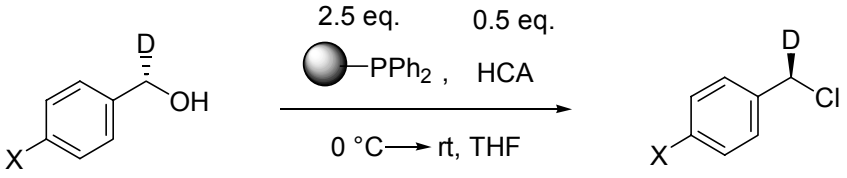

20 **21**

entry	X	ee of (*S*)-**20***	$[\alpha]_D^{21}$ of (*S*)-**20**	yield	$[\alpha]_D^{21}$ of (*R*)-**21**
a	H	96%	+ 1.34° (neat)	64%	- 1.52° (*c* 6.9, THF)**
b	OTIPS	98%	+ 0.30° (neat)	96%	- 0.39° (*c* 15.4, THF)***
c	OCH_3	92%	+ 0.91° (neat)	97%	- 0.18° (*c* 16.6, THF)
d	OBn	95%	+ 0.59° (*c* 5.1, THF)	quant.	- 0.37° (*c* 13.6, THF)
e	NO_2	95%	+ 2.46° (*c* 6.1, THF)	quant.	- 1.31° (*c* 6.9, THF)

*estimated by ^{1}H NMR analysis of (-)-camphanate derivative, **$[\alpha]_D^{25}$ = - 1.53° reported for specific rotation of optically pure material,[119] ***$\geq$ 82% ee by analysis of alkylation reaction product.

Table 3.1 Chlorination studies using HCA / polymer-supported TPP.

As depicted in Table 3.1, the yield of the chlorination reaction is essentially quantitative in most cases except in the simple benzyl case where somewhat lower yields are observed. Optical rotation data for only one of the chlorides, the benzyl chloride **21a**, has been previously reported in the literature. The specific rotation of **21a** generated using the current conditions is comparable to the rotation reported for the optically pure material.[119] The data reported for 4-triisopropylsilyloxy chloride, entry **21b**, is derived from the labeled tyrosine synthesis and is determined from the alkylation product **17**. Although this represents an indirect stereochemical analysis of the chloride, it establishes the lower limit for its optical purity at 82% ee. Optical rotation data for entries **21c-e** have not previously been reported in the literature, therefore, this method

cannot be used to determine optical purity. If desired, the optical purity of these materials could be indirectly analyzed using the alkylation strategy similar to that used for **21b**. In spite of this, the specific rotations for these compounds demonstrate that the products obtained are chiral and do possess rotations of opposite sign from the starting material suggesting similar inversion of the benzylic center.

3.6 Efforts Toward Other ^{15}N-Labeled β-Deuterated Amino Acids

3.6.1 Serine derivative

This synthetic strategy was originally proposed as a route to a variety of amino acids containing prochiral β-methylene protons including aromatic, aliphatic, and heteroatom side chain containing amino acids. The synthesis of a doubly labeled serine derivative was originally planned to represent a heteroatom containing side chain amino acid. Depicted in Scheme 3.14 is the proposed route to a serine derivative using ethyl hippurate as the glycine equivalent. Alkylation of **7** with methyl formate-*d* would yield the α-formyl derivative. Asymmetric reduction of the formyl moiety would yield the stereoselectively deuterated hydroxymethyl side-chain of serine.

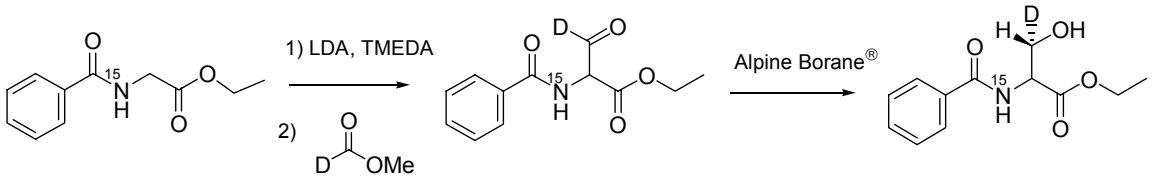

7

Scheme 3.14 Proposed synthesis of a doubly labeled serine derivative.

Initial methods development work was done with unlabeled ethyl hippurate and ethyl formate to establish optimal conditions for the alkylation reaction. Those conditions were found to be the treatment ethyl hippurate with 5 equivalents of LDA and excess methyl formate. From analysis of the crude reaction products, it was apparent that the major isolated material was a mixture of multiple components. Analysis by ^{1}H NMR spectroscopy suggested that a mixture of keto and enol tautomers of the α-formyl material were present (Figure 3.14).

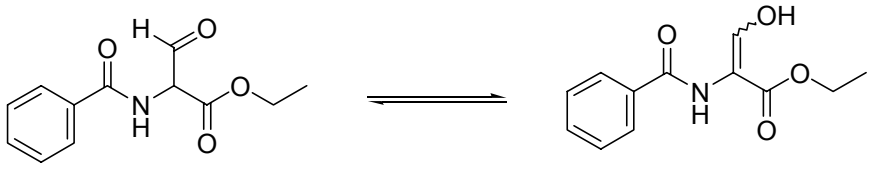

Figure 3.14 Keto-enol equilibrium of α-formyl hippurate derivative.

The conditions used to quench the alkylation reaction and isolate the product were investigated in an effort to minimize the percentage of the enol form of the product that was formed. Limited success with this approach led to attempts to reduce the crude product mixture with both $NaBH_4$ and Alpine Borane® in an effort to obtain the protected serine derivative directly. The enolization of the product represented a major obstacle to the synthesis of this material. Not only did it interfere with the reduction of the formyl group, it would also result in the loss of any stereochemistry introduced at the α-carbon. Therefore, if the L-amino acid derivative was to be synthesized, conditions would have to be found that eliminated or minimized enolization of the product. At this early stage in the project, it was decided to focus on the aromatic amino acids which did not possess this complicating issue.

3.6.2 Histidine and tryptophan derivatives

The strategy is currently being extended to include the other β-methylene unit containing aromatic amino acids, histidine and tryptophan. The synthesis of the doubly labeled materials is being conducted primarily by our collaborator, Dr. Michael J. Panigot at Arkansas State University. However, much of the work in the development of unlabeled electrophiles for the synthesis of the histidine derivative has been carried out in our laboratory. The synthesis of a labeled histidine derivative is dependent on the alkylation of **7** with an enantioselectively deuterated imidazole derivative. Based on previous results, efforts have been focused on the generation of chloromethyl imidazole derivatives as potential electrophiles. A key intermediate for model reactions was *N*-benzyl-4-hydroxymethylimidazole (Scheme 3.15).

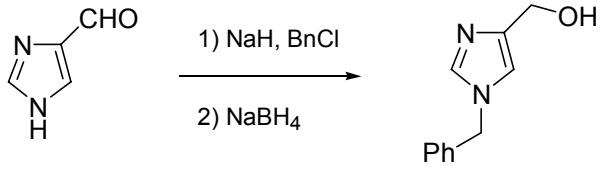

Scheme 3.15 Synthesis of *N*-benzyl-4-hydroxymethylimidazole.

Treatment of 4-formylimidazole with sodium hydride followed by benzyl chloride yielded the *N*-benzylimidazole derivative. Reduction of the formyl group with sodium borohydride gave the hydroxymethyl derivative. Several chlorination conditions were evaluated for the functional group interconversion including Mitsunobu, CCl_4/TPP, and thionyl chloride. The most interesting of those conditions investigated was the previously described HCA/TPP conditions. It has previously been established that these conditions can be used to generate optically active benzylic chlorides from the enantioselectively deuterated alcohols. Using these conditions, the *N*-benzyl-4-

chloromethylimidazole derivative has been synthesized from the hydroxymethyl derivative (Scheme 3.16). Unfortunately, the reaction was not high yielding and only produced enough product to make a putative identification..

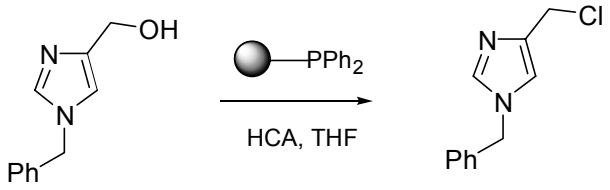

Scheme 3.16 Synthesis of a chloromethylimidazole derivative using HCA/TPP conditions.

Although this reaction was done on an achiral substrate, once the chirally deuterated hydroxymethylimidazole derivative is prepared, these conditions, once optimized, could be used to generate the enantioselectively deuterated chloride. This chloride could then be used to alkylate glycine template **7** in a similar manner as previously described to generate the doubly labeled histidine derivative. The synthesis of the enantioselectively deuterated 4-hydroxymethylimidazole derivative is currently being completed in Dr. Panigot's laboratory. Once in hand, this material will be used for further chlorination and alkylation studies.

In addition to the histidine work, Dr. Panigot's laboratory is currently developing the synthesis of a doubly labeled tryptophan derivative using the described strategy. Current efforts are focused on developing an optimal electrophilic species from the chiral indole derivative (Figure 3.15).

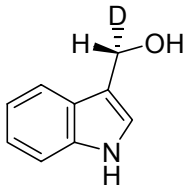

Figure 3.15 Deuterated hydroxymethyl indole derivative to be used for the labeled tryptophan synthesis.

3.7 Synthesis of Stable-Isotope Labeled Cysteine Derivatives

We were recently asked by Dr. John L. Markley from the Department of Biochemistry at the University of Wisconsin-Madison to synthesize two stable-isotope labeled cysteine derivatives to facilitate his NMR research. Dr. Markley is interested in studying the paramagnetic properties of iron-sulfur proteins using NMR spectroscopy. Paramagnetic proteins are characterized by the existence of one or more pairs of unpaired electrons in at least one of the protein's oxidation states.[120] The unpaired electrons often are present in a cofactor such as flavin, a heme with a bound metal center, or a metal cluster. Iron-sulfur proteins are one type of paramagnetic protein and are involved in many different biological processes including enzyme catalysis, gene regulation, and electron transfer.[120] The paramagnetic centers present in iron-sulfur proteins lead to hyperfine-shifted resonances of those residues involved with metal binding. Unfortunately, the paramagnetic centers also result in signal broadening in the NMR spectrum which complicates determining sequence-specific assignments. These assignments are critical for studying the structure and dynamics of these metal binding centers which are defined by the hyperfine-shifted resonances. These shifted resonances originate from critical residues under investigation as they are directly involved with catalysis or electron transfer. Various NMR experiments are used to study

these shifted resonance in these proteins, and these experiments rely on isotopically labeled amino acids.

We have synthesized two stable-isotope labeled derivatives of fully protected cysteine derivatives to be used in solid-phase syntheses of these proteins. These labeled proteins will then be used to facilitate NMR studies of the iron-sulfur redox protein rubredoxin.[120] Rubredoxins represent the simplest type of iron-sulfur proteins as characterized by the iron-sulfur bonding patterns. X-ray crystallography studies have established rubredoxins contain a single iron ion coordinated tetrahedrally by four cysteines.[120] Shown in Scheme 3.17 are the details of the synthesis of (2*S*)-[3,3-$^2H_2$]-*S*-trityl-*N*-fluorenylmethoxycarbonyl-cysteine (**24**). All of the chemistry was optimized using unlabeled starting material before the final labeled syntheses were performed.

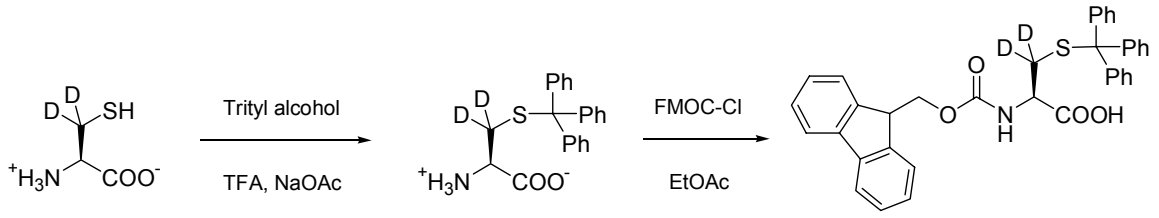

22 (97%) **23** (quant.) **24**

Scheme 3.17 Synthesis of labeled cysteine derivative **24**.

Treatment of [3,3-$^2H_2$]-L-cysteine (**22**) with triphenylmethanol (trityl alcohol), sodium acetate, and trifluoroacetic acid (TFA) yielded the *S*-trityl protected material **23** in excellent yield.[121] The next step was the direct acylation of the amine group using 9-fluorenylmethyl (FMOC) chloroformate in ethyl acetate under refluxing conditions.[122,123] Also, synthesized in a similar fashion was the uniformly ^{15}N, ^{13}C labeled derivative **25** (Figure 3.16). The synthesis of this material also proceeded with excellent yield.

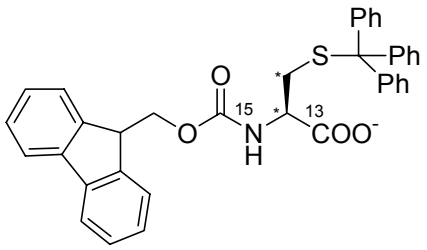

25

Figure 3.16 Structure of (2*S*)-[^{15}N, U-^{13}C]-*S*-trityl-*N*-FMOC-cysteine (**25**).

The amino acids were synthesized in our laboratory and sent to Dr. Markley where they have been incorporated into various rubredoxin mutants with altered redox properties using peptide solid phase synthesis methods. Current efforts in Dr. Markley's lab are focused obtaining sequence specific assignments using the labeled proteins and continuing studies of the altered redox properties of these mutant proteins using NMR methods.

3.8 Summary

A simple yet versatile strategy for the chemical synthesis of ^{15}N-labeled stereoselectively β-deuterated amino acids has been described. The utility of the method was first demonstrated with the synthesis of a phenylalanine derivative. This chapter summarizes our efforts to extend the strategy to include a tyrosine derivative. The use of a 4-oxygenated benzylic electrophile has a significant impact on the chemistry that is required. Several electrophiles have been investigated in the alkylation reaction, as well as alternative glycine equivalents. The current synthetic route to the labeled tyrosine derivative relies on a 4-triisopropylsilyoxy protected benzyl chloride in the alkylation of a (-)-8-phenylmenthylhippurate ester.

As a result of our interest in stereoselectively deuterated benzylic chlorides, we have investigated the HCA/polymer-supported TPP chlorination conditions on a small series of benzylic alcohols. It appears that these reaction conditions generate the optically active chloride from the corresponding alcohol in high yield with a high degree of inversion. Finally, we have prepared protected stable-isotope labeled cysteine derivatives to be used by our collaborators to facilitate NMR studies of iron-sulfur containing proteins. Current efforts are focused on fully characterizing the apparent epimerization observed at the benzylic position of the tyrosine derivative, and optimizing the final deprotection strategy to minimize this process. In addition, our collaborators are currently working on key components of the synthesis that will be used to elaborate this strategy to doubly labeled histidine and tryptophan derivatives.

PART 2. SYNTHESIS OF MECHANISTIC PROBES OF RETINOID ACTION

CHAPTER 4

SYNTHESIS OF MECHANISTIC PROBES OF RETINOID ACTION

4.1 Statement of the Problem

N-(4-Hydroxyphenyl)retinamide (4-HPR), a synthetic amide analog of retinoic acid, has been studied extensively as a cancer chemopreventive and chemotheraupeutic agent. However, the mechanism through which 4-HPR exerts its biological effects remains unclear. It has been demonstrated that 4-HPR binds with virtually no affinity to the nuclear retinoid receptors (RARs and RXRs) and that it induces apoptosis in most tumor cells. This is in direct contrast to retinoic acid, which binds to the RARs with high affinity and induces differentiation in tumor cells. These data suggest that 4-HPR and retinoic acid may act, at least in part, at different cellular targets. In an effort to identify possible alternative targets of 4-HPR binding, we have synthesized a series of photo/affinity label analogs. Details of the syntheses and preliminary chemical reactivity are presented.

4.2 Introduction to Retinoids

The term “retinoid” refers to natural and synthetic compounds structurally related to and/or possessing similar biological activity as vitamin A (retinol; ROL) (Figure 4.1). The naturally occurring retinoids are fat-soluble polyene containing compounds that play essential roles in many normal mammalian processes including vision, reproduction,

metabolism, differentiation, bone development, embryonic development, and immune function.[124] Shown in Figure 4.1 is a general structure of the major naturally occurring retinoids with the commonly accepted numbering convention.

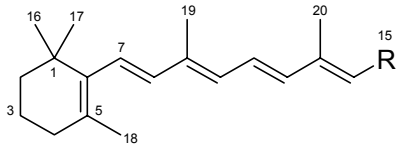

R = CH_2OH (retinol, ROL, vitamin A)

R = CHO (retinal, RAL)

R = COOH (retinoic acid, RA)

Figure 4.1 Structure of the major naturally occurring retinoids.

Vitamin A is an essential nutrient that is obtained through dietary sources originating from provitamin A carotenoids in vegetables or retinyl ester stores from animal sources. One of the primary functions of ROL is to serve as a precursor for the other significant naturally occurring retinoids, retinal (RAL) and retinoic acid (RA) (Figure 4.1). *In vivo*, RAL is synthesized from the reversible oxidation of ROL. The primary function of RAL is to serve as the visual pigment chromophore in the visual cycle. A comprehensive discussion of the visual cycle is not the intent of this document, therefore, the reader is directed to an additional reference for further reading.[124] Retinoic acid is produced from the irreversible oxidation of RAL and is associated with many biological functions including maintenance of growth and epithelial cell differentiation. Other than in visual and some aspects of reproduction function, it is commonly accepted that RA is the active form of vitamin A, and its pleiotropic effects are mediated by nuclear retinoid receptors.

4.3 Retinoid Receptors

The discovery of retinoic acid receptors in 1987 was a quantum leap forward in understanding the mechanism of action of these compounds.[125,126] Since those initial reports, two classes of receptors have been identified: retinoic acid receptors (RARs) and retinoid X receptors (RXRs). The natural ligands for the RARs include both all-*trans*-RA (atRA) and 9-*cis*-RA while the RXRs only bind 9-*cis*-RA (Figure 4.2).

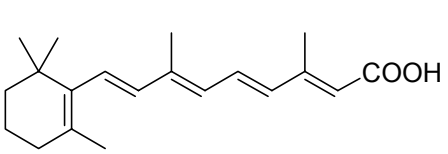

all-*trans*-RA (atRA)

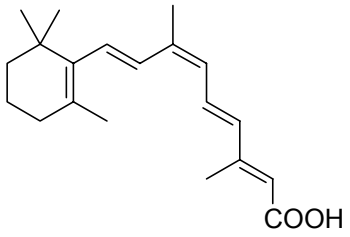

9-*cis*-RA

Figure 4.2 Structures of atRA and 9-*cis*-RA.

Three receptor subtypes have been characterized for each of the RARs and RXRs: α, β, and γ.[124] These receptor isoforms are expressed in unique patterns during development and in the mature organism. The role of the different subtypes as mediators of different functions is suggested by these unique expression patterns during development and in the adult organism.[124]

The retinoid receptors (RARS and RXRs) are just one class of receptors that belong to the superfamily of steroid/thyroid hormone receptors.[127] In general, these receptors regulate gene expression by interacting with specific DNA sequences present in the target gene promoter regions. These sequences are known as hormone response elements (HREs) and help to convey specificity to gene transcription. Different classes of receptors recognize unique HREs, therefore, each receptor class activates different

target genes. This superfamily of receptors is characterized by their modular structure consisting of six functional domains within the protein which are designated A through F (Figure 4.3).

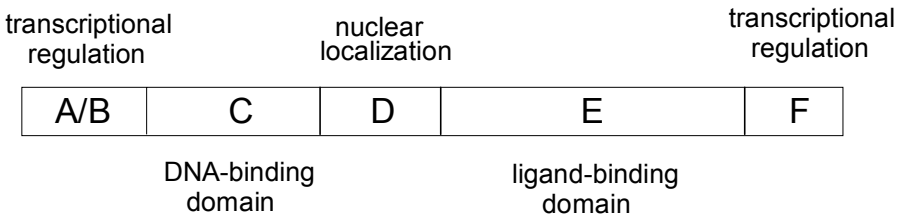

Figure 4.3 Representation of the modular structure of steroid/thyroid superfamily of receptors.

The major functional domains are the DNA binding domain (C) and the ligand binding domain (E). The DNA binding domain is defined by two zinc finger DNA binding motifs which interact with the HREs and is, therefore, responsible for the targeting of receptors to the appropriate HREs.[127] The ligand binding domain has several functions including hormone binding receptor, homo- and/or heterodimerization, formation of heat shock protein complexes, and transcriptional activation and repression.[127] Domains A, B, and F are also involved with transcriptional activation and help to provide specificity to gene activation. Domain D is termed the hinge region and contains the nuclear localization signal.

Activation of the RARs and RXRs requires ligand binding which results in the dimerization of these receptors.[124] The RARs function as a heterodimer comprised of a RXR partner, while RXR functions can be mediated by the formation of homodimers or heterodimers with the vitamin D receptor, thyroid hormone receptor, peroxisome proliferator activated receptor, and various orphan receptors.[124] Thus, the activation of

the RXR pathway can result in the signaling of many other receptor systems. The dimeric receptors bind to retinoid HREs termed retinoic acid response elements (RAREs) or retinoid X receptor response elements (RXREs) found in the promoter regions of retinoid sensitive genes. In general, the retinoid response elements are characterized by nucleotide sequences consisting of direct repeats of AGGTCA separated by only a few nucleotides, however, the RARs have been found to bind to a number of RAREs.[128]

There are several ways by which the retinoid receptors regulate gene transcription. When the receptor dimer forms a ternary complex with DNA, the result is a conformational change that either results in transcription or repression of the target gene and subsequent modulation of the mRNA levels. Target gene transcription and up regulation of mRNA levels occur when additional *trans* acting transcription factors are recruited to the complex. When corepressors are recruited, the result is the down regulation of the gene products. The RARs and RXRs can also regulate gene function indirectly through their interaction with other transcriptional factors.[128] For example, the activator protein-1 (AP-1) binds to AP-1 sites in the promoter region of target genes. The cyclic AMP response elements binding protein (CBP) binds to AP-1 to up regulate gene transcription from the AP-1 sites. However, in the presence of retinoids, a complex is formed between retinoid receptors and CBP which inhibits CBP's ability to activate gene transcription.[129,130]

The mechanisms by which RARs and RXRs mediate their actions are complex. Considering the different receptor classes, receptor subtype variability, RARE/RXRE variability, heterogeneous tissue distribution, and the existence of "cross-talk" with "non-retinoid" signaling pathways, it is clear that much research needs to be done to further

elucidate these mechanisms. It is also apparent that within this complex signaling pathway, there exists the possibility that “alternative” or yet to be discovered pathways may exist.

4.4 Therapeutic Uses of Retinoids

Retinoic acid and its analogs have found uses as therapeutics because of their antiproliferative effects in tissue epithelium. Both naturally occurring and synthetic retinoids have been used clinically in the treatment of dermatological disorders such as psoriasis, cystic acne, and cutaneous disorders of keratinization.[124] In addition, many analogs have been studied as chemopreventives and chemotherapeutic agents for the treatment of numerous cancers. Various analogs have been studied, undergone clinical trials, or have found clinical uses for leukemia, breast, lung, cervical, ovarian, head and neck, skin, bladder, liver, pancreatic, and oral cancers.[124,131-135] Although many retinoids have been investigated as therapeutics, their efficacy is often limited by their liver toxicity, teratogenicity, and skin toxicity.[124,135] Perhaps the most studied retinoid analog for cancer chemoprevention and chemotherapy is the synthetic analog *N*-(4-hydroxyphenyl)retinamide (4-HPR) also known as Fenretinide® (Figure 4.4).

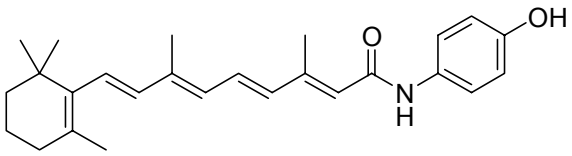

Figure 4.4 Structure of *N*-(4-hydroxyphenyl)retinamide.

N-(4-hydroxyphenyl)retinamide was originally synthesized by Gander and Gurney in 1978.[136] The biological activity was described by Moon and co-workers.[137] In

that report, 4-HPR was found to have significant activity in reversing keratinization in vitamin A deficient hamster tracheal organ culture, an assay used to monitor differentiation activity. Subsequent studies have demonstrated that 4-HPR possesses promising chemoprevention activity in many malignancies including breast, prostate, bladder, and skin cancers.[131-133] The incorporation of the hydroxyphenyl moiety into the parent structure results in a more effective, less toxic chemopreventive agent as compared to atRA. This reduced toxicity is due in part to 4-HPR's minimal accumulation in the liver and the increased chemoprevention activity has been attributed to its greater accumulation in fat tissue, prostate, and muscle.[138,139] The most significant side-effects observed with 4-HPR treatment are impaired dark adaptation or nightblindness and dry skin, however, these quickly subside once treatment is discontiuned.[128]

4.5 Mechanism of 4-HPR Action

Much research has been conducted in an effort to determine if the actions of 4-HPR are mediated by the nuclear retinoid receptors. There is a substantial body of evidence to suggest that 4-HPR operates by both receptor dependent and independent pathways. For example, in some cancer cell lines, treatment with 4-HPR induces RARβ expression, [140,141] and transactivation studies have shown that 4-HPR can activate RARα, RARβ, and RXR.[142] It has also been demonstrated that RAR antagonists can block 4-HPR-induced apoptosis.[143,144] There is also substantial data to suggest that 4-HPR's actions are receptor independent.[145] For example, 4-HPR and related analogs have been shown to possess virtually no affinity for the nuclear receptors.[146] In addition, 4-HPR has been shown to be an effective inducer of apoptosis in cells that are unresponsive to RA treatment and cells that have been genetically manipulated to not

express the retinoid receptors.[147] Finally, one of the most interesting observations is that in many cancer cell lines, RA induces differentiation while 4-HPR induces apoptosis.[148]

Induction of apoptosis is an almost uniform response of cells to treatment with 4-HPR.[148] Apoptosis or "programmed cell death" can be viewed as a macromolecular synthesis dependent mechanism of cell death.[148] It can be initiated by a variety of stimuli and appears to be a complex, multifaceted process that is cell-type and cell-line dependent. Apoptosis is distinct from pathologically based necrotic cell death. Apoptotic cell death is associated with cell shrinkage, chromatin condensation, membrane blebbing, and the formation of apoptotic bodies.[148] By comparison, cell death by necrosis is accompanied by swelling and rupture, leakage of cellular contents and induction of an inflammatory response.[148]

The antiproliferative effects of 4-HPR have been demonstrated in many tumor cell lines, however, its mechanism of action is still unclear. Although 4-HPR has demonstrated some atRA-like effects, the majority of its actions are unique. The current body of evidence suggests that its activity may occur through an alternative mechanism of action rather than mediation via the nuclear retinoid receptors. We are interested in further elucidating this alternative mechanism or mechanisms to discover the molecular targets of 4-HPR.

Our lab has a primary interest in the synthesis of molecules that are designed to probe the mechanism by which 4-HPR and related compounds mediate their action.[149-152] One fundamental concern is that some of the activity observed with 4-HPR may be due, in part, to small quantities of RA, which is liberated by limited hydrolysis of the amide bond. Many of the molecules synthesized in our laboratory are metabolically stable analogs of 4-HPR, which possess enhanced chemopreventive and/or

chemotherapeutic activity with reduced RA-like effects. One molecule that would greatly aid these types of studies is a highly potent RAR antagonist. Use of this type of compound in biological evaluation studies would ensure that the receptor mediated pathways are blocked. It would also be used to demonstrate that limited hydrolysis may be occurring by abolishing any RA-like effects. One such antagonist has been described by Chandraratna and co-workers.[153] The compound, termed AGN193109, is shown in Figure 4.5.

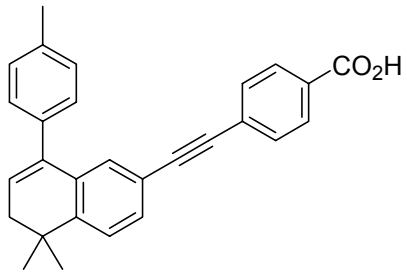

Figure 4.5 Structure of RAR antagonist AGN193109.

In that initial disclosure, the authors report that AGN193109 binds to all three subtypes of the RARs with very high affinity, K_d = 2-3 nm. This represents a 4-6 fold higher affinity than RA showed in the same assay. In addition, AGN193109 showed no transactivation activity in a gene transcription assay, even at receptor saturating concentrations.

4.6 Synthesis of RAR antagonist

Since the antagonist was not available to us, the synthesis of the antagonist was patterned after a published procedure.[154] The first two steps in the synthesis are shown in Scheme 4.1. The first reaction in the sequence was a Grignard reaction of acetone with the magnesium bromide species obtained from 1-bromo-3-phenylpropane to form

the tertiary alcohol. The alcohol was then treated with phosphorous pentoxide and methanesulfonic acid to yield the cyclized product.

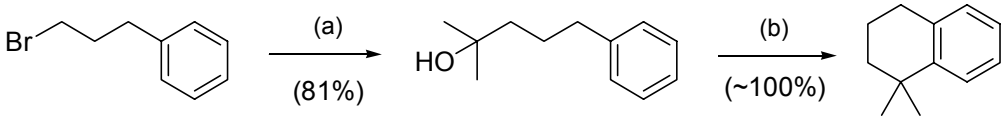

Scheme 4.1 Annulation reaction sequence of the AGN193109 synthesis. (a), i, Mg, diethyl ether, reflux; ii, acetone, rt, 4N HCl, 0 °C; (b) P_2O_5, CH_3SO_3H.

The cyclic product was then treated with chromium trioxide in benzene to oxidize the benzylic position to give the ketone derivative in good yield (Scheme 4.2). Bromination of the aromatic ring was accomplished by treating the ketone with aluminium chloride and bromine to give the precursor for the alkyne coupling reactions.

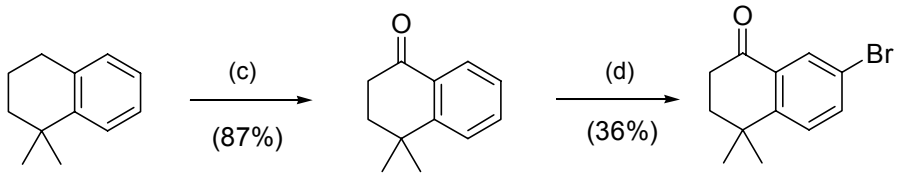

Scheme 4.2 Synthesis of aryl bromo-ketone intermediate. (c) HOAc, acetic anhydride, CrO_3, benzene, 0 °C; (d) $AlCl_3$, Br_2, CH_2Cl_2, reflux.

It was of interest to note that the use of anhydrous aluminium chloride was required to mediate the bromination reaction. In all cases when partially hydrated reagent was used, the α-dibromo product (Figure 4.6) was isolated as the exclusive product as determined by ^{1}H NMR spectroscopy.

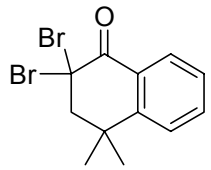

Figure 4.6 Structure of putative side-product from bromination.

The next series of steps involved the introduction of the alkyne moiety and took advantage of the Sonogashira coupling reaction (Scheme 4.3).[155] In the first coupling, treatment of the bromo-ketone with (trimethylsilyl)acetylene in the presence of bis(triphenyphosphine)palladium(II) chloride, copper(I) iodide, and triethylamine gave the terminal alkyne in excellent yield. In the second coupling, the terminal alkyne was reacted with ethyl 4-iodobenzoate under the same conditions to give the desired product in essentially quantitative yield

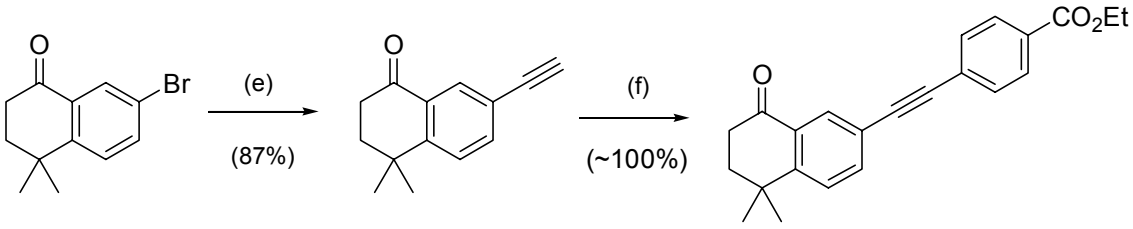

Scheme 4.3 The Sonogashira[155] couplings in the synthesis of AGN193109. (e) (trimethylsilyl)acetylene, 5 mol% $Pd(PPh_3)_2Cl_2$, CuI, NEt_3, 100 °C, sealed bottle; (f) ethyl 4-iodobenzoate, 5 mol% $Pd(PPh_3)_2Cl_2$, CuI, NEt_3.

The final steps in the synthesis are shown in Scheme 4.4. The conversion of the ketone to the vinyl triflate species was accomplished using 2-[*N*,*N*-bis(trifluoromethylsulfonyl)amino]-5-chloropyridine as a triflating agent to trap the lithium enolate derived from the ketone.[156] Reaction of the vinyl triflate with the organozinc

species derived from 4-bromotoluene under Heck conditions gave the vinyl tolyl derivative in high yield.[157] Hydrolysis of the ethyl ester yielded the final product.

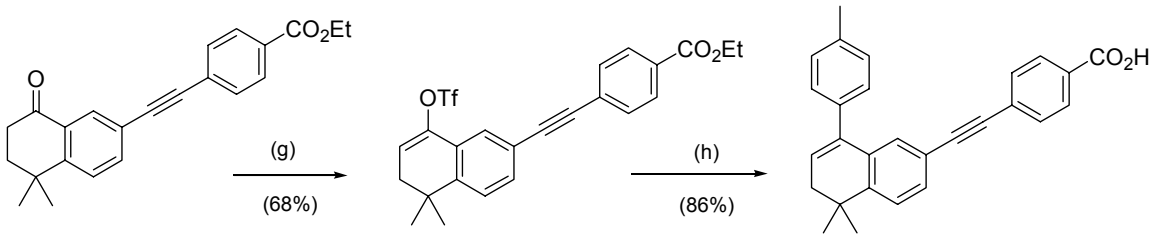

Scheme 4.4 Final two steps in the synthesis of AGN193109. (g) LDA, 2-[*N*,*N*-bis(trifluoromethylsulfonyl)amino]-5-chloropyridine, THF, -78 – 0 °C; (h) i, 4-bromotoluene, *t*-BuLi, $ZnCl_2$, $Pd(PPh_3)_4$ THF; ii, lithium hydroxide hydrate, THF/H_2O 4:1.

This compound is currently being used by our collaborators in the laboratory of Dr. Margaret Clagett-Dame at the University of Wisconsin-Madison for the biological evaluation of synthetic 4-HPR analogs.

4.7 Synthesis of Affinity Label Analogs of *N*-(4-hydroxyphenyl)retinamide

Affinity labeling is a technology that has been developed to study the interactions between biological molecules. It is used to help characterize the spatial relationship between a ligand and its corresponding receptor. The term “ligand” can be used in many different contexts, but often refers to enzyme substrates, allosteric effectors, haptens, neurotransmitters, hormones, or other biochemical entities of interest.[158] These ligands bind to receptors in the course of exerting their biological action. The term “receptor” usually refers to enzymes, immunoglobulins, or other macromolecules which bind neurotransmitters, hormones, or other similar molecules.[158] The goal of an affinity labeling experiment is often to locate the portion of a receptor that is involved in ligand

binding.[158] Two types of affinity labeling experiments are commonly conducted: electrophilic affinity labeling and photoaffinity labeling (Figure 4.7).

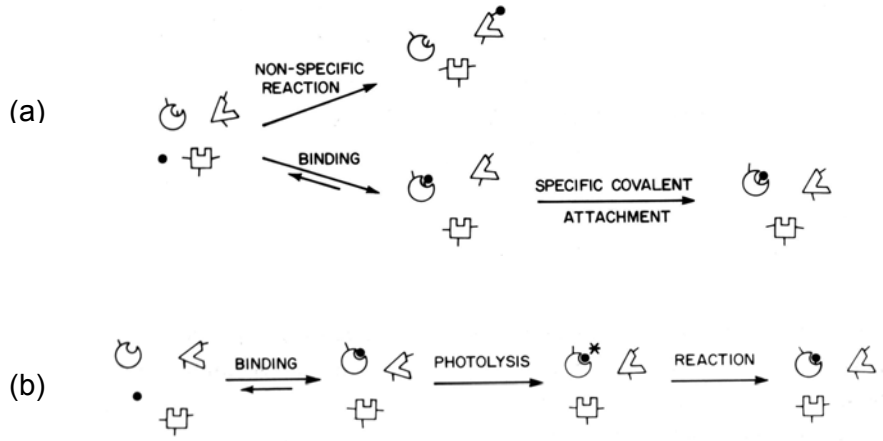

Figure 4.7 Schematic representation of affinity labeling experiments. (a) electrophilic affinity labeling; (b) photoaffinity labeling. (figure taken from reference 158)

In an electrophilic affinity labeling experiment, the ligand contains an electrophilic group that can react with nucleophilic centers in the receptor. When the ligand binds to the receptor, a proximal nucleophile in the binding site reacts with the electrophilic moiety in the ligand forming a covalent bond between the two species. Common electrophilic groups used in labeling experiments include: α-halo ketones, epoxides, haloacetamides, and isothiocyanates.[159] In a photoaffinity labeling experiment, the ligand contains a latent reactive group that is selectively activated upon irradiation with ultraviolet (UV) or visible light. Upon irradiation, the photoreactive group in the ligand forms a reactive intermediate which then alkylates the receptor forming a covalent bond between the ligand and receptor. Common photoreactive groups employed in photoaffinity experiments include: aryl azides, diazo compounds, diazirines, enones, and halogenated substrates.[160] Depending on the technique employed and the chosen ligand, the covalently modified receptor can be analyzed by a variety of methods.

Common approaches include radiolabeling, spectroscopic analysis including fluorescence measurements, visualization by staining, and hydrolysis followed by fragment analysis using mass spectrometry or HPLC.[160]

A comparison of the two methods reveals that both techniques are commonly used to provide structural information about interactions of a ligand-receptor complex. For recent examples of electrophilic affinity labeling[161-164] and photoaffinity labeling[165-168] the reader is directed to the cited references. Each of the two methods, although similar in result, possesses their own advantages and disadvantages, and are often used in conjunction to complement the other.

An analysis of the two methods reveals that photoaffinity labeling offers several theoretical advantages over electrophilic affinity labeling.[158] The inert ligand of a photoaffinity experiment is preferable because it allows binding experiments and biological activity to be determined with minimal difficulty. These photoreactive ligands can be treated just as the "natural" ligands with minimal likelihood of degradation of the compounds. However, the presence of a highly reactive group, as in the case of electrophilic affinity experiments, occasionally complicates these preliminary experiments as care must be taken to avoid decomposition of the test compound. An additional advantage is the unmasking of the reactive species is initiated in a controlled manner with the use of irradiation to activate the photolabel. One of the problems associated with electrophilic affinity labeling experiments is the non-specific reaction of the ligand with nucleophiles other than those present in the ligand binding site. These nonspecific interactions often occur during the association of the ligand with the receptor, but before a binding equilibrium has been established. Finally, the reactive intermediates formed upon irradiation of photoaffinity labeling probes are usually more

reactive than those groups employed in electrophilic affinity labeling experiments.[158] A highly reactive species helps to ensure that covalent modification occurs in the ligand binding site before the ligand has an opportunity to equilibrate out of the binding pocket.

The most common reactive intermediates in photoaffinity labeling are carbenes and nitrenes which are neutral divalent carbon and monovalent nitrogen containing species respectively. These materials are highly reactive and can undergo several different reaction pathways. Shown in Figure 4.8 are some typical reactions of carbenes.[158] Nitrenes are generally less reactive than carbenes, however, they can also undergo analogous reactions as those depicted below.

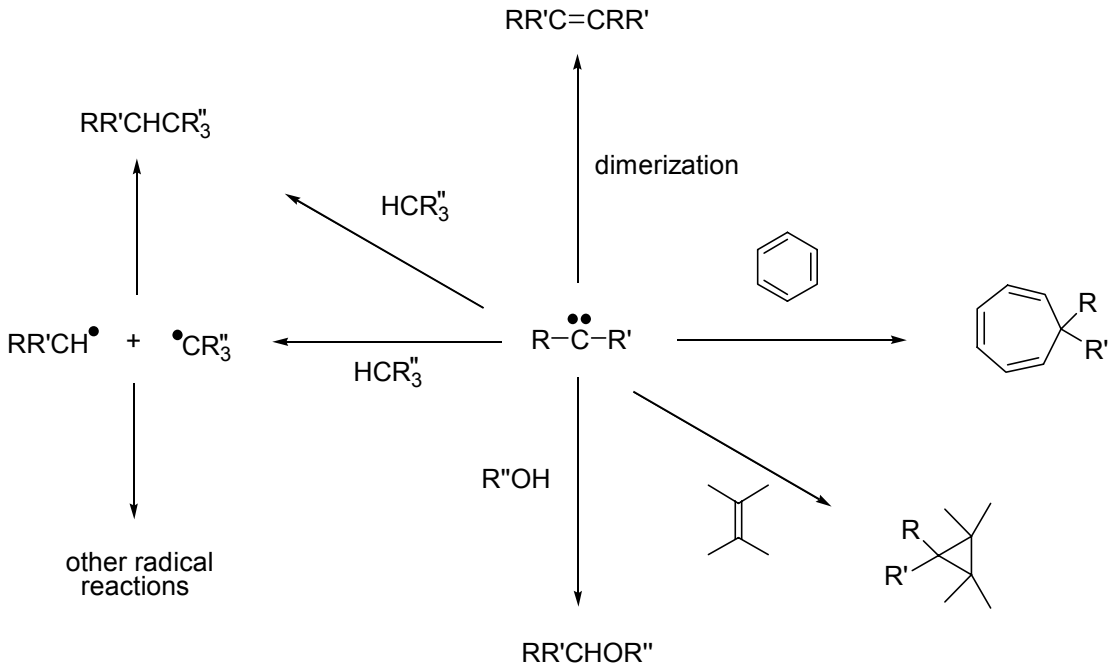

Figure 4.8 Typical reactions of carbenes.[158]

Besides reacting with nucleophilic groups, carbenes and nitrenes are capable of reacting by carbon-hydrogen bond insertion with saturated hydrocarbons and by addition

to unsaturated compounds including aromatic molecules. Due to this reactivity, a nucleophilic center need not be present to mediate the labeling reaction. Therefore, carbene and nitrene reactions are independent of the nature of the ligand binding site and can be used to label many types of receptors, not only those that contain nucleophilic sites.

Perhaps the most significant limitation of photoaffinity labeling experiments is that cross-linking often proceeds with low efficiencies. This can be especially true with the use of nitrenes as the labeling species.[160] A survey of the literature reveals that aryl azides have been the most popular photoaffinity labeling reagents[160] to date, consequently aryl nitrenes have been studied quite extensively. The popularity of aryl azides is due in part to their ease of preparation. Although aryl azides have been utilized comprehensively in affinity labeling, photolabeling experiments involving nitrenes can suffer from low labeling efficiencies.[160] This lack of efficiency has been explained by an examination of the photochemistry of aryl azides.[160,169] Irradiation of phenyl azide produces a singlet nitrene, which can undergo intersystem crossing to the ground state triplet (Figure 4.9).[160,169]

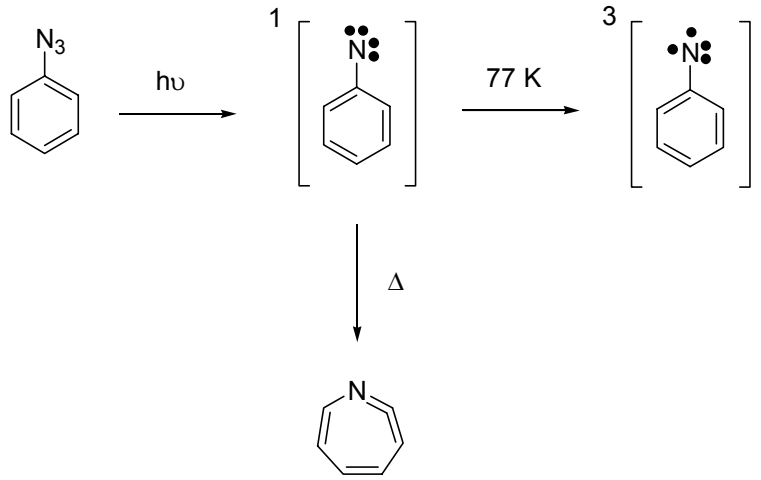

Figure 4.9 Photochemistry of phenyl nitrene.[160,169]

However, the energy barrier for the conversion of the singlet state to the triplet state is sufficiently high that at low temperatures, chemistry from the singlet species can be observed.[160] In general, the singlet nitrene species is preferred for labeling experiments due to its greater reactivity. The singlet phenyl nitrene undergoes ring expansion to give a ketenimine azepine.[160] This compound can react with nucleophiles, however its long lifetime and stability are not ideal for rapid reaction.[160] The triplet nitrene species behaves as a diradical, and can either undergo recombination or hydrogen abstraction followed by a radical coupling reaction. Electron withdrawing groups on the aromatic nucleus have been used to increase the reactivity of aryl nitrenes by diminishing the population of the triplet species and by increasing the electrophilicity of the ring expansion products arising from the singlet nitrene.[158]

One area of interest in our laboratory is the elucidation of the mechanism by which 4-HPR (Figure 4.4) exerts its chemopreventive/chemotherapeutic effects.[149-152,170-172] As previously described the mechanism of 4-HPR is complex and remains unclear. One question that has yet to be answered is whether some of the biological effects of 4-

HPR and related analogs are due, in part, to small quantities of RA being liberated by limited hydrolysis of the amide bond. Retinoic acid is a very potent inducer of cell differentiation, therefore, limited hydrolysis of 4-HPR may produce sufficient quantities of RA to invoke a response. This sequence of events would help explain the apparent dual mechanism of action of 4-HPR and related analogs. In an effort to answer this question, research from our laboratory has resulted in the synthesis and biological evaluation of several metabolically stable analogs of 4-HPR.[149,151,170,171]

Biological evaluation of these compounds by our collaborators suggests that limited hydrolysis of retinamides may play a role in the production of retinoic acid like effects.[149,170] These observations support the hypothesis that 4-HPR may act, at least in part, at a different molecular target other than the nuclear retinoid receptors. As a result of these studies, we are beginning efforts to discover these possible alternative targets with the use of affinity label analogs of 4-HPR. Previous work from our laboratory has led to the synthesis of a small library of 43 analogs of 4-HPR.[173] These compounds were prepared in an effort to discover more potent analogs of 4-HPR and to develop a structure-activity relationship (SAR) of the aromatic portion of the molecule. Shown in Table 4.1 are the anilinamide analogs of 4-HPR that were prepared. Of these compounds that were prepared, 7 novel analogs showed antiproliferative activity in MCF-7 cells, a human mammary tumor cell line. A subset of these also possessed apoptotic activity in MCF-7 cells similar to that of 4-HPR (unpublished results). Although no SAR is readily apparent, this data suggests that substitution of the aromatic ring is tolerated and can produce compounds with activity similar to that of 4-HPR. In addition to these analogs, a few other biologically active 4-HPR analogs with simple substitution of the aromatic ring have been described in the literature.[174-176] Some of these analogs

have proven to be more potent than 4-HPR against some cancer cell lines. Additionally, analogs reported from our group, although involving more than simple aromatic substitutions, also suggest that derivatives of the aromatic ring are tolerated, and in some cases, lead to a more potent compound.[177]

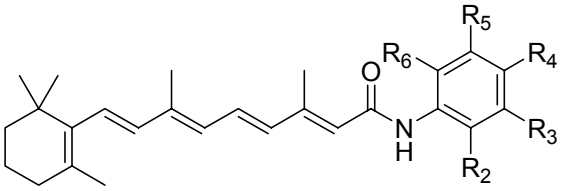

R_2	R_3	R_4	R_5	R_6
H[a,b]	H	OH	H	H
CH_3[b]	H	OH	H	H
CH_3	H	OH	CH_3	H
OH	H	CH_3	H	H
OH	H	H	CH_3	H
OH	H	H	$C(CH_3)_3$	H
OH	H	H	H	CH_3
H[a,b]	OH	CH_3	H	H
CH_3	OH	H	H	H
H	OH	OCH_3	H	H
Cl	H	OH	H	H
H[a,b]	Cl	OH	H	H
OH	H	H	Cl	H
H	Cl	OH	Cl	H
H	Br	OH	Br	H
OH	Cl	CH_3	Cl	H
NO_2	H	OH	H	H
H	NO_2	OH	H	H
OH[a,b]	H	NO_2	H	H
OH[a]	H	H	NO_2	H
OH	CO_2CH_3	H	H	H
OH	CO_2H	H	H	H
OH[a]	H	CO_2CH_3	H	H
OH	H	CO_2H	H	H
OH	H	H	H	CO_2CH_3
OH	H	H	H	CO_2H
H	OH	CO_2CH_3	H	H
H	OH	CO_2H	H	H
H[a]	CO_2CH_3	OH	H	H
H	CO_2H	OH	H	H
OH	H	H	CO_2CH_3	H
OH	H	$SO_2CH_2CH_3$	H	H
CH_2OH	H	H	H	H
H[a]	CH_2OH	H	H	H
H[a]	H	NH_2	H	H
CO_2CH_3	H	H	H	H
CO_2H[a]	H	H	H	H
H	H	OCH_2CH_3	H	H

* [a]compounds with growth inhibition activity; [b]compounds with apoptosis inducing activity

Table 4.1 Library of anilinamide analogs* of 4-HPR previously prepared.[173]

It was hypothesized that a good starting point for these studies was the synthesis of several electrophilic and photoaffinity label analogs of 4-HPR. It was believed that the synthesis of these initial compounds could be guided by the limited SAR obtained from our library of analogs and their preparation should be relatively straightforward. Examination of the active compounds from Table 4.1 reveals that a wide range of functional groups are tolerated at the 4-position as well as the 2-position. Functional groups that are accepted at the 4-position include methoxy, methyl, nitro, carbomethoxy, and amino moieties; hydroxy, methyl, and carboxylic acid groups are apparently tolerated at the 2-position. It was hoped that by using this information, several electrophilic and photoaffinity label analogs could be synthesized which incorporated simple haloacetamido, isothiocyanato, and azido substitutions. The acetamido group is a "nonclassical" bioisostere replacement for the hydroxy moiety.[178] Thus, it is reasonable to expect that the haloacetamido compounds may possess similar activity as 4-HPR or some of the other hydroxy containing analogs. Rationale for some of the azido derivatives can perhaps be derived from examining data from the nitro containing analogs (Table 4.1). The 2-hydroxy-4-nitro analog indicates that a dipolar substitutent is tolerated at the 4-position when a 2-position hydroxyl is present. With this information in hand, initial efforts were focused on the generation of the electrophilic affinity label analogs.

4.8 Synthesis of Electrophilic Affinity Label Analogs

Initial efforts were focused on the synthesis of the analogs shown in Figure 4.10. It was believed that these compounds would be accessible in a straightforward manner and would provide a good starting point for labeling studies.

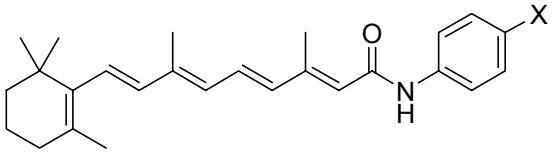

X
$NHCOCH_2Cl$
$NHCOCH_2Br$
$NHCOCH_3$
NCS

Figure 4.10 Electrophilic affinity label analogs of 4-HPR and the 4-acetamido analog.

The haloacetamido derivatives would be prepared as potential electrophilic labels and the 4-acetamido analog would be synthesized as a model compound. These types of compounds can be directly prepared from the amino compound which makes *N*-(4-aminophenyl)retinamide (4-AmPR) a key intermediate (Figure 4.11)

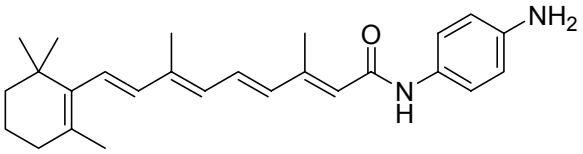

Figure 4.11 Structure of 4-AmPR.

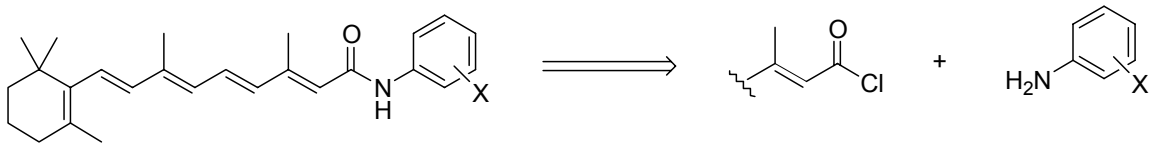

Figure 4.12 Retrosynthesis of retinamide analogs.

In general, these retinamide analogs are synthesized using a coupling reaction involving retinoyl chloride and the appropriate aniline precursor (Figure 4.12). Key elements of this type of disconnection include the synthesis of the appropriate aniline precursor and the generation of the acid chloride. The anilines represent important intermediates, but can be obtained in a simple manner. The HCA/TPP system,[111,173] the same conditions also used in the preparation of deuterated benzyl chlorides (Chapter 3), has proven to be a valuable means of obtaining the unstable retinoyl chloride in an acid free manner. The minimization of acidic by-products reduces acid-catalyzed processes which can lead to isomerization and decomposition of the labile polyene structure. Another method to generate retinoyl chloride is the treatment of retinoic acid with thionyl choride. This more conventional approach has also proven successful when working with these acid sensitive compounds. During the course of these syntheses, both methods were used. However, the thionyl chloride method was used more often due to the scale of the reactions. The stoichiometry required using the polymer supported phosphine would necessitate relatively large amounts of the costly resin (~$30/g). In spite of the non-acid free conditions of the thionyl chloride route, these conditions were found to give adequate results with no significant acid catalyzed degradation being observed.

The first compound synthesized was the model compound *N*-(4-acetamidophenyl)retinamide (4-AcPR) (Scheme 4.5). This compound was prepared because it represents a stable model of the haloacetamide derivatives and its biological activity has never been investigated.

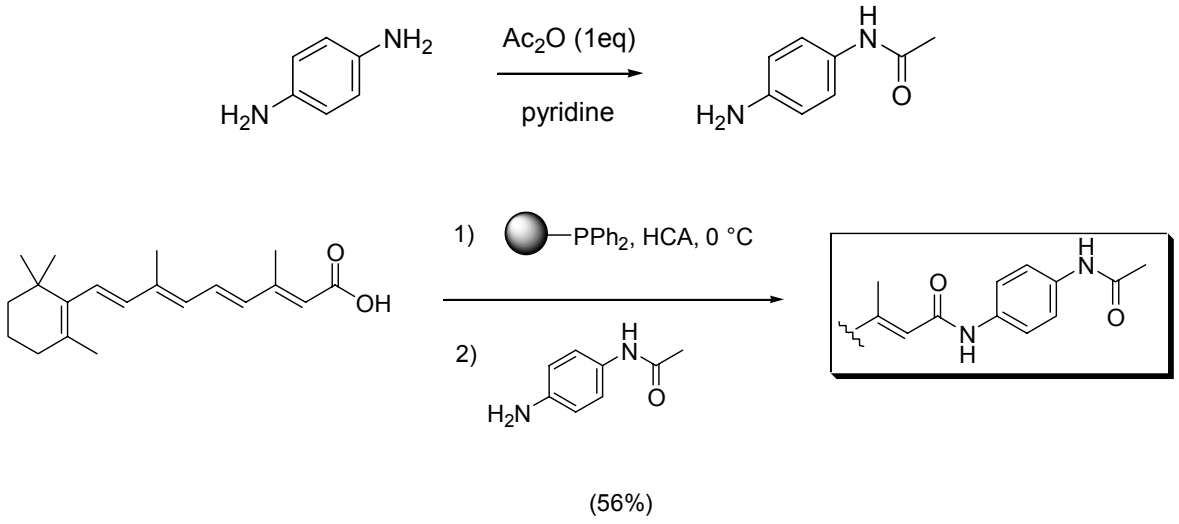

(56%)

Scheme 4.5 Synthesis of 4-AcPR.

Monoacetylation of 4-aminoaniline gave 4-acetamidoaniline which was then coupled to retinoyl chloride generated from polymer supported TPP and HCA. The final product was obtained as a yellow solid in 56% yield after purification using preparative TLC on silica gel. Monoacetylation of 4-aminoaniline was achieved using acetic anhydride in pyridine. However, the yield of the desired product was low regardless of the reaction conditions that were employed. Several methods were investigated, including acetic anhydride in acetic acid and acylation with acetyl chloride, but they too proved unsatisfactory. A different route to the anilines would be used in the synthesis of the other derivatives.

The next compounds to be synthesized were the 4-chloro- and 4-bromoacetamido derivatives. A key intermediate in these syntheses was *N*-(4-trifluoroacetamido)phenyl retinamide (4-TfaPR). This material was obtained from the coupling of 4-trifluoroacetamidoaniline with retinoyl chloride generated using thionyl chloride (Scheme 4.6). The trifluoroacetamido group was selected as a protecting group because it could be selectively cleaved under basic conditions to yield 4-AmPR.

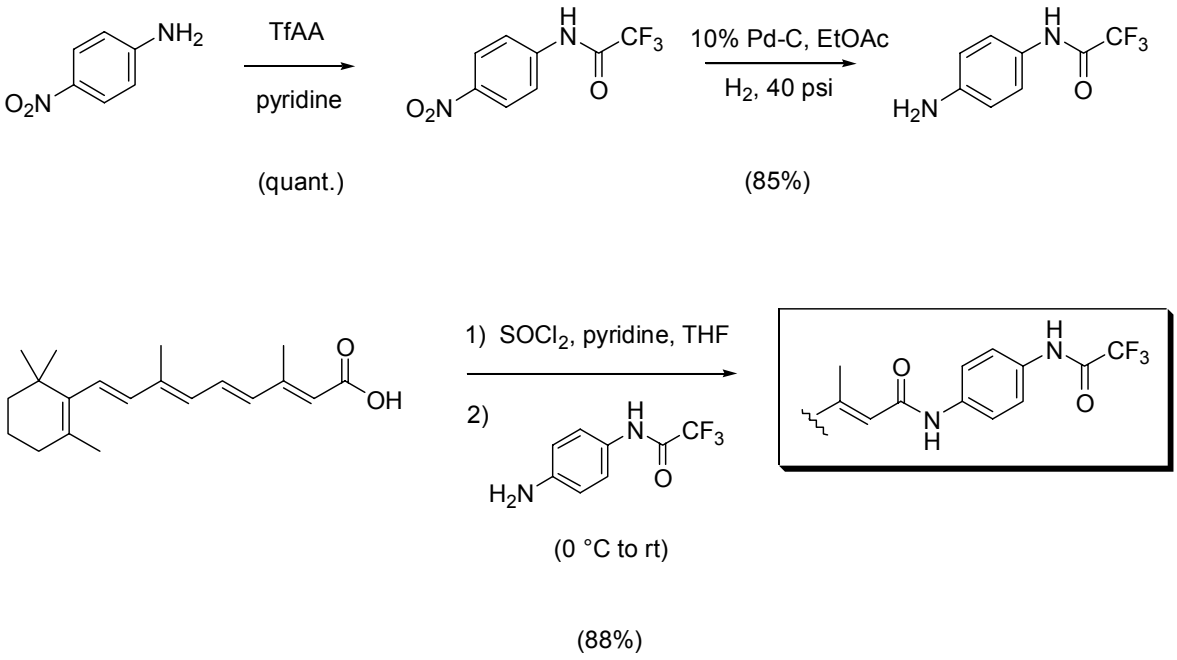

Scheme 4.6 Synthesis of 4-TfaPR.

The aniline precursor was synthesized starting from 4-nitroaniline. The amine was acylated using trifluoroacetic anhydride in pyridine which yielded the trifluoroacetamide in quantitative yield. The nitro group was then reduced to give the trifluoroacetanilide with high efficiency using hydrogen over 10% palladium-carbon catalyst in ethyl acetate. Although starting from the nitro derivative required an

additional synthetic operation, the overall yield of the process compared to the analogous procedure used in the synthesis of the 4-acetamido derivative (Scheme 4.5), was much higher. 4-TfaPR was obtained as a yellow solid in 88% yield after purification using column chromatography on silica gel.

The next step was the base catalyzed cleavage of the trifluoroacetamide to give the amino derivative. This reaction was carried out using 5 N potassium hydroxide in a methanol/THF solution and yielded 4-AmPR as an orange solid in 67% yield (Scheme 4.7).

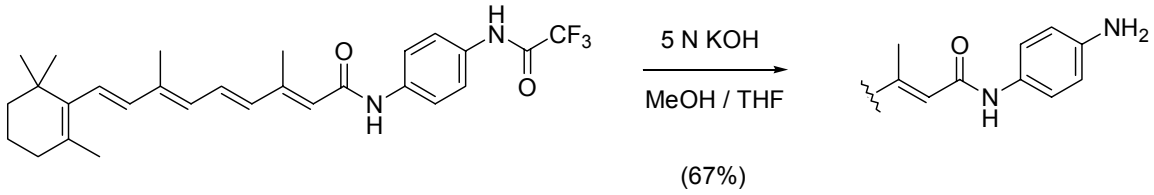

Scheme 4.7 Hydrolysis of 4-TfaPR.

With 4-AmPR in hand as the pentultimate product, the synthesis of the haloacetamido derivatives was straightforward (Scheme 4.8).

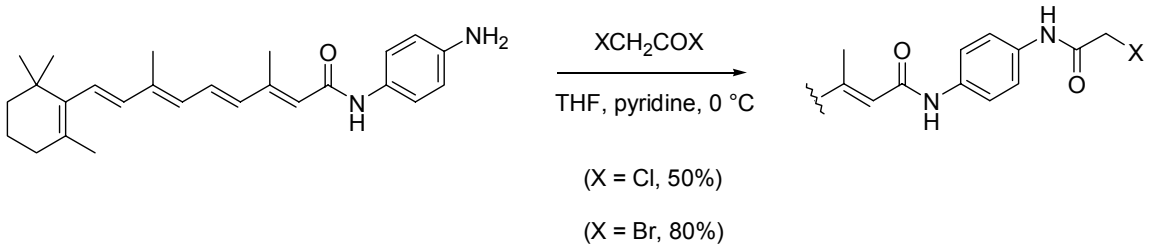

Scheme 4.8 Synthesis of haloacetamido derivatives.

4-AmPR was treated with excess chloroacetyl chloride in THF and pyridine at 0 °C to give the chloroacetamide in 50% yield after purification using prepative TLC. The bromoacetamide was prepared in a similar fashion using bromoacetyl bromide and was obtained in 80% yield after purification. Caution had to be taken to avoid decomposition of the bromide during purification. In early attempts, it was observed that exposure to silica gel for extended periods of time resulted in the degradation of the bromoacetamide. In contrast, the chloroacetamide appeared to be relatively stable to the purification conditions.

The final electrophilic affinity label to be synthesized was *N*-(4-isothiocyanatophenyl)retinamide (4-NCSPR). Isothiocyanates are commonly employed in electrophilic affinity labeling reactions, [163,179] and it was believed this compound would be easily accessible from the free amine. There are several methods available for the synthesis of isothiocyanates from the corresponding amine, including the reaction of amines with thiophosgene and the addition of amines to carbon disulfide.[180] Model reactions conducted on aniline derivatives using carbon disulfide proved unsatisfactory, and it was thought best to avoid reactions involving highly toxic phosgene. Therefore, alternative methods were investigated. A paper by Albanese and Penso reports the synthesis of isothiocyanates directly from *N*-monosubstituted trifluoroacetamides in the presence of potassium carbonate and sodium hydroxide.[181] In that work, they describe the synthesis of several simple isothiocyanates in moderate to good yield using these conditions. They propose the synthesis is mediated by the alkylation of the nitrogen anion with carbon disulfide to give the *N*-acyldithiocarbamate anion. This intermediate then undergoes a concerted rearrangement-elimination process to give the desired product and the thiocarboxylate anion (Scheme 4.9).

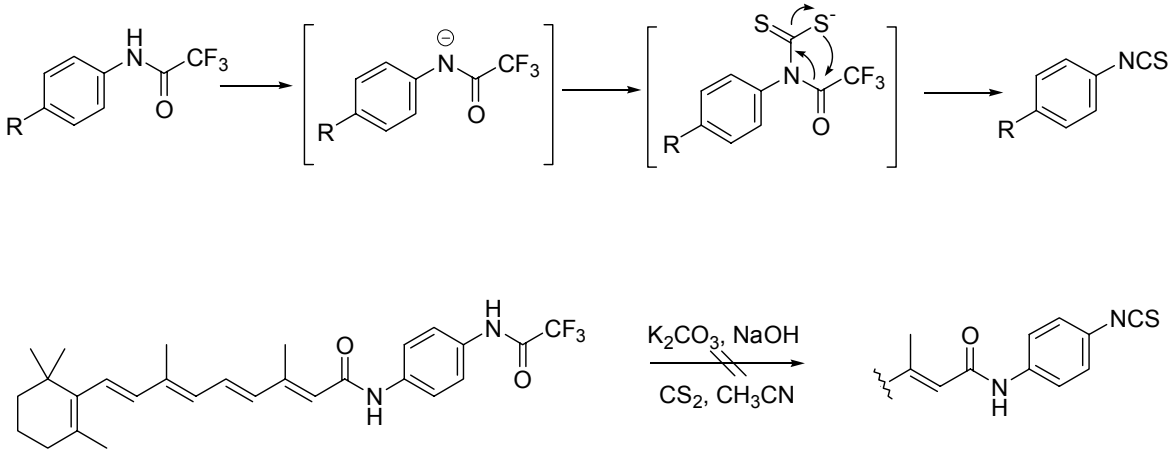

Scheme 4.9 Attempted synthesis of 4-NCSPR from 4-TfaPR.

Unfortunately, this method proved to be unsuccessful for the synthesis of the isothiocyanate derivative. The next route investigated utilized *N*-(4-azidophenyl)retinamide (4-AzPR) as the starting material. This material is one of the photoaffinity labels that will be discussed later, however, its use as a precursor to 4-NCSPR will be presented at this time. The reduction of azides with TPP was first reported by Staudinger, and consequently is known as the Staudinger reaction (Figure 4.13).[182] Molina and co-workers report that the iminophosphoranes generated in the Staudinger reaction can be treated with carbon dioxide or carbon disulfide to generate thiocyanates and isothiocyanates respectively.[183]

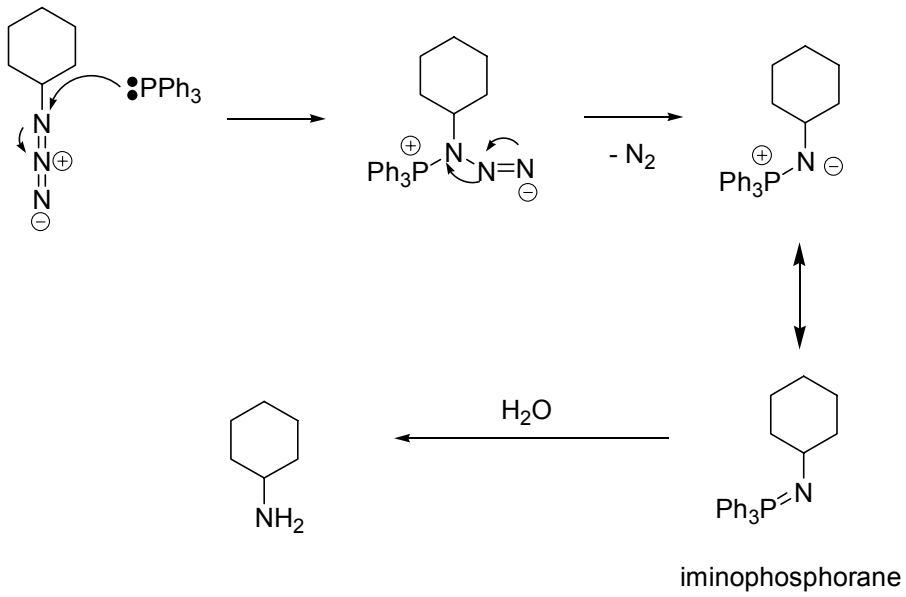

Figure 4.13 General mechanism of the Staudinger reaction.

Using these reaction conditions, 4-NCSPR was generated as a yellow solid in 55% yield after purification using preparative TLC (Scheme 4.10**)**. The use of the resin-bound phosphine seemed to facilitate the reaction, as initial attempts with soluble TPP were not successful. Use of the resin also facilitated product isolation.

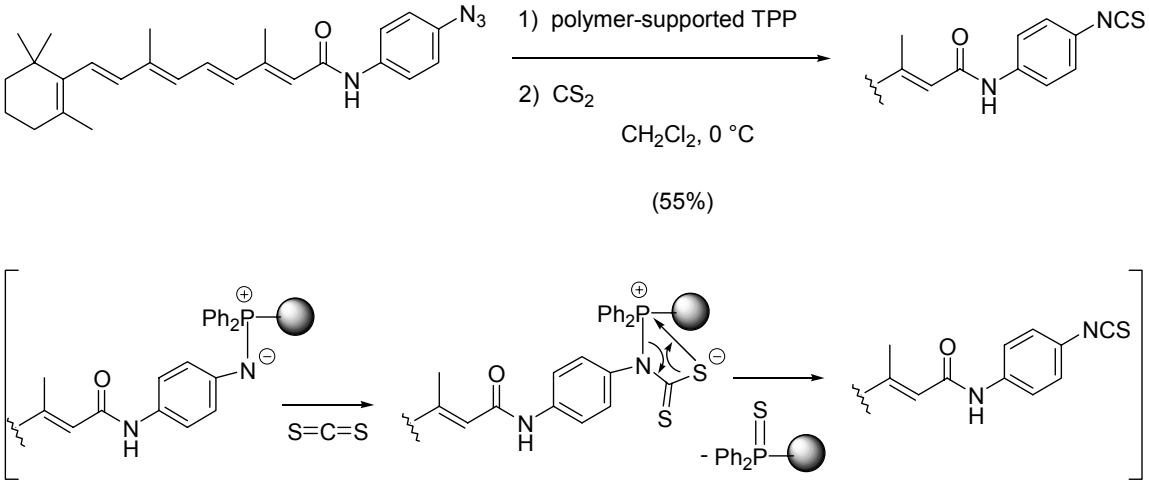

Scheme 4.10 Synthesis of 4-NCSPR using Staudinger conditions.

These compounds, the haloacetamides and the isothiocyanate, represent our first efforts on the synthesis of electrophilic affinity label analogs of 4-HPR. These compounds are currently being evaluated by Dr. Clagett-Dame's laboratory for their ability to inhibit growth and induce apoptosis in human mammary tumor cells. Future synthetic efforts will be guided by the results obtained from this preliminary biological evaluation. With these initial analogs in hand, our attention shifted to the synthesis of potential photoaffinity label analogs.

4.9 Synthesis of Photoaffinity Labels

Photoaffinity labeling has proven to be a successful technique in obtaining structural information regarding retinoids and the proteins with which they interact. For several examples the reader is directed to the following references.[168,184-188] This strategy has had the greatest impact on our current understanding of the visual cycle. As a result of these numerous studies, many photoaffinity label analogs of retinal are known. These include analogs incorporating fluoroazides,[185] diazo derivatives,[186,187] and diazirino moieties.[188]

As described previously (Table 4.1), *N*-(2-hydroxy-4-nitrophenyl)retinamide showed promising antiproliferative and apoptotic activity in the MCF-7 mammary tumor cell line. Therefore, it may be reasonable to expect, based on dipolar similarities, that replacing the nitro group with an azido group may give a compound with similar activity. Shown in Figure 4.14 are the azido derivatives that were synthesized.

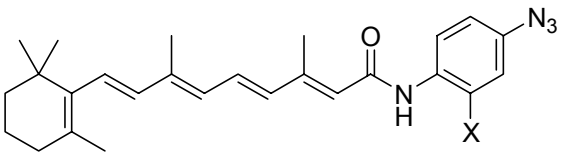

(X = H, OH)

Figure 4.14 General structure of 4-azido photoaffinity labels.

It was believed that these compounds would be easily obtainable using similar chemistry as that employed in the syntheses of the electrophilic affinity labels. Using the same retinoylation reaction, it would be possible to generate aryl azides by incorporating azidoanilines into the synthesis. The first compound synthesized was 4-AzPr that was previously introduced. The details of the synthesis are depicted in Scheme 4.11.

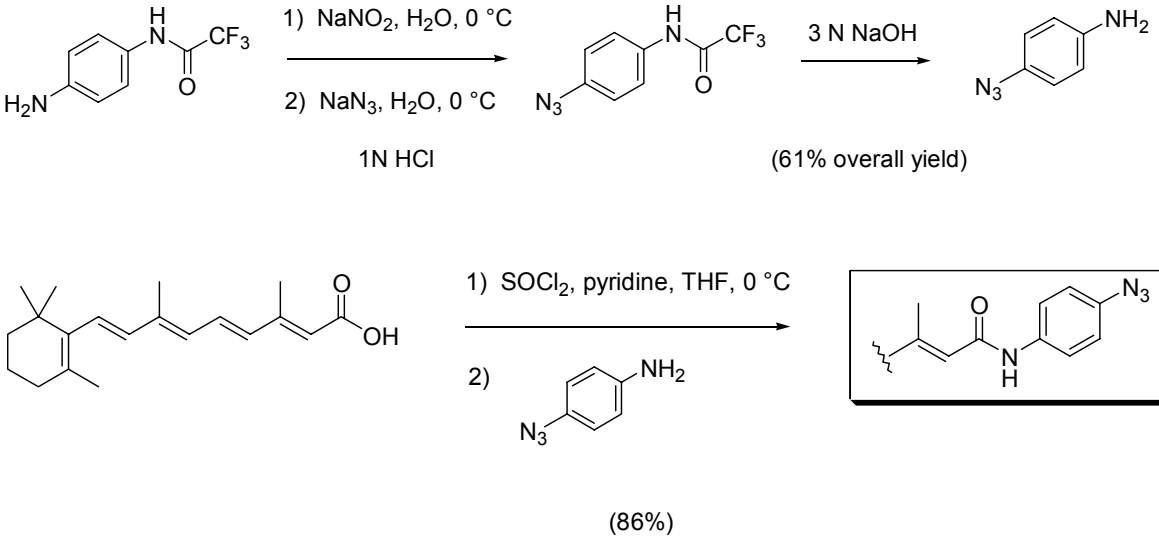

Scheme 4.11 Synthesis of 4-AzPR.

The azidoaniline was obtained from the previously synthesized 4-trifluoroacetamidoaniline. Diazotization of the aniline followed by base cleavage of the trifluoroacetamido moiety yielded the aniline precursor in 61% overall yield. The retinoylation reaction yielded 4-AzPR as a yellow solid in 86% yield after chromatography on silica gel.

The next compound synthesized was *N*-(4-azido-2-hydroxyphenyl)retinamide (4-AzOHPR). It is reasonable to expect, based on the activity data in Table 4.1, that this compound may possess similar activity as the 2-hydroxy-4-nitro analog. In addition, the incorporation of the hydroxy group into the aromatic ring may offer different kinetic behavior of the photoactivation process.[158] These types of substitutions may be important for reactivity "tuning" of future cross-linking experiments. The details of this synthesis are shown in Scheme 4.12.

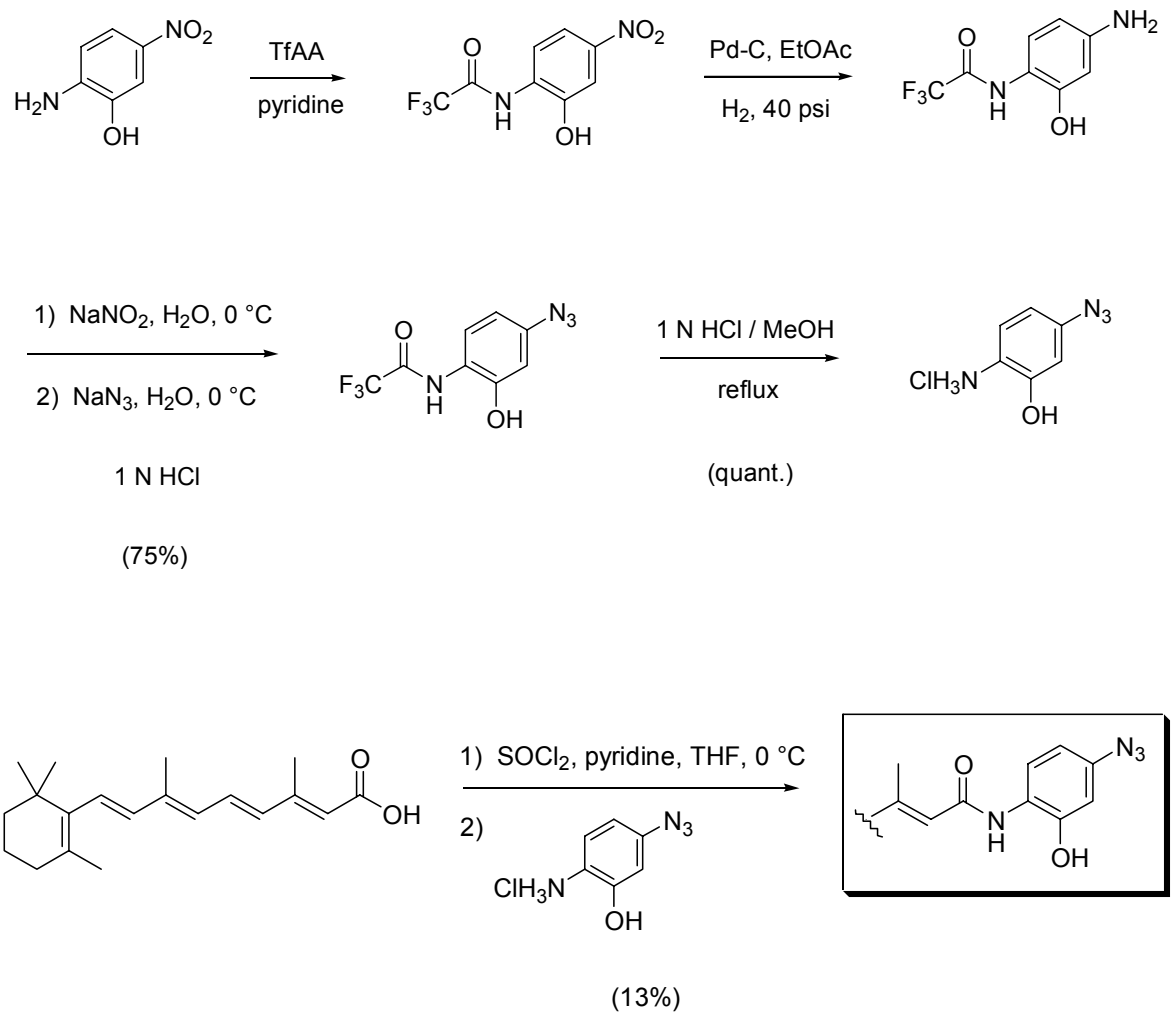

Scheme 4.12 Synthesis of 4-AzOHPR.

The 4-azido-2-hydroxyaniline was obtained in a good yield using a similar strategy as that previously described. However, the trifluoroacetamido protecting group was cleaved using acidic conditions. The basic conditions used previously with similar compounds to effect this transformation, led to complicated mixtures of products that could not easily be purified. One of the difficulties that hindered isolation was the solubility of the product aniline in aqueous systems. This made purification by extraction relatively difficult. Therefore, it was decided to use the acidic conditions, which

facilitated product isolation by abolishing the need for extractions. Evaporation of the reaction mixture provided the crude product as the hydrochloride salt, which was used without further purification. The aniline hydrochloride was stirred with pyridine prior to the retinoylation. The coupling reaction produced 4-AzOHPR as a yellow solid in a disappointing yield of 13% after purification using preparative TLC. Although this yield was satisfactory for these preliminary investigations, current efforts are focused on the optimization of this reaction, especially in consideration of planned future reactions incorporating radioiodinated anilines.

4.10 Preliminary Photochemical Behavior of Photoaffinity Labels

Preliminary studies were conducted to investigate the photochemical behavior of the azido derivatives. The goal of these early experiments was to establish a basic understanding of the kinetics of the photoactivation of these materials. The test compounds were irradiated with an ultraviolet (UV) source and changes in the UV spectrum were recorded as a function of time. This simple kinetic study provides useful information that will be used in future cross-linking studies.

The compounds were prepared as methanolic solutions and irradiated at a wavelength of 254 nm. A wavelength of 254 nm was selected because it used the most convenient light source for these preliminary investigations, and it was desirable to observe the effects of irradiation of the azido group as opposed to the polyene portion of the molecule. It was hoped that by conducting the experiment in this manner, any observable changes could be attributed to the photoactivation of the azide. Phenyl azide has an absorption maximum at 250 nm with the characteristic shoulders of an aryl azide appearing at 277 and 286 nm.[158] The absorption maximum of 4-HPR is at approximately 370 nm.

The first experiment to be conducted was a control experiment involving the irradiation of acetanilide and 4-azidotrifluoroacetanilide (Figure 4.15). This experiment was performed to investigate whether photoactivation of an aryl azide could be observed under the test conditions.

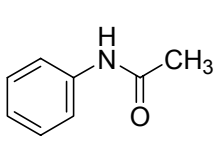

acetanilide

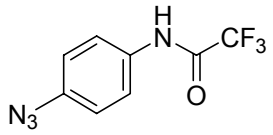

4-azidotrifluoroacetanilide

Figure 4.15 Structures of acetanilide and 4-azidotrifluoroacetanilide.

A UV spectrum was recorded of acetanilide dissolved in methanol. This spectrum would serve as a reference spectrum. The test solution was then irradiated from a fixed distance with a UV source emitting at 254 nm. After irradiation for measured periods of time, the UV spectrum was recorded. After 30 minutes of exposure, as expected the UV spectrum showed no changes relative to the reference spectrum (data not shown). Next, the experiment was repeated with 4-azidotrifluoroacetanilide. After 30 minutes of exposure, the UV spectrum revealed a significant change (Figure 4.16). These results established that under the conditions that were employed, an observable response from the azide was possible.

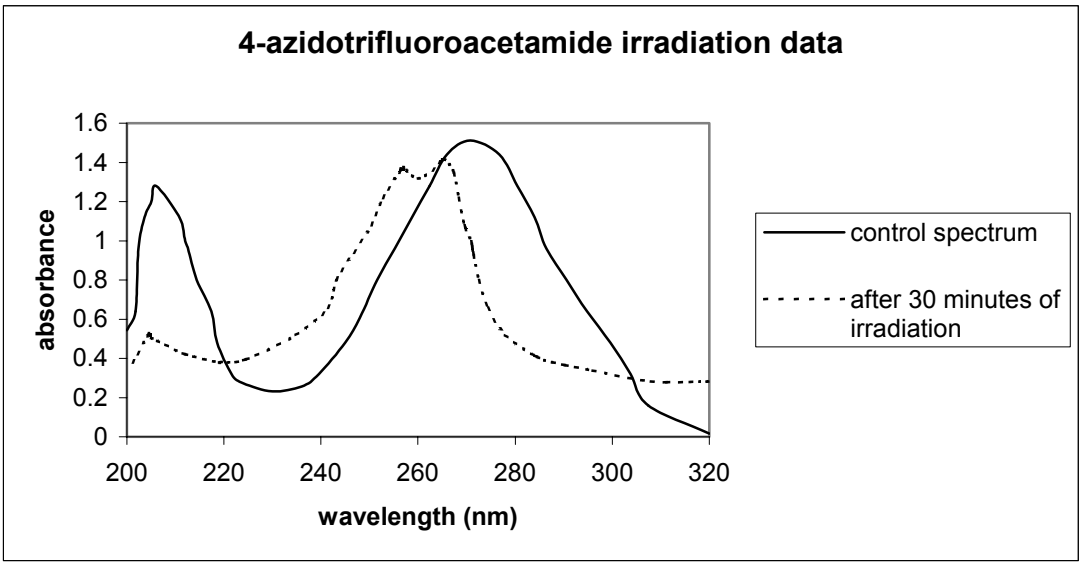

Figure 4.16 Data from model irradiation studies.

The next experiment conducted was a control experiment to determine if 4-HPR would be stable to the irradiation conditions. A methanolic solution of 4-HPR was prepared and treated as described above, however, the total irradiation time was three hours. Data from that experiment is summarized in Figure 4.17. These results indicate that 4-HPR is stable under the irradiation conditions for at least three hours.

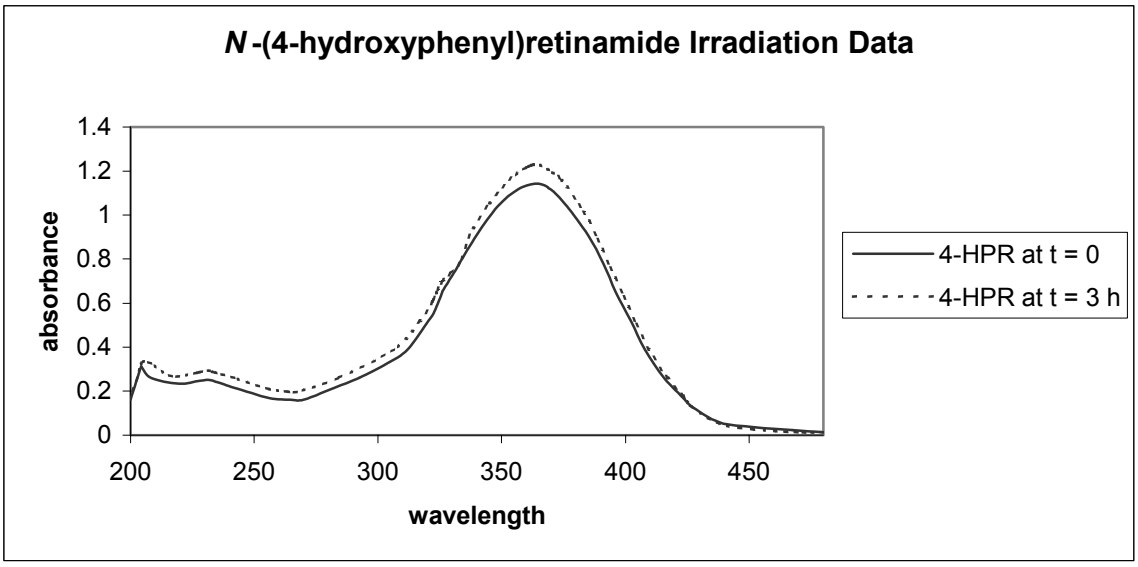

Figure 4.17 Data from 4-HPR irradiation experiments.

The next compounds to be examined were the azido-retinamides. Data for 4-AzPR and 4-AzOHPR are shown in Figures 4.18 and 4.19 respectively. The compounds were irradiated for a period of two hours. These data indicate that upon irradiation, some structural changes have occurred. The change in the UV spectrum of 4-AzOHPR appears to be more dramatic, however, further characterization of the activation products needs to be performed.

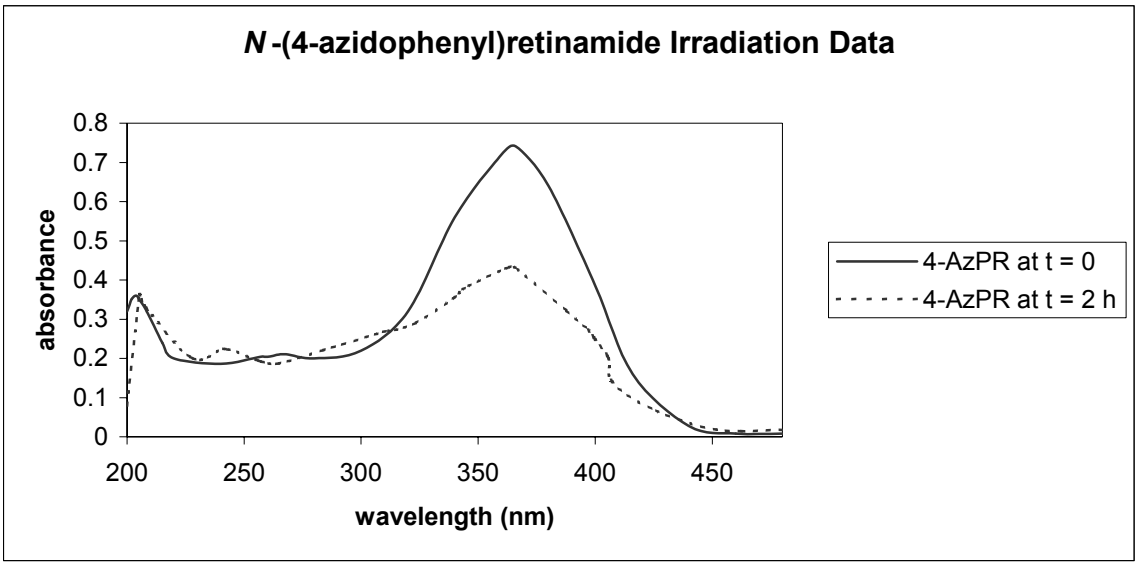

Figure 4.18 Data from 4-AzPR irradiation experiments.

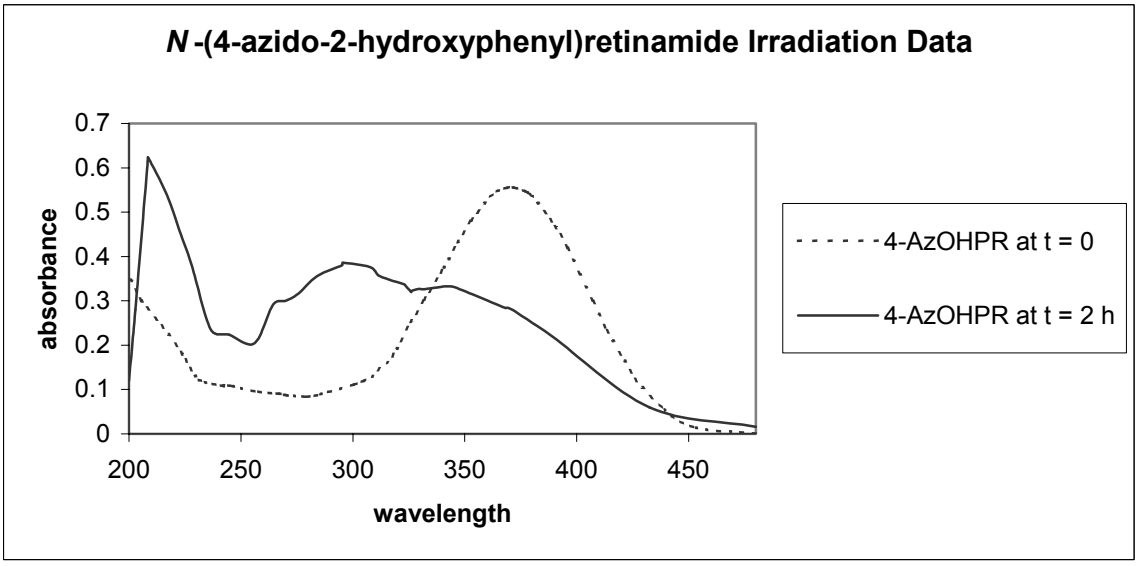

Figure 4.19 Data from 4-AzOHPR irradiation experiments.

The kinetics of the 4-AzOHPR irradiation experiment is shown in Figure 4.20. At various time-points throughout the experiment, UV spectra were recorded. The change in absorbance at 371 nm was recorded as a function of time. This wavelength was selected because it showed the greatest change during the irradiation experiment. Initial inspection of this data suggests that perhaps two different processes are occurring as evident from the two apparent slopes.

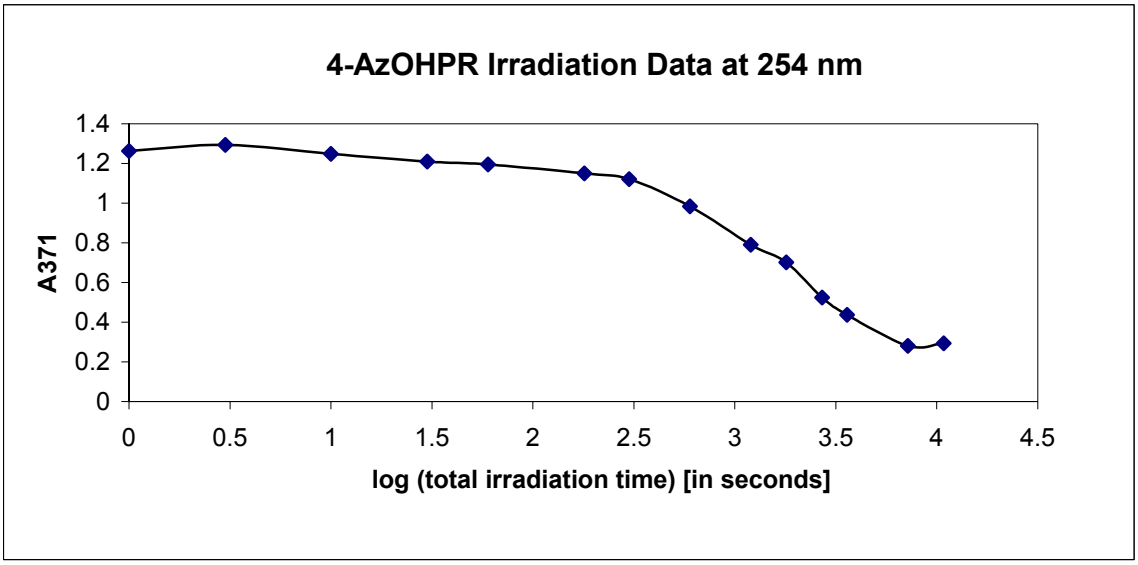

Figure 4.20 Data from kinetic analysis of 4-AzOHPR irradiation.

These preliminary chemical investigations represent the beginning of the evaluation process of these compounds. These compounds are currently be evaluated by our collaborators for their antiproliferative activity in MCF-7 cells. Results from this study will be used to direct further synthetic efforts. For future cross-linking studies it will be necessary to optimize the photoactivation process of these compounds with respect to the activation of the compound and compatibility with the biological components of the

assay. The apparent long irradiation times at 254 nm required in these initial investigations may not be compatible with biological components, although labeling experiments that use this wavelength have been reported.[160] It may be necessary to alter the wavelength employed in the cross-linking experiments, however, that will ultimately be decided by the photoactive group incorporated into the ligand. In addition, other 4-HPR photoaffinity labels could be prepared. As previously, discussed, there are many photoaffinity analogs of retinal that have been prepared. Many of these compounds incorporate the photoreactive centers on the cyclohexenyl portion of the molecule. This would not be an ideal approach in the current study because it is the aromatic portion of the compounds that is of most interest. By maintaining the labeling moiety on the aromatic ring, the possibility of cross-linking with an RA target should hydrolysis occur is lessened. Nonetheless, it is likely that alternative 4-HPR photoaffinity analogs could be prepared by adapting some of the retinal strategies to the current work.

4.11 Summary

The mechanism by which 4-HPR exerts its antiproliferative effects remains unclear. The work described in this Chapter details our efforts to further understand the mechanism of action of 4-HPR. The potent RAR antagonist AGN193109 was synthesized to facilitate mechanistic studies of various 4-HPR analogs generated in our laboratory. This compound is currently being used by our collaborators in these studies and will continue to be an invaluable tool for future investigations. Using information from a previously synthesized library of 4-HPR analogs, we have prepared a series of affinity analogs in an effort to discover possible alternative targets of 4-HPR binding. A series of electrophilic affinity label analogs were synthesized including 4-ClAcPR, 4-BrAcPR, and 4-NCSPR. In addition, a series of photoaffinity label analogs were

prepared including 4-AzPR and 4-AzOHPR. The photochemical behavior of the azido analogs was characterized using simple irradiation assays. These preliminary experiments will provide a reference for future evaluations. All of the affinity label analogs are currently undergoing biological evaluation by our collaborators. Current efforts with the photoaffinity labels are focused on generating an iodinated analog of 4-AzOHPR (Figure 4.21). Data from Table 4.1 shows that one of the active compounds contained a 3-chloro substituent. We would like to further explore the tolerance for halogenation of the aromatic ring. The iodinated compound represents a critical analog because of its role as a model for preparing a radio-labeled ligand. The incorporation of radioactive ^{125}I into the affinity label would be a significant step towards developing a viable probe as it would provide a ligand which is readily observable during the experiment and would greatly facilitate identifying cross-linked conjugates.

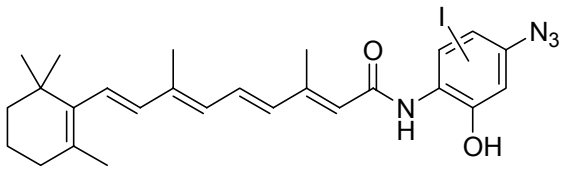

Figure 4.21 Iodinated analog of 4-AzOHPR.

Several attempts have been made to prepare this compound, unfortunately, none have been successful to date. The current strategy being investigated involves iodination of the aniline precursors using the well-known chloramine T and sodium iodide conditions.[189] Initial efforts were directed at introducing the iodo substituent to the various aniline derivatives. In addition, attempts have been made to directly iodinate 4-

AzOHPR. Model reactions with 4-HPR have revealed that the retinoid was stable to the reaction conditions. Unfortunately, this strategy has not been successful as of yet.

CHAPTER 5

Experimental Section

5.1 General Information

All moisture sensitive reactions were conducted using oven or flame-dried glassware cooled and maintained under an argon atmosphere. Effort was made to conduct all operations involving moisture sensitive reagents with technique such as reagent additions via syringe or cannula. Commercial argon was dried by passage through a gas washing bottle filled with concentrated sulfuric acid followed by a drying tube containing calcium sulfate. Anhydrous THF and diethyl ether was obtained by distillation from sodium/potassium benzophenone ketyl immediately prior to use. Anhydrous dichloromethane was obtained by distillation from calcium hydride immediately prior to use. Butyllithium concentrations were determined by titration against diphenylacetic acid. Normal phase analytical TLC was performed using EM Science silica gel 60 F_{254} aluminum-backed plates. Normal phase preparative TLC was performed using Analtech uniplate silica gel GF glass plates. Reverse phase analytical TLC was performed using Analtech UNIBOND octadecyl modified silica gel with UV 254 glass plates; reverse phase preparative TLC was performed using Whatman PLKC18F silica gel glass plates. Visualization of TLC plates was accomplished using UV light, phosphomolybdic acid or *p*-anisaldehyde staining, or sulfuric acid/ethanol charring depending on the properties of the molecules. Open column chromatography was

performed using silica gel 60 (70-230 mesh) from EM Separations; flash column chromatograpy was performed using silica gel (230-400 mesh) from Fisher Scientific. EM Separations LiChroprep® RP-18 (40-60 μm) was used for reverse phase flash column chromatography. Melting points were determined using a Thomas-Hoover capillary apparatus and are uncorrected. Optical rotations were obtained using a Perkin-Elmer 241 polarimeter. Analytical scale HPLC analyses were performed using a Beckman Ultrasphere ODS column (4.6 x 250 mm) using UV detection. Semi-preparative HPLC was performed using a Zorbax ODS column (9.4 x 250 mm) with UV detection. UV spectra were recorded using a Beckman DU®-40 spectrophotometer. Infrared spectra were acquired as films on AgCl plates using a Nicolet Protégé 460 FTIR. Nuclear magnetic resonance spectra were acquired on a Bruker DRX400 operating at 400 MHz (^{1}H) and 100 MHz (^{13}C) unless otherwise indicated and referenced to non-deuterated solvent resonances. Nitrogen-15 NMR spectra were recorded at 40.5 MHz and referenced externally to a ^{15}N-glycine sample in D_2O (31.5 ppm). Deuterium NMR spectra were recorded at 92 MHz. Mass spectrometry was performed using a Micromass QTOF spectrometer at The Ohio State University Campus Chemical Instrumentation Center (CCIC). Catalytic hydrogenation was conducted on a Parr hydrogenation apparatus model 3911. Diazomethane was generated using a Diazald® kit from Aldrich. Cambridge Isotope Laboratories supplied ^{15}N-glycine and D_2O.

5.2 General Methods and Procedures

5.2.1 Alkylation of hippurate esters

The procedure used for the alkylation of hippurate esters was adapted from McIntosh.[77] All operations were performed to exclude moisture (section 5.1). A 0.5 M

solution of LDA was prepared by the addition of a solution of *n*-BuLi (1 eq) in hexanes to a solution of diisopropylamine (1 eq) in dry THF at -78 °C. The solution was stirred for 10 min and then TMEDA was added (1eq). The solution was allowed to warm to room temperature and then recooled to -78 °C. Hippurate ester (0.5 eq) was dissolved in dry THF (0.25 M solution) and added slowly. This mixture was stirred at -78 °C for 1 h after which electrophile (slight excess), dissolved in dry THF (0.5 M solution), was added slowly. The mixture was stirred for the time indicated (usually 1-6 h). The reaction was then quenched at the indicated temperature by the addition of 1 N HCl. The solution was allowed to warm to room temperature, diluted with ethyl acetate, and the phases were separated. The organic phase was dried and evaporated to yield material that was analyzed by ^{1}H NMR or HPLC. Subsequently, the crude product was purified using chromatography.

5.2.2 Synthesis of deuterated aldehydes

The procedure used for the synthesis of deuterated aldehydes was adapted from Bennett[80] and consists of three steps: 1) synthesis of the morpholineacetonitrile derivative, 2) proton-deuteron exchange, and 3) hydrolysis of the deuterated morpholineacetonitrile. The procedure that follows was used for the preparation of benzaldehyde-α-*d* and is representative of the other deuterated aldehydes. The reaction times and temperatures, as well as the method of purification varied slightly depending on the aldehyde. For example, benzaldehyde-α-*d* was obtained from the crude reaction mixture and was used without further purification; other aldehydes were chromatographed or recrystallized.

Step 1. A round bottom flask equipped with a magnetic stir bar and reflux condenser was charged with morpholine (20 mL) and cooled to 0 °C. Perchloric acid (70%, 9.5 mL, 0.11 mol) was added dropwise to the stirred solution followed by the careful addition of benzaldehyde (0.11 mol). The cooled mixture solidified as a yellow solid that dissolved upon warming to 70 °C. After 4 h at 70 °C, the mixture was cooled to rt, and an aqueous solution of KCN (0.12 mol, minimal water) was added. The reaction mixture was then warmed to 90 °C for 1 h and then cooled to rt. After cooling, the reaction mixture was poured onto ice with stirring. The resulting precipitate was collected, washed with water, recrystallized from absolute ethanol, and dried under high vacuum at 40 °C for 12 h.

Step 2. All operations were performed to exclude moisture (section 5.1). A dry, argon flushed round bottom flask equipped with a magnetic stir bar and reflux condenser was charged with the product from Step 1 (50 mmol) and THF (50 mL). Sodium hydride (95%, 99 mmol) was carefully added and the mixture was heated to 40 °C for 1 h during which time the reaction mixture turned pink in color. The reaction mixture was then cooled to 0 °C and deuterium oxide (1.0 mol) was carefully added dropwise quenching the pink color. The mixture was stirred for 30 min at 0 °C, acidified (pH 1-2) by the addition of freshly distilled thionyl chloride, and poured onto ice with stirring. The resulting precipitate was collected, washed with water, and dried.

Step 3. A round bottom flask equipped with a magnetic stir bar and reflux condenser was charged with the product from Step 2 (25 mmol) and 2 N HCl (60 mL). The suspension was refluxed for 12 h under an argon atmosphere after which the resulting two phase mixture was cooled to rt and extracted with diethyl ether. The combined organic phases were washed with saturated sodium bicarbonate, water, and

brine. The organic solution was dried over magnesium sulfate, filtered, and concentrated under reduced pressure at ambient temperature to give an oil that was used without further purification.

5.2.3 Asymmetric reduction with Alpine Borane®

The following procedure was used for the asymmetric reduction of benzaldehyde-α-*d* with Alpine Borane®. Similar procedures were used for the other deuterated aldehydes with slight variations in the final purification of the alcohols.

A THF solution of 0.5 M *R*-Alpine-Borane® (70 mL; 35 mmol) was added to benzaldehyde-α-*d* (2.3 g, 21.5 mmol). The mixture was stirred at rt for 12 h and then heated to reflux for 1.5 h. After cooling to rt, acetaldehyde (5 mL) was added and the mixture was stirred for 30 min after which the solvent was removed using a rotary evaporator. Some of the pinene by-products were then removed using a rotary evaporator under high vacuum at 50 °C for 5 h. The remaining orange oil was dissolved in diethyl ether (75 mL) and cooled to 0 °C. Ethanolamine (2.1 g, 35 mmol) was added and the mixture was stirred for 30 min at 0 °C during which time a white solid precipitated from the mixture. The mixture was filtered and washed with diethyl ether. The filtrate was concentrated and the resulting oil was dissolved in 10% aq MeOH and washed several times with heptane. Isopropanol was added to the methanolic fraction and the solution was concentrated on a rotary evaporator. The resulting yellow oil was chromatographed on silica gel (95:5 hexanes / ethyl acetate) to yield 2.0 g of a colorless oil.

5.2.4 Halogenations using CX_4/PPh_3

The following procedure was used for the halogenation of benzylic alcohols with carbon tetrahalides and TPP. All operations were performed to exclude moisture (section 5.1). Anhydrous carbon tetrachloride and dichloromethane were the solvents used for chlorination and bromination reactions respectively.

Chlorinations. To a 1 M solution of alcohol (1 eq) in CCl_4 at 0 °C was added TPP (2 eq). The reaction was maintained at 0 °C and monitored by TLC; upon disappearance of starting material, the solvent was reduced in volume with a stream of argon. The reaction mixture was then directly loaded onto a chromatographic column and purified using silica gel.

Brominations. To a 1 M solution of alcohol (1 eq) in dichloromethane at 0 °C was added CBr_4 (2 eq). After stirring for 10 min at 0 °C, TPP (2 eq) was added. The remaining operations were similar to those presented above.

5.2.5 Halogenations using Mitsunobu conditions

The procedure used for the halogenation reactions using Mitsunobu conditions has been described by Manna and co-workers.[91] All operations were performed to exclude moisture (section 5.1). To a solution of TPP in anhydrous THF (0.4 M) at 0 °C was added DEAD (2 eq). After stirring for 20 min, the lithium halide (1 eq) was added to the reaction mixture followed by the alcohol (1 eq) in a minimal volume of THF. The reaction mixture was maintained at 0 °C and monitored by TLC; upon disappearance of starting material, the solvent was reduced in volume with a stream of argon. The reaction mixture was then directly loaded onto a chromatographic column and purified using silica gel.

5.2.6 Halogenations using HCA/polymer-supported PPh_3

The procedure used for the halogenation reactions using the HCA/polymer-supported TPP was adapted from Villeneuve and Chan.[111] All operations were conducted to exclude moisture (section 5.1). Polymer-supported TPP was washed thoroughly with THF and dried under high vacuum at 100 °C for 12 h prior to use. To a dry, argon flushed flask equipped with a magnetic stir bar was added TPP resin (~3 mmol/g, 1.89 mmol) and anhydrous THF (25 mL). The suspension was cooled to 0 °C at which time HCA (0.5 eq) was added. After stirring at 0 °C for 20 min, a solution of the alcohol (1.0 eq) in anhydrous THF was added dropwise. The reaction mixture was stirred at 0 °C for 1 h and then warmed to rt. When TLC of the reaction mixture revealed no remaining starting material, the resin was removed from the mixture using gravity filtration through filter paper. The resin was washed with dichloromethane and the filtrate was concentrated under reduced pressure. The product chloride was then purified using silica gel chromatography.

5.2.7 Evaluation of deuterated electrophiles

A key property of the electrophiles was the ability to alkylate the chiral enolate derived from (-)-8-phenylmenthyl hippurate with good chemical and stereochemical yield. The electrophiles were used as described in section 5.2.1 and the yields of each reaction were determined. Stereochemical analysis of the reaction products was performed using NMR spectroscopy and HPLC as described in section 5.1.

5.2.8 Synthesis of (-)-camphanamide derivatives

The procedure used for the preparation of diastereomeric derivatives of labeled benzylic alcohols and amino acids was adapted from Williams and co-workers.[88]

Toluene and pyridine was used as the solvent for derivatizations of alcohols while a mixture of toluene and 10% potassium carbonate was used for derivatization of the amino acids. A solution of the alcohol or amino acid in a small amount of solvent was added to a solution of (-)-camphanic chloride (2 eq) in toluene at 0 °C. The reaction mixture was stirred for 30 min at 0 °C and then 5 h at 25 °C. The workup for derivatization of alcohols involved concentrating the reaction mixture under reduced pressure. The workup for derivatization of amino acids involved washing the reaction mixture with chloroform, acidifying the aq layer with 1 N HCl, and extracting the aq layer with dichloromethane. Crude products were analyzed by NMR spectroscopy, and purified when necessary using preparative TLC.

5.2.9 Catalytic hydrogenation

Catalytic hydrogenations were conducted on a Parr hydrogenator apparatus under 40 psi of hydrogen. The reactions were performed over 10% palladium on carbon in ethyl acetate. The typical reaction time was approximately 6 h. Reaction workup involved filtration of the reaction mixture through a pad of Celite and concentration of the filtrate under reduced pressure.

5.2.10 Synthesis of 4-HPR analogs

The procedure used to synthesize the retinamide analogs was dependent on the preparation of retinoyl chloride. Two methods were used to generate the acyl chloride, 1) HCA/polymer-supported TPP and 2) thionyl chloride. All operations were conducted to exclude moisture (section 5.1).

HCA/polymer-supported method. A dry, argon flushed round bottom flask equipped with a magnetic stir bar was charged with RA (1 eq), TPP resin (2.5 eq), and

anhydrous THF (~0.5 M in RA). The reaction mixture was cooled to 0 °C and HCA (0.5 eq) was added. After stirring at 0 °C for 1h, the aniline derivative was added.

Thionyl chloride method. Under similar conditions as described above, a THF solution of RA and pyridine (5 eq) at 0 °C was treated with thionyl chloride (1.1 eq). After stirring at 0 °C for 1h , the aniline derivative was added.

Upon generation of the retinoyl chloride, solutions of the aniline derivatives (1.2 eq) in anhydrous THF and pyridine were added dropwise at 0 °C. Upon completion of addition, the reaction mixture was warmed to rt and stirred for 12 h after which the reaction was quenched with the addition of methanol. After stirring for 30 min, the mixture was diluted with water and the phases separated. The aq phase was extracted with ethyl acetate. The combined organic phases were washed with water, saturated sodium bicarbonate, and brine. The organic solution was dried over sodium sulfate, filtered, and concentrated under reduced pressure. The crude products were then purified by chromatography.

5.2.11 UV Irradiation of 4-HPR photoaffinity label analogs

The source used for the irradiation experiments was a Mineralight® Lamp model UVG-11 (115 V, 60 Hz, 0.16 amps) intended to be used to visualize TLC plates. Methanolic solutions of the compounds were irradiated from a fixed distance of approximately 3 cm at 254 nm for the time indicated. At various timepoints during the experiments, UV spectra were recorded.

5.3 Analytical Data

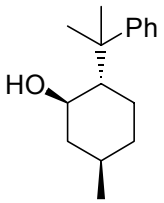

(-)-8-phenylmenthol. The chiral auxiliary was prepared according to the published procedure of Ort.[87] colorless oil: $[\alpha]^{21}_{D}$ -30.5° (neat); ^{1}H NMR ($CDCl_3$, δ): 0.75-1.90 (m, 9H); 0.87 (d, 3H, *J* = 5.7 Hz), 1.29 (s, 3H), 1.42 (s, 3H,), 3.55 (dt, 1H, *J* = 10.0 Hz), ^{13}C NMR ($CDCl_3$, δ): 21.95, 25.93, 26.62, 27.33, 31.45, 34.81, 39.87, 45.62, 53.85, 72.52, 125.22, 125.52, 127.88, 150.83.

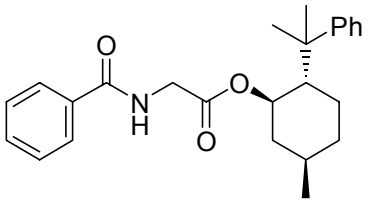

(-)-8-phenylmenthylhippurate (1). A mixture of hippuric acid (2.0 g, 11.2 mmol), (-)-8-phenylmenthol (0.75 g, 3.2 mmol), and *p*-toluenesulfonic acid (100 mg) in toluene (50 mL) was refluxed under Dean-Stark conditions. The reaction was monitored by TLC. Upon the disappearance of the alcohol, the reaction was cooled to rt. Saturated sodium bicarbonate was added (15 mL) and the mixture was stirred for 15 min. The phases were separated and the organic phase was washed with water, brine, and concentrated to yield the crude product which was further purified using flash chromatography to yield a white solid (1.2 g, 93%).

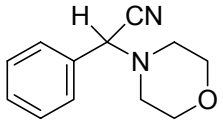

α-phenyl-4-morpholineacetonitrile.[80] This compound was prepared from benzaldehyde (11.5 g) as described in section 5.2.2 (step 1) to give white needles after recrystallization from absolute ethanol (18.8 g, 91%): mp 67-68 °C (lit. 68-70 °C);[80] IR (cm^{-1}): 1117 (s), 2857 (m), 1453 (m), 1007 (m), 866 (m), 701 (m), 2227 (w); ^{1}H NMR ($CDCl_3$, δ): 2.27-2.38 (m, 4H), 3.45-3.57 (m, 4H), 4.65 (s, 1H), 7.15-7.22 (m, 3H), 7.34-7.36 (m, 2H); ^{13}C NMR ($CDCl_3$, δ): 49.79, 62.31, 66.55, 115.03, 127.80, 128.61, 128.79, 132.55; HRMS-ES (*m*/*z*): $[M + Na]^+$ calcd for 225.1004; found 225.0991.

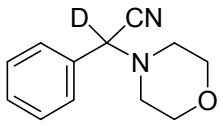

α-phenyl-4-morpholineacetonitrile-α-*d*.[80] This compound was prepared from α-phenyl-4-morpholineacetonitrile (10 g) as described in section 5.2.2 (step 2) to give a white crystalline solid (9.91, 99%; 99% ^{2}H incorporation determined by ^{1}H NMR): mp 67-68 °C (lit. 69-70 °C)[80]; IR (cm^{-1}): 1118 (s), 2864 (m), 1453 (m), 1015 (m), 862 (m), 700 (m), 2229 (w); ^{1}H NMR ($CDCl_3$, δ): 2.42 (t, 4H, *J* = 4.4 Hz), 3.51-3.60 (m, 4H), 7.15-7.28 (m, 3H), 7.38-7.40 (m, 2H); ^{13}C NMR ($CDCl_3$, δ): 49.75, 61.85 (t, *J* = 22.1 Hz), 66.60, 115.00, 127.82, 128.74, 128.97, 132.46; HRMS-ES (*m*/*z*): $[M + Na]^+$ calcd for 226.1082; found 226.1070.

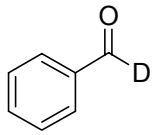

benzaldehyde-α-*d*. This compound was prepared from α-phenyl-4-morpholineacetonitrile-α-*d* (5 g) as described in section 5.2.2 (step 3) to give an oil (2.5 g, 93%; 98% ^{2}H incorporation determined by ^{1}H NMR): ^{1}H NMR ($CDCl_3$, δ): 7.39-7.68 (m, 3H), 7.87 (d, 2H, *J* = 4.9 Hz), 10.01 (s, residual CHO).

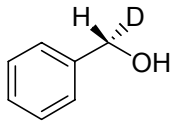

(*S*)-(+)-benzyl-α-*d* alcohol (2).[82] This compound was prepared from benzaldehyde-α-*d* (2.3 g) as described in section 5.2.3 to yield a colorless oil (2.0 g, 87%, > 96% ee): $[\alpha]^{21}_{D}$ +1.34° (neat)[82]; IR (cm^{-1}): 3349 (s), 2924 (s), 1452 (s), 1406 (s), 1320 (s), 1043 (s), 1024 (s), 723 (s), 697 (s), 3029 (m), 1205 (m), 2137 (w), 1949 (w); ^{1}H NMR ($CDCl_3$, δ): 1.90 (s, 1H), 4.64 (t, 1H, *J* = 1.8 Hz), 7.26-7.37 (m, 5H); ^{13}C NMR ($CDCl_3$, δ): 64.20 (t, *J* = 22.1 Hz), 126.79, 127.23, 128.21, 140.64; HRMS-EI (70 eV) *m*/*z*: M^{+} calcd for 109.0637; found 109.0569.

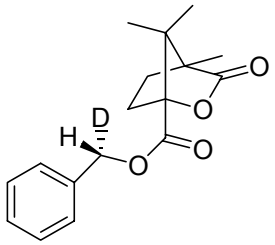

Stereochemical analysis of 2. The optical purity of **2** was determined using ^{1}H NMR spectroscopy of the (-)-camphanate ester derivative (Figure 2.13) as described in section 5.2.8.[88] The product was purified using silica gel preparative TLC and analyzed by ^{1}H NMR: ^{1}H NMR (800 MHz, $CDCl_3$, δ): 5.35 (broad s, major), 5.39 (broad s, minor), major/minor > 98:2.

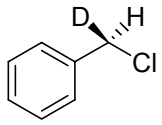

(*R*)-(-)-benzyl-α-*d* chloride. This compound was prepared from **2** using the methods described in section 5.2.4-5.2.6 to give a colorless oil: $[\alpha]^{21}_D$ -1.52° (*c* 6.9, THF, method 5.2.6); ^{1}H NMR ($CDCl_3$, δ): 4.53 (s, 1H), 7.28-7.36 (m, 5H); ^{13}C NMR ($CDCl_3$ δ): 45.76 (t, *J* = 23 Hz), 128.18, 128.28, 128.38, 137.29; HRMS-EI (70 eV) *m*/*z*: M^+ calcd for 127.02980; found 127.03019.

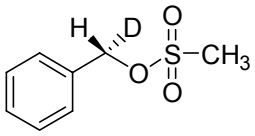

(*S*)-(+)-benzyl-α-*d* mesylate (3e). All operations were conducted to exclude moisture (section 5.1). Methanesulfonyl chloride (0.66 ml, 8.5 mmol) was added to a THF solution of (*S*)-(+)-benzyl-α-d alcohol (750 mg, 6.87 mmol), DMAP (84 mg, 0.69 mmol),

and NEt_3 (1.43 mL, 10.3 mmol) at 0 °C. The reaction mixture was stirred at 0 °C for 1 h and then diluted with water and extracted with ethyl acetate. The solvent was evaporated and the crude product was chromatographed on silica gel (1:1 hexanes/ethyl acetate) to yield 1.1 g of colorless oil (86%): $[\alpha]^{21}_{D}$ +0.47° (*c* 12.8, ethyl acetate); ^{1}H NMR (250 MHz, $CDCl_3$, δ): 2.87 (s, 3H), 5.21 (t, 1H, *J* = 1.7 Hz), 7.35-7.45 (m, 5H); ^{13}C NMR (62.9 MHz, $CDCl_3$, δ): 38.39, 71.23 (t, *J* = 23.1 Hz), 128.90, 129.42; HRMS-ES (*m*/*z*): $[M + Na]^+$ calcd for 210.0327; found 210.0319.

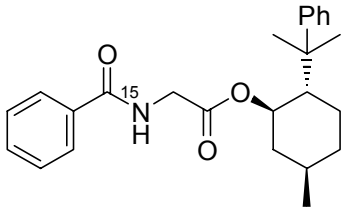

^{15}N-(-)-8-phenylmenthylhippurate (7). This compound was prepared in a similar manner as that described for **1** using ^{15}N-glycine as a starting material. ^{1}H NMR ($CDCl_3$, δ): 0.87 (d, 3H, *J* = 6.5 Hz), 0.89-1.02 (m), 1.15-2.11 (m), 3.41 (dd, 1H, *J* = 18.4 Hz, *J* = 5.7), 3.58 (dd, 1H, *J* = 18.4 Hz, *J* = 4.6 Hz), 4.91 (dd, 1H, *J* = 10.7 Hz, *J* = 4.6 Hz), 6.05 (dt, 1H, *J* = 91.4 Hz, *J*= 5.0 Hz), 7.12-7.73 (m, 10H).

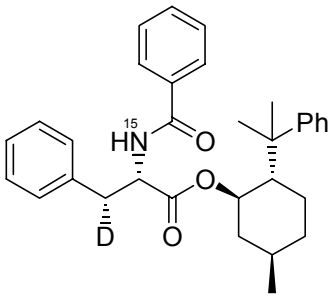

(2*S*, 3*R*)-(-)-*N*-benzoyl-[3-^{2}H,^{15}N]-phenylalanine-(-)-8-phenylmenthyl ester (8). This compound was prepared from **7** (600 mg) and **3e** (300 mg) as described in section 5.2.1. Electrophile addition was conducted at -42 °C. The reaction was stirred at this temperature for 12 h after which the reaction was quenched with 1 N HCl (10 mL) and allowed to warm to room temperature. After stirring for 30 min, the phases were separated and the aqueous phase was extracted with ethyl acetate. The organic phases were combined, washed with water, diluted with isopropanol, and concentrated to give an orange oil. HPLC and ^{1}H NMR analysis of the crude product revealed 92% de at the 2-position with the (2*S*)-epimer as the major product and 74% de at the 3-position. The crude product was partially purified on silica gel (85:15 hexanes/ethyl acetate) yielding 660 mg of **8** as a mixture of the (2*S*) and (2*R*)-epimers (89%). A portion of the mixture was then further purified using semi-preparative HPLC (80% MeOH/H_2O) to yield 83 mg of a white solid which was used for all analytical measurements: $[\alpha]^{21}_{D}$ -12.11° (*c* 4.1, ethyl acetate); HPLC (85% MeOH / H_2O, λ = 254 nm) $t_{R(2S,\ 3R/S)}$ = 20.0 min; IR (cm^{-1}): 2955 (s), 2924 (s), 1729 (s), 1666 (s), 1479 (s), 700 (s), 3360 (m), 3060 (m), 1602 (m), 1497 (m), 1368 (m), 1210 (m); ^{1}H NMR ($CDCl_3$, δ): 0.81-1.02 (m, 5H), 1.03-1.31 (m, 8H), 1.68 (d, *J* = 12.5 Hz, 1H), 1.83 (dt, *J* = 13.8 Hz, 3.4 Hz, 2H), 2.09 (dt, *J* = 11.3 Hz, 3.4 Hz, 1H), 2.70-2.79 (m, residual CH), 3.00 (d, *J* = 5.8 Hz, 1H), 4.23 (dd, *J* = 7.5 Hz, 6.5 Hz, 1H), 4.81 (dt, *J* = 10.8 Hz, 4.3 Hz, 1H), 6.29 (dd, *J* = 91.1 Hz, 7.5 Hz, 1H), 7.00-7.69

(m, 15H); ^{13}C NMR ($CDCl_3$, δ): 21.73, 23.89, 26.45, 28.85, 29.31, 31.29, 34.48, 36.91 (t, *J* = 19.2 Hz), 39.49, 41.58, 50.41, 53.16, 53.29, 76.21, 125.25, 125.41, 126.66, 126.98, 128.08, 128.23, 128.51, 129.53, 131.49, 134.34, 134.43, 136.20, 151.54, 166.52 (d, *J* = 16.2 Hz), 170. 83; ^{15}N NMR ($CHCl_3$, δ): 112.01 (d, *J* = 91.1 Hz); HRMS-ES (*m*/*z*): [M + Na]$^+$ calcd for $C_{32}H_{36}D^{15}NO_3Na$ 508.2828; found 508.2806.

Stereochemical analysis of 8. Retention times from HPLC analyses were determined using phenylalanine standards prepared from authentic L- and DL-phenylalanine. The reference amino acids were benzoylated and the crude products esterified with (-)-8-phenylmenthol. Optically pure (2*R*)-epimer was obtained from fractional crystallization of the racemate mixture containing solution.

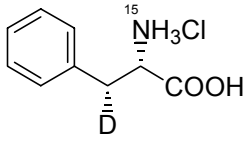

(2*S*, 3*R*)-[3-^{2}H,^{15}N]-phenylalanine hydrochloride (9). Chromatographed **8** was treated with 6 N HCl under refluxing conditions in a sealed vessel for 36 h after which the reaction mixture was extracted with ethyl acetate. TLC analysis of the organic phases revealed unreacted **8** which was isolated and re-submitted to the hydrolysis conditions. This process was repeated until the organic phase was devoid of starting material. The aqueous phases were pooled, diluted with isopropanol, and concentrated to give crude **9** which was recrystallized from isopropanol/water (86%): mp 190-200 °C dec; $[\alpha]^{20}_D$ -10.75° (*c* 5.0, H_2O); ^{1}H NMR (D_2O, δ): 2.98-3.04 (m, residual 1H), 3.14 (broad triplet, 1H), 3.96 (d, *J* = 5.2 Hz, 1H), 7.16-7.29 (m, 5H); ^{13}C NMR (D_2O / MeOH, δ): 36.34 (t, *J* =

19.6 Hz), 55.92 (d, J = 7.7 Hz), 128.47, 129.80, 130.00, 135.22, 173.52; ^{15}N NMR (D_2O, δ): 39.80; HRMS-ES (m/z): $[M + H]^+$ calcd for 168.0901; found 168.0897.

Stereochemical Analysis of 9. The optical purity of **9** was assessed using the (-)-camphanamide methyl ester derivative.[98] HPLC analysis of the derivatized material showed a 76% de at the 2-position, and deuterium NMR studies revealed a 72% de at the 3-position.

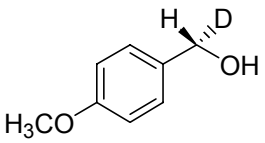

(*S*)-(+)-4-methoxybenzyl-α-*d* alcohol (10). $[\alpha]^{21}_D$ +0.91° (neat); ^{1}H NMR ($CDCl_3$, δ): 3.79 (s, 3H), 4.58 (t, br, 1H), 6.87 (d, 2H, J = 8.6 Hz), 7.27 (d, 2H, J = 8.6Hz); ^{13}C NMR ($CDCl_3$, δ): 55.26, 64.50 (t, J = 22.0 Hz), 113.89, 128.63, 133.09, 159.12; HRMS-ES (m/z): $[M + Na]^+$ calcd for 162.0641; found 162.0645.

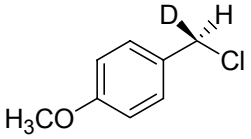

(*R*)-(-)-4-methoxybenzyl-α-*d* chloride (11). $[\alpha]^{21}_D$ –0.18° (*c* 16.6, THF); ^{1}H NMR ($CDCl_3$, δ): 3.79 (s, 3H), 4.53 (t, br, 1H, J = 1.6 Hz), 6.87 (d, 2H, J = 8.8 Hz), 7.30 (d, 2H, J = 8.8Hz); ^{13}C NMR (acetone-d_6): 45.89 (t, J = 23.2 Hz), 55.15, 113.99, 129.91, 159.52, 175.42; HRMS-EI (70 eV) m/z: M^+ calcd for 157.04037; found 157.04137.

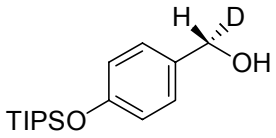

(*S*)-(+)-4-triisopropylsilyloxybenzyl-α-*d* alcohol (15). $[\alpha]^{21}_{D}$ +0.30° (neat); ^{1}H NMR ($CDCl_3$, δ): 1.08 (d, 18H, *J* = 7.04 Hz), 1.23 (m 3H), 4.57 (t, br, 1H), 6.85 (d, 2H, Hz), 7.20 (d, 2H, 8.6 Hz); HRMS-ES (*m*/*z*): $[M + Na]^+$ calcd for 304.1835; found 304.1837.

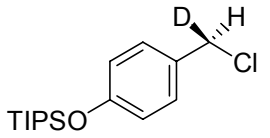

(*R*)-(-)-4-triisopropylsilyloxybenzyl-α-*d* chloride (16). $[\alpha]^{21}_{D}$ -0.39° (*c* 15.4, THF); ^{1}H NMR ($CDCl_3$, δ): 1.09 (d, 18H, *J* = 7.4 Hz), 1.25 (m, 3H), 4.63 (t, br, 1H), 6.89 (d, 2H, *J* = 8.5 Hz), 7.31 (d, 2H, *J* = 8.5Hz); ^{13}C NMR ($CDCl_3$, δ): 13.27, 18.15, 46.45 (t, *J* = 23.2 Hz), 120.65, 131.07, 131.50, 156.93; HRMS-ES (*m*/*z*): $[M + Na]^+$ calcd for 322.1480; found 322.1470.

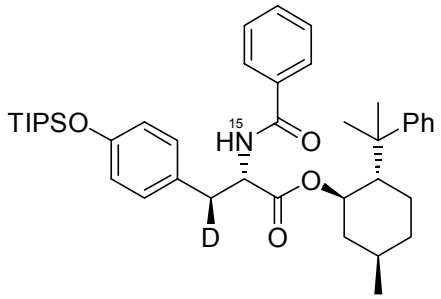

(2*S*, 3*S*)-*N*-benzoyl-*O*-triisopropylsilyl-[3-^{2}H,^{15}N]-tyrosine-(-)-8-phenylmenthyl ester (17). $[\alpha]^{21}_{D}$ +11.2° (*c* 13.5, THF); ^{1}H NMR ($CDCl_3$, δ): 0.85-1.30 (m), 0.88 (d, 3H, *J* = 6.6 Hz), 1.04 (s), 1.06 (s), 1.65-1.86 (m, 5H), 2.06 (dt, 1H, *J* = 11.8 Hz, 3.5 Hz), 2.65 (t, b, 1H, *J* = 3.7 Hz), 4.17 (dt, 1H, *J* = 2.4, 1.3), 4.78 (dt, 1H, *J* = 10.7 Hz, *J* = 4.2 Hz), 6.27

(dd, 1H, *J* = 91.4 Hz, 7.5 Hz), 6.71 (d, 2H, *J* = 8.3 Hz), 6.85 (d, 2H, *J* = 8.3 Hz), 7.24-7.26 (m, 4H), 7.37-7.50 (m, 4H), 7.66 (d, 2H, *J* = 7.2 Hz); ^{13}C NMR ($CDCl_3$, δ): 12.26, 14.12, 17.83, 20.93, 21.62, 23.82, 26.37, 28.81, 31.24, 34.41, 35.99 (t, *J* = 18.9 Hz), 39.40, 41.54, 50.33, 53.15, 53.27, 60.28, 76.06, 119.80, 125.19, 125.34, 126.92, 128.02, 128.43, 130.37, 131.42, 134.29, 134.37, 151.23, 154.90, 166.31, 166.47, 170.91; (HPLC 95% MeOH/H_2O): t_r = 20.2 min, 15.6 min.

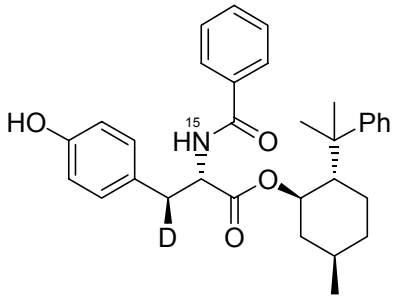

(2*S*, 3*S*)-*N*-benzoyl-[3-^{2}H,^{15}N]-tyrosine-(-)-8-phenylmenthyl ester (18). ^{1}H NMR ($CDCl_3$, δ): 0.89-1.29 (m), 0.90 (d, 3H, *J* = 6.4 Hz), 1.02 (s), 1.20 (s), 1.47 (s, b, 1H), 1.70 (d, 1H, J = 12.7 Hz), 1.84 (dt, 2H, J = 13.8, J = 3.1), 2.12 (dt, 1H, *J* = 11.6 Hz, 3.1 Hz), 2.65 (m, 1H), 4.20 (t, 1H, *J* = 6.1), 4.86 (dt, 1H, *J* = 11.0 Hz, *J* = 4.2 Hz), 6.44 (dd, 1H, *J* = 91.2 Hz, 7.9 Hz), 6.70 (d, 2H, *J* = 8.8 Hz), 6.88 (d, 2H, *J* = 8.8 Hz), 7.17-7.30 (m, 4H), 7.37-7.51 (m, 4H), 7.68 (d, 2H, *J* = 7.2 Hz); ^{13}C NMR ($CDCl_3$, δ): 12.24, 14.07, 17.62, 20.95, 21.69, 23.37, 26.28, 29.12, 31.19, 34.35, 36.10 (m), 39.34, 41.48, 50.23, 53.36, 53.49, 60.45, 76.19, 115.37, 125.16, 125.35, 126.94, 128.01, 128.53, 130.35, 131.66, 133.83, 133.91, 151.51, 155.49, 167.03, 167.19, 170.98; (HPLC 85% MeOH/H_2O): t_r = 8.4 min, 15.6 min.

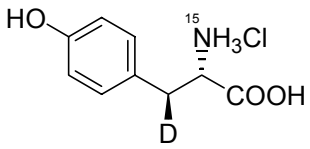

(2*S*, 3*S*)-[3-^{2}H,^{15}N]-tyrosine (19). ^{1}H NMR (D_2O, δ): 2.2 (dd, b, 1H, *J* = 7.5 Hz, *J* = 2.2 Hz), 3.10 (residual ^{1}H, t, b, 3.4 Hz), 4.08 (d, 1H, *J* = 7.5 Hz), 6.75 (d, 2H, *J* = 8.3 Hz), 7.05 (d, 2H, *J* = 8.3 Hz); ^{13}C NMR (D_2O/MeOH, δ): 35.25 (t, *J* = 19.6 Hz), 55.13, 116.56, 126.40, 131.47, 155.87, 172.43; HRMS-ES (*m*/*z*): $[M]^+$ calcd for 184.0958; found 184.0951.

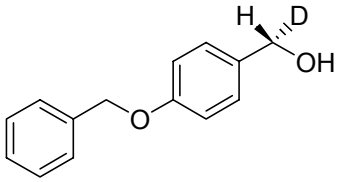

(*S*)-(+)-4-benzyloxybenzyl-α-*d*-alcohol (20d). $[\alpha]^{21}_{D}$ +0.59° (*c* 5.1, THF); ^{1}H NMR ($CDCl_3$, δ): 2.07 (s, br, 1H), 4.55 (s, br, 1H), 5.06 (s, 2H), 6.96 (d, 2H, *J* = 8.8 Hz), 7.27 (d, 2H, *J* = 8.8 Hz), 7.31-7.45 (m, 5H); ^{13}C NMR ($CDCl_3$, δ): 22.1 (t, *J* = 22.1 Hz), 69.90, 114.79, 127.32, 127.84, 128.46, 128.52, 133.26, 136.84, 158.23; HRMS-ES (*m*/*z*): $[M + Na]^+$ calcd for 238.0954; found 238.0946.

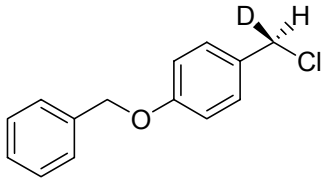

(*R*)-(-)-4-benzyloxybenzyl-α-*d*-chloride (21d). $[\alpha]^{21}_{D}$ -0.37° (*c* 13.6, THF); ^{1}H NMR ($CDCl_3$, δ): 4.53 (s, br, 1H), 5.05 (s, 2H), 6.93 (d, 2H, J = 8.6 Hz), 7.28-7.42 (m, 7H); ^{13}C

NMR ($CDCl_3$, δ): 45.64 (t, *J* = 23.0 Hz), 62.71, 66.15, 69.47, 75.46, 114.78, 127.39, 127.66, 128.29, 130.10, 137.13, 158.81; HRMS-ES (*m*/*z*): $[M + Na]^+$ calcd for 256.0615; found 256.0617.

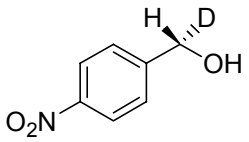

(*S*)-(+)-4-nitrobenzyl-α-*d* alcohol (20e). $[\alpha]^{21}_D$ +2.46° (*c* 6.1, THF); ^1H NMR ($CDCl_3$, δ): 4.81 (s, 1H), 7.52 (d, 2H, *J* = 8.8 Hz), 8.21 (d, 2H, *J* = 8.8 Hz); ^{13}C NMR ($CDCl_3$, acetone-d_6, δ): 62.24 (t, *J* = 23 Hz), 123.03, 126.79, 146.78, 150.19; HRMS-ES (*m*/*z*): $[M + Na]^+$ calcd for 177.0386; found 177.0378.

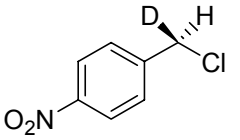

(*R*)-(-)-4-nitrobenzyl-α-*d* chloride (21e). $[\alpha]^{21}_D$ -0.1.31° (*c* 6.9, THF); ^1H NMR (acetone-d_6, δ): 4.81 (s, 1H), 7.71 (d, 2H, *J* = 8.6 Hz), 8.21 (d, 2H, *J* = 8.6 Hz); ^{13}C NMR (acetone-d_6, δ): 43.98 (t, *J* = 23 Hz), 123.54, 129.58, 144.82, 147.57; HRMS-EI (70 eV) *m*/*z*: M^+ calcd for 172.01488; found 172.01506.

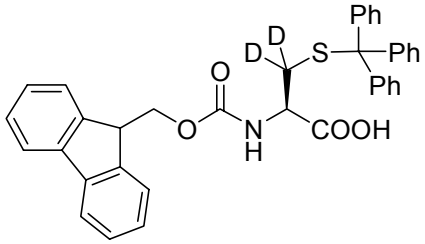

(2*S*)-[3,3-$^2H_2$]-*N*-FMOC-*S*-trityl-cysteine (24). (2S)-[3,3-$^2H_2$]-cysteine was treated as described by Fukase to generate the *S*-trityl material.[121] Briefly, the amino acid was

dissolved in trifluoroacetic acid and to this stirred solution was added trityl alcohol (1 eq) in one portion. The mixture was stirred at rt for 30 min and concentrated under reduced pressure. The residue was dissolved in diethyl ether and the pH was adjusted with 10% sodium acetate until a precipitate formed. The precipitate was collected and washed with diethyl ether and water (97%). This material was added to a solution of FMOC chloride (1.1 eq) in ethyl acetate and refluxed for 12 h under an argon atmosphere.[122,123,190] Concentration of the organic solution gave a residue which was purified using silica gel column chromatography (quant.): ^{1}H NMR ($CDCl_3$ δ): 4.20-4.4.25 (m, 2H), 4.36-4.42 (m, 2H), 5.11 (d, 1H, *J* = 7.9 Hz), 7.17-7.75 (m, 23H).

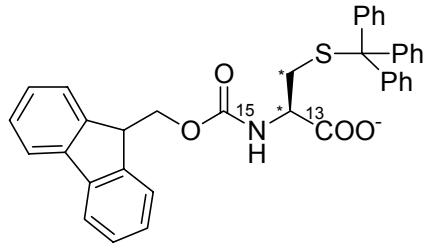

(2*S*)-[U-^{15}N,^{13}C]-*N*-FMOC-*S*-trityl-cysteine (25). This compound was prepared in a similar manner as described for (2*S*)-[3,3-$^{2}H_2$]-*N*-FMOC-*S*-trityl-cysteine. Uniformly labeled cysteine was treated with trifluoroacetic acid and trityl alcohol to give the *S*-trityl protected material (quant.). This material (900 mg) was treated with FMOC chloride under refluxing conditions to yield 1.3 g of a solid (87%): ^{1}H NMR ($CDCl_3$ δ): 2.45 (s, br, 1H), 2.80 (s, br, 1H), 4.30 (s, br, 4H), 5.10 (d, br, 1H, *J* = 92.0 Hz), 7.00-7.75 (m, 23H).

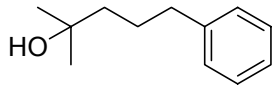

2-hydroxy-2-methyl-5-phenylpentane. A dry, argon flushed 3-neck rb flask equipped with a reflux condenser and magnetic stir bar was charged with magnesium (6.6 g, 0.27 mol) and anhydrous diethyl ether (100 mL). To this mixture was added via cannula a solution of 1-bromo-3-phenylpropane (38 mL, 0.25 mol) in anhydrous diethyl ether (50 mL). After 5 mL of the bromide solution had been added, addition was stopped until Grignard reagent formation had begun indicated by the mixture turning a gray color and magnesium being consumed. The rest of the bromide solution was added over 1.5 h. The reaction mixture was refluxed at 35 °C for 20 min, then cooled to rt and anhydrous acetone (20 mL) was carefully added via cannula over 1 h. The reaction mixture was stirred overnight at rt. The next morning the mixture was cooled to 0 °C and carefully quenched with 4 N HCl. The mixture was stirred for 1 h at 0 °C. The phases were separated and the aq phase was extracted with diethyl ether. The combined organic phases were washed with water, brine, dried over magnesium sulfate, and filtered. The filtrate was concentrated and fractionally distilled under high vacuum to yield 36.2 g of a pale yellow oil (81%): ^{1}H NMR ($CDCl_3$ δ): 1.19 (s, 6H), 1.34 (s, br, 1H), 1.48-1.52 (m, 2H), 1.64-1.62 (m, 2H), 2.61 (t, 2H, *J* = 7.5 Hz), 7.15-7.28 (m, 4H).

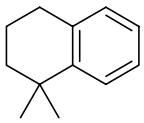

1,2,3,4-tetrahydro-1,1-dimethylnaphthalene. A dry, argon flushed 500 mL rb flask equipped with a magnetic stir bar was charged with phosphorous pentoxide (19 g, 67

mmol) and methane sulfonic acid (100 mL). The mixture was heated to 105 °C under argon until the phosphorous pentoxide had dissolved. The reaction mixture was cooled to rt and 2-hydroxy-2-methyl-5-phenylpentane (20 g, 112 mmol) was slowly added with stirring. The mixture was stirred for 3 h, after which time, it was poured onto ice with stirring. The ice mixture was diluted with diethyl ether with stirring. The phases were separated and the aq. phase extracted with diethyl ether. The combined organic extracts were washed with water, brine, dried over magnesium sulfate, and filtered. The filtrate was concentrated to yield an oil which was distilled under high vacuum to give 19.2 g of a yellow oil (quant.): ^{1}H NMR ($CDCl_3$ δ): 1.28 (s, 6H), 1.64-1.67 (m, 2H), 1.76-1.83 (m, 2H), 2.76 (t, 2H, *J* = 6.3 Hz), 7.04-7.33 (m, 4H).

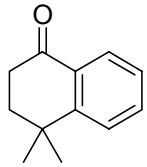

4,4-dimethyl-1-tetralone. A solution of glacial acetic acid (160 mL) and acetic anhydride (80 mL) was cooled to 0 °C and chromium trioxide (12 g) was carefully added in small portions. The mixture was stirred at 0 °C for 30 min before benzene (60 mL) was added. 1.2,3,4-tetrahydro-1,1-dimethylnaphthalene (9.0 g) was added slowly as a solution in benzene (14 mL). The reaction mixture was stirred at 0 °C for 4h. The solution was diluted with water and extracted with ether. The combined organic layers were washed with water, sodium bicarbonate, brine, dried over magnesium sulfate, and filtered. The organic solution was concentrated and the residue distilled under high vacuum to give 8.5 g of oil (87%): ^{1}H NMR ($CDCl_3$ δ): 1.38 (s, 6H), 2.01 (t, 2H, *J* = 6.7 Hz), 2.72 (t, 2H, *J* = 6.7 Hz), 7.24-7.51 (m, 3H), 8.00 (dd, 1H, *J* = 7.8 Hz, *J* = 1.1 Hz).

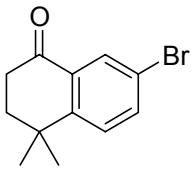

7-bromo-4,4-dimethyl-1-tetralone. A dry, argon flushed rb flask equipped with a dry-ice condenser and a drying tube was charged with aluminum chloride (5.0 g) and anhydrous dichloromethane (minimal amount). To the stirred mixture was added 4,4-dimethyl-1-tetralone at rt followed by the careful addition of bromine. The mixture was stirred for 2 h, heating the mixture to 70 °C was required to maintain stirring. The reaction was quenched by the slow addition of ice-cold 6 N HCl. The mixture was extracted with diethyl ether and the combined organic phases were washed with water, sodium bicarbonate, and brine. The organic solution was dried over magnesium sulfate, filtered, and concentrated under reduced pressure. The residue was purified using chromatography on silica gel to give 1.3 g of an orange oil (36%): ^{1}H NMR ($CDCl_3$ δ): 1.36 (s, 6H), 1.99 (t, 2H, *J* = 6.7 Hz), 2.71 (t, 2H, *J* = 6.7 Hz), 7.37 (d, 1H, *J* = 8.2), 7.59 (dd, 1H, *J* = 8.2 Hz, *J* = 2.2 Hz), 8.12 (d, 1H, *J* = 2.2 Hz).

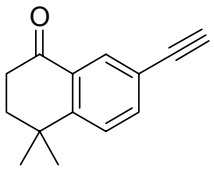

4,4-dimethyl-7-ethynyl-1-tetralone. A dry, argon flushed pressure flask flask equipped with a magnetic stir bar was charged with 7-bromo-4,4-dimethyl-1-tetralone (256 mg, 1.0 mmol) and triethylamine. To this stirred solution was added Pd(PPh3)2Cl2 (0.05 mmol) and CuI (0.05 mmol). The solution was flushed with argon for 5 min and TMS-acetylene (10 mmol) was added. The flask was sealed and heated to 100 °C for 24 h. The

reaction mixture was filtered through Celite and washed with diethyl ether. Concentration of the filtrate gave a residue which was dissolved in methanol. To this solution was added potassium carbonate and the mixture was stirred for 8 h at rt. The reaction mixture was filtered and diluted with ether. The phases were separated and the aq. phase was extracted with diethyl ether. The combined organic phases were washed with water, 1 N HCl, and brine. The organic solution was dried over magnesium sulfate, filtered, and concentrated. Purification by chromatography on silica afforded 175 mg of a light brown solid (87%): ^{1}H NMR ($CDCl_3$ δ): 1.36 (s, 6H), 2.01 (t, 2H, *J* = 6.9 Hz), 2.71 (t, 2H, *J* = 6.9 Hz), 3.04 (s, 1H), 7.37 (d, 1H, *J* = 8.2), 7.59 (dd, 1H, *J* = 8.2 Hz, *J* = 1.8 Hz), 8.12 (d, 1H, *J* = 1.8 Hz).

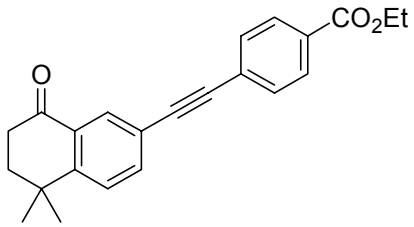

4-[(5,6,7,8-tetrahydro-5,5-dimethyl-8-oxo-2-naphthalenyl)ethynyl]-benzoic acid ethyl ester. To a dry, argon flushed rb flask was added a solution of 4,4-dimethyl-7-ethynyl-1-tetralone (74 mg) in triethylamine (2 mL), 4-iodoethylbenzoate (113 mg), $Pd(PPh_3)_2Cl_2$ (87 mg), and CuI (24 mg). The mixture was stirred for 18 h and filtered through Celite. The filtrate was concentrated and the residue purified using chromatography on silica gel to give 137 mg (quant.) of a faintly yellow solid: ^{1}H NMR ($CDCl_3$ δ): 1.36 (m, 9H), 2.01 (t, 2H, *J* = 6.5 Hz), 2.73 (t, 2H, *J* = 6.5 Hz), 4.36 (q, 2H, *J* = 7.1 Hz), 7.37-7.66 (m, 5H), 8.01 (d, 1H, *J* = 8.4 Hz), 8.18 (d, 1H, *J* = 1.8 Hz).

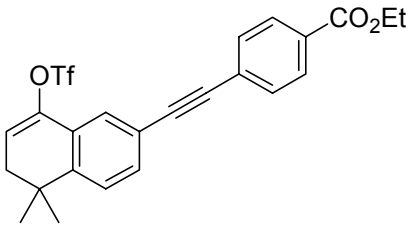

4-[[5,6-dihydro-5,5-dimethyl-8-[[(trifluoromethyl)sulfonyl]oxy]-2-naphthalenyl]ethynyl]-benzoic acid ethyl ester. To a solution of LDA prepared at -78 °C (1.1 eq) was added a solution of 4-[(5,6,7,8-tetrahydro-5,5-dimethyl-8-oxo-2-naphthalenyl)ethynyl]-benzoic acid ethyl ester (1 eq) in anhydrous THF. The enolate solution was stirred at -78 °C for 30 min and a THF solution of 2-[*N*,*N*-bis(trifluoromethylsulfonyl)-amino]-5-chloropyridine (1.1 eq) was added. The reaction mixture was stirred at -78 °C for 1 h, then at 0 °C for 2.5 h. TLC analysis of an aliquot showed no remaining starting material. The reaction was quenched at 0 °C with the addition of saturated ammonium chloride. The reaction mixture was extracted with ethyl acetate. The combined organic phases were washed with 1 N NaOH, water, brine, and dried over sodium sulfate. Concentration of the organic solution gave a residue which was purified using chromatography on silica gel to give a yellow oil (68%): ^{1}H NMR ($CDCl_3$ δ): 1.30 (s, 6H), 1.39 (t, 3H, *J* = 7.1 Hz), 2.42 (d, 1H, *J* = 4.8 Hz), 4.37 (q, 2H, *J* = 7.1 Hz), 7.30 (d, 1H, *J* = 8.0 Hz), 7.48-7.51 (m, 2H), 7.58 (d, 2H, *J* = 8.2 Hz), 8.01 (d, 2H, *J* = 8.2 Hz).

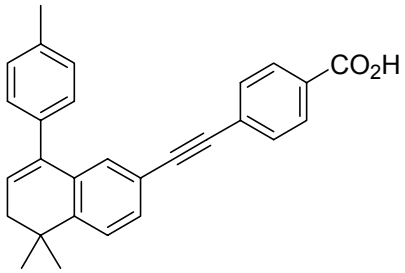

4-[[5,6-dihydro-5,5-dimethyl-8-(4-methylphenyl)-2-naphthalenyl]ethynyl]-benzoic acid. A solution of 4-lithiotoluene was prepared by the addition of *t*-butyl lithium (2.2 mmol) to a solution of 4-bromotoluene in anhydrous THF (1.5 mL) at -78 °C. The solution was stirred for 30 min at -78 °C and a THF solution of zinc chloride (1.49 mmol, 2.4 mL) was added. The solution was warmed to rt, stirred for 30 min, and added via cannula to a THF solution of 4-[[5,6-dihydro-5,5-dimethyl-8-[[(trifluoromethyl)sulfonyl]oxy]-2-naphthalenyl]ethynyl]-benzoic acid ethyl ester (0.74 mmol, 3 mL) and $Pd(PPh_3)_4$ (0.03 mmol). The reaction mixture was warmed to 50 °C for 1 h, cooled to rt, and diluted with saturated ammonium chloride. The aq phase was extracted with ethyl acetate and the combined organic layers washed with water and brine and dried over sodium sulfate. Concentration of the organic solution afforded a yellow solid which was purified using flash chromatography on silica gel to give 267 mg of a white solid which was stirred with lithium hydroxide in THF/water for 12 h at rt to yield a white solid (86%, over 2 steps): mp 270-272 °C; UV (ethanol) λ_{max}, nm (ε): 281 (28,000); ^{1}H NMR (DMSO-d_6 δ): 1.26 (s, 6H), 2.29-2.46 (m, 5H), 5.96 (t, 1H, *J* = 4.6 Hz), 7.01 (s, 1H), 7.23 (q, 4H, *J* = 8.1 Hz), 7.47 (s, 2H), 7.60 (d, 2H, *J* = 8.4 Hz), 7.87 (d, 2H, *J* = 8.4 Hz); ^{13}C NMR (DMSO-d_6 δ): 21.17, 28.11, 33.76, 38.34, 88.42, 92.34, 119.55, 125.01, 126.90, 127.46, 128.25, 128.63, 129.56, 129.85, 130.78, 131.27, 131.87,

134.25, 137.01, 137.23, 138.19, 138.46, 146.53, 167.03; HPLC (85% MeOH/H_2O): t_r = 8.7 min; HRMS-ES (*m*/*z*): $[M + Na]^+$ calcd for 415.1674; found 415.1700.

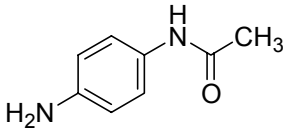

4-acetamidoaniline. Acetic anhydride (0.9 mL, 9.2 mmol) was added dropwise to a solution of 4-aminoaniline (1.0 g, 9.2 mmol) in pyridine (25 mL) at rt. The reaction mixture was stirred for 4 h then diluted with water and extracted with ethyl acetate. The combined organic phases were washed with water, brine, and diluted with toluene. Concentration of the organic solution gave a solid that was recrystallized from ethanol at -30 °C. ^{1}H NMR (acetone-d_6, δ): 1.94 (s, 3H), 4.78 (br, s, 2H), 6.49 (d, 2H), 7.19 (d, 2H), 9.5 (s, 1H).

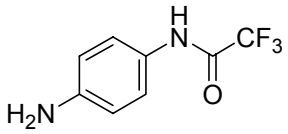

4-trifluoroacetamidoaniline. Trifluoroacetic anhydride (2.5 mL, 17.7 mmol) was added dropwise to a solution of 4-nitroaniline (2.0 g, 14.5 mmol) in pyridine (50 mL) at rt. The reaction mixture was stirred overnight. The reaction mixture was diluted with toluene and concentrated under reduced pressure to give an orange solid. The solid was dissolved in ethyl acetate, washed with 0.5 N HCl, water, and brine. Concentration of the organic phase yielded 3.4 g of an orange solid (quant.). A portion of this solid (1.0 g) was subjected to catalytic hydrogenation as described in section 5.2.9 and

chromatographed on silica to yield 500 mg of a light brown solid. ^{1}H NMR (acetone-d_6, δ): 4.62 (br, s, 2H), 6.69 (d, 2H), 7.37 (d, 2H), 9.89 (br, s, 1H).

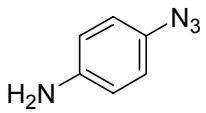

4-azidoaniline. To a solution of 4-trifluoroacetamidoaniline (500 mg, 2.5 mmol) in 1 N HCl (20 mL) at 0 °C was added a cooled aq solution of sodium nitrite (254 mg, 3.7 mmol). The reaction mixture was stirred for 15 min after which time a chilled aq solution of sodium azide (3.7 mmol) was added resulting in the immediate formation of flocculate ppt. After stirring for 1h at 0 °C, the reaction mixture was filtered and precipitate was washed with water and collected. The light brown solid was dissolved in 4 N sodium hydroxide and stirred at 0 °C for 3 h. The reaction mixture was diluted with water and extracted with ethyl acetate. Concentration of the pooled organic phases yielded 199 mg (61%): ^{1}H NMR (acetone-d_6, δ): 4.70 (br, s, 2H), 6.72 (d, 2H), 6.79 (d, 2H).

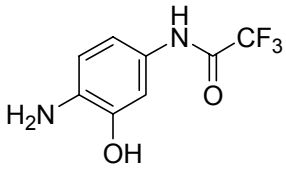

2-amino-5-trifluoroacetamidophenol. Trifluoroacetic anhydride (4.6 mL, 32.4 mmol) was added dropwise to a solution of 2-amino-5-nitroaniline (5.0 g, 32.4 mmol) in pyridine (100 mL) at rt. The reaction mixture was stirred overnight. The reaction mixture was diluted with toluene and concentrated under reduced pressure to give an orange solid. The solid was dissolved in ethyl acetate, washed with 0.5 N HCl, water, and brine. Concentration of the organic phase yielded the crude product. This solid was subjected

to catalytic hydrogenation as described in section 5.2.9 and purified by extraction to give 5.0 g of a brown solid. 1H NMR (acetone-d_6, δ): 4.69 (br, s, 2H), 6.21 (dd, 1H, J = 8.6 Hz, J = 2.4 Hz), 6.32 (d, 1H, J= 2.4 Hz), 7.41 (d, 1H, J = 8.6 Hz), 8.60 (s, br, 1H), 9.15 (s, br, 1H).

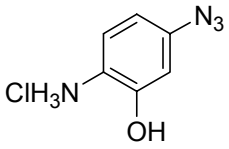

4-azido-2-hydroxyaniline hydrochloride. To a solution of 2-amino-5-trifluoroacetamidophenol (1.0 g, 4.5 mmol) in 1 N HCl (50 mL) at 0 °C was added a cooled aq solution of sodium nitrite (470 mg, 6.8 mmol). The reaction mixture was stirred for 15 min after which time a chilled aq solution of sodium azide (443 mg, 6.8 mmol) was added resulting in the immediate formation of flocculent precipitate. After stirring for 1 h at 0 °C, the reaction mixture was filtered and the precipitate was washed with water and collected to give 830 mg of a brown solid. A portion of this material was dissolved in 1 N HCl and was refluxed for 12 h. Concentration of the aq phase yielded a solid that was used without further purification.

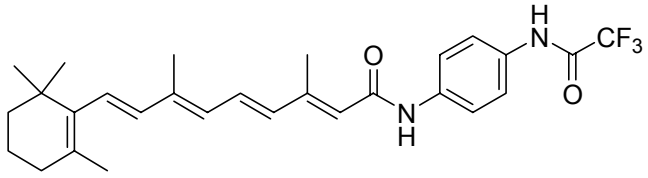

***N*-(4-trifluoroacetamidophenyl)retinamide.** This compound was prepared as described in section 5.2.10 (method 2) using RA (1.0 g) and 4-trifluoroacetamidoaniline (748 mg, 1.1 eq). The crude product was purified using column chromatography on silica gel to give a yellow solid (88%): ^{1}H NMR (acetone-d_6, δ): 1.00 (s, 6H), 1.43-1.46

(m, 2H), 1.56-1.61 (m, 2H), 1.68 (s, 3H), 1.98-2.03 (m, 5H), 2.39 (s, 3H), 6.00 (s, 1H), 6.13-6.35 (m, 4H), 7.06 (dd, 1H, *J* = 15.9 Hz, *J* = 11.3 Hz), 7.62 (d, 2H, *J* = 8.9 Hz), 7.73 (d, 2H, *J* = 8.9 Hz), 9.29 (s, 1H), 10.19 (s, 1H); ^{13}C NMR (acetone-d_6, δ): 12.79, 13.56, 19.83, 21.82, 33.54, 34.82, 40.32, 120.25, 122.10, 123.04, 128.71, 130.12, 130.74, 130.83, 132.40, 136.81, 138.40, 138.55, 139.35, 150.32, 165.67; HPLC (92% MeOH/H_2O): t_r = 8.0 min; HRMS-ES (*m/z*): $[M + Na]^+$ calcd for $C_{28}H_{33}F_3N_2O_2Na$ 509.2392; found 509.2408.

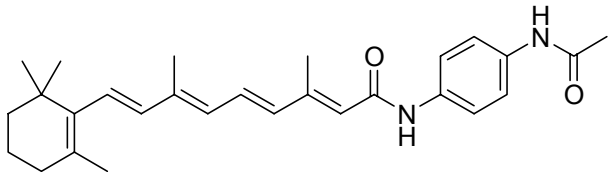

***N*-(4-acetamidophenyl)retinamide.** This compound was prepared as described in section 5.2.10 (method 2) using RA (75 mg) and acetanilide (75 mg). The crude product was purified using silica gel preparative TLC to give a yellow solid (56%): ^{1}H NMR (DMSO-d_6, δ): 1.02 (s, 6H), 1.44-1.45 (m, 2H), 1.58 (m, 2H), 1.69 (s, 3H) 1.98-2.08 (m, 8H), 2.34 (s, 3H), s (6.00, 1H), 6.15-6.38 (m, 4H), 6.99 (dd, 1H, *J* = 15.9 Hz, *J* = 11.8 Hz), 7.48 (d, 2H, *J* = 8.9 Hz), 7.55 (d, 2H, *J* = 8.9 Hz), 9.85 (s, 1H), 9.94 (s, 1H); ^{13}C NMR (DMSO-d_6, δ): 12.45, 13.14, 18.60, 21.36, 23.72, 28.68, 32.48, 33.73, 119.23, 122.60, 127.33, 129.22, 129.95, 134.54, 134.66, 135.89, 136.83, 137.17, 138.02, 147.88, 164.35, 167.73; HPLC (92% MeOH/H2O): t_r = 7.0 min; HRMS-ES (*m/z*): $[M + Na]^+$ calcd for 455.2674; found 455.2689.

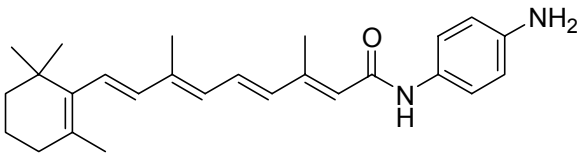

***N*-(4-aminophenyl)retinamide**. To 2 mL of a 5 N KOH in MeOH/THF (5:1) solution was added (*N*-(4-trifluoroacetamidophenyl)retinamide (102 mg, 0.21 mmol). The reaction mixture was stirred overnight under an argon atmosphere. Purification by silica gel preparative TLC afforded 68 mg of the title compound (67%): ^{1}H NMR (acetone-d_6, δ): 1.00 (s, 6H), 1.43-1.46 (m, 2H), 1.58 (m, 2H), 1.68 (s, 3H), 1.99 (m, 5H), 2.75 (s, 3H), 4.39 (s, 2H), 5.98 (s, 1H), 6.11-6.33 (m, 4H), 6.57 (d, 2H, *J* = 8.7 Hz) 7.00 (dd, 1H, *J* = 15.3 Hz, *J* = 11.4 Hz) 7.38 (d, 2H, *J* = 8.7 Hz), 8.82 (s, 1H); ^{13}C NMR (acetone-d_6 δ): 12.83, 13.45, 19.90, 21.88, 33.59, 34.87, 40.37, 115.14, 121.55, 124.02, 128.45, 130.00, 130.05, 130.84, 131.02, 137.25, 138.53, 138.62, 138.83, 145.34, 148.68, 165.02; (HPLC 92 % MeOH/H_2O): t_r = 8.76 min; HRMS-ES (*m/z*): $[M + Na]^+$ calcd for 413.2569; found 413.2574.

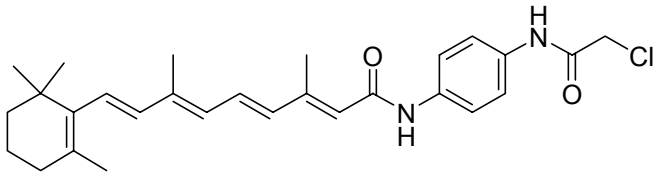

***N*-(4-chloroacetamidophenyl)retinamide**. A dry, argon flushed round bottom flask equipped with a magnetic stir bar was charged with *N*-(4-aminophenyl)retinamide (25 mg, 0.064 mmol) and THF (2 mL) and cooled to 0°C. To this stirred solution was added chloroacetyl chloride (10.9 mg, 0.096 mmol). The solution was stirred at 0 °C for 1.5 h, then diluted with water and extracted with ethyl acetate. The product was purified using silica gel preparative TLC (50% ethyl acetate/hexanes): ^{1}H NMR (acetone-d_6, δ): 1.01

(s, 6H), 1.44-1.47 (m, 2H), 1.58-1.60 (m, 2H), 1.68 (s, 3H), 2.01 (m, 5H), 2.40 (s, 3H), 4.20 (s, 2H), 6.00 (s, 1H), 6.14-6.35 (m, 4H), 7.05 (dd, 1H, *J* = 15.9 Hz, *J* = 11.5 Hz), 7.57 (d, 2H, *J* = 8.9 Hz), 7.66 (d, 2H, *J* = 8.7 Hz), 9.19 (s, 1H), 9.33 (s, 1H); ^{13}C NMR (acetone-d_6, δ): 12.68, 13.38, 19.71, 21.75, 33.42, 34.69, 40.15, 43.92, 119.97, 120.06, 120.57, 120.67, 123.11, 128.50, 129.98, 130.49, 130.79, 136.79, 138.32, 138.41, 139.12, 149.88, 164.80, 165.38; (HPLC 92 % MeOH/H_2O): t_r = 10.22 min; HRMS-ES (*m/z*): [M + Na]$^+$ calcd for 489.2285; found 489.2266.

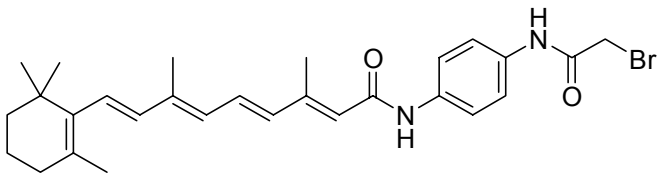

***N*-(4-bromoacetamidophenyl)retinamide**. Synthesis was performed as described for *N*-(4-chloroacetamidophenyl)retinamide except using bromoacetyl bromide. The product was purified using column chromatography on silica gel (100% ethyl acetate): ^{1}H NMR (acetone-d_6, δ): 1.04 (s, 6H), 1.47-1.50 (m, 2H), 1.61-1.64 (m, 2H), 1.71 (s, 3H), 2.03-2.09 (m, 5H), 2.42 (d, 3H, *J* = 0.7 Hz), 4.01 (s, 2H), 6.02 (s, 1H), 6.16-6.38 (m, 4H), 7.05 (dd, 1H, *J* = 15.4 Hz, *J* = 11.3 Hz), 7.59 (d, 2H, *J* = 8.8 Hz), 7.69 (d, 2H, *J* = 8.8 Hz), 9.21 (s, 1H), 9.47 (s, 1H); ^{13}C NMR (acetone-d_6, δ): 12.72, 13.42, 19.75, 21.79, 33.46, 34.74, 40.19, 120.04, 120.12, 120.39, 120.48, 123.17, 128.54, 130.02, 130.53, 130.83, 134.91, 136.83, 138.36, 138.44, 139.16, 149.92, 164.94, 165.41; HRMS-ES (*m/z*): [M + Na]$^+$ calcd for 533.1780; found 533.1771.

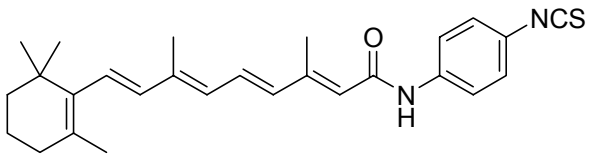

***N*-(4-isothiocyanatophenyl)retinamide.** A dry, argon flushed 3-neck round bottom flask equipped with a magnetic stir bar was charged with polymer-supported TPP (240 mg, 0.72 mmol) and CH_2Cl_2 (5 mL) and cooled to 0 °C. To this stirred suspension was added via cannula a CH_2Cl_2 solution of *N*-(4-azidophenyl)retinamide (98 mg, 0.24 mmol). The reaction mixture was stirred at 0 °C for 1 h, after which, CS_2 (0.03 mL, 0.50 mmol) was added via a syringe. The stirred suspension was maintained under an argon atmosphere and was allowed to warm to rt overnight. The contents of the reaction mixture were filtered, concentrated, and chromatographed on silica gel (20% ether/hexanes) to yield 56 mg of a yellow solid (55%): ^{1}H NMR (acetone-d_6 δ): 1.04 (s, 6H), 1.47-1.50 (m, 2H), 1.61-1.64 (m, 2H), 1.71 (s, 3H), 2.04 (m, 5H), 2.43 (d, 3H, *J* = 0.8 Hz), 6.02 (s, 1H), 6.16-6.38 (m, 4H), 7.12 (dd, 1H, *J* = 15.9 Hz, *J* = 11.3 Hz), 7.32 (d, 2H, *J* = 8.9 Hz), 7.81 (d, 2H, *J* = 8.9 Hz), 9.43 (s, 1H); ^{13}C NMR (acetone-d_6, δ): 12.88, 13.69, 19.91, 21.90, 33.62, 34.89, 40.39, 120.84, 122.72, 125.98, 127.05, 128.91, 130.24, 130.86, 131.15, 136.72, 138.43, 138.61, 139.66, 140.30, 151.06, 165.74, 165.82; HPLC (92% MeOH/H_2O): t_r = 17.0 min; HRMS-ES (*m/z*): $[M + Na]^+$ calcd for 455.2133; found 455.2130.

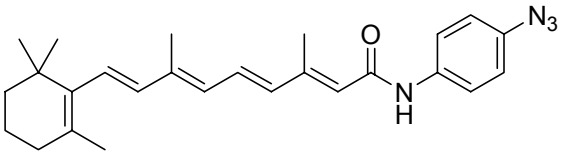

***N*-(4-azidophenyl)retinamide**. This compound was prepared as described in section 5.2.10 (method 2) using RA (343 mg, 1.14 mmol) and 4-azidoaniline (199 mg, 1.49 mmol). The crude product was purified by trituration with hexanes to give a yellow solid (86%): ^{1}H NMR (acetone-d_6, δ): 1.06 (s, 6H), 1.49-1.52 (m, 2H), 1.63-1.65 (m, 2H), 1.73 (s, 3H), 2.11 (m, 5H), 2.45 (d, 3H, J = 0.9 Hz), 6.03 (s, 1H), 6.18-6.43 (m, 4H), 7.03-7.15 (m, 3H), 7.81 (d, 2H, J = 8.1 Hz), 9.31 (s, 1H); ^{13}C NMR (acetone-d_6, δ): 12.87, 13.63, 19.91, 21.90, 33.62, 34.89, 40.39, 120.09, 121.39, 123.03, 128.78, 130.19, 130.82, 130.91, 135.18, 136.87, 138.01, 138.46, 138.61, 139.42, 150.39, 165.59; (HPLC 92% MeOH/H_2O): t_R = 13.59 min; HRMS-ES (*m/z*): $[M + Na]^+$ calcd for 439.2474; found 439.2470.

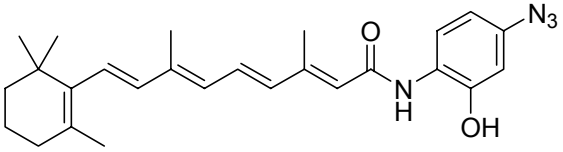

***N*-(2-hydroxy-4-azidophenyl)retinamide**. This compound was prepared as described in section 5.2.10 (method 2) using RA (100 mg, 0.33 mmol) and 4-azido-2-hydroxyaniline hydrochloride (82 mg, 0.44 mmol). The product was purified using silica gel preparative TLC (13 %): ^{1}H NMR (acetone-d_6, δ): 1.01 (s, 6H), 1.44-1.47 (m, 2H), 1.57-1.63 (m, 2H), 1.69 (s, 3H), 2.02 (m, 5H), 2.41 (d, 3H, J = 0.7 Hz), 6.15-6.39 (m, 5H), 6.53-6.6.58 (m, 2H), 7.13 (dd, 1H, J = 15.5 Hz, J = 11.7 Hz), 7.44 (d, 1H, J = 8.4 Hz), 9.32 (s, 1H); ^{13}C NMR (acetone-d_6, δ): 12.73, 13.62, 19.71, 21.77, 33.44, 34.70,

40.16, 109.14, 110.98, 121.20, 123.90, 125.26, 128.90, 130.14, 130.69, 131.53, 136.40, 137.93, 138.25, 138.39, 139.90, 150.79, 152.00, 167.29; (HPLC 92% MeOH/H_2O): t_R = 13.65 min; HRMS-ES (*m/z*): $[M + Na]^+$ calcd for 455.2423; found 455.2414..

APPENDIX

NMR Terms

Definitions of some of the terms commonly encountered in protein NMR literature are presented below in alphabetical order.[191] These definitions are rooted in the fundamentals of NMR theory, which can not be fully explained within this document. Therefore, the unfamiliar reader is directed to another reference as a starting point for additional reading.[192]

The term "correlation spectroscopy" refers to a multi-dimensional method in which peaks appear at the coordinates of two nuclei related by a mutual interaction. Examples of mutual interactions between nuclei include *J*-coupling, nuclear Overhauser enhancement (NOE), or chemical exchange. The term "correlation time" (τ_c) can be defined as a parameter related to the mean time during which a molecule maintains its spatial geometry. For a vector between nuclei, τ_c is approximately equal to the average time for it to rotate through an angle of one radian. Correlation time provides a measure of the tumbling rate of a molecule in solution which in turn, is most closely related to the size of the molecule.

The term "dipolar mechanism" refers to a direct through-space interaction, as opposed to a through-bond interaction, of two nuclear magnetic moment vectors. "Heteronuclear correlation spectroscopy" can be defined as correlation spectroscopy in which different types of nuclei are related by their mutual spin coupling. For example, a ^{13}C resonance can be defined by a ^{1}H resonance which is related or correlated to the ^{13}C

resonance by some interaction between the two nuclei. The "magnetization vector" (M) is the resultant of the individual magnetic moment vectors for an ensemble of a particular type of nuclei. "Nuclear Overhauser enhancement" (NOE) is the change in intensity of the resonance of one nucleus when the polarization of other nuclei are not at equilibrium. The nuclei must relax each other by through space interactions, the dipolar mechanism. The distance between the interacting nuclei is described by *r* and the NOE response is proportional to r^{-6}. The result is that NOE interactions are limited to nuclei within five Å of each other. The nuclear Overhauser enhancement is often used for signal enhancement in ^{13}C NMR by nonselective proton irradiation and to determine spatial proximity of nuclei by selective irradiation of one nucleus and observation of any change in the intensity of other resonances.

"Polarization" can be defined as excess nuclear magnetic moment vectors aligned with or opposed to B_o. The term "spin-coupling" (*J*-coupling) is the effect of the spin state of one nucleus on the energy of another nucleus. This effect is transmitted through intervening bonding electrons, in direct contrast to the dipolar mechanism which is transmitted through space. "Spin coupling constant" is a measure of the *J*-coupling interaction between two nuclei expressed in hertz (Hz). "Spin-lattice relaxation time" (T_1) is the time constant for the process of the magnetization vector, M, returning to its equilibrium position along the z-axis of B_o after being perturbed from equilibrium. The process is characterized by the transfer of absorbed energy from the molecule to its surroundings (lattice). "Spin-spin relaxation time" (T_2) is the time constant for the loss of magnetization due to chemical and spin exchange with other nuclei. This process is characterized by the transfer of absorbed energy between nuclei; T_2 processes also include T_1 processes. These are just a few of the fundamental definitions needed to

comprehend protein NMR theory. Again, the unfamiliar reader is directed to the reference cited above for further reading.

NMR Spectra

The following pages contain NMR spectra of key compounds. These spectra are included because they provide illustrative examples of stereochemical analysis or measurement of isotope incorporation. In the case of the affinity label analogs, a representative set of NMR data is included using the model compound *N*-(4-trifluoromethylacetamidophenyl)retinamide.

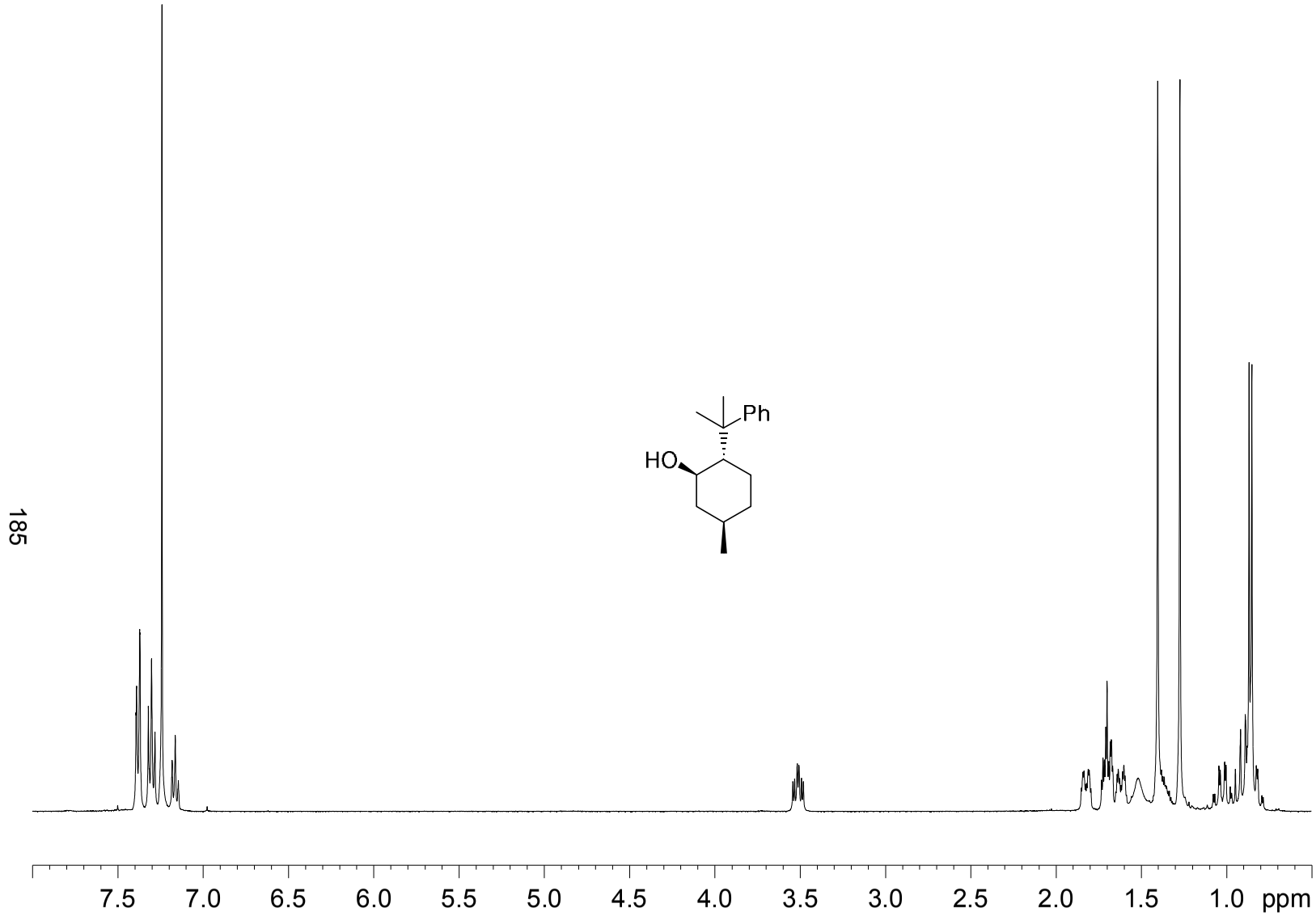

Spectrum 1 ^{1}H NMR spectrum (400 MHz) of (-)-8-phenylmenthol in $CDCl_3$.

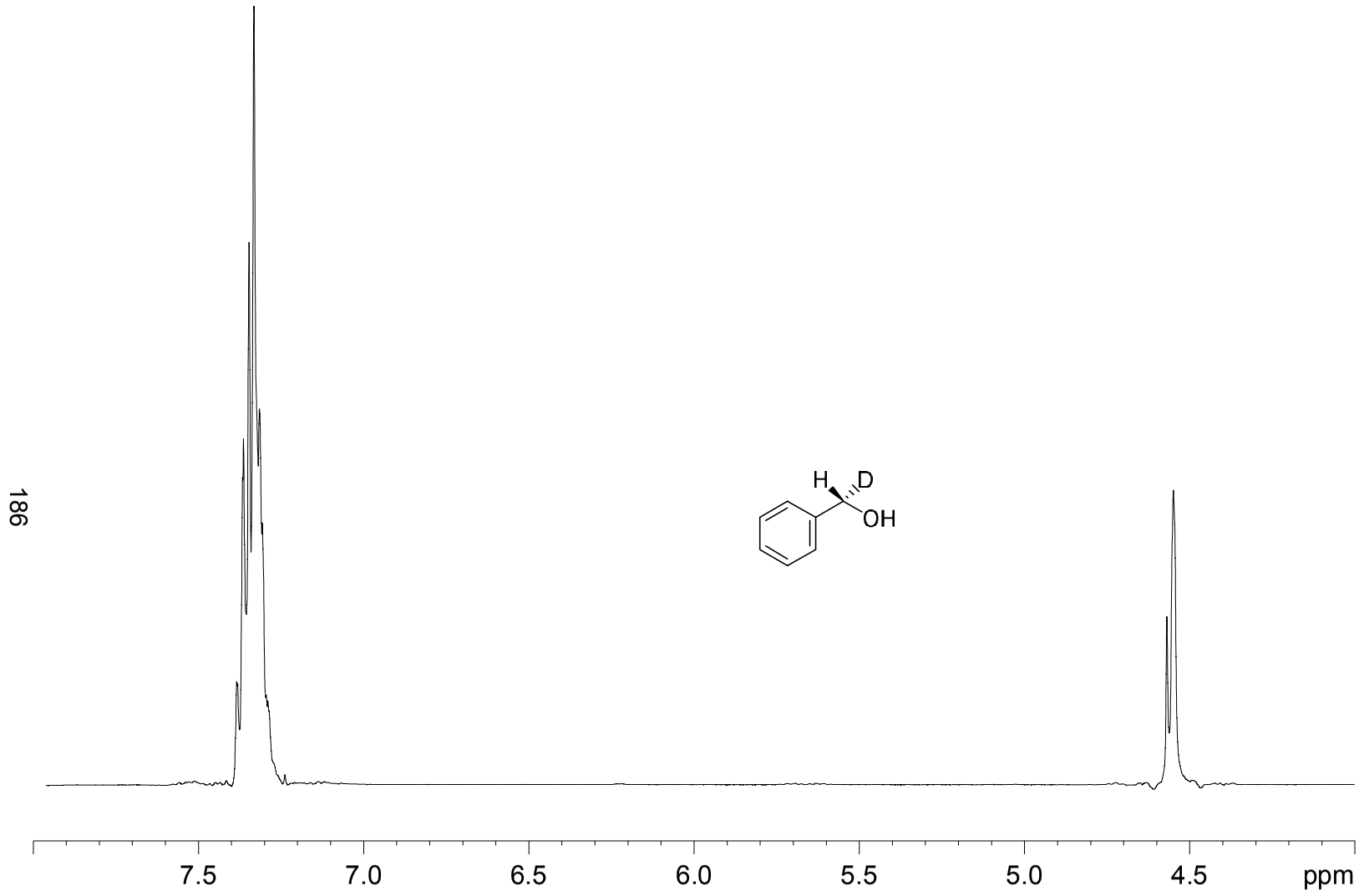

Spectrum 2 ^{1}H NMR spectrum (400 MHz) of (*S*)-(+)-benzyl-α-*d* alcohol (**2**) in $CDCl_3$.

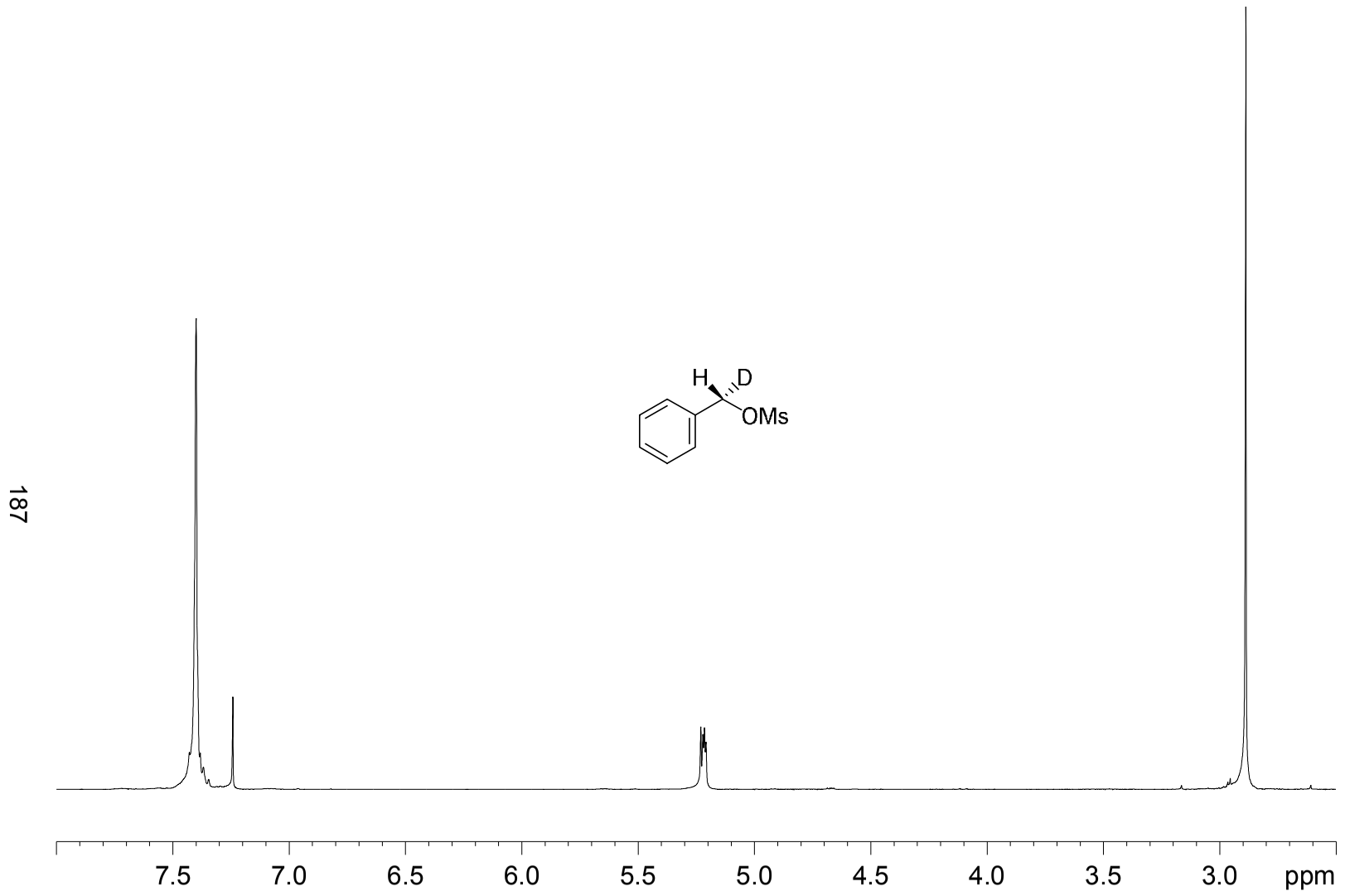

Spectrum 3 ^{1}H NMR spectrum (400 MHz) of (*S*)-(+)-benzyl-α-*d* mesylate (**3e**) in $CDCl_3$.

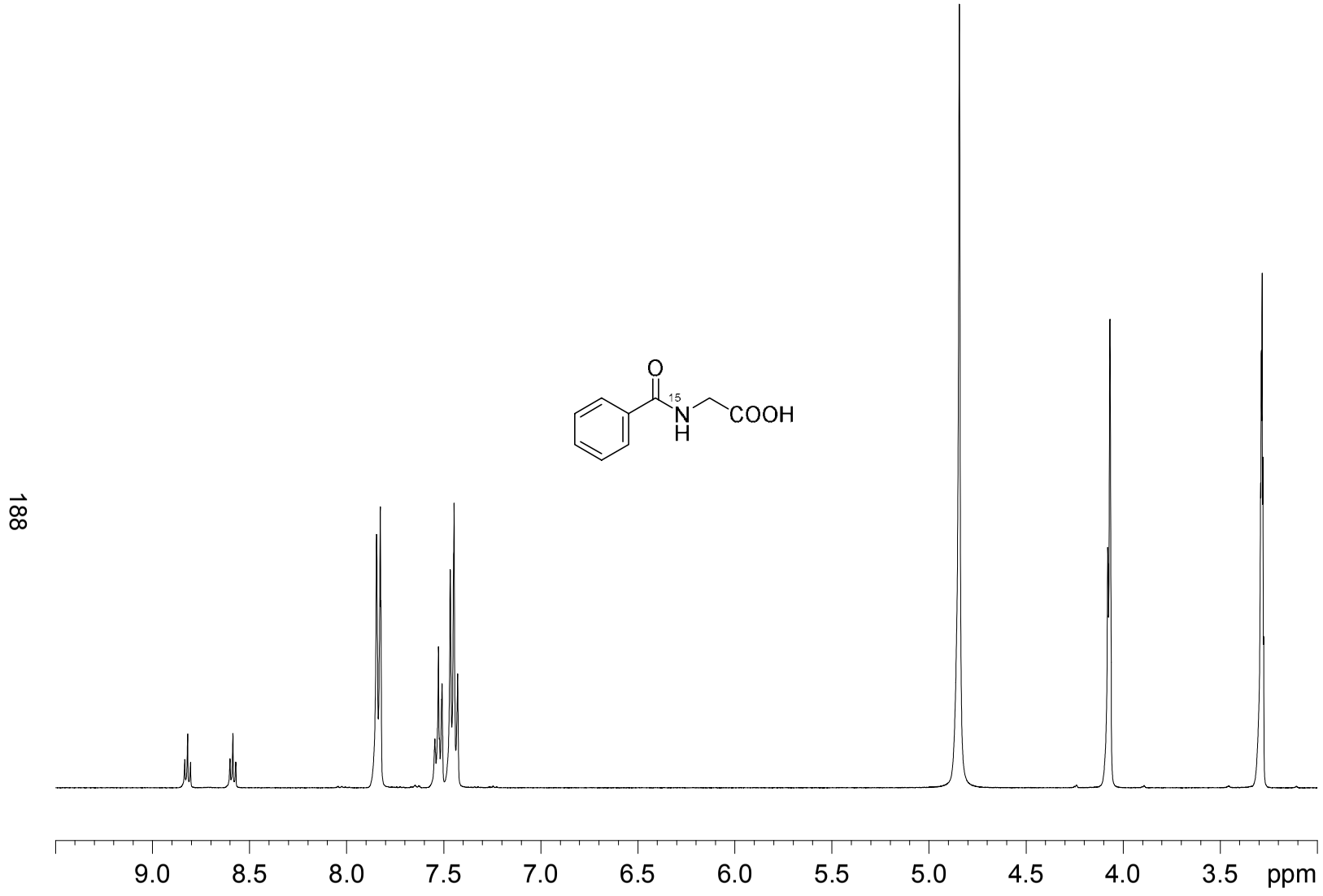

Spectrum 4 ^{1}H NMR spectrum (400 MHz) of ^{15}N-hippuric acid in MeOH-d_4.

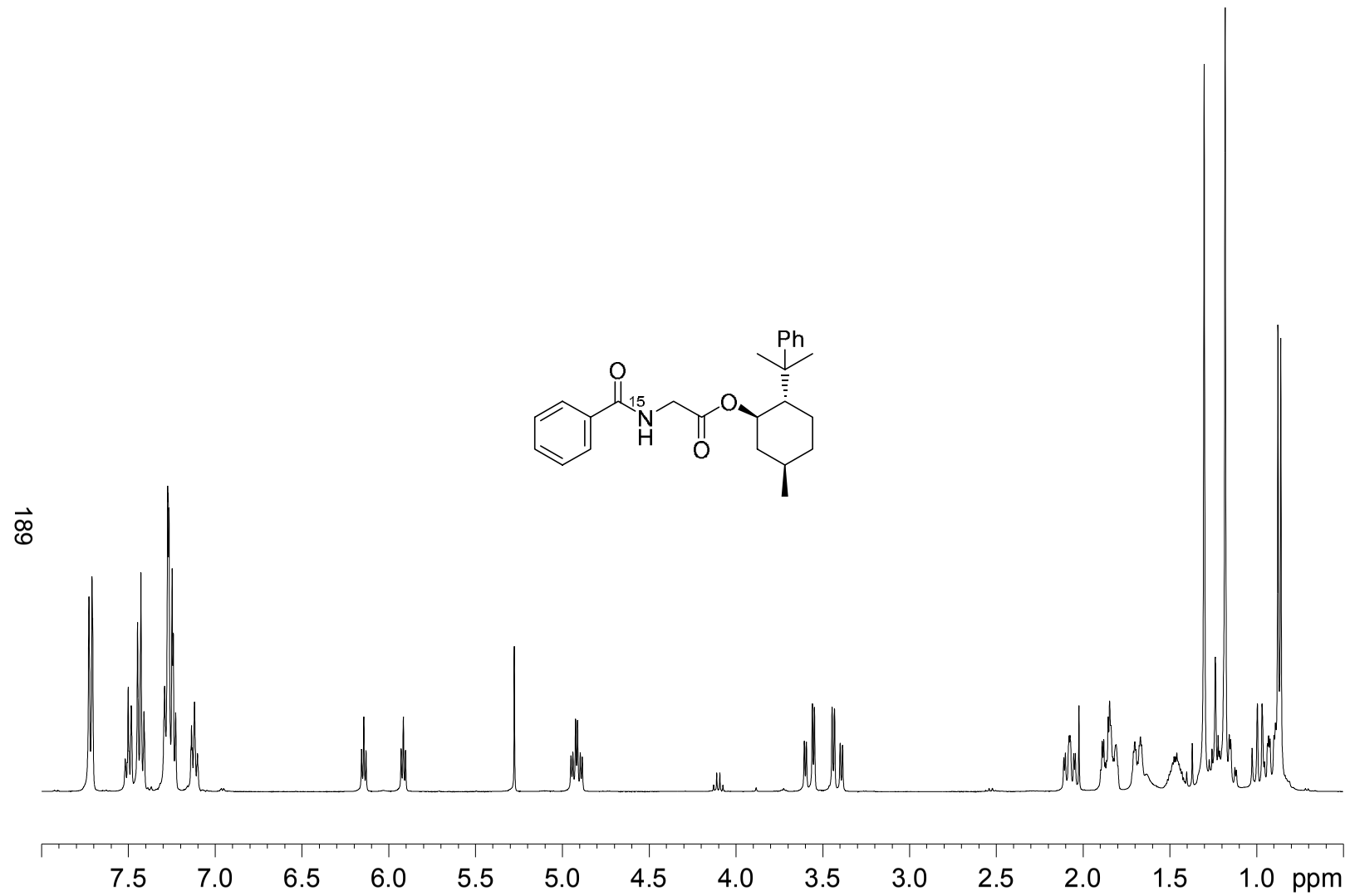

Spectrum 5 ^{1}H NMR spectrum (400 MHz) of ^{15}N-(-)-8-phenylmenthylhippurate (**7**) in $CDCl_3$.

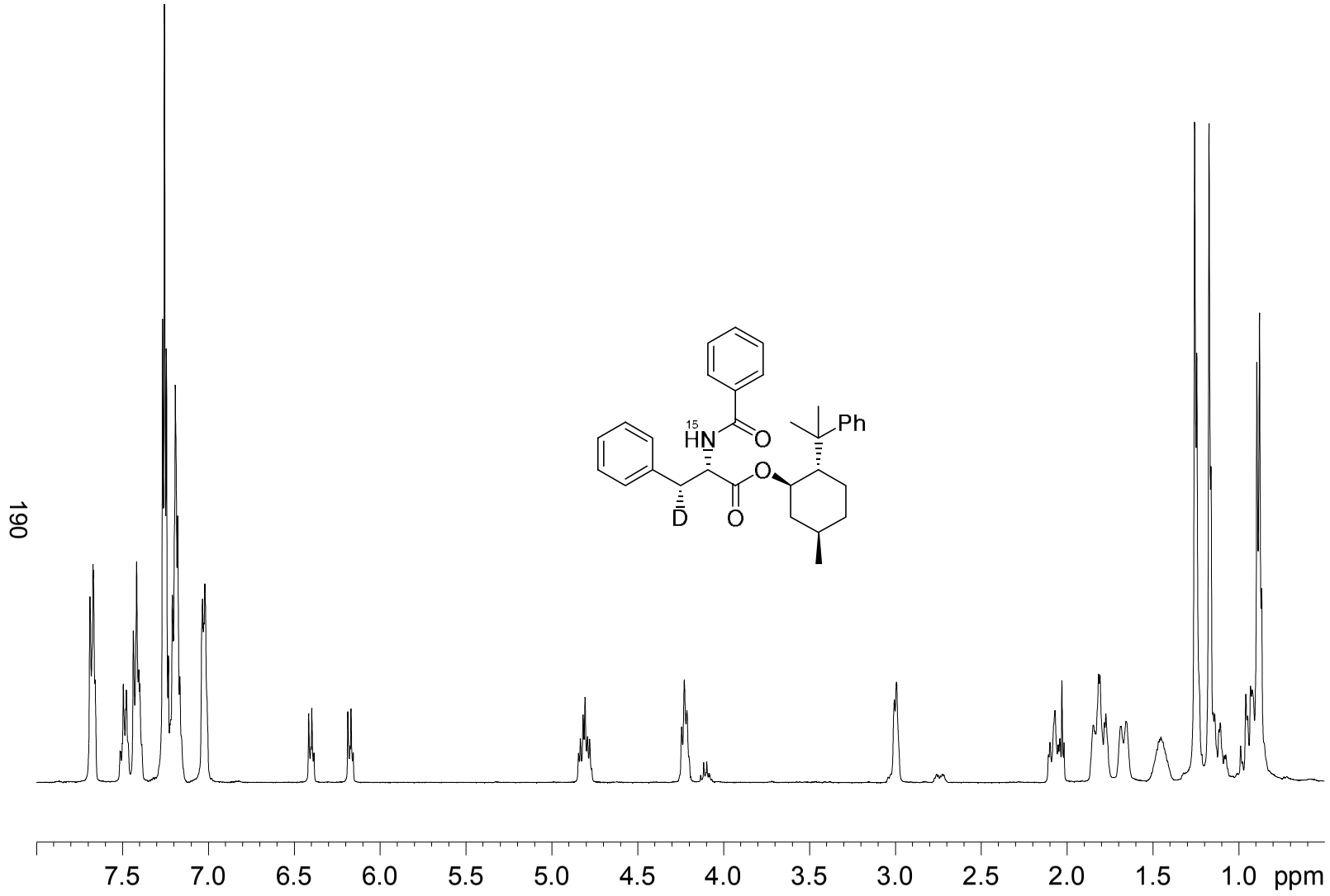

Spectrum 6 ^{1}H NMR spectrum (400 MHz) of (2*S*, 3*R*)-(-)-*N*-benzoyl-[3-^{2}H,^{15}N]-phenylalanine-(-)-8-phenylmenthyl ester (**8**) in $CDCl_3$.

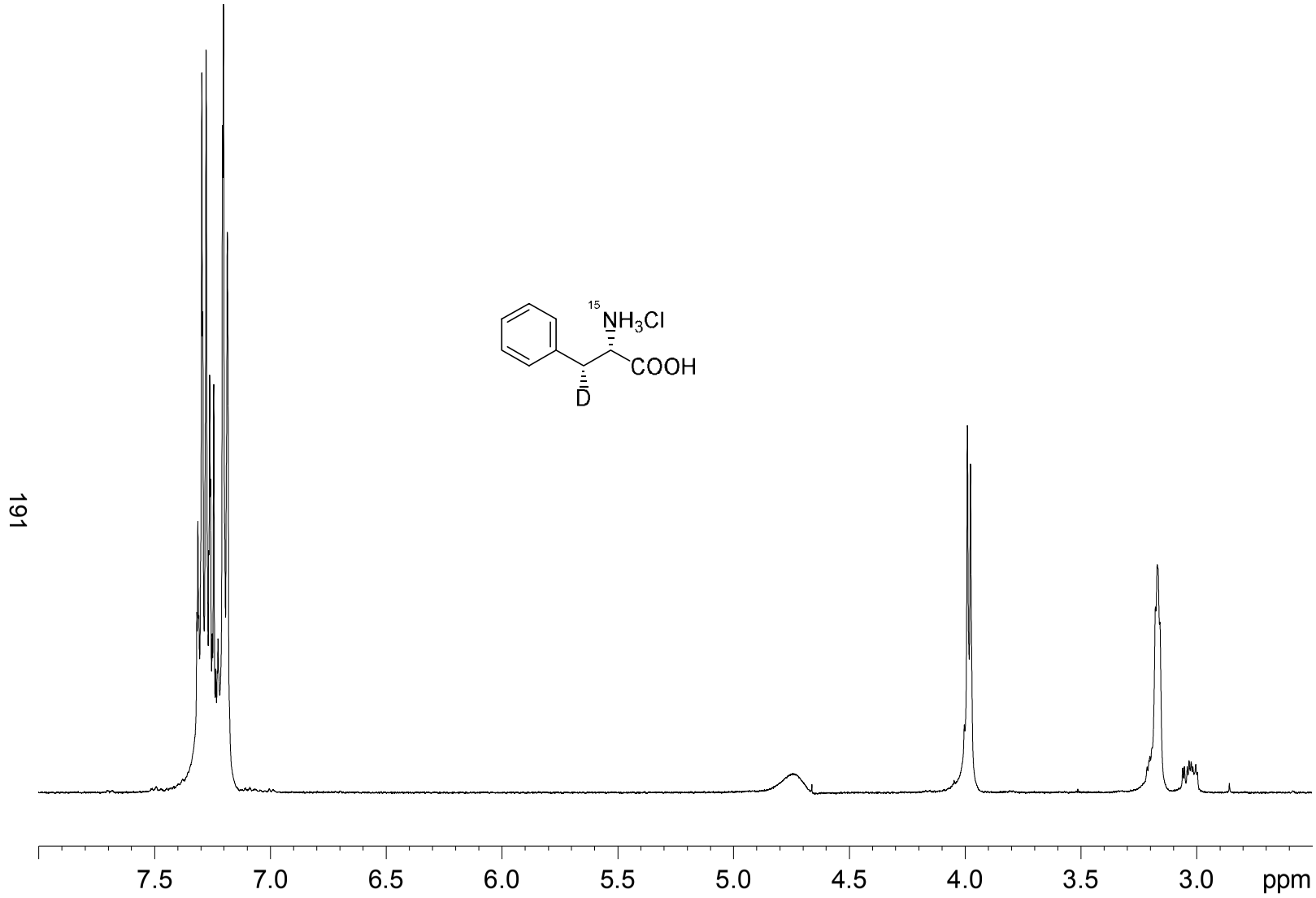

Spectrum 7 ^{1}H NMR spectrum (400 MHz) of (2*S*, 3*R*)-[3-^{2}H,^{15}N]-phenylalanine hydrochloride (**9**) in D_2O.

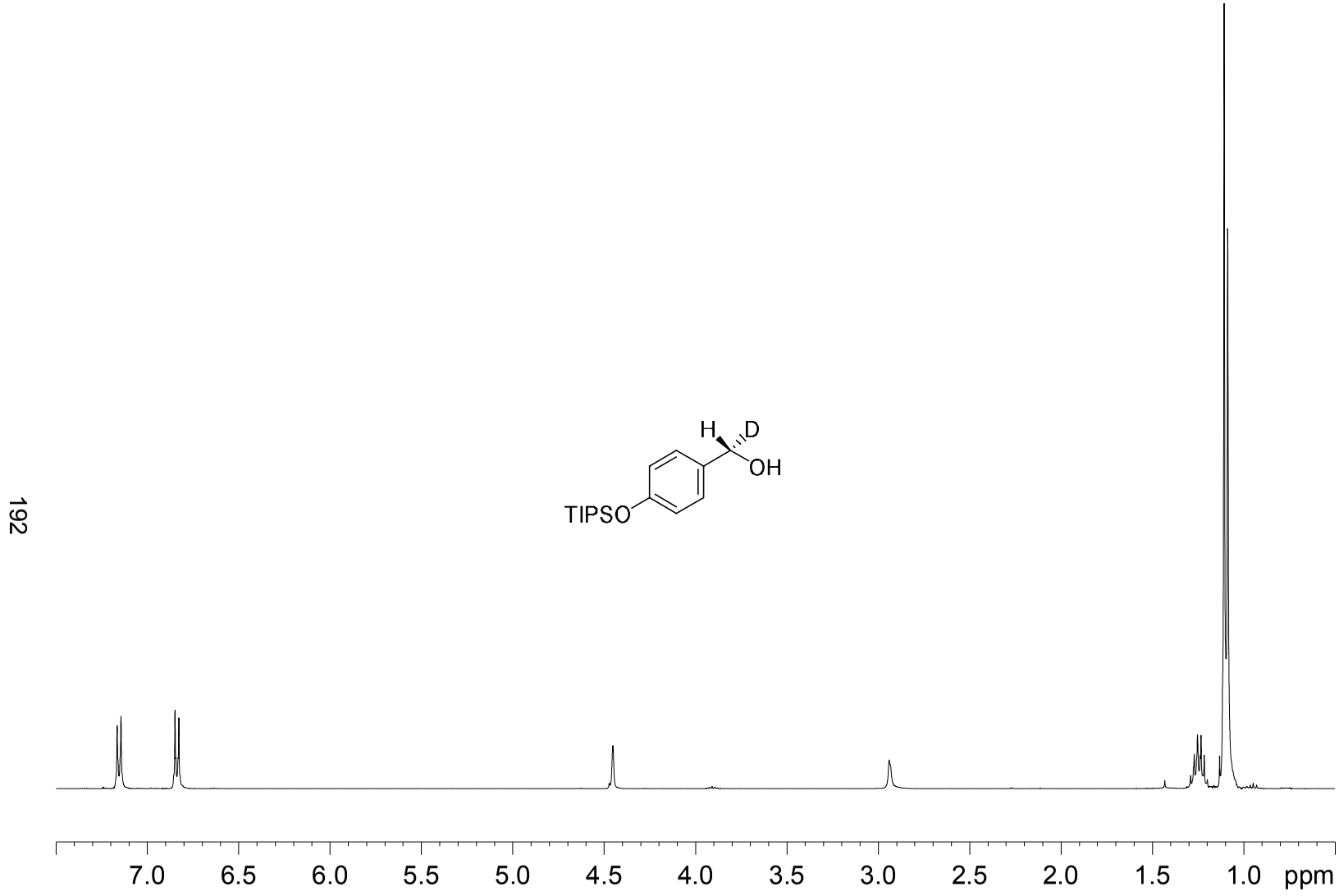

Spectrum 8 ^{1}H NMR spectrum (400 MHz) of (*S*)-(+)-4-triisopropylsilyloxybenzyl-α-*d* alcohol (**15**) in $CDCl_3$.

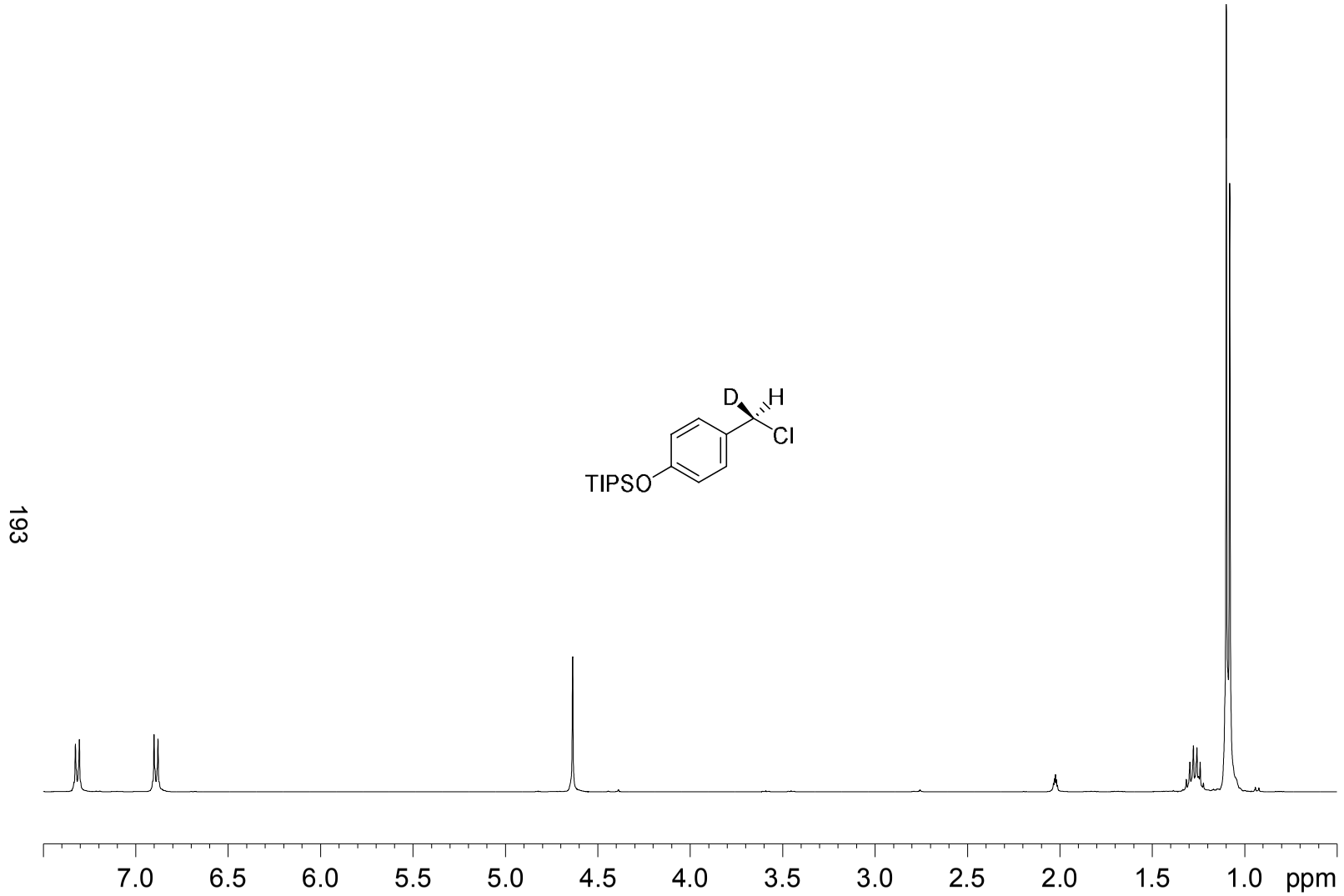

Spectrum 9 ^{1}H NMR spectrum (400 MHz) of (*R*)-(-)-4-triisopropylsilyloxybenzyl-α-*d* chloride (**16**) in $CDCl_3$.

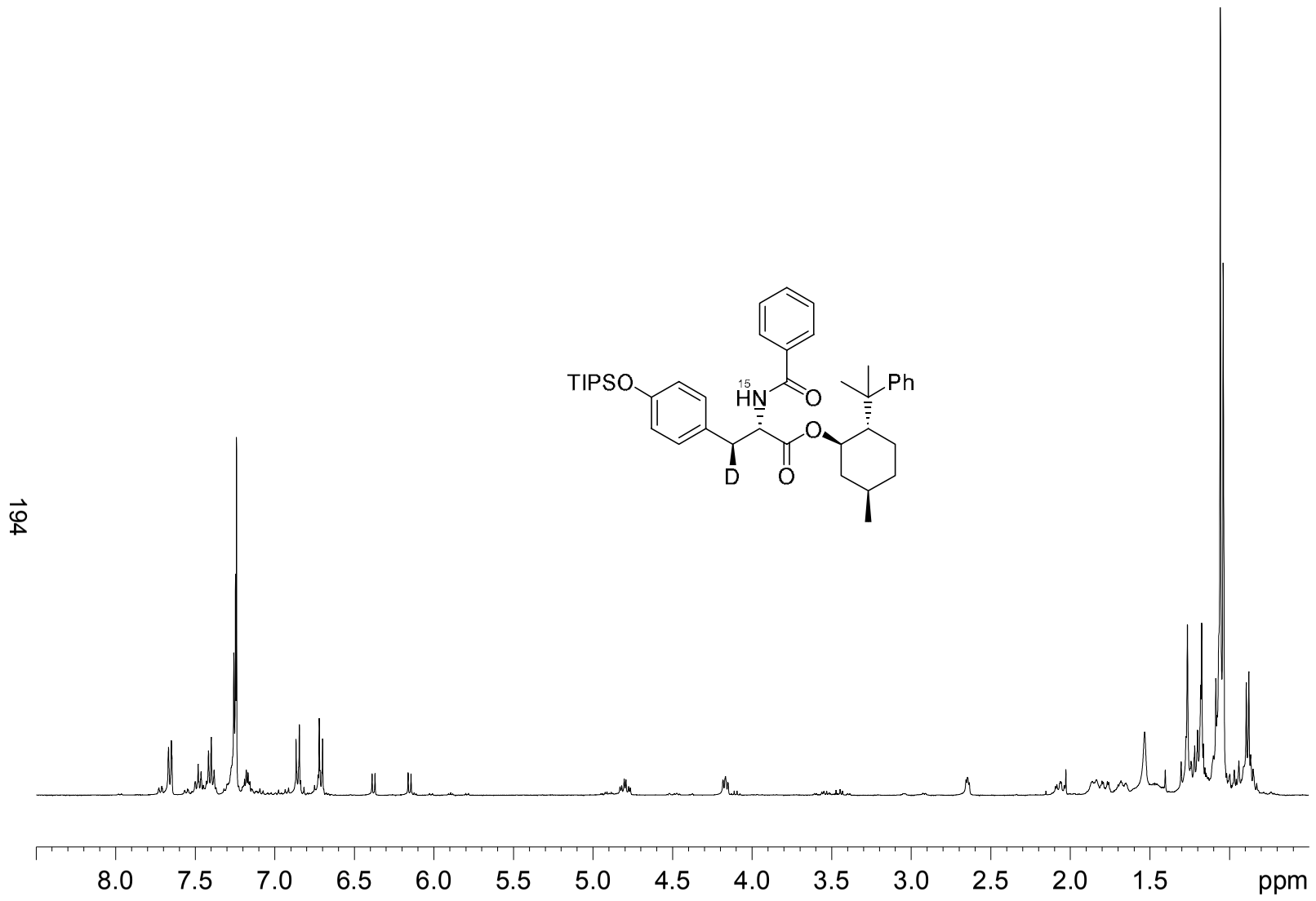

Spectrum 10 ^{1}H NMR spectrum (400 MHz) of (2*S*, 3*S*)-(+)-*N*-benzoyl-*O*-triisopropylsilyl-[3-^{2}H,^{15}N]-tyrosine-(-)-8-phenylmenthyl ester (**17**) in $CDCl_3$.

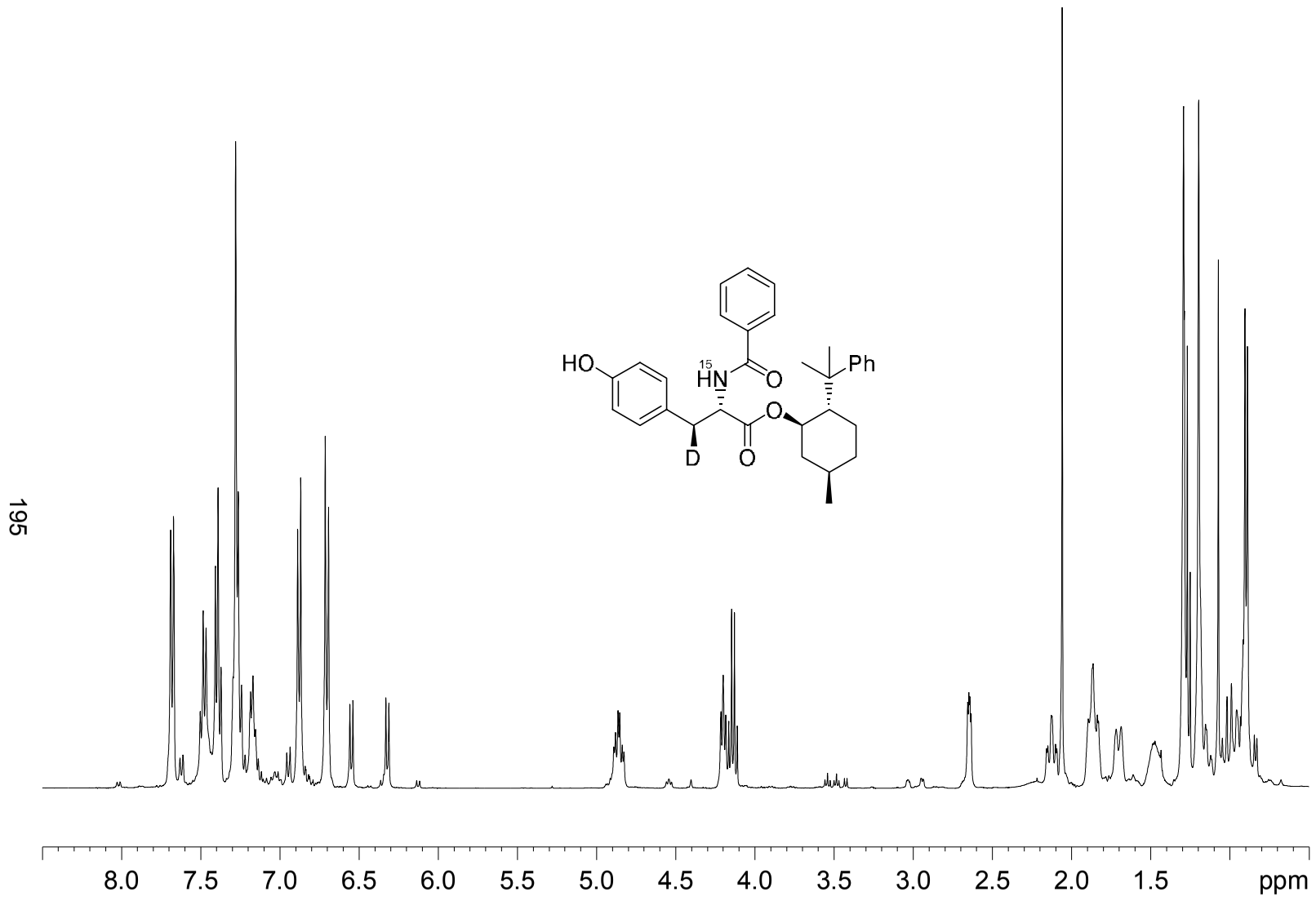

Spectrum 11 ^{1}H NMR spectrum (400 MHz) of (2*S*, 3*S*)-*N*-benzoyl-[3-^{2}H,^{15}N]-tyrosine-(-)-8-phenylmenthyl ester (**18**) in $CDCl_3$.

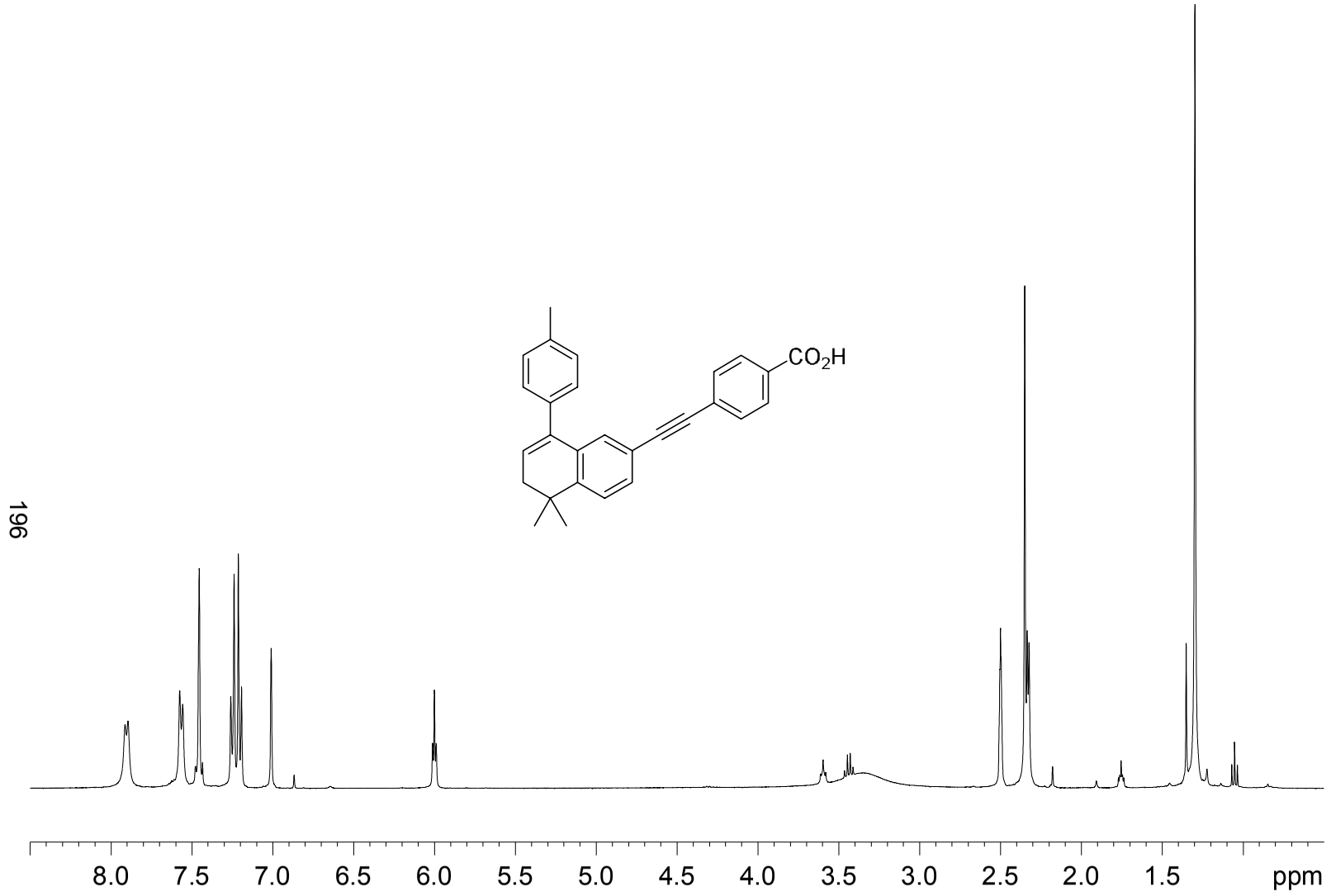

Spectrum 12 ^{1}H NMR spectrum (400 MHz) of 4-[[5,6-dihydro-5,5-dimethyl-8-(4-methylphenyl)-2-naphthalenyl]ethynyl]-benzoic acid in DMSO-d_6.

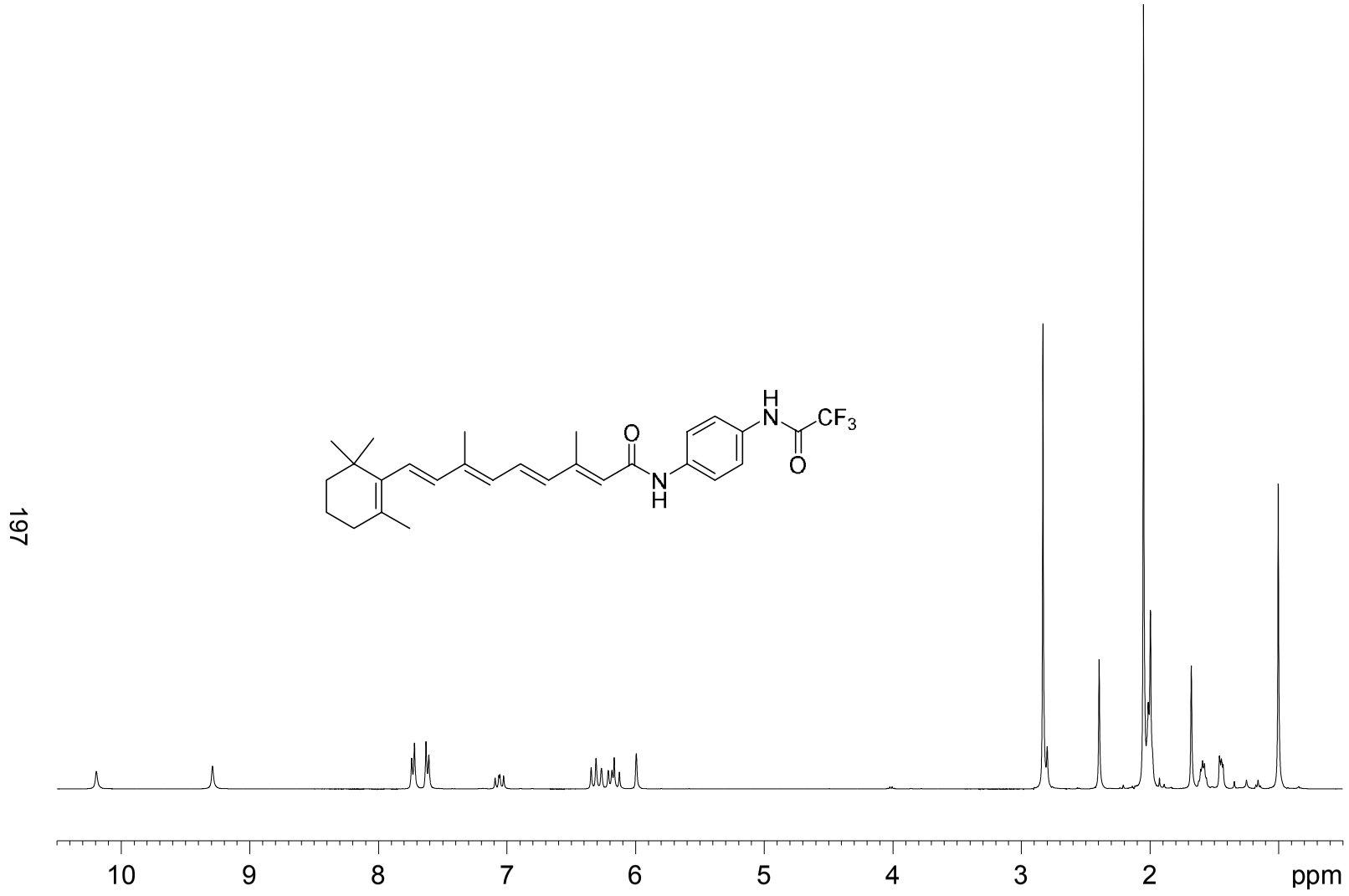

Spectrum 13 ^{1}H NMR spectrum (400 MHz) of *N*-(4-trifluoroacetamidophenyl)retinamide in acetone-d_6.

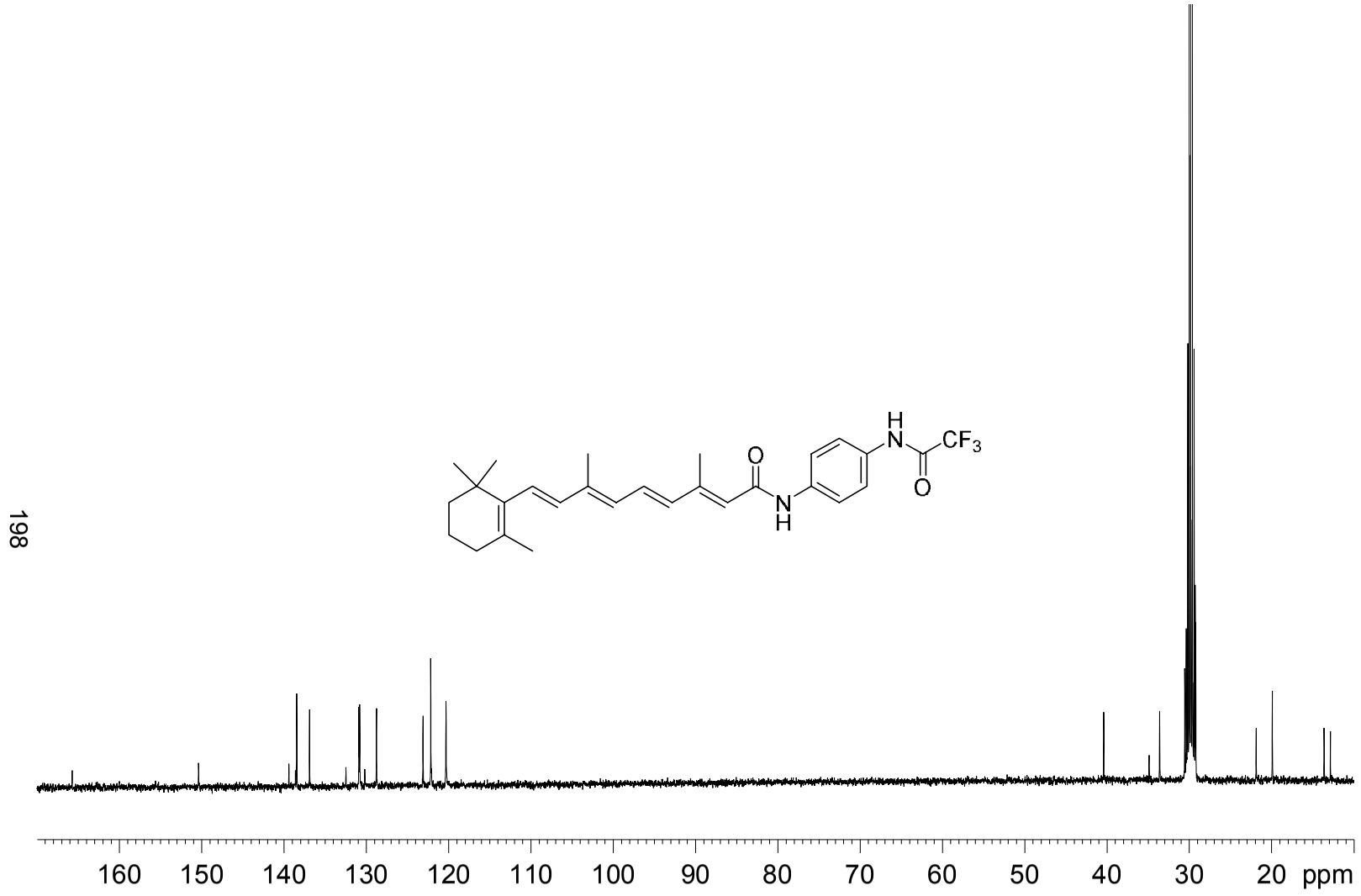

Spectrum 14 ^{13}C NMR spectrum (400 MHz) of *N*-(4-trifluoroacetamidophenyl)retinamide in acetone-d_6.

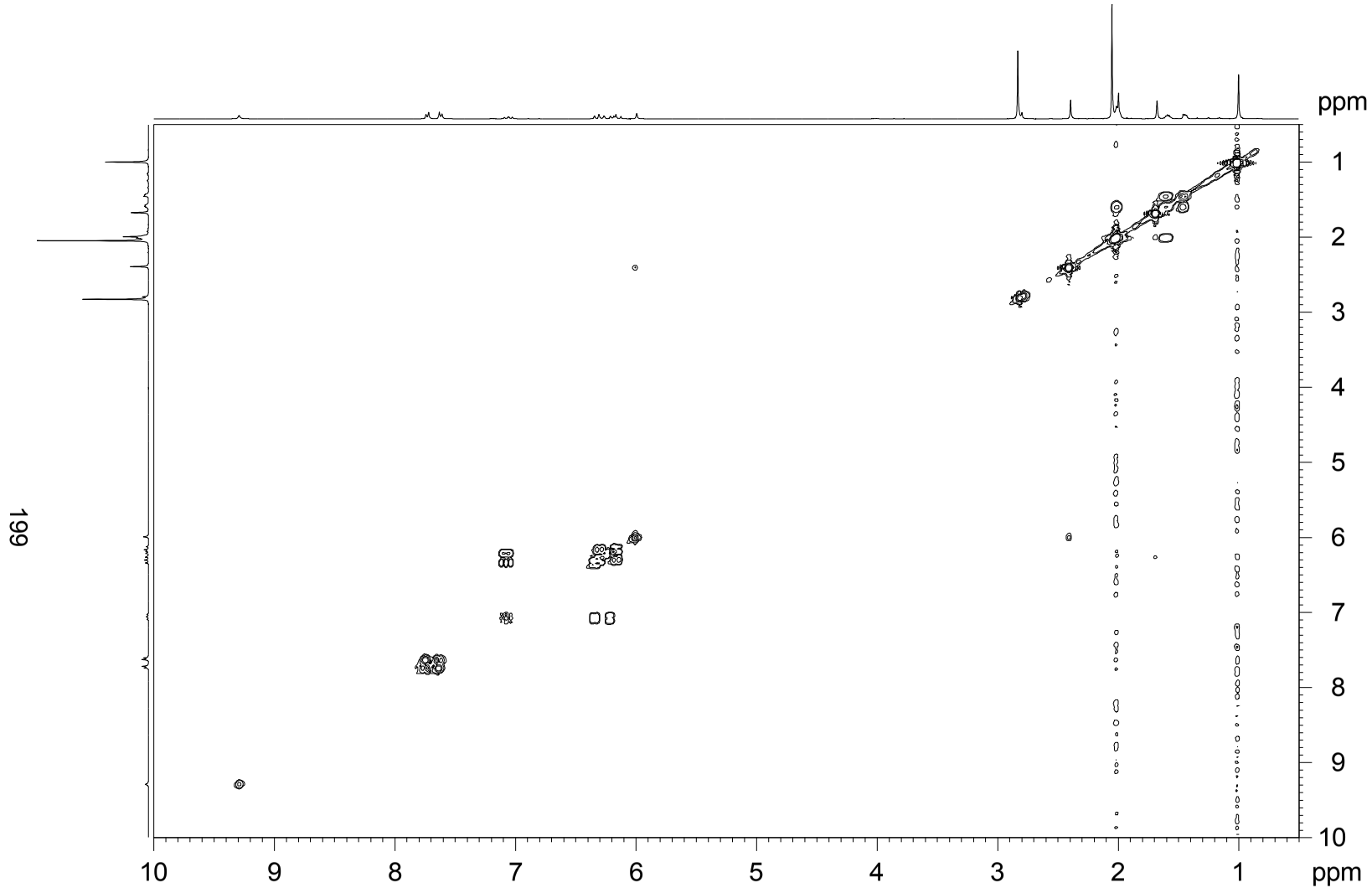

Spectrum 15 Gradient-selected ^{1}H-^{1}H COSY NMR spectrum (400 MHz) of *N*-(4-trifluoroacetamidophenyl)retinamide in acetone-d_6.

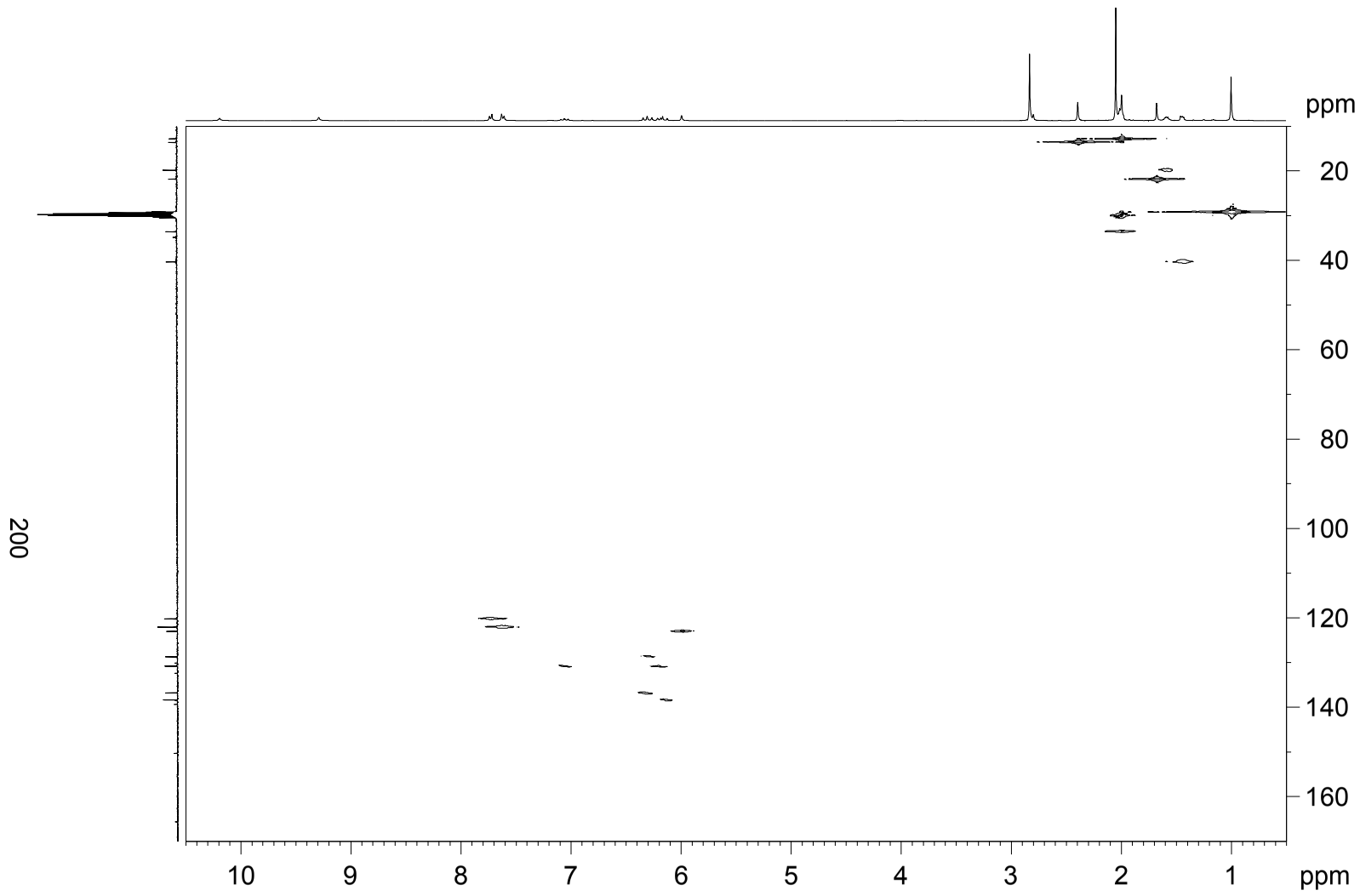

Spectrum 16 Gradient-selected ^{1}H-^{13}C HMQC NMR spectrum (400 MHz) of *N*-(4-trifluoroacetamidophenyl)retinamide in acetone-d_6.

REFERENCES

(1) *Synthesis and Applications of Isotopically Labeled Compounds*; Pleiss, U.; Voges, R., Eds.; Wiley, 2001.

(2) *Synthesis and Applications of Isotopically Labeled Compounds 1994*; Allen, J.; Voges, R., Eds.; Wiley, 1995.

(3) *Synthesis and Applications of Isotopically Labelled Compounds 1991*; Buncel, E.; Kabalka, G. W., Eds.; Elsevier, 1992.

(4) Young, D. W. Stereochemistry of metabolic reactions of amino-acids. *Top. Stereochem.* **1994**, *21*, 381-465.

(5) Vederas, J. C. The use of stable isotopes in biosynthetic studies. *Nat. Prod. Rep.* **1987**, *4*, 277-337.

(6) Mann, J. In *Secondary Metabolism*; 2nd ed.; Oxford University Press: New York, 1987.

(7) Wüthrich, K. The second decade-into the third millenium. *Nat. Struct. Biol.* **1998**, *5*, 492-495.

(8) Clore, G. M.; Gronenborn, A. M. NMR structures of proteins and protein complexes beyond 20,000 M(r). *Nat. Struct. Biol.* **1997**, *4*, 849-853.

(9) Gronenborn, A. M.; Clore, G. M. Structures of protein complexes by multidimensional heteronuclear magnetic resonance spectroscopy. *Crit. Rev. Biochem. Mol. Biol.* **1995**, *30*, 351-385.

(10) Arrowsmith, C. H.; Wu, Y. S. NMR of large (> 25 kDa) proteins and protein complexes. *Prog. Nucl. Magn. Reson. Spectrosc.* **1998**, *32*, 277-286.

(11) Bodo, G.; Dintzis, H. M.; Kendrew, J. C.; Wyckoff, H. W. Crystal structure of myoglobin. V. Low-resolution three-dimensional Fourier synthesis of sperm-whale myoglobin crystals. *Proc. Roy. Soc. (London)* **1959**, *A253*, 70-102.

(12) Clore, G. M.; Gronenborn, A. M. Structures of larger proteins in solution: three- and four-dimensional heteronuclear NMR spectroscopy. *Science* **1991**, *252*, 1390-1399.

(13) Evans, J. N. S. In *Biomolecular NMR Spectroscopy*; Oxford: New York, 1995.

(14) Williamson, M. P.; Havel, T. F.; Wüthrich, K. Solution conformation of proteinase inhibitor IIA from bull seminal plasma by ^{1}H nuclear magnetic resonance and distance geometry. *J. Mol. Biol.* **1985**, *182*, 295-315.

(15) Kaptein, R.; Zuiderweg, E. R. P.; Scheek, R. M.; Boelens, R.; Van Gunsteren, W. F. A protein structure from nuclear magnetic resonance data. The lac repressor headpiece. *J. Mol. Biol.* **1985**, *182*, 179-182.

(16) Clore, G. M.; Gronenborn, A. M.; Brunger, A. T.; Karplus, M. Solution conformation of a heptadecapeptide comprising the DNA binding helix F of the cyclic AMP receptor protein of Escherichia coli. Combined use of ^{1}H nuclear magnetic resonance and restrained molecular dynamics. *J. Mol. Biol.* **1985**, *186*, 435-455.

(17) Fiaux, J.; Bertelsen, E. B.; Horwich, A. L.; Wüthrich, K. NMR analysis of a 900K GroEL-GroES complex. *Nature* **2002**, *418*, 207-211.

(18) Goto, N. K.; Kay, L. E. New developments in isotope labeling strategies. *Curr. Opin. Struct. Biol.* **2000**, *10*, 585-592.

(19) McIntosh, L. P.; Dahlquist, F. W. Biosynthetic incorporation of ^{15}N and ^{13}C for assignment and interpretation of nuclear magnetic resonance spectra of proteins. *Q. Rev. Biophys.* **1990**, *23*, 1-38.

(20) Venters, R. A.; Huang, C. C.; II, B. T. F.; Trolard, R.; Spicer, L. D.; Fierke, C. A. High level $^{2}H/^{13}C/^{15}N$ labelling of proteins for NMR studies. *J. Biomol. NMR* **1995**, *5*, 339-344.

(21) Stockman, B. J. NMR spectroscopy as a tool for structure-based drug design. *Prog. Nucl. Magn. Reson. Spectrosc.* **1998**, *33*, 109-151.

(22) Havel, T. F. An evaluation of computational strategies for use in the determination of protein structure from distance constraints obtained by nuclear magnetic resonance. *Prog. Biophys. Mol. Biol.* **1991**, *56*, 43-78.

(23) Clore, G. M.; Gronenborn, A. M. Determination of three-dimensional structures of proteins and nucleic acids in solution by nuclear magnetic resonance spectroscopy. *Crit. Rev. Biochem. Mol. Biol.* **1989**, *24*, 479-564.

(24) Braun, W. Distance geometry and related methods for protein structure determination from NMR data. *Q. Rev. Biophys.* **1987**, *19*, 115-157.

(25) Xu, R. X.; Olejniczak, E. T.; Fesik, S. W. Stereospecific assignments and χ_1 rotamers for FKBP when bound to ascomycin from $^{3}J_{H\alpha,H\beta}$ and $^{3}J_{N,H\beta}$ coupling constants. *FEBS Lett.* **1992**, *305*, 137-143.

(26) Hyberts, S. G.; Maerki, W.; Wagner, G. Stereospecific assignments of side-chain protons and characterization of torsion angles in Eglin c. *Eur. J. Biochem.* **1987**, *164*, 625-635.

(27) Wagner, G.; Braun, W.; Havel, T. F.; Schaumann, T.; Go, N.; Wüthrich, K. Protein structures in solution by nuclear magnetic resonance and distance geometry. The polypeptide fold of the basic pancreatic trypsin inhibitor determined using two different algorithms, DISGEO and DISMAN. *J. Mol. Biol.* **1987**, *196*, 611-639.

(28) Karplus, M. J. Contact electron-spin coupling of nuclear magnetic moments. *J. Chem. Phys.* **1959**, *30*, 11-15.

(29) Karplus, M. J. Vicinal proton coupling in nuclear magnetic resonance. *J. Am. Chem. Soc.* **1963**, *85*, 2870-2871.

(30) Bystrov, V. F. Spin-spin coupling and the conformational states of peptide systems. *Prog. Nucl. Magn. Reson. Spectrosc.* **1976**, *10*, 41-81.

(31) IUPAC-IUB IUPAC-IUB Commission on biochemical nomenclature. Abbreviations and Symbols for the description of the conformation of polypeptide chains. *Biochemistry* **1970**, *9*, 3471-3479.

(32) Güntert, P.; Braun, W.; Billeter, M.; Wüthrich, K. Automated stereospecific proton NMR assignments and their impact on the precision of protein structure determinations in solution. *J. Am. Chem. Soc.* **1989**, *111*, 3997-4004.

(33) Nilges, M.; Clore, G. M.; Gronenborn, A. M. Proton NMR stereospecific assignments by conformational data-base searches. *Biopolymers* **1990**, *29*, 813-822.

(34) Bax, A.; Vuister, G. W.; Grzesiek, S.; Delaglio, F.; Wang, A. C.; Tschudin, R.; Zhu, G. Measurement of homo- and heteronuclear *J* couplings from quantitative *J* correlation. *Methods Enzymol.* **1994**, *239*, 79-105.

(35) Weisemann, R.; Lohr, F.; Ruterjans, H. HNCCH-TOCSY, a triple resonance experiment for the correlation of backbone $^{13}C\alpha$ and ^{15}N resonances with aliphatic side-chain proton resonances and for measuring vicinal ^{13}CO, $^{1}H\beta$ coupling constants in proteins. *J. Biomol. NMR* **1994**, *4*, 587-593.

(36) LeMaster, D. M. Deuterium labelling in NMR structural analysis of larger proteins. *Q. Rev. Biophys.* **1990**, *23*, 133-174.

(37) Lemaster, D. M.; Richards, F. M. NMR sequential assignment of *Escherichia* coli thioredoxin utilizing random fractional deuteriation. *Biochemistry* **1988**, *27*, 142-150.

(38) LeMaster, D. M. Chiral β and random fractional deuteration for the determination of protein sidechain conformation by NMR. *FEBS Lett.* **1987**, *223*, 191-196.

(39) Otting, G.; Wüthrich, K. Heteronuclear filters in two-dimensional [^{1}H,^{1}H]-NMR spectroscopy: Combined use with isotope labelling for studies of macromolecular conformation and intermolecular interactions. *Q. Rev. Biophys.* **1990**, *23*, 39-96.

(40) Bax, A.; Weiss, M. A. Simplification of two-dimensional NOE spectra of proteins by ^{13}C labeling. *J. Magn. Reson.* **1987**, *71*, 571-575.

(41) Fesik, S. W.; Gampe, R. T., Jr.; Rockway, T. W. Application of isotope-filtered 2D NOE experiments in the conformational analysis of atrial natriuretic factor (7-23). *J. Magn. Reson.* **1987**, *74*, 366-371.

(42) Diercks, T.; Coles, M.; Kessler, H. Applications of NMR in drug discovery. *Curr. Opin. Chem. Biol.* **2001**, *5*, 285-291.

(43) Hicks, R. P. Recent advances in NMR: expanding its role in rational drug design. *Curr. Med. Chem.* **2001**, *8*, 627-650.

(44) Roberts, G. C. K. Applications of NMR in drug discovery. *Drug Discov. Today* **2000**, *5*, 230-240.

(45) Mosberg, H. I.; Sobczyk-Kojiro, K.; Subramanian, P.; Crippen, G. M.; Ramalingam, K.; Woodard, R. W. Combined use of stereospecific deuteration, NMR, distance geometry, and energy minimization for the conformational analysis of the highly δ opioid receptor selective peptide [D-Pen2,D-Pen5]enkephalin. *J. Am. Chem. Soc.* **1990**, *112*, 822-829.

(46) Etzkorn, F. A.; Travins, J. M. Stereoselective deuterium labeling of pro*R* β-protons in the NMR structure determination of a helix-turn-helix turn peptide mimic. *J. Pept. Res.* **2000**, *55*, 436-446.

(47) Etzkorn, F. A.; Travins, J. M.; Hart, S. A. In *Rare Protein Turns. Helix-Turn-Helix, γ-Turn And Cis-Proline Mimics*; Abell, A., Ed.; JAI Press Inc.: Greenwich, 1999; Vol. 2, p 125-163.

(48) Akam, M. Hox genes. From master genes to micromanagers. *Curr. Biol.* **1998**, *8*, R-676-R678.

(49) Anglister, J. Use of deuterium labelling in NMR studies of antibody combining site structure. *Q. Rev. Biophys.* **1990**, *23*, 175-203.

(50) Walker, J. R.; Curley, R. W., Jr. Improved synthesis of (*R*)-glycine-*d*-^{15}N. *Tetrahedron* **2001**, *57*, 6695-6701.

(51) Curley, R. W., Jr.; Panigot, M. J.; Hansen, A. P.; Fesik, S. W. Stereospecific assignments of glycine in proteins by stereospecific deuteration and ^{15}N labeling. *J. Biomol. NMR* **1994**, *4*, 335-340.

(52) Mittermaier, A.; Kay, L. E. χ_1 Torsion angle dynamics in proteins from dipolar couplings. *J. Am. Chem. Soc.* **2001**, *123*, 6892-6903.

(53) Oba, M.; Terauchi, T.; Miyakawa, A.; Kamo, H.; Nishiyama, K. Stereoselective deuterium-labeling of diastereotopic methyl and methylene protons of L-leucine. *Tetrahedron Lett.* **1998**, *39*, 1595-1598.

(54) Oba, M.; Nakajima, S.; Nishiyama, K. Substituent-dependent asymmetric synthesis of L-*threo*- and L-*erythro*-[2,3-$^2H_2$]-phenylalanine from chiral (*Z*)-dehydrophenylalanine. *Chem. Commun. (Cambridge)* **1996**, 1875-1876.

(55) Oba, M.; Ueno, R.; Fukuoka, M.; Kainosho, M.; Nishiyama, K. Synthesis of L-*threo*- and L-*erythro*-[1-^{13}C, 2,3-$^2H_2$]-amino acids: novel probes for conformational analysis of peptide side chains. *J. Chem. Soc., Perkin Trans. 1* **1995**, 1603-1609.

(56) Easton, C. J.; Hutton, C. A. Synthesis of each stereoisomer of [3-$^2H_1$]phenylalanine and evaluation of the stereochemical course of the reaction of (*R*)-phenylalanine with (*S*)-phenylalanine ammonia-lyase. *J. Chem. Soc., Perkin Trans. 1* **1994**, 3545-3548.

(57) Wightman, R. H.; Staunton, J.; Battersby, A. R.; Hanson, K. R. Studies of enzyme-mediated reactions. I. Syntheses of deuterium- or tritium-labelled (3*S*)- and (3*R*)-phenylalanines: stereochemical course of the elimination catalysed by L-phenylalanine ammonia-lyase. *J. Chem. Soc., Perkin Trans. 1* **1972**, *18*, 2355-2364.

(58) Nagai, U.; Kobayashi, J. Simultaneous synthesis of both diastereomers of stereoselectively β-deuterated phenylalanines, (2*S*,3*R*)- and (2*R*,3*R*)-PhCHDCH(NH2)COOH. *Tetrahedron Lett.* **1976**, 2873-2874.

(59) Kirby, G. W.; Michael, J. Stereoselective β-labeling of aromatic amino acids with deuterium and tritium. *J. Chem. Soc., Perkin Trans. 1* **1973**, 115-120.

(60) Kirby, G. W.; Michael, J. Labeling of aromatic amino-acids stereoselectively with tritium in the β-methylene group: stereochemistry of hydroxylation in the biosynthesis of hemanthamine. *J. Chem. Soc. D.* **1971**, 187-188.

(61) Oba, M.; Terauchi, T.; Owari, Y.; Imai, Y.; Motoyama, I.; Nishiyama, K. Stereo-divergent synthesis of L-*threo*- and L-*erythro*-[2,3-$^2H_2$]-amino acids using optically active dioxopiperazine as a chiral template. *J. Chem. Soc., Perkin Trans. 1* **1998**, 1275-1282.

(62) Duthaler, R. O. Recent developments in the stereoselective synthesis of α-amino acids. *Tetrahedron* **1994**, *50*, 1539-1650.

(63) Williams, R. M.; Hendrix, J. A. Asymmetric synthesis of arylglycines. *Chem. Rev.* **1992**, *92*, 889-917.

(64) Williams, R. M. In *Synthesis of Optically Active α-Amino Acids*; Pergamon: Oxford, 1989.

(65) O'Donnell, M. J., Ed. α-Amino Acid Synthesis. *Tetrahedron* **1988**, *44(17)*.

(66) Caddick, S.; Parr, N. J.; Pritchard, M. C. Preparation of α-amino-carboxylic acid derivatives via diastereoselective reactions of glycine enolate equivalents. *Tetrahedron* **2001**, *57*, 6615-6626.

(67) Soloshonok, V. A.; Tang, X.; Hruby, V. J. Large-scale asymmetric synthesis of novel sterically constrained 2',6'-dimethyl- and α–2',6'-trimethyltyrosine and phenylalanine derivatives via alkylation of chiral equivalents of nucleophilic glycine and alanine. *Tetrahedron* **2001**, *57*, 6375-6382.

(68) Berkowitz, D. B.; McFadden, J. M.; Sloss, M. K. Engineering acyclic stereocontrol in the alkylation of vinylglycine-derived dianions: asymmetric synthesis of higher α-vinyl amino acids. *J. Org. Chem.* **2000**, *65*, 2907-2918.

(69) Chinchilla, R.; Mazon, P.; Najera, C. Asymmetric synthesis of α-amino acids using polymer-supported Cinchona alkaloid-derived ammonium salts as chiral phase-transfer catalysts. *Tetrahedron: Asymmetry* **2000**, *11*, 3277-3281.

(70) Reyes, A.; Juaristi, E. Stereoselective alkylation of C2-symmetric chiral *N*-phthaloylglycinamides in the preparation of enantiopure α-amino acids. *Tetrahedron: Asymmetry* **2000**, *11*, 1411-1423.

(71) Myers, A. G.; Schnider, P.; Kwon, S.; Kung, D. W. Greatly simplified procedures for the synthesis of α-amino acids by the direct alkylation of pseudoephedrine glycinamide hydrate. *J. Org. Chem.* **1999**, *64*, 3322-3327.

(72) Myers, A. G.; Gleason, J. L.; Yoon, T.; Kung, D. W. Highly practical methodology for the synthesis of D- and L-α-amino acids, *N*-protected α-amino acids, and *N*-methyl-α-amino acids. *J. Am. Chem. Soc.* **1997**, *119*, 656-673.

(73) Berkowitz, D. B.; Smith, M. K. Enantiomerically enriched α-methyl amino acids. Use of an acyclic, chiral alanine-derived dianion with a high diastereofacial bias. *J. Org. Chem.* **1995**, *60*, 1233-1238.

(74) Alvarez-Ibarra, C.; Csakye, A. G.; Maroto, R.; Quiroga, M. L. Asymmetric alkylation of 8-phenylmenthyl *N*-[bis(methylthio)methylene]glycinate enolates. Synthesis of D- and L-α-amino acids from a single chiral precursor. *J. Org. Chem.* **1995**, *60*, 7934-7940.

(75) McIntosh, J. M.; Peters, S. Alkylations of 2-arylcyclohexyl hippurates. Stereochemical influence of π-electrons. *Synthesis* **1999**, 635-638.

(76) McIntosh, J. M.; Kiser, E. J.; Tian, Z. The stereochemistry of hippurate alkylation. *Can. J. Chem.* **1998**, *76*, 147-151.

(77) McIntosh, J. M.; Thangarasa, R.; Foley, N. K.; Ager, D. J.; Froen, D. E.; Klix, R. C. The alkylation of menthyl hippurate and some related materials: a reinvestigation. *Tetrahedron* **1994**, *50*, 1967-1974.

(78) Deslongchamps, P. In *Stereoelectronic effects in organic chemistry*; Organic Chemistry Series; Pergamon Press: New York, 1983; Vol. 1.

(79) Jones, G. B.; Chapman, B. J. π-Stacking effects in asymmetric synthesis. *Synthesis* **1995**, 475-497.

(80) Bennett, D. J.; Kriby, G. W.; Moss, V. A. Deuteration and tritiation of aryl aldehydes in the formyl group and the synthesis of (+-)-3,4-dihydroxy[β-$^2H_2$]phenylalanine. *J. Chem. Soc., C* **1970**, 2049-2051.

(81) Midland, M. M.; Tramontano, A.; Zderic, S. A. Preparation of optically active benzyl-α-*d* alcohol via reduction by *B*-3α-pinanyl-9-borabicyclo[3.3.1]nonane. A new highly effective chiral reducing agent. *J. Am. Chem. Soc.* **1977**, *99*, 5211-5213.

(82) Midland, M. M.; Greer, S.; Tramontano, A.; Zderic, S. A. Chiral trialkylborane reducing agents. Preparation of 1-deuterio primary alcohols of high enantiomeric purity. *J. Am. Chem. Soc.* **1979**, *101*, 2352-2355.

(83) Schotten, C. *Ber.* **1884**, *17*, 2544.

(84) Baumann, E. *Ber.* **1886**, *19*, 3218.

(85) Steiger, R. E. Benzoylation of amino acids. *J. Org. Chem.* **1944**, *9*, 396-400.

(86) Corey, E. J.; Ensley, H. E. Preparation of an optically active prostaglandin intermediate via asymmetric induction. *J. Am. Chem. Soc.* **1975**, *97*, 6908-6909.

(87) Ort, O. (-)-8-Phenylmenthol [1*R*-(1α, 2β, 5α)-5-methyl-2-(1-methyl-1-phenylethyl)cyclohexanol]. *Org. Synth.* **1987**, *65*, 203-214.

(88) Williams, R. M.; Zhai, D.; Sinclair, P. J. Asymmetric synthesis of (*R*)- and (*S*)-[2-$^2H_1$]-glycine. *J. Org. Chem.* **1986**, *51*, 5021-5022.

(89) Downie, I. M.; Holmes, J. B.; Lee, J. B. Preparation of alkyl chlorides under mild conditions. *Chem. Ind. (London)* **1966**, 900-901.

(90) Hooz, J.; Gilani, S. S. H. Rapid, mild procedure for the preparation of alkyl chlorides and bromides. *Can. J. Chem.* **1968**, *46*, 86-87.

(91) Manna, S.; Falck, J. R.; Mioskowski, C. A convenient preparation of alkyl halides and cyanides from alcohols by modification of the Mitsunobu procedure. *Synth. Commun.* **1985**, *15*, 663-668.

(92) Weiss, R. G.; Snyder, E. I. Stereochemistry of chloride formation from alcohols and thiols by use of triphenylphosphine and carbon tetrachloride. *Chem. Commun.* **1968**, 1358-1359.

(93) Weiss, R. G.; Snyder, E. I. Conversion of some bicycloheptanols to chlorides using triphenylphosphine-carbon tetrachloride. Stereochemistry and mechanistic implications. *J. Org. Chem.* **1970**, *35*, 1627-1632.

(94) Appel, R. Tertiary phosphane/tetrachloromethane, a versatile reagent for chlorination, dehydration, and phosphorus-nitrogen linking. *Angew. Chem.* **1975**, *87*, 863-874.

(95) Mitsunobu, O.; Yamada, M. Preparation of esters of carboxylic and phosphoric acid via quaternary phosphonium salts. *Bull. Chem. Soc. Jpn.* **1967**, *40*, 2380-2382.

(96) Mitsunobu, O. The use of diethyl azodicarboxylate and triphenylphosphine in synthesis and transformation of natural products. *Synthesis* **1981**, 1-28.

(97) Weiss, R. G.; Snyder, E. I. Stereochemistry of displacement reactions at the neopentyl carbon. Further observations on the triphenylphosphine-polyhalomethane-alcohol reaction. *J. Org. Chem.* **1971**, *36*, 403-406.

(98) Arnold, L. D.; Drover, J. C. G.; Vederas, J. C. Conversion of serine β-lactones to chiral α-amino acids by copper-containing organolithium and organomagnesium reagents. *J. Am. Chem. Soc.* **1987**, *109*, 4649-4659.

(99) Amelung, W.; Brodowski, S. *In vitro* quantification of hydrolysis-induced racemization of amino acid enantiomers in environmental samples using deuterium labeling and electron-impact ionization mass spectrometry. *Anal. Chem.* **2002**, *74*, 3239-3246.

(100) Csapó, J.; Csapó-Kiss, Z.; Wágner, L.; Tálos, T.; Martin, T. G.; Folestad, S.; Tivesten, A.; Némethy, S. Hydrolysis of proteins performed at high temperatures and for short times with reduced racemization, in order to determine the enantiomers of D- and L-amino acids. *Anal. Chim. Acta* **1997**, *339*, 99-107.

(101) D'aniello, A.; Petrucelli, L.; Gardner, C.; Fisher, G. Improved method for hydrolyzing proteins and peptides without inducing racemization and for determing their true D-amino acid content. *Anal. Biochem.* **1993**, *213*, 290-296.

(102) Liardon, R.; Jost, R. Racemization of free and protein-bound amino-acids in strong mineral acid. *Int. J. Pept. Res.* **1981**, *18*, 500-505.

(103) Greene, T. W.; Wuts, P. G. M. In *Protective Groups in Organic Synthesis*; 2nd ed.; John Wiley & Sons, Inc.: New York, 1991.

(104) Li, G.; Patel, D.; Hruby, V. J. An efficient procedure for the demethylation of aryl-methyl ethers in optically pure unusual amino acids. *Tetrahedron Lett.* **1993**, *34*, 5393-5396.

(105) Jung, M. E.; Lyster, M. A. Quantitative dealkylation of alkyl ethers via treatment with trimethylsilyl iodide. A new method for ether hydrolysis. *J. Org. Chem.* **1977**, *42*, 3761-3764.

(106) Bhatt, M. V.; Kulkarni, S. U. Cleavage of ethers. *Synthesis* **1983**, 249-282.

(107) Meyer, L.; Poirier, J.-M.; Duhamel, P.; Duhamel, L. Chiral auxiliaries with a switching center: new tools in asymmetric synthesis. Application to the synthesis of enantiomerically pure (*R*)- and (*S*)-α-Amino Acids. *J. Org. Chem.* **1998**, *63*, 8094-8095.

(108) Earnshaw, C.; Wallis, C. J.; Warren, S. Synthesis of *E*- and *Z*-vinyl ethers by the Horner-Wittig reaction. *J. Chem. Soc., Perkin Trans. 1* **1979**, 3099-3106.

(109) Magid, R. M.; Fruchey, O. S.; Johnson, W. L. Hexachloroacetone/triphenylphosphine: a reagent for the regio- and stereoselective conversion of allylic alcohols into chlorides. *Tetrahedron Lett.* **1977**, 2999-3002.

(110) Magid, R. M.; Fruchey, O. S.; Johnson, W. L.; Allen, T. G. Hexachloroacetone/triphenylphosphine: a mild reagent for the regioselective and stereospecific production of allylic chlorides from the alcohols. *J. Org. Chem.* **1979**, *44*, 359-363.

(111) Villeneuve, G. B.; Chan, T. H. A rapid, mild and acid-free procedure for the preparation of acyl chlorides including formyl chloride. *Tetrahedron Lett.* **1997**, *38*, 6489-6492.

(112) Amouri, H.; Bras, J. L. Taming reactive phenol tautomers and *o*-quinone methides with transition metals: a structure-reactivity relationship. *Acc. Chem. Res.* **2002**, *35*, 501-510.

(113) Kiehlmann, E.; Li, E. P. M. Isomerization of dihydroquercetin. *J. Nat. Prod.* **1995**, *58*, 450-455.

(114) Matsuura, S.; Niu, C.-H.; Cohen, J. S. Pyridinium polyhydrogen fluoride, a deprotecting reagent in peptide chemistry. *J. Chem. Soc., Chem. Comm.* **1976**, *12*, 451-452.

(115) Carey, F. A.; Sundberg, R. J. In *Advanced Organic Chemistry Part A: Structure and Mechanisms*; 3rd ed.; Plenum Press: New York, 1990.

(116) Moss, R. A.; Kim, H.-R. The stereochemical course of fragmentation of benzyloxychlorocarbene. *Tetrahedron Lett.* **1990**, *31*, 4715-4718.

(117) Streitwieser, A., Jr.; Walsh, T. D.; Wolfe, J. R., Jr. Stereochemistry of acetolysis of alkyl sulfonates. *J. Am. Chem. Soc.* **1965**, *87*, 3682-3685.

(118) Streitwieser, A., Jr.; Wolfe, J. R., Jr. Stereochemistry of the primary carbon. XI. Ethanolysis of optically active benzyl-α-*d p*-toluenesulfonate. *J. Am. Chem. Soc.* **1959**, *81*, 4912-4914.

(119) Becker, Y.; Stille, J. K. Stereochemistry of oxidative addition of benzyl-α-*d* chloride and bromide to tris(triethylphosphine)palladium(0). Direct observation of optical activity in a carbon-palladium σ-bonded complex. *J. Am. Chem. Soc.* **1978**, *100*, 838-844.

(120) Cheng, H.; Markley, J. L. NMR spectroscopic studies of paramagnetic proteins: iron-sulfur proteins. *Annu. Rev. Biophys. Biomol. Struct.* **1995**, *24*, 209-237.

(121) Fukase, K.; Wakamiya, T.; Shiba, T. Synthetic study on peptide antibiotic nisin. II. The synthesis of ring B. *Bull. Chem. Soc. Jpn.* **1986**, *59*, 2505-2508.

(122) Ronwin, E.; Horn, D. E. Solvent significance in the mechanism of direct acylation. Reactions in cyclic ethers. *J. Org. Chem.* **1965**, *30*, 2821-2826.

(123) Ronwin, E.; Warren, C. B. The mechanism of the direct acylation of amino acids and related compounds in nonaqueous solvents. *J. Org. Chem.* **1964**, *29*, 2276-2279.

(124) *The Retinoids: Biology, Chemistry, and Medicine*; 2nd ed.; Sporn, M. B.; Roberts, A. B.; Goodman, D. S., Eds.; Raven Press: New York, 1994.

(125) Petkovich, M.; Brand, N. J.; Krust, A.; Chambon, P. A human retinoic acid receptor which belongs to the family of nuclear receptors. *Nature* **1987**, *330*, 444-450.

(126) Giguére, V.; Ong, E. S.; Segui, P.; Evans, R. M. Identification of a receptor for the morphogen retinoic acid. *Nature* **1987**, *330*, 624-629.

(127) Carson-Jurica, M. A.; Schrader, W. T.; O'Malley, B. W. Steroid receptor family: structure and functions. *Endocr. Rev.* **1990**, *11*, 201-220.

(128) Fontana, J. A.; Rishi, A. K. Classical and novel retinoids: Their targets in cancer therapy. *Leukemia* **2002**, *16*, 463-472.

(129) Kamei, Y.; Xu, L.; Heizel, T.; Torchia, J.; Kurokawa, R.; Gloss, B.; Lin, S. C.; Heyman, R. A.; Rose, D. W.; Glass, C. K.; Rosenfeld, M. G. A CBP integrator complex mediates transcriptional activation and AP-1 inhibition by nuclear receptors. *Cell* **1996**, *85*, 403-414.

(130) Chakravarti, D.; La Morte, V.; Nelson, M. C.; Nakajima, T.; Schulman, I.; Juguilon, H.; Montminy, M.; Evans, R. M. Role of CBP/300 in nuclear receptor signalling. *Nature* **1996**, *383*, 99-103.

(131) Ohshima, M.; Ward, J. M.; Wenk, M. L. Preventive and enhancing effects of retinoids on the development of naturally occurring tumors of skin, prostate gland, and endrocrine pancreas in aged male ACI/segHapBR rats. *J. Natl. Cancer Inst.* **1985**, *74*, 517-524.

(132) Pollard, M.; Luckert, P. H.; Sporn, M. B. Prevention of primary prostate cancer in Lobund-Wistar rats by *N*-(4-hydroxyphenyl)retinamide. *Cancer Res.* **1991**, *51*, 3610-3611.

(133) Ulukaya, E.; Wood, E. J. Fenretinide and its relation to cancer. *Cancer Treatment News* **1999**, *25*, 229-235.

(134) Niles, R. M. Recent advances in the use of vitamin A (retinoids) in the prevention and treatment of cancer. *Nutrition* **2000**, *16*, 1084-1089.

(135) Sun, S.-Y.; Lotan, R. Retinoids as chemopreventive and therapeutic agents. *Drugs of the Future* **1998**, *23*, 621-634.

(136) Gander, R.; Gurney, J. A. All-*trans*-retinoic acid esters and amides. U.S. Patent 4,108,880, Aug. 22, 1978.

(137) Moon, R. C.; Thompson, H. J.; Becci, P. J.; Grubbs, C. J.; Gander, R. J.; Newton, D. L.; Smith, J. M.; Phillips, S. L.; Henderson, W. R.; Mullen, L. T.; Brown, C. C.; Sporn, M. B. *N*-(4-Hydroxyphenyl)retinamide, a new retinoid for prevention of breast cancer in the rat. *Cancer Res.* **1979**, *39*, 1339-1346.

(138) Swanson, B. N.; Zaharevitz, D. W.; Sporn, M. B. Pharmacokinetics of *N*-(4-hydroxyphenyl)-all-*trans*-retinamide in rats. *Drug Metab. Dispos.* **1980**, *8*, 168-172.

(139) Mehta, R. G.; Moon, R. C.; Hawthorne, M.; Formelli, F.; Costa, A. Distribution of fenretinide in the mammary gland of breast cancer patients. *Eur. J. Cancer* **1991**, *27*, 138-141.

(140) Sabichi, A. L.; Hendricks, D. T.; Bober, M. A.; Birrer, M. J. Retinoic acid receptor beta expression and growth inhibition of gynecologic cancer cells by the synthetic retinoid *N*-(4-hydroxyphenyl) retinamide. *J. Natl. Cancer Inst.* **1998**, *90*, 597-605.

(141) Liu, G.; Wu, M.; Levi, G.; Ferrari, N. Inhibition of cancer cell growth by all-*trans*-retinoic acid and its analog *N*-(4-hydroxyphenyl) retinamide: a possible mechanism of action via regulation of retinoid receptors expression. *Int. J. Cancer* **1998**, *78*, 248-254.

(142) Fanjul, A. N.; Delia, D.; Pierotti, M. A.; Rideout, D.; Yu, J. Q.; Pfahl, M.; Qiu, J. 4-Hydroxyphenyl retinamide is a highly selective activator of retinoid receptors. *J. Biol. Chem.* **1996**, *271*, 22441-22446.

(143) Sun, S. Y.; Yue, P.; Lotan, R. Induction of apoptosis by *N*-(4-hydroxyphenyl)retinamide and its association with reactive oxygen species, nuclear retinoic acid receptors, and apoptosis-related genes in human prostate carcinoma cells. *Mol. Pharmacol.* **1999**, *55*, 403-410.

(144) Lovat, P. E.; Ranalli, M.; Annichiarrico-Petruzzelli, M.; Bernassola, F.; Piacentini, M.; Malcolm, A. J.; Pearson, A. D. J.; Melino, G.; Redfern, C. P. F. Effector mechanisms of fenretinide-induced apoptosis in neuroblastoma. *Exp. Cell Res.* **2000**, *260*, 50-60.

(145) Sheikh, M. S.; Shao, Z. M.; Li, X. S.; Ordonez, J. V.; Conley, B. A.; Wu, S.; Dawson, M. I.; Han, Q.-X.; Chao, W. *N*-(4-hydroxyphenyl)retinamide (4-HPR)-mediated biological actions involve retinoid receptor-independent pathways in human breast carcinoma. *Carcinogenesis* **1995**, *16*, 2477-2486.

(146) Sani, B. P.; Shealy, Y. F.; Hill, D. L. *N*-(4-hydroxyphenyl)retinamide: interactions with retinoid-binding proteins/receptors. *Carcinogenesis* **1995**, *16*, 2531-2534.

(147) Delia, D.; Aiello, A.; Lombardi, L.; Pelicci, P. G.; Grignani, F.; Formelli, F.; Menard, S.; Costa, A.; Veronesi, U. *N*-(4-hydroxyphenyl)retinamide induces apoptosis of malignant hemopoietic cell lines including those unresponsive to retinoic acid. *Cancer Res.* **1993**, *53*, 6036-6041.

(148) Wu, J. M.; DiPietrantonio, A. M.; Hsieh, T. C. Mechanism of fenretinide (4-HPR)-induced cell death. *Apoptosis* **2001**, *6*, 377-388.

(149) Weiss, K. L.; Alshafie, G.; Chapman, J. S.; Mershon, S. M.; Abou-Issa, H.; Clagett-Dame, M.; Curley, R. W., Jr. An unhydrolyzable analogue of N-(4-hydroxyphenyl)retinamide: synthesis and preliminary biological studies. *Bioorg. Med. Chem. Lett.* **2001**, *11*, 1583-1586.

(150) Walker, J. R.; Alshafie, G.; Abou-Issa, H.; Curley, R. W., Jr. An improved synthesis of the *C*-linked glucuronide of *N*-(4-hydroxyphenyl)retinamide. *Bioorg. Med. Chem. Lett.* **2002**, *12*, 2447-2450.

(151) Curley, R. W., Jr.; Abou-Issa, H.; Panigot, M. J.; Repa, J. J.; Clagett-Dame, M.; Alshafie, G. Chemopreventive activities of *C*-glucuronide/glycoside analogs of retinoid-*O*-glucuronides against breast cancer development and growth. *Anticancer Res.* **1996**, *16*, 757-763.

(152) Curley, R. W., Jr.; Robarge, M. J. Recent advances in the development of retinoids. *Curr. Med. Chem.* **1996**, *3*, 325-342.

(153) Johnson, A. T.; Klein, E. S.; Gillett, S. J.; Wang, L.; Song, T. K.; Pino, M. E.; Chandraratna, R. A. S. Synthesis and characterization of a highly potent and effective antagonist of retinoic acid receptors. *J. Med. Chem.* **1995**, *38*, 4764-4767.

(154) Klein, E. S.; Johnson, A. T.; Standeven, A. M.; Beard, R. L.; Gillett, S. J.; Duong, T. T.; Nagpal, S.; Vuligonda, V.; Teng, M.; Chandraratna, R. A. Preparation of benzopyrans, benzothiopyrans, 1,2-dihydroquinolines and 5,6-dihydroanaphthalenes as retinoid compounds having negative hormone and/or antagonist activities. US Patent 5877207, 1997.

(155) Sonogashira, K.; Tohda, Y.; Hagihara, N. Convenient synthesis of acetylenes. Catalytic substitutions of acetylenic hydrogen with bromo alkenes, iodo arenes, and bromopyridines. *Tetrahedron Lett.* **1975**, 4467-4470.

(156) Comins, D. L.; Dehghani, A. Pyridine-derived triflating reagents: an improved preparation of vinyl triflates from metallo enolates. *Tetrahedron Lett.* **1992**, *33*, 6299-6302.

(157) Crisp, G. T.; Glink, P. T. Palladium-catalyzed Heck couplings of L-vinylglycine derivatives with vinyl and aryl halides and triflates. *Tetrahedron* **1992**, *48*, 3541-3556.

(158) Bayley, H. In *Photogenerated Reagents in Biochemistry and Molecular Biology*; Laboratory Techniques in Biochemistry and Molecular Biology; Elsevier: New York, 1983; Vol. 12.

(159) Coleman, R. F. In *Protein Function*; Creighton, T. E., Ed.; IRL Press: Oxford, 1997, p 155-183.

(160) Fleming, S. A. Chemical reagents in photoaffinity labeling. *Tetrahedron* **1995**, *51*, 12479-12520.

(161) McCurdy, C. R.; Le Bourdonnec, B.; Metzger, T. G.; Kouhen, R. E.; Zhang, Y.; Law, P. Y.; Portoghese, P. S. Naphthalene dicarboxaldehyde as an electrophilic fluorogenic moiety for affinity labeling: application to opioid receptor affinity labels with greatly improved fluorogenic properties. *J. Med. Chem.* **2002**, *45*, 2887-2890.

(162) Portoghese, P. S.; El Kouhen, R.; Law, P. Y.; Loh, H. H.; Le Bourdonnec, B. Affinity labels as tools for the identification of opioid receptor recognition sites. *Farmaco* **2001**, *56*, 191-196.

(163) Maeda, D. Y.; Ishmael, J. E.; Murray, T. F.; Aldrich, J. V. Synthesis and evaluation of *N*,*N*-dialkyl enkephalin-based affinity labels for δ opioid receptors. *J. Med. Chem.* **2000**, *43*, 3941-3948.

(164) Aliau, S.; Delettre, G.; Mattras, H.; El Garrouj, D.; Nique, F.; Teutsch, G.; Borgna, J.-L. Steroidal affinity labels of the estrogen receptor α. 4. electrophilic 11β-aryl derivatives of estradiol. *J. Med. Chem.* **2000**, *43*, 613-628.

(165) Garbus, I.; Roccamo, A. M.; Barrantes, F. J. Identification of threonine 422 in transmembrane domain .alpha.M4 of the nicotinic acetylcholine receptor as a possible site of interaction with hydrocortisone. *Neuropharmacology* **2002**, *43*, 65-73.

(166) Lequin, O.; Bolbach, G.; Frank, F.; Convert, O.; Girault-Lagrange, S.; Chassaing, G.; Lavielle, S.; Sagan, S. Involvement of the second extracellular loop (E2) of the neurokinin-1 receptor in the binding of substance P: photoaffinity labeling and modeling studies. *J. Biol. Chem.* **2002**, *277*, 22386-22394.

(167) Hashimoto, M.; Hatanaka, Y.; Sadakane, Y.; Nabeta, K. Synthesis of tag introducible (3-trifluoromethyl)phenyldiazirine based photoreactive phenylalanine. *Bioorg. Med. Chem. Lett.* **2002**, *12*, 2507-2510.

(168) Radominska-Pandya, A.; Chen, G. Photoaffinity labeling of human retinoid X receptor β. (RXRβ) with 9-*cis*-retinoic acid: identification of phytanic acid, docosahexaenoic acid, and lithocholic acid as ligands for RXRβ. *Biochemistry* **2002**, *41*, 4883-4890.

(169) Schuster, G. B.; Platz, M. S. Photochemistry of phenyl azide. *Adv. Photochem.* **1992**, *17*, 69-143.

(170) Abou-Issa, H.; Curley, R. W., Jr.; Alshafie, G. A.; Weiss, K. L.; Clagett-Dame, M.; Chapman, J. S.; Mershon, S. M. Chemotherapeutic evaluation of 4-hydroxybenzylretinone (4-HBR), a nonhydrolyzable *C*-linked analog of *N*-(4-hydroxyphenyl) retinamide (4-HPR) against mammary carcinogenesis. *Anticancer Res.* **2001**, *21*, 3839-3844.

(171) Abou-Issa, H. M.; Alshafie, G. A.; Curley, R. W., Jr.; Wong, M. F.; Clagett-Dame, M.; Repa, J. J.; Sikri, V. Chemopreventive activity of a *C*-glucuronide analog of *N*-(4-hydroxyphenyl)retinamide-*O*-glucuronide against mammary tumor development and growth. *Anticancer Res.* **1999**, *19*, 999-1004.

(172) Abou-Issa, H.; Curley, R. W., Jr.; Panigot, M. J.; Tanagho, S. N.; Sidhu, B. S.; Alshafie, G. A. Chemotherapeutic evaluation of *N*-(4-hydroxyphenyl)retinamide-*O*-glucuronide in the rat mammary tumor model. *Anticancer Res.* **1997**, *17*, 3335-3340.

(173) Mershon, S. M. Chemical studies of *N*-(4-hydroxyphenyl)retinamide and analogs. Masters Thesis, The Ohio State University, 2001.

(174) Sun, S.-Y.; Yue, P.; Kelloff, G. J.; Steele, V. E.; Lippman, S. M.; Hong, W. K.; Lotan, R. Identification of retinamides that are more potent than *N*-(4-hydroxyphenyl)retinamide in inhibiting growth and inducing apoptosis of human head and neck and lung cancer cells. *Cancer Epidemiol. Bio. Prev.* **2001**, *10*, 595-601.

(175) Clifford, J. L.; Sabichi, A. L.; Zou, C.; Yang, X.; Steele, V. E.; Kelloff, G. J.; Lotan, R.; Lippman, S. M. Effects of novel phenylretinamides on cell growth and apoptosis in bladder cancer. *Cancer Epidemiol. Bio. Prev.* **2001**, *10*, 391-395.

(176) Rui, H. Research and development of cancer chemopreventive agents in China. *J. Cell. Biochem.* **1997**, *27*, 7-11.

(177) R. W. Curley, J.; Abou-Issa, H.; Panigot, M. J.; Repa, J. J.; Clagett-Dame, M.; Alshafie, G. Chemopreventive activities of *C*-glucuronide/glycoside analogs of retinoid-*O*-glucuronides against breast cancer development and growth. *Anticancer Res.* **1996**, *16*, 757-764.

(178) Thornber, C. W. Isosterism and molecular modification in drug design. *Chem. Soc. Rev.* **1979**, *8*, 563-580.

(179) Kirkovsky, L.; Mukherjee, A.; Yin, D.; Dalton, J. T.; Miller, D. D. Chiral nonsteroidal affinity ligands for the androgen receptor. 1. Bicalutamide analogues bearing electrophilic groups in the B aromatic ring. *J. Med. Chem.* **2000**, *43*, 581-590.

(180) Smith, M. B.; March, J. In *March's Advanced Organic Chemistry: Reactions, Mechanisms, and Structure*; 5th ed.; John Wiley & Sons, Inc., 2001.

(181) Albanese, D.; Penso, M. Synthesis of isothiocyanates by reaction of amides with carbon disulfide in the presence of solid potassium carbonate/sodium hydroxide mixture. *Synthesis* **1991**, 1001-1002.

(182) Staudinger, H.; Meyer, J. New organic compounds of phosphorus. III. Phosphinemethylene derivatives and phosphinimines. *Helv. Chim. Acta* **1919**, *2*, 635-646.

(183) Molina, P.; Alajarin, M.; Arques, A. Convenient improved syntheses of isocyanates or isothiocyanates from amines. *Synthesis* **1982**, 596-597.

(184) Tomas, P.; Ledesma, A.; Rial, E. Photoaffinity labeling of the uncoupling protein UCP1 with retinoic acid: ubiquinone favors binding. *FEBS Lett.* **2002**, *526*, 63-65.

(185) Beischel, C. J.; Knapp, D. R.; Govindjee, R.; Ebrey, T. G.; Crouch, R. K. Azidotetrafluorophenyl retinal analog: synthesis and bacteriorhodopsin pigment formation. *Photochem. Photobiol.* **1994**, *60*, 64-68.

(186) Boehm, M. F.; Gawinowicz, M. A.; Foucault, A.; Derguini, F.; Nakanishi, K. Photoaffinity labeling studies of bacteriorhodopsin with [15-^{3}H]-3-diazo-4-keto-all-*trans*-retinal. *J. Am. Chem. Soc.* **1990**, *112*, 7779-7782.

(187) Ding, W. D.; Tsipouras, A.; Ok, H.; Yamamoto, T.; Gawinowicz, M. A.; Nakanishi, K. Photoaffinity labeling of bacteriorhodopsin. *Biochemistry* **1990**, *29*, 4898-4904.

(188) Huang, K. S.; Radhakrishnan, R.; Bayley, H.; Khorana, H. G. Orientation of retinal in bacteriorhodopsin as studied by crosslinking using a photosensitive analog of retinal. *J. Biol. Chem.* **1982**, *257*, 13616-13623.

(189) Kometani, T.; Watt, D. S.; Ji, T. Iodination of phenols using chloramine and sodium iodide. *Tetrahedron Lett.* **1985**, *17*, 2043-2046.

(190) Cardinali, F.; Ziggiotti, A.; Viscomi, G. C. Scaling-up procedure from the range of milligrams to grams for the purification of amino acid derivatives in displacement chromatography. *J. Chromatogr.* **1990**, *499*, 37-45.

(191) King, R. W.; Williams, K. R. A glossary of NMR terms. *J. Chem. Ed.* **1990**, *67*, A100-A105.

(192) Sanders, J. K. M.; Hunter, B. K. In *Modern NMR Spectroscopy A Guide for Chemists*; 2nd ed.; Oxford University Press: New York, 1997.